Activation and Disruption of Brain Microvascular Endothelial Cells by Interleukin 2

By

Lukasz S Wylezinski

Dissertation

Submitted to the Faculty of the

Graduate School of Vanderbilt University

in partial fulfillment of the requirements

for the degree of

DOCTOR OF PHILOSOPHY

in

Molecular Physiology and Biophysics

December, 2016

Nashville, Tennessee

Approved:

Alyssa Hasty, Ph.D.

Roger Colbran, Ph.D.

David Harrison, M.D.

Luc Van Kaer, Ph.D.

To My Ever-Loving and

Infinitely Supportive

Family

ACKNOWLEDGEMENTS

The work reported here as well as my development into a scientist could not have been possible without the unending guidance, help and support of my mentor Dr. Jacek Hawiger. I eternally thank him for allowing me to pursue my scientific training beginning as an undergraduate at Vanderbilt University throughout the completion of this degree. His belief in my potential as a scientist underscored my decision to continue towards this achievement. I am also grateful to my Dissertation Committee members; Professors Alyssa Hasty, Roger Colbran, David Harrison and Luc Van Kaer. Their direction and support allowed for the successful completion of my work. Additionally, I would like to thank Dr. Kate Ellacott, a member of my thesis Committee prior to her departure to the United Kingdom from Vanderbilt University, for her constructive criticism and support. The Committee's guidance was instrumental in the successful completion of my project and my growth as a scientist. I would like to thank the Department of Molecular Physiology and Biophysics for providing a welcoming and stimulating environment contributing to my scientific development.

I am grateful to all of the Hawiger laboratory members that I encountered during my training for the immense help and support they provided. In particular I would like to wholeheartedly thank the following individuals. I am indebted to Dr. Jozef Zienkiewicz for continuous support, friendship and everlasting advice throughout my course of being a part of the laboratory. Dr. Antonio DiGiandomenico was instrumental in nurturing my scientific curiosity by providing abundant direction and continuous aid during the beginning of my research endeavors. I thank Dr. Daniel Moore for his insightful discussion and suggestions throughout the course of my time at Vanderbilt University. Furthermore, while too many to

individually thank the numerous members of the Hawiger laboratory both past and present (Ruth Ann Veach, Danya Liu, Yan Liu, Sydney Elizer, Jenny Watchmaker, Amy Armitage and Huan Qiao) have been most helpful in my studies and I thank them for their assistance and friendship.

Finally and most importantly, I'd like to thank my family and friends who have stood by me throughout my journey. My friends have been indispensable in providing the support necessary to complete this degree. My parents have provided unwavering support and advice throughout my training ensuring a successful outcome. I wish to thank them for being the ultimate role models and for their steadfast love.

Acknowledgements of Support

This work would not have been possible without the financial support of NIH Grants HL069452, HL085833, HL069765, the Vanderbilt Immunotherapy Program, the Vanderbilt University Medical School Department of Medicine and the Vanderbilt Clinical and Translational Science Award UL1TR000445.

TABLE OF CONTENTS

LIST OF TABLES

Table

Page

LIST OF FIGURES

Figure **Page**

LIST OF ABBREVIATIONS

AJ	Adherens Junction
ANOVA	Analysis of Variance
BBB	Blood Brain Barrier
bEnd.3	Murine Brain Microvascular Endothelial Cell
b-FGF	Basic Fibroblast Growth Factor
BMEC	Brain Microvascular Endothelial Cell
CBA	Cytometric Bead Array
CBF	Cerebral Blood Flow
CRADD/RAIDD	Caspase and Receptor Interacting Protein Adaptor with Death Domain
DMEM	Dulbecco's Modified Eagle's Medium
EBM-2	Endothelial Basal Medium 2
ECM	Extra Cellular Matrix
hCMEC/D3	Human Brain Microvascular Endothelial Cell
HEK	Human Embryonic Kidney
HEPES	4-(2-hydroxyethyl)-1-piperazineethanesulfonic acid
HI-FBS	Heat-Inactivated Fetal Bovine Serum

IKK	I Kappa B Kinase
IL	Interleukin
IL2R	Interleukin 2 Receptor
kDa	Kilo Dalton
LPS	Lipopolysaccharide
MCP1	Monocyte Chemoattractant Protein 1
MEF	Mouse Embryonic Fibroblast
NFκB	Nuclear Factor Kappa B
NIH	National Institutes of Health
NP-40	Nonidet P-40
p120	p120-catenin
PBS	Phosphate-Buffered Saline
PECAM	Platelet Endothelial Cell Adhesion Molecule
qPCR	Quantitative Real Time Polymerase Chain Reaction
RelA	NFκB p65
RT	Reverse Transcription
SDS	Sodium Dodecyl Sulfate

SDS-PAGE	Sodium Dodecyl Sulfate Polyacrylamide Gel Electrophoresis
SHP2	Src Homology 2 Domain-Containing Protein-Tyrosine Phosphatase 2
TJ	Tight Junction
TNF	Tumor Necrosis Factor
VE-cadherin	Vascular Endothelial Cadherin
VLS	Vascular Leak Syndrome
vWF	von Willebrand Factor

Chapter I

INTRODUCTION

Vascular System

The Vascular System in Physiology and Disease

The human vascular system is indispensable for normal physiological development and survival due to its foremost function of being a closed conduit for the circulation of blood. The blood imports oxygen, nutrients, ions and water to all organs in the body and exports carbon dioxide as well as other noxious molecules from these organs. Few processes in the body have as daunting an impact on human health and development as angiogenesis and vasculogenesis; from disorders characterized by excessive angiogenesis to diseases resulting from insufficient vessel growth and function (1). Vasculature throughout the body undergoes continuous remodeling and maturation until a complete circulatory system is formed which measures close to 60,000 miles in a normal human if laid continuously end to end (2). This is most apparent in the brain where the vascular system establishes an intricate network of blood vessels responsible for sustaining the brain with its high metabolic demands. *In vivo* remodeling and maintenance of the cerebral microvasculature has been elegantly documented in a murine model system exhibiting extensive expansion and pruning that continues postnatally and declines with age (3).

Characterization of the vessels that comprise the circulatory system depend on their anatomical and functional differences. Arteries that carry blood from a pumping heart and veins that carry blood back to the heart form the macrovascular system. Between arteries and veins

lays a vast network of tiny blood vessels that form the microcirculation. The microvascular bed is comprised of the arterioles, capillaries and venules which possess the largest surface area of the circulation. For comparison, the surface area of the skin of a normal 75 kg man is close to 2 m^2 while the surface area of the microcirculation has been estimated at 800-1000 m^2 (4,5). This expansive microvascular bed is critically involved in blood-tissue exchange (Fig.1) (6,7). The diameter of blood vessels within the human body varies from 4 μm to 25 mm (typically lower than 300 μm in microvessels) whereas endothelial cell thickness ranges from less than 0.1 μm to 1 μm (8). These vast differences allow the circulatory system to account for the diverse needs of the human body and thus adapt to requirements of each particular organ. Comparatively, red blood cells have an approximate diameter ranging from 6 μm to 8 μm while immune cells are larger; lymphocyte diameter ranges from 7 μm to 20 μm, monocyte diameter ranges from 15 μm to 25 μm and neutrophils diameter ranges from 12 μm to 15 μm (9). These cellular diameters at times may be larger than the microvessels through which they travel requiring the microvasculature to retain elasticity allowing the passage of these blood cells.

Constituents of the Microvascular System (Microcirculation)

As depicted in Figure 1, the circulation encompasses blood vessels of multiple sizes and characteristics that include differing inner surface area, velocity of blood flow and wall shear rate. As blood travels through arteries from the heart, the inner surface area of the vasculature increases both at the arterioles and the microcirculation which comprises the largest surface area (as indicated by the central peak in Fig.1). Concomitantly, the velocity of the blood flow is slowed

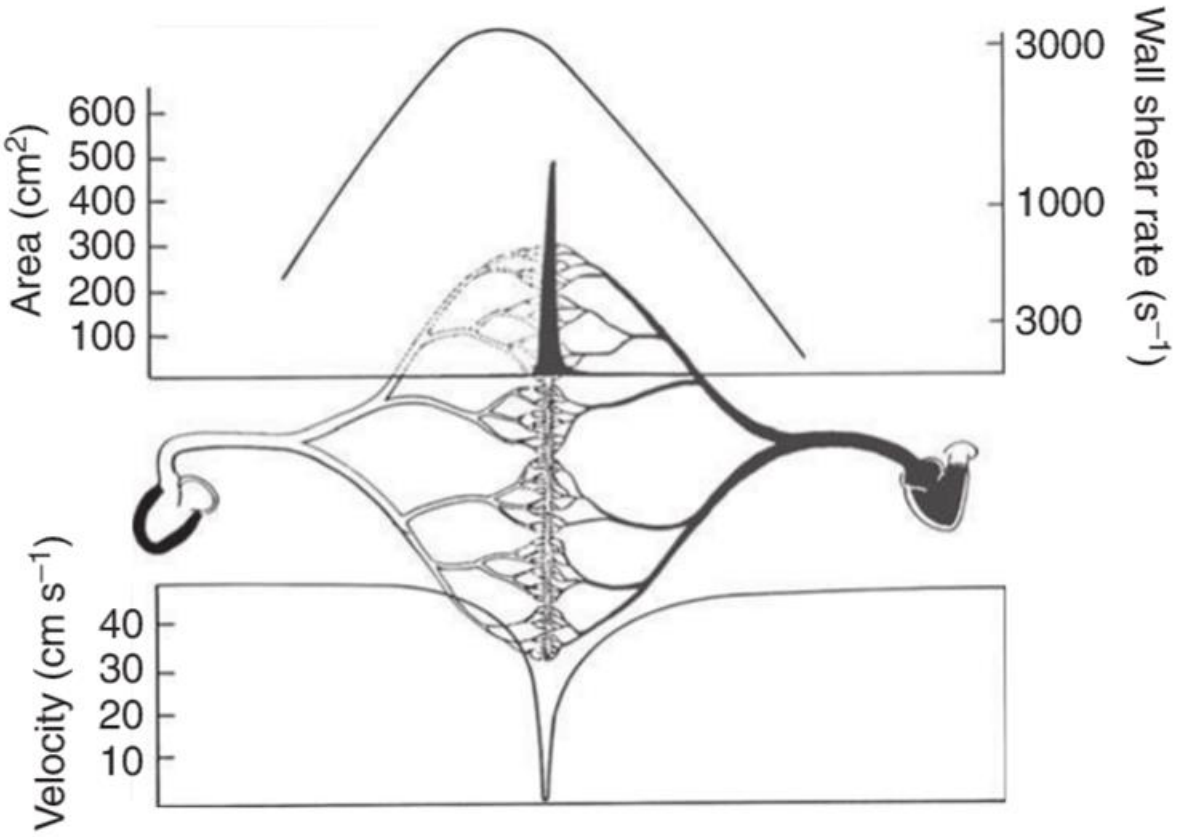

Figure 1. A Global View of the Circulatory System

Arterial circulation is depicted on the left and venous on the right. Microcirculation comprises the greatest endothelial surface area (left axis of the upper panel), as represented by the central solid peak. The upper panel right axis represents wall shear rate (s^{-1}), with the curve reaching its highest values on the arterial side of the microcirculation (pre-capillary arterioles). The lower panel comprises the velocity of blood flow, and indicates that the slowest values correlate with post-capillary venules, the terrain of white blood cell emigration. Figure from Hawiger, J. et al, 2015, *J Thromb Haemost* **13**, 1743-1756.

upon entering the microcirculation with minimal velocity occurring at the post-capillary venules where the majority of blood-tissue exchange occurs. Furthermore, wall shear rate increases as arterial blood flow approaches the microvasculature but then falls as blood moves into the venous circulation (7). This organization of blood circulation provides the most efficient mechanism for delivery and exchange of water, ions as well as nutrients at the blood-tissue interface.

Endothelial cells comprise the innermost lining of the vascular wall and are instrumental in forming the lumen of the vascular system. They work alone or in concert with other supporting cells to develop the required characteristics within each organ. At the tiniest blood vessels, solitary endothelial cell monolayers comprise the capillary tubes while other larger vessels require a more complex cellular organization including vascular smooth muscle cells and pericytes. The microvascular endothelium is tasked with sustaining the metabolic requirements and diverse functions of a given organ while also maintaining two other major functions: preservation of blood fluidity through inherent anti-clotting mechanisms and a second critical capacity, formation of the blood-tissue barrier. The microvascular endothelium is able to selectively allow the movement of water, nutrients, growth factors, hormones as well as certain cells into the surrounding tissues thereby maintaining physiological function of each organ systems. Concurrently, the microvascular endothelium excludes any constituents within the bloodstream that would prove harmful to the surrounding tissue (6).

The microvascular endothelium must exhibit specific selectivity and strike a delicate balance as each organ system possesses distinct requirements. While the macrovascular endothelium is non-fenestrated and continuous thus allowing tightly controlled permeability, some microvascular endothelium is discontinuous with open pores (lacking a basal lamina

underneath the endothelial cells) allowing cellular trafficking in organs (8). The most dramatic example of this occurs in the spleen. The spleen deviates from the standard pattern of arterioles, capillaries and venules found in most other organs and employs an "open" microcirculation where specialized microvessels exhibit gaps between their endothelial lining cells permitting blood cells and blood-borne materials to enter from the circulation (10). The liver also requires considerable blood-tissue interaction, thus the microvasculature specific to this organ contains endothelial fenestrae which allow dynamic exchange by responding to changes in perfusion and blood flow rates. Microvascular circulation in the liver also uniquely contains clusters of pores or so called "sieve plates" occupying ~6-8% of the endothelial surface, that lack a diaphragm and a basal lamina thus facilitating extensive exchange of material between the blood and liver tissue (11). As with the spleen, the liver also permits the interaction of immune cells with the surrounding tissue facilitating the development of immune tolerance.

In contrast to the previous two organs that demonstrate broad exchange between the microvasculature and tissue, the microcirculation of the lung exhibits a much tighter barrier excluding blood-borne cells. One of the major differences between systemic and pulmonary microvascular networks is the organization of capillaries in a dense anastomosing mesh of capillary segments (12). In contrast to the brush-like capillary beds common in the systemic circulation which are designed to meet minimum respiratory and nutritional requirements, the purpose of the alveolar microvascular network is to maximize the surface area available for gas exchange (O_2 and CO_2). In the adult human pulmonary microvascular surface area is on the scale of 100 m^2 and above (12). Skeletal muscle microvasculature is differently organized with capillaries running in parallel to the muscle fibers. Microvascular endothelial cells in the capillaries and arterioles play an important part in the regulation of microcirculation by sensing

and conducting the initial impulse for dilation during muscle contraction thus adjusting perfusion levels leading to heterogeneous blood flow (13). As opposed to the "open" circulation of the spleen, the specialized microvasculature of the brain exhibits the most restricted interface with the surrounding tissue, essentially excluding most circulating molecules and cells from the central nervous system (CNS) (see section below on the Blood Brain Barrier).

To recapitulate, microvascular characteristics and functional requirements can vary greatly from one organ to another. Endothelial cells, responsible for the formation of the microvasculature in each of these organs, are instrumental in regulating the proper exchange of water, metabolites and plasma proteins as well as the trafficking of immune cells when their recruitment is necessary for an immune or inflammatory response. Many physiological and disease conditions contribute to phenotypic changes in the microvasculature that occurs in response to diverse factors including shear stress, hypoxia, or molecular mediators (8). As the principle cell type responsible for ensuring proper microvascular capacity at the blood-tissue interface, endothelial cells must preserve their structural and functional integrity which is of paramount importance in maintaining physiologic homeostasis.

Furthermore, the heterogeneity of endothelial cells comprising the microcirculation in specific organs can result in diverse responses when challenged with similar insults. Endothelial cells from each particular microvascular bed have distinct and dynamic gene transcription profiles resulting in selective involvement in different disease states (14). Despite the shared general characteristics, endothelial cells from specific microvascular beds have a number of unique features and indeed, many human vascular diseases are restricted to particular vessels (8). Understanding endothelial cell response to a multitude of inflammatory insults is critical to preserving microvascular stability and organ health (see section below on Inflammation).

Blood Brain Barrier

General Features of Brain Circulation

The brain is a highly vascularized organ due to the extensive metabolic requirement for its physiologic function (Fig. 2). Formation of the specialized microvascular system found in the brain requires the interaction of a number of cell types including brain microvascular endothelial cells, the basement membrane, and various other cell types, including astrocytes, glial cells and neurons that are located close to the capillaries. Blood vessels supplying the brain must shield it from toxic substances in the blood, deliver nutrients, and allow harmful compounds to diffuse from the brain back into the bloodstream. Brain microvasculature is very intricate and reaches the deepest areas of the organ. Generally, capillaries in the brain may be as small as 7 μm to 10 μm in average diameter, and the average intercapillary distance is approximately 40 μm meaning that every neuron is within 20 μm of a capillary (15). Such proximity and compact organization ensures that every cell within the CNS is properly oxygenated and maintained. Brain microvascular endothelial cells are an essential part of the neurovascular unit that comprises the blood brain barrier (see below).

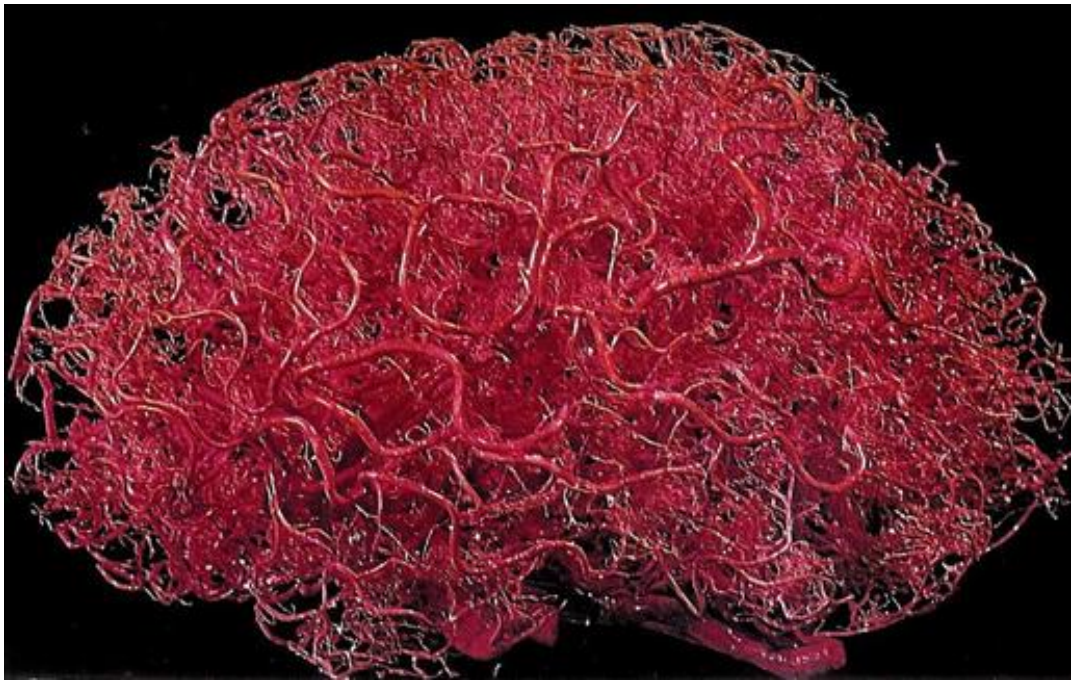

Figure 2. The Brain is a Highly Vascularized Organ

A representative casting of the extensive and intricate vascular system in the human brain. Larger vessels are apparent on the exterior of the casting while smaller microvessels are abundantly localized in the middle of the model. Image from Google Image Search

Characterization of the Blood Brain Barrier

Named for its ability to prevent the uncontrolled leakage of substances from the blood into the brain, the blood brain barrier (BBB) has emerged as a complex, dynamic, adaptable interface that controls the exchange of substances, including signaling molecules, between the CNS and the blood (16). Distinct specialization of the BBB depends on a number of cell types working in concert to form the "neurovascular unit" capable of providing the central nervous system a demarcation zone accessible to the bloodstream. Brain microvascular endothelial cells (BMECs) are surrounded by or closely associated with pericytes, astrocytes, perivascular endfeet, microglia and neuronal processes (17). The cells that make up the neurovascular unit communicate with the parenchyma of the CNS, adapting their behavior to serve its needs, responding to pathological conditions, and in some cases participating in the onset, maintenance or progression of disease (16). Microvascular endothelial cells form the lumen of the capillary and are surrounded by extracellular basal membrane with pericytes facing the brain parenchyma (Fig. 3). For a long time, the existence of pericytes and their function were underappreciated, but during recent years, these cells have gained increasing attention as obligatory constituents of blood microvessels and important regulators of vascular development, stabilization, maturation, and remodeling (18). Astrocytes and neurons are able to interact directly with endothelial cells or the encompassing pericytes. The concept of the neurovascular unit emphasizes that BMECs are in intimate and constant crosstalk with astrocytes, microglia, neurons, pericytes as well as circulating immune cells allowing for the BBB to refine its functions and facilitate brain-body communication (16).

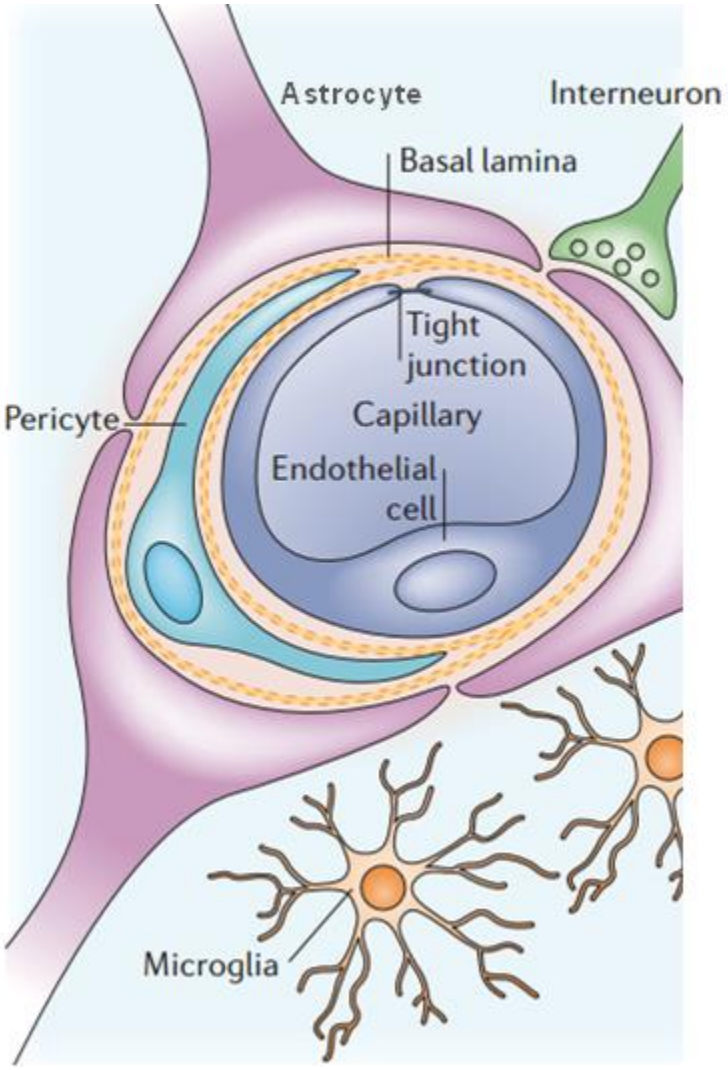

Figure 3. Cellular Constituents of the Blood Brain Barrier

The blood brain barrier 'neurovascular unit' is formed by capillary endothelial cells, surrounded by basal lamina, pericytes and astrocytic perivascular endfeet. Astrocytes provide the cellular link to the neurons. The figure also shows microglial cells. Adapted from Abbott, N.J. et al, 2006, *Nat Rev Neurosci* **7**, 41-53.

Endothelial Barrier Function

The barrier formed between the bloodstream and the CNS is of paramount importance in protecting delicate brain structure thereby allowing efficient neural activity. Hence, the importance of endothelial barrier function is most pronounced at the BBB that maintains an environment allowing proper function of the CNS by tightly controlling the passage of water, ions and other molecules while instantaneously delivering nutrients and oxygen according to current neuronal needs. Even water molecules, the prerequisite molecules to life, are transferred into the brain under strict control. During normal physiologic conditions in the brain the movement of water molecules is mainly directed by specific proteins that belong to the Aquaporins family, in particular Aquaporin 4 (AQP4). AQP4 protein complexes are strategically localized at astrocyte endfoot plasma membranes, in close contact with endothelial cells in the neurovascular unit, to constitutively regulate the flux of excess water derived from the metabolic breakdown of brain glucose and ions/neurotransmitters released by neural activity (19). While water molecules can cross the plasma membrane directly and perhaps, to a small extent through some glucose transporters and ion channels, several studies support a major role for AQP4 in determining BBB water permeability (20). At this point, it is still unclear to what extent AQP4 plays a role in the development of increased microvascular permeability during BBB disruption.

Importantly, the BBB also protects the brain from toxins, certain drugs and pathogens, (21). The brain endothelium has a range of passive and active features resulting in a much lower degree of endocytosis/transcytosis activity than does peripheral endothelium contributing to this transport-barrier property of the BBB (17). The vast majority of hydrophilic drugs, peptides and proteins are restricted from entry into the CNS under physiologic conditions. The restriction of

small molecule transport into the brain under normal physiologic conditions also extends to blood-borne immune cells.

Immune Privilege of the Brain

Early studies in the brain, in which minimal immunological response to transplanted antigenic material was observed, led to the concept of the brain as an "immune privileged site" that evolved from separation of immune cells found in the bloodstream from the brain parenchyma (22). Presently, it is recognized that "CNS immune privilege" is not absolute and it is more accurately described as an immunologically specialized site rather than immunologically privileged (23). Under normal conditions, antigen-activated lymphocytes are capable of only low-level surveillance throughout the CNS limiting entry to a fraction of the immune cells observed in other tissues (24). Larger numbers of immune cells are able to transverse the BBB only upon the activation of an inflammatory response. An intact BBB is essential for forming and maintaining a microenvironment that allows neuronal circuits to function properly by controlling leukocyte trafficking across the BBB (21). The tightly regulated barrier function of brain microvascular endothelial cells is formed by endothelial junctional protein complexes.

The Blood Brain Barrier is Maintained by Discrete Protein Complexes

Intercellular junctions made up of a complex network of adhesive proteins organized into adherens junctions (AJ) and tight junctions (TJ) maintain BBB function in brain microvascular endothelial cells (25). Each of these junctional complexes is characterized by the presence of

proteins from two distinct families, the cadherins and catenins in AJs while claudins and occludin make up TJs. Vascular endothelial cadherin (VE-cadherin) is specifically responsible for endothelial AJ assembly and barrier architecture as it anchors the transcellular interaction between plasma membranes of adjoining cells. VE-cadherin, as a transmembrane protein, recruits cytoplasmic catenins through its cytosolic tail, specifically β-catenin and p120-catenin, thus facilitating the connection of these protein complexes to the actin cytoskeleton (26). Tyrosine phosphorylation of VE-cadherin and β-catenin is strongly reduced in confluent monolayers as tyrosine phosphorylation of β-catenin decreases the affinity of its binding to the cadherin tail (27). Tight junctions are comprised of the transmembrane proteins occludin and the claudin family of proteins (Fig.4) (17). Tight junctions are important due to their primary responsibility of limiting movement of molecules across the endothelial barrier. These junctions restrict even the movement of small ions such as Na^+ and Cl^- as well as segregating the apical and basal domains of the cell membrane (a "fence-like" function) so that the endothelium can take on a polarized state (17). The term "barrier" suggests a relatively fixed structure, but it is now known that many features of the BBB phenotype can vary (28). The BBB is not simply a barrier that blocks water, small molecules and cells but a complex, interactive, ever-adapting interface that serves the signaling needs of the CNS and facilitates communication between the brain and peripheral organs (16). Activation of microvascular endothelial cells in the presence of a proinflammatory microenvironment leads to the disruption of these protein complexes and deterioration of normal physiologic function. A full understanding of the processes underlying microvascular disruption could prove pivotal in discovering new therapeutic targets to limit neuronal toxicity that underlies a number of neurologic disorders.

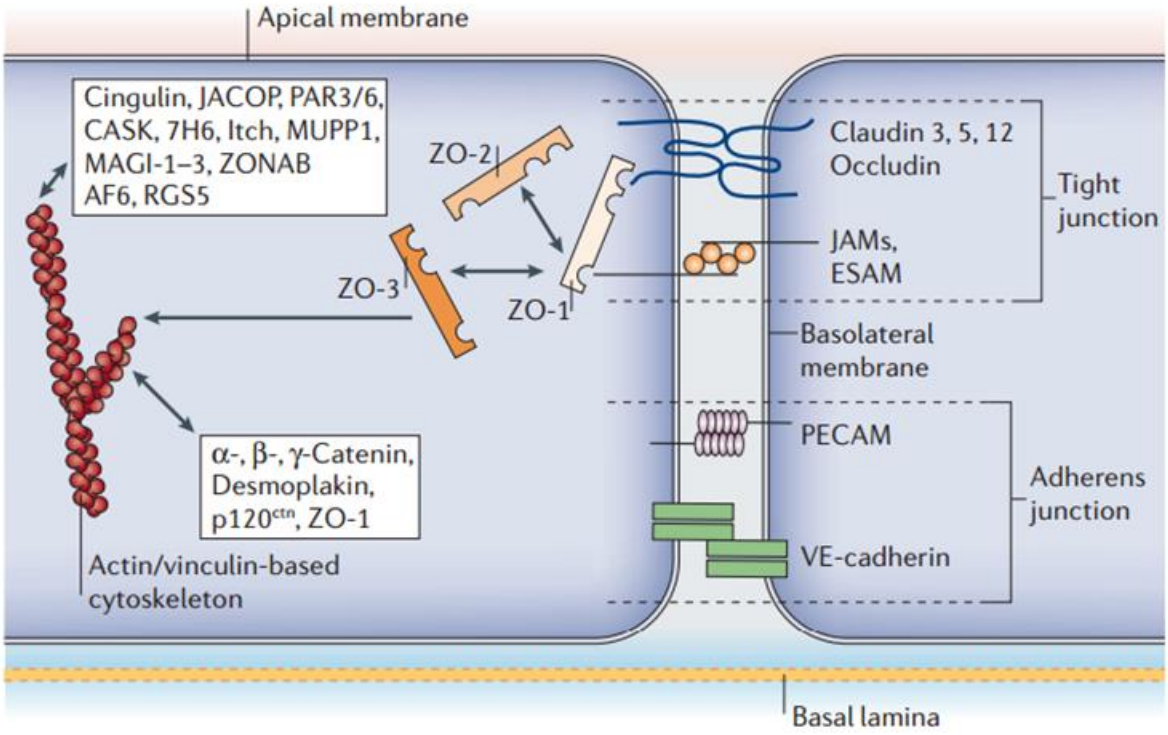

Figure 4. Simplified Schematic Depiction Showing the Molecular Composition of Endothelial Junctions

In epithelial cells, tight and adherens junctions are strictly separated from each other, but in endothelial cells these junctions are intermingled. The most important molecule of endothelial adherens junctions is VE-cadherin. In addition, the platelet–endothelial cell adhesion molecule (PECAM) mediates homophilic adhesion. The chief linker molecules between adherens junctions and the cytoskeleton are the catenins, while desmoplakin and p120 catenin (p120ctn) are also involved. Occludin and the claudins — proteins with four transmembrane domains and two extracellular loops — are the most important membranous components. The junctional adhesion molecules (JAMs) and the endothelial selective adhesion molecule (ESAM) are members of the immunoglobulin superfamily. Many first-order adaptor proteins are located within the cytoplasm, including zonula occludens 1, 2 and 3 (ZO-1–3) and Ca^{2+} dependent serine protein kinase (CASK), that bind to the intramembrane proteins. Among the second-order adaptor molecules, cingulin is important, and junction-associated coiled-coil protein (JACOP) may also be present. Signaling and regulatory proteins include multi-PDZ-protein 1 (MUPP1), the partitioning defective proteins 3 and 6 (PAR3/6), MAGI-1–3 (membrane-associated guanylate kinase with inverted orientation of protein–protein interaction domains), ZO-1-associated nucleic acid-binding protein (ZONAB), afadin (AF6), and regulator of G-protein signaling 5 (RGS5). All of these adaptor and regulatory/signaling proteins control the interaction of the membranous components with the actin/ vinculin-based cytoskeleton. Itch, E3 ubiquitin protein ligase. Figure from Abbott, N.J. et al, 2006, *Nat Rev Neurosci* **7**, 41-53.

Disruption of the Blood Brain Barrier

Disruption of the BBB leads to increased translocation of water, ions, plasma proteins as well as poorly regulated exchange of other molecules and infiltrating immune cells across the BBB affecting the delicate CNS environment (Fig.5) (21). Breakdown of the BBB impacts all of the constituents of the neurovascular unit but in particular astrocytes, which are normally tasked with a number of housekeeping functions, including regulation of ion homeostasis, water transport and amino acid neurotransmitter metabolism (29). Preserving a uniform internal environment within the CNS is essential for normal neuronal activity. Lost integrity of the neurovascular unit deleteriously impacts the surrounding neural tissue as maintenance of a stable osmotic environment is lost and normally excluded biologically active molecules are able to enter the CNS (29). It is noteworthy that disruption of physiologic barrier function underlies the development of neurodegenerative diseases including Multiple Sclerosis and Neuromyelitis Optica (21,30). It remains unknown whether BBB breakdown is an initiating event or a downstream consequence in these diseases.

The process of increased immune cell infiltration begins with disruption of endothelial cell organization and results in a breach of the BBB. Leukocyte extravasation from the bloodstream is a multistep process that depends on several factors including fluid dynamics within the vasculature and molecular interactions between circulating lymphocytes and endothelial cells (23,24,30). These interactions are mediated by emitted cytokines and chemokines that are able to initiate a feed-forward auto-regulatory loop. Interaction between activated immune cells and the endothelium occurs during the initiation and progression of Multiple Sclerosis. While its initiation is still unresolved, formation of multiple sclerotic lesions results from trafficking of autoreactive T cells from the periphery into the CNS parenchyma

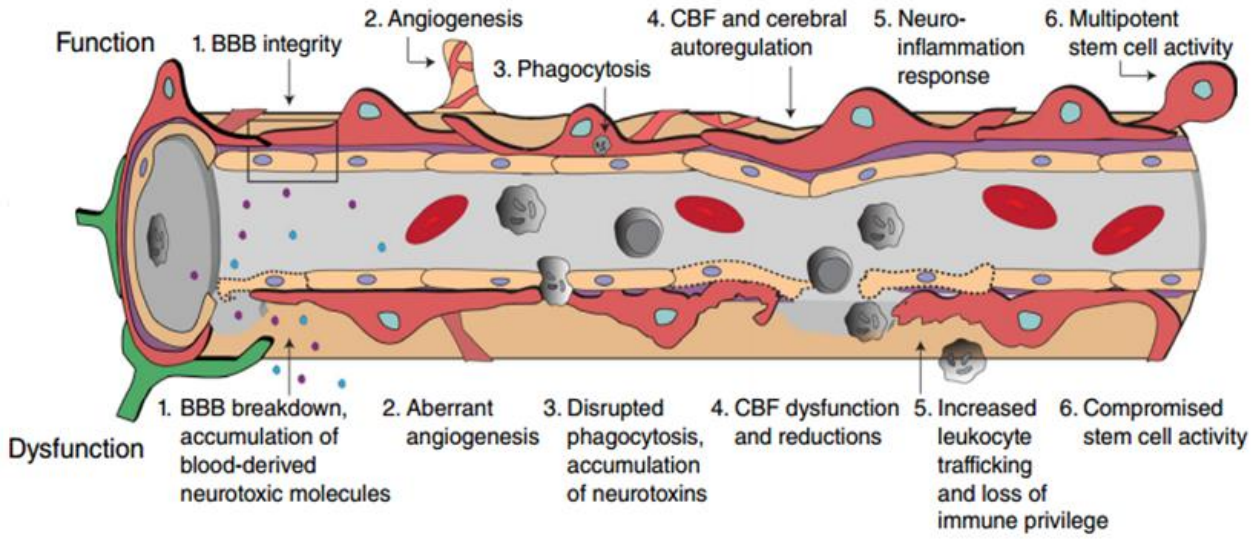

Figure 5. Blood Brain Barrier Regulation under Normal Physiologic Conditions (top row) and BBB Breakdown Following Injury (bottom row)

Under physiological conditions (top row), pericytes regulate (1) BBB integrity, i.e., tight or adherens junctions and transcytosis across the BBB; (2) angiogenesis, i.e., microvascular remodeling, stability and architecture; (3) phagocytosis/pinocytosis, i.e., clearance of toxic particles and metabolites from the CNS; (4) Cerebral blood flow (CBF) and capillary diameter; (5) neuroinflammation manifested by leukocyte trafficking into the brain among other features and (6) multipotent stem cell activity. Pericyte dysfunction (bottom row) is characterized by (1) BBB breakdown causing leakage of neurotoxic blood-derived molecules into the brain (for example, fibrinogen, thrombin, plasminogen, erythrocyte-derived free iron and anti-brain antibodies); (2) aberrant angiogenesis; (3) impaired phagocytosis causing CNS accumulation of neurotoxins; (4) CBF dysfunction and ischemic capillary obstruction; (5) increased leukocyte trafficking promoting neuroinflammation; and (6) impaired stem cell-like ability to differentiate into neuronal and hematopoietic cells. Pericyte dysfunction is present in numerous neurological conditions and can contribute to disease pathogenesis. Figure from Sweeney, M.D., et al, 2016, *Nat Rev Neurosci* **19**, 771-783.

leading to their attack of neurons (31). Recruitment of activated leukocytes can also prove destructive to the brain through excessive expression of proinflammatory mediators, cytokines and chemokines (30). For instance BMEC stimulation by Interleukin 1 beta (IL-1β) leads to fever and lethargy (32), exemplifying the direct impact this cytokine has on the CNS.

Inflammation

Inflammation Affecting the Vascular System

As stated by Elias Metchnikoff in 1891, 'The main factor in all inflammatory states consists in a lesion of the vessels which are attacked by an irritating cause" (7). These "irritating causes" can be microbial, autoimmune, metabolic, and/or physical (trauma, burns and irradiation). Inflammatory insults brought on by pathogenic microbes, metabolic products or traumatic injury lead to activation of endothelial cells and a loss of their barrier function manifest by increased permeability and subsequent swelling of the surrounding tissue (edema). Since antiquity, inflammation was recognized and characterized by four cardinal signs: rubor (redness), calor (increased heat), tumor (swelling) and dolor (pain) (33). Injury of the vasculature features prominently in the development of these signs. Increased blood flow due to vasodilation results in development of redness and increased heat at the site of injury. The expression of inflammation and hemostasis-related proteins following endothelial activation is notably dependent on the vascular bed and the nature of the stimulus (8).

Vascular inflammation is a daunting issue in modern medicine because it mediates a number of diseases including atherosclerosis, stroke, hypertension and sepsis (7,34-36). Cardiovascular disease is the leading global cause of death, accounting for more than 17.3 million deaths per year, a number that is expected to grow to more than 23.6 million by 2030 (34). Direct and indirect costs of cardiovascular diseases and stroke including health expenditures and lost productivity total more than $316.6 billion (34). About 75 million American adults (32%) live with hypertension resulting in direct and indirect costs totaling more than $48.6 billion (35). Sepsis, developing from a collapse of microvascular circulation, is one of the ten leading causes of death worldwide (7). Thus, protection of endothelial cells from excessive activation due to proinflammatory insults is a chief concern. This protection hinges upon a delicate balance between the inducers and physiologic suppressors of inflammation in endothelial cells during the course of disease. Physiologic suppressors of inflammation encompass ubiquitin modifier A20, suppressors of cytokine signaling (SOCS) 1 and 3 as well as caspase and receptor interacting protein adaptor with death domain (CRADD/RAIDD) (37-40). Relative deficiency of these physiologic anti-inflammatory regulators may contribute to reversible or irreversible endothelial injury, detachment, and cell death known as “anoikis”. Anoikis or “homelessness” is a form of programmed cell death due to the loss of contact with the extracellular matrix (ECM). Anchorage-dependent cells use ECM derived signals to maintain viability and tissue integrity (41).

Activation of the endothelium leading to increased permeability plays a crucial role in the development of vascular injury and its resolution. A proinflammatory environment induces a switch in gene transcription from generating a protective anti-coagulant, anti-adhesive and anti-inflammatory endothelial surface to one that is dominated by pro-coagulant, pro-adhesive and

pro-thrombotic mediators (8). Vascular permeability results in accumulation of parenchymal and interstitial fluid impairing organ function by increasing the distance required for the diffusion of oxygen and compromising microvascular perfusion because of increased interstitial pressure (42). Increased microvascular permeability is a characteristic of a multitude of deleterious diseases.

Vascular Leak Syndrome: A Complication of Interleukin 2 Action during Cancer Immunotherapy

Another disorder emblematic of the dangers associated with excessive vascular permeability is the vascular leak syndrome (VLS). VLS is characterized by a generalized increase in extravasation of fluids along with proteins from the capillary vessels into the tissues resulting in interstitial edema, a decrease in microcirculatory perfusion and ultimately culminating in different types/severities of organ damage in various pathological conditions (43). Patients present with transient but severe hypotension that results in vascular collapse and shock, hemoconcentration and ultimately anasarca (generalized massive edema) because of the accumulation of fluids and macromolecules in tissues (44). Development of this dangerous ailment results from loss of endothelial barrier function and may prove fatal if left untreated. Treatment of VLS can be difficult as the signs and symptoms widely vary among patients. With no defined course of medical care, most patients receive various regimens to decrease systemic edema such as diuretics, intermittent exogenous oxygen or intubation with mechanical ventilation support to counteract lung edema or pulmonary insufficiency and vassopressors to maintain renal perfusion and blood pressure (43). VLS has been described as the major dose-

limiting toxicity of cancer immunotherapy with IL2 (Fig.6) (45). Important work has been done documenting the effect of IL2 immunotherapy on pulmonary endothelial cells (46). These findings suggest that use of IL2-antibody complexes targeting specific IL2 receptor subunits may reduce the adverse side effect of severe pulmonary edema. Due to the differences exhibited by endothelial cells in specific microvascular beds we were interested in identifying the mechanism of IL2 action on brain microvascular endothelial cells. This mechanism of IL2-induced VLS affecting the brain and causing neuropsychiatric disorders is still unclear and requires further study.

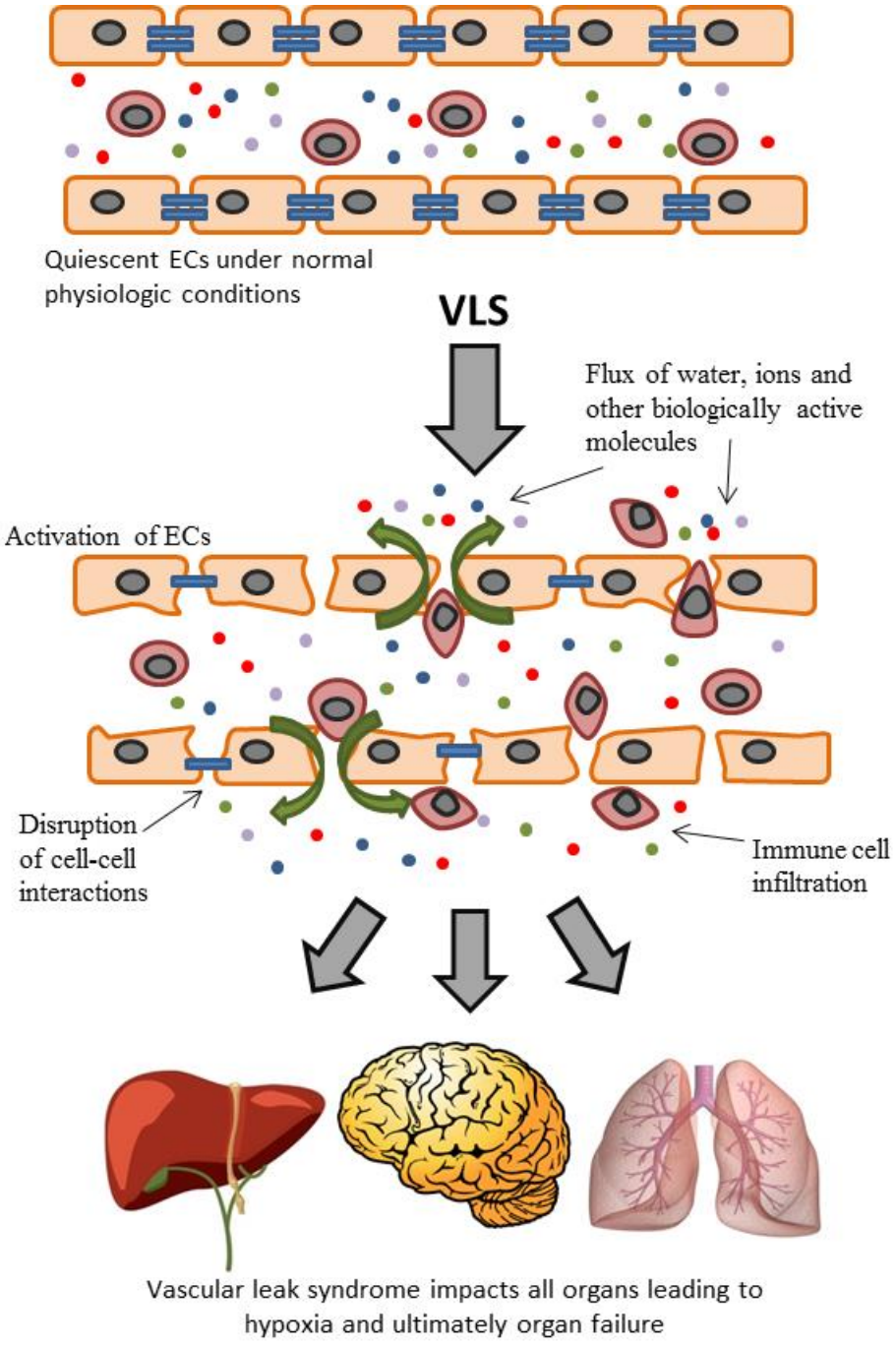
Quiescent ECs under normal physiologic conditions
VLS
Flux of water, ions and other biologically active molecules
Activation of ECs
Disruption of cell-cell interactions
Immune cell infiltration
Vascular leak syndrome impacts all organs leading to hypoxia and ultimately organ failure

Figure 6. Overview of Vascular Leak Syndrome Following Breakdown of the Blood-Tissue Barrier

Vascular Leak Syndrome caused by IL2 immunotherapy induces endothelial damage resulting in increased extravasation of water, proteins, ions, and electrolytes culminating in a decrease in plasma osmolarity. Vascular activation leads to changes in cellular morphology and loss of cell-cell interactions at adherens junctions and tight junctions. Tissue edema impacting organs such as the liver, brain and lungs reduces capillary circulation resulting in decreased perfusion and tissue hypoxia. Loss of microvascular endothelium function is deleterious for the organ systems.

Transcription Factor Nuclear Factor κB, a Master Regulator of Immunity

Nuclear Factor κB Signaling

NFκB (RelA, RelB, cRel, NFκB1 and NFκB2) is a family of transcription factors sharing the Rel homology domain (47) and functionally denoted by us as one of the stress-responsive transcription factors (SRTFs) along with nuclear factor of activated T cells (NFAT), cFos and cJun (forming the AP1 complex) and signal transducer and activator of transcription (STAT) 1 (48). NFκB p65 (RelA) is known as a pleomorphic transcription factor, expressed in most mammalian cells, able to induce hundreds of genes responsible for critical roles in many normal physiological processes as well as diverse pathologic conditions most notably, inflammation and cancer (49). Activation of NFκB leads to its translocation to the nucleus and transcriptional activity upon binding to specific κB target sites within the DNA. This transcription factor is sequestered in the cytoplasm when bound to a class of proteins referred to as inhibitors of NFκB or IκB proteins. Binding of IκBα obscures the RelA nuclear localization sequence. Release of RelA from these inhibitors is initiated by IκB kinase mediated phosphorylation, subsequent polyubiquitination and proteasomal degradation of IκB proteins (50). Following removal of IκB, the nuclear localization sequence (NLS) is recognized by nuclear transport shuttles that belong to the importin/karyopherins alpha family (51). This complex is then guided by importin beta toward the nuclear pore, for nuclear translocation. Once inside the nucleus NFκB binds to κB regulatory elements and begins transcription (Fig. 7). Post-translational modification of NFκB, in particular phosphorylation, has been documented to increase DNA binding capacity (52). A fully phosphorylated NFκB transcription factor is then able to transcribe a multitude of target genes

impacting a number of cellular processes. Activation of lymphocytes by IL2 is well known for inducing NFκB signaling (53). This fact, along with the prior detailed documentation of pulmonary endothelial expression of IL2 receptor, suggests that IL2 signaling in BMEC may result in NFκB p65 (RelA) activation.

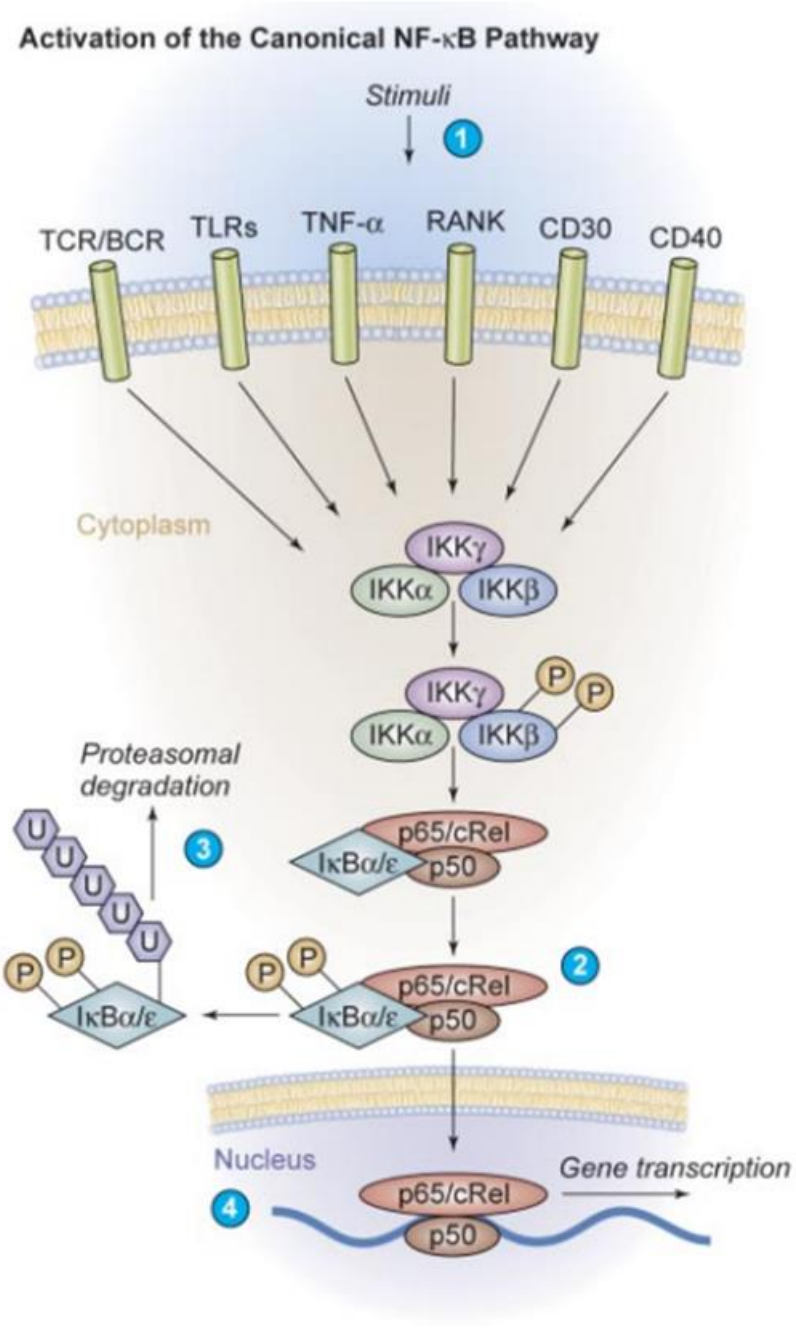
Activation of the Canonical NF-κB Pathway
Stimuli
1
TCR/BCR
TLRs
TNF-α
RANK
CD30
CD40
Cytoplasm
IKKγ
IKKα
IKKβ
P
P
Proteasomal degradation
3
U
U
U
U
U
p65/cRel
IκBα/ε
p50
2
Nucleus
4
Gene transcription

Figure 7. Activation of the Canonical Pathway of NFκB

Many agonists activate the canonical pathway of NFκB, including proinflammatory cytokines such as IL-1β, TNF-α, or pathogen-associated molecular patterns that bind to TLRs, ligands for the antigen receptors TCR/BCR, or lymphocyte co-receptors such as CD40, CD30, or receptor activator of NFκB (RANK) (1). Activated IKK phosphorylates IκB proteins on 2 conserved serine residues and induces IκB polyubiquitinylation (2), which in turn induces their recognition by the proteasome and causes successive proteolytic degradation (3). Following the IκB degradation, the cytoplasmic NFκB dimers are released, bound by nuclear transport adaptors importins/karyophherins alpha/beta and translocated to the nucleus, where gene transcription is activated (4). Figure from Jost, P.J. and Ruland, J., 2007, *Blood* ***109,*** 2700-2707.

Activation of Endothelial Cells is Mediated by Nuclear Factor κB Signaling

Disruption of endothelial barrier function develops following activation of the endothelium. The NFκB pathway is an important player in endothelial activation. Cell adhesion molecules e.g. intercellular cell adhesion molecule 1 (ICAM1) and selectins, members of the immunoglobulin superfamily, are up-regulated by proinflammatory factors and sequentially mediate rolling, adhesion, and transmigration of leukocytes from the bloodstream to underlying tissues (54). Endothelial cells become activated in response to leukocyte engagement and/or to leukocyte-derived cytokines resulting in an upregulation of cell adhesion molecules as well as further cytokine expression which leads to an escalation of the inflammatory cascade (24). Genes encoding these cell adhesion molecules and other mediators of inflammation are controlled by stress-responsive transcription factors exemplified by NFκB, master regulator of immunity and inflammation. Increased expression of interleukin 6 (IL6), macrophage chemotactic protein 1 (MCP1), ICAM1 and vascular cell adhesion molecule 1 (VCAM1) among others, have been linked to the NFκB pathway in endothelial cells (47,54,55). The emerging link between IL2, NFκB activation and vascular permeability led us to further study these interactions in brain microvascular endothelial cells.

Interleukin 2

Interleukin 2 Signaling

IL2, a 15.5 kDa cytokine, was initially discovered as a mediator of expansion and maintenance of T lymphocytes (56). The importance of IL2 in immunobiology is well documented. IL2 is able to deliver both stimulatory and regulatory signals to lymphocytes by interacting with either a trimeric receptor complex consisting of IL2Rα (CD25), IL2Rβ (CD122) and IL2Rγ (CD132, γc) or the dimeric IL2Rβγ (57). While both receptor complexes are able to transmit signals following IL2 ligation, the trimeric ("high affinity") complex shows a 10-100 fold higher affinity than that of the dimeric ("intermediate affinity") receptor complex (Fig. 8) (57,58). The IL2 receptor complex signals through three main signaling pathways, the mitogen-activated protein kinase (MAPK) pathway, the signal transducer and activator of transcription (STAT) pathway and the phosphoinositide 3-kinase (PI3K-AKT) signaling pathway (Fig. 9) (59). Pulmonary endothelial cells have been shown to induce an increase in vascular permeability following engagement of the trimeric IL2Rαβγ (46). Expression of IL2Rα subunit on endothelial cells was identified as the culprit in development of vascular leak in the lungs. This led us to postulate that BMECs may also express this receptor complex and be responsible for brain edema following IL2 stimulation. While previous studies have been undertaken to understand IL2 activation of endothelial cells, particularly pulmonary endothelial cells, to our knowledge investigations focusing on IL2 activation of brain microvascular endothelial cells have not been described (46,60-62).

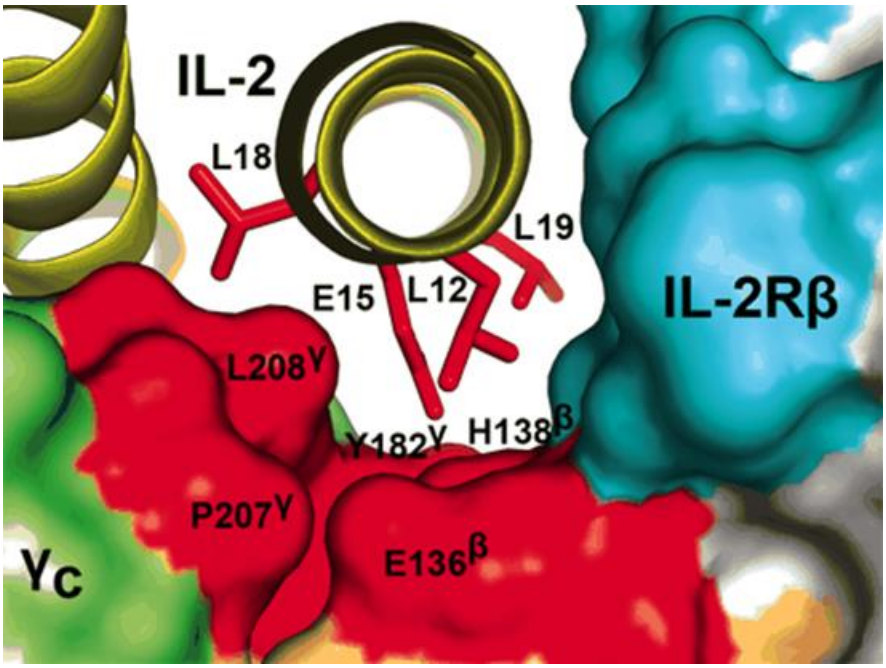

Figure 8. Three-way Junction between IL2, IL2Rβ, and γ_c

IL2 (yellow ribbon representation), IL2Rβ (cyan), and γ_c (green) form a three-way junction at the heart of the high-affinity IL2 signaling complex. The network of residues that mediate these contacts (colored red) provides a compelling structural basis for cooperativity in the IL2/IL2R complex assembly. Figure from Stauber, D.J., et al, 2005, *Proc. Natl. Acad. Sci. U. S. A.* **103**, 2788-2793.

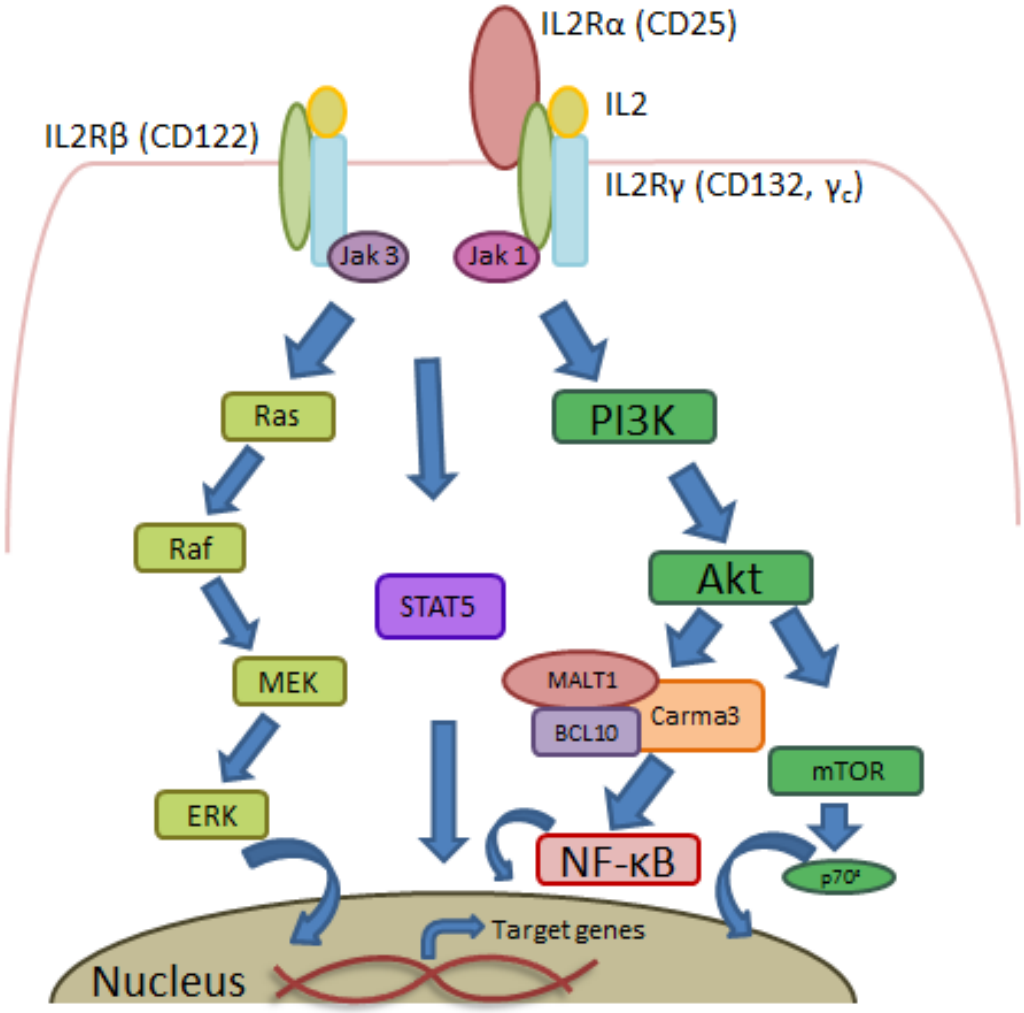

Figure 9. Major Interleukin 2 Signaling Pathways

IL2 signaling emanating from the trimeric (IL2Rαβγ) or dimeric (IL2Rβγ) receptor complex involves three major signaling pathways. Following ligation of IL2 to the receptor complex Janus family tyrosine kinases (JAK1 and JAK3) are activated and are responsible for further signaling down the signal transducer and activator of transcription (STAT) signaling pathway, the phosphoinositide 3-kinase (PI3K-Akt) signaling pathway, and the mitogen-activated protein kinase (MAPK) signaling pathway. New evidence points to the activation of NFκB by the PI3K-Akt pathway through activation of the CARMA 3 signalosome. The MALT1-BCL10-CARMA1 complex in immune cells is able to drive nuclear NFκB localization resulting in transcription of its target genes in addition to the other signaling pathways.

Interleukin 2: A Mainstay of Early Cancer Immunotherapy

The ability to mediate T cell survival and function suggests that IL2 administration would drive expansion of tumor infiltrating lymphocytes. This hypothesis led to pioneering efforts to harness IL2 for initiation of cancer immunotherapy programs in patients with renal cell carcinoma and malignant melanoma. Initial administration in humans was undertaken by Dr. Steven A. Rosenberg and his team at the National Cancer Institute in 1985 when twenty patients received a wide variety of different regimens and doses of recombinant IL2 (56). Following optimization of different administration protocols, IL2 was demonstrated to be a successful cancer treatment showing an objective and durable regression in ~20% to ~30% of tumors in patients suffering from renal cell carcinoma or melanoma (63,64). More recent advances have allowed physicians to utilize adoptive transfer of natural or genetically modified autologous human antitumor T cells expanded *in vitro* to treat a variety of cancer types (64). These immunotherapy protocols have been refined and expanded leading to an increase in positive outcomes. Thus, IL2 cancer immunotherapy was approved by the U.S. Food and Drug Administration (FDA) for the treatment of malignant melanoma and renal cell carcinoma.

Interleukin 2-Induced Vascular Leak Syndrome

While partially successful, the major dose-limiting toxicity of IL2 immunotherapy is the development of vascular leak syndrome (VLS) in treated patients (64). As described above, VLS leads to increased vascular permeability that results in extravasation of proteins, water and electrolytes culminating in decreases in both serum albumin levels and plasma osmolarity (43). VLS is thought to occur secondary to endothelial injury, causing increased vascular permeability

which results in patient hypotension, edema and increased body weight endangering a number of organ systems (65). VLS of multiple severities has been documented in patients, thus entrenching VLS as one of the most dangerous side effects of IL2 cancer immunotherapy treatment. Tissue edema is accompanied by elevated tissue pressure, decreasing capillary circulation resulting in decreased microcirculatory perfusion and hypoxia (43). Cessation of IL2 immunotherapy results in rapid resolution of these side effects documenting IL2's direct involvement in the initiation and progression of VLS (32,64). Thus, identification of the mechanisms through which IL2 acts may provide new targets to combat this dangerous complication of cancer immunotherapy.

Interleukin 2 Immunotherapy's Impact on the Central Nervous System (CNS)

As with other organ systems throughout the body, IL2-induced VLS also impacts the central nervous system manifested by a rise in brain water content that is attributed to increased permeability of the brain microvascular endothelium. CNS toxicity with substantial neuropsychiatric presentation has been documented in patients undergoing IL2 immunotherapy (32). IL2, as with other cytokines which have been previously shown to impact the CNS (e.g. IL-1β), influences neural activity. Neuropsychiatric manifestations of IL2 immunotherapy ranged from minor agitation requiring minimal supervision to severe agitation and combative behavior that necessitated the use of neuroleptic agents (32). Patients also developed a number of symptoms over the course of IL2 immunotherapy including delusions, malaise, fatigue, confusion and a general depressed level of consciousness (32,66). These adverse effects of IL2 must be delicately balanced with the positive outcome of IL2 antitumor immune response. Initial

onset of psychiatric problems most commonly appeared at the end of each treatment phase, particularly on the last day of IL2 administration (32). These observations suggest that cumulative and escalating exposure to IL2 becomes deleterious to the CNS through an increasingly more disruptive effect of IL2 on the BBB. Furthermore, IL2's association with models of other neurological disorders underscores the negative aspects of IL2 action on the CNS. Understanding the mechanistic basis for development of increased brain microvascular permeability and neurological toxicity will allow more successful treatments utilizing IL2 while reducing deleterious side effects.

Formulation of Working Hypothesis and Experimental Strategy

While much work has been undertaken to identify the role of immune cell signaling in the induction of vascular permeability, surprisingly little has been learned about the molecular underpinnings of IL2-induced signaling in BMECs that are an integral part of the neurovascular unit comprising the BBB. The lack of knowledge regarding IL2-induced dysregulation of brain microvasculature motivated me to study the mechanism of IL2 action in BMECs. It is well known that there are important phenotypic differences in endothelium throughout the vascular tree encompassing major organs such as the brain, lungs, liver and spleen. These organs are all impacted by Vascular Leak Syndrome, a complication of cancer immunotherapy with IL2. Therefore, my hypothesis is focused on BMECs as the main target of IL2 action in the brain. I posited that BMECs would respond to IL2 through its cognate receptor previously not identified in these cells. I hypothesized further that binding of IL2 to its putative receptor complex would

evoke signaling pathways that are mediated by transcription factor NFκB akin to those noted in immune cells e.g. lymphocytes. I also hypothesized that IL2 would induce increased permeability in BMECs monolayers. Thus, in an effort to further our understanding of the mechanism of disease evoked by IL2, my thesis studies endeavored to provide new insight into the initiation and development of brain microvascular permeability induced by IL2 in order to allow development of novel treatments for patients suffering from these effects.

IL2 therapy induces expression of inflammatory cytokines and chemokines in a similar pattern to those elicited following challenge with bacterial endotoxin and termed a "cytokine storm" (45). The vast majority of these proinflammatory mediators are controlled by the transcription factor NFκB (67) further strengthening my hypothesis to focus on the NFκB pathway in BMECs. Thus, my first aim was to demonstrate that IL2 stimulation of BMECs through the newly identified IL2 receptor complex would lead to activation of the NFκB pathway resulting in the expression of proinflammatory cytokines and chemokines. In an effort to document NFκB activation I took a three-pronged approach documenting degradation of IκBα, increased presence of phosphorylated NFκB in nuclear extracts from IL2 stimulated BMECs and by utilizing immunofluorescence to visualize an increase in nuclear NFκB. I further verified activation of NFκB by measuring the expression of proinflammatory mediators IL6 and MCP1.

IL2 therapy also leads to the induction of VLS characterized by increased systemic organ edema and weight gain seen in patients receiving this form of cancer immunotherapy (64). Endothelial dysfunction following IL2 stimulation disrupts endothelial interactions and integrity. Adherens junctions along with tight junctions are part of the unique network of complex protein interactions responsible for forming the endothelial blood-tissue barrier (25). Hence, my second aim was to document changes seen in brain microvascular endothelial monolayer permeability as

well as unraveling the underlying mechanism for increased permeability. I evaluated IL2-induced permeability of the BMEC monolayer in Transwell chambers. The mechanism of increased BMEC monolayer permeability was investigated by monitoring the changes in adherens junction components, namely VE-cadherin, p120-catenin and β-catenin, using co-immunoprecipitation as well as immunofluorescence. Further mechanistic documentation was performed by monitoring the phosphorylation state of adherens junction proteins as well as expression levels of phosphatases associated with adherens junctions.

Importantly, the microvascular effects of IL2 also play a role in the development of Multiple Sclerosis and other chronic neurological disorders. The potential mechanism of IL2-induced disruption of brain microcirculation has not been previously determined in these conditions. Here we report that IL2 is able to directly signal through the intermediate affinity IL2 receptor complex expressed on BMECs. Furthermore, signaling through this receptor complex leads to activation of the transcription factor NFκB resulting in the perpetuation of an inflammatory environment characterized by increased expression of pleotropic cytokine IL6 and chemokine MCP1. NFκB activation was documented in BMECs following IL2 stimulation and in accordance with my hypothesis, activated BMECs led to expression of NFκB dependent proinflammatory mediators in a concentration dependent manner. Based on this analysis, a novel IL2 signaling pathway activating NFκB and resulting in activation of BMECs is described. Concurrently, activation of BMECs ultimately results in increased permeability across BMEC monolayers through disruption of the adherens junction protein complex. Increased post-translational modification of VE-cadherin, in particular phosphorylation, leads to destabilization of the adherens junction and formation of intercellular gaps. Loss of tightly organized brain microvascular endothelial junctions potentiates an increase in vascular permeability. These

studies provide a novel and comprehensive account of IL2 action on BMECs and provide a mechanism to explain increased brain edema experienced by patients receiving IL2 cancer immunotherapy.

Chapter II

ANALYSIS OF ENDOTHELIAL ACTIVATION BY IL2

Wylezinski L.S. and Hawiger J., Interleukin 2 Activates Brain Microvascular Endothelial Cells Resulting in Destabilization of Adherens Junctions. *Journal of Biological Chemistry*, 2016. **291,** 22913-22923.

Synopsis

Perturbation of the endothelium results in deleterious effects on organs and their function. Upon disruption, biologically diverse molecules are able to flow into the surrounding tissue accompanied by activated immune cells thereby impacting organ homeostasis. The brain is no exception as the delicate milieu of the CNS is particularly sensitive to environmental change. Dysregulation of brain microvascular endothelial cells, tasked with formation of the BBB, is known to result in or potentiate a number of central nervous system maladies. Here we report that IL2, a well-known and important cytokine in immunobiology, is able to activate brain microvascular endothelial cells leading to the induction of NFκB. IL2 is able to signal through the intermediate affinity IL2 receptor complex located on the endothelial cell surface resulting in activation of the NFκB signaling pathway. NFκB activation has been shown to induce the production of a number of proinflammatory cytokines/chemokines as well as cell surface adhesion molecules that further exacerbate injury by increasing immune cell response. Based on our results, IL2 is able to initiate endothelial dysregulation and potentiate a proinflammatory environment.

Introduction

The development of systemic vascular leak syndrome by patients undergoing IL2 cancer immunotherapy underlines the effect of IL2 on the vascular endothelium. Cognizant of the fact that IL2 is involved in the development of both vascular leak syndrome as well as neurotoxicity we were interested in deciphering the impact of IL2 on brain microvascular endothelial cells. To our knowledge no previous work has been done to identify the mechanism of IL2 induced activation of BMECs. Understanding the process of activation of BMECs by IL2 would provide better insight into the development of brain edema. We utilized both human and murine brain microvascular endothelial cell monolayers to replicate a cardinal feature of the BBB. The known link between IL2 and NFκB in immune cells as well as the proinflammatory role NFκB plays in endothelial cells led us to investigate this axis in BMECs. We hypothesized that binding of IL2 to its receptor complex would evoke signaling pathways that are mediated by transcription factor NFκB akin to those noted in immune cells e.g. lymphocytes. We further hypothesized that NFκB would potentiate a proinflammatory environment and ultimately lead to increased microvascular permeability.

Results

In order to validate the phenotypic features of the BMEC lines used in this study, we documented expression of two well-known endothelial markers. Platelet cell adhesion molecule

1 (PECAM1), a member of the immunoglobulin gene superfamily that concentrates at intercellular junctions (68). Additionally, von Willebrand factor (vWF) is a multimeric plasma glycoprotein constitutively expressed by endothelial cells (69). Utilizing real time PCR (Table 1; Table 2), I was able to show that constitutive expression of both PECAM1 and vWF are significantly displayed in human and murine BMECs compared to control cell types, human embryonic kidney cells (HEKs) and murine embryonic fibroblasts (MEFs) (Fig. 10). These results verify the phenotypic features of brain microvascular endothelial cells thereby allowing us to use them for experimental modeling of the endothelial interactions at the BBB.

Table 1

Human oligonucleotide PCR primer sequences
h = Human

Gene		Primer sequences (5' to 3')
hvWF	Forward	5-TGCTGACACCAGAAAAGTGC-3
	Reverse	5-AGTCCCCAATGGACTCACAG-3
hPECAM1	Forward	5-GATAATTGCCATTCCCATGC-3
	Reverse	5-GGGTTTGCCCTCTTTTTCTC-3
hIL2a	Forward	5-ATCAGTGCGTCCAGGGATAC-3
	Reverse	5-GTGACGAGGCAGGAAGTCTC-3
hIL2b	Forward	5-GCTGATCAACTGCAGGAACA-3
	Reverse	5-TGTCCCTCTCCAGCACTTCT-3
hIL2g	Forward	5-CCACTCTGTGGAAGTGCTCA-3
	Reverse	5-AGGTTCTTCAGGGTGGGAAT-3

Table 1. Human Oligonucleotide Primer Sequences

Table 2

Murine oligonucleotide PCR primer sequences
m= Murine

Gene		Primer sequences (5' to 3')
mvWF	Forward	5-TTCATCCGGGACTTTGAGAC-3
	Reverse	5-AGCCTTGGCAAAACTCTTCA-3
mPECAM1	Forward	5-ATGACCCAGCAACATTCACA-3
	Reverse	5-CACAGAGCACCGAAGTACCA-3
mIL2a	Forward	5-TACAAGAACGGCACCATCCTAA-3
	Reverse	5-TTGCTGCTCCAGGAGTTTCC-3
mIL2b	Forward	5-GGCTCTTCTTGGAGATGCTG-3
	Reverse	5-GCCAGAAAAACAACCAAGGA-3
mIL2g	Forward	5-CTGGGGGAGTCATACTGTAGAGG-3
	Reverse	5-AGGCTTCCGGCTTCAGAGAAT-3

Table 2. Oligonucleotide Primer Sequences

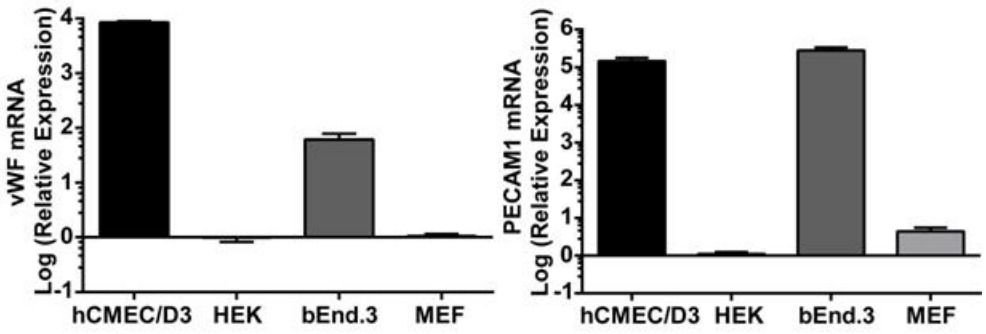

Figure 10. Expression of Endothelial Cell Markers vWF, PECAM1

Constitutive transcript levels of endothelial cell markers vWF and PECAM1 were assessed by qPCR. Following normalization to GAPDH, mRNA levels are presented as increased-fold change from species-specific non-endothelial cells: HEK 293 cells and MEFs.

Interleukin 2 Receptor Complex

We embarked on identification of IL2 receptors on BMECs as a prerequisite for their activation by IL2. Trimeric high affinity IL2 receptor complexes (IL2Rα, IL2Rβ and IL2Rγ) were initially documented to activate the NFκB signaling pathway in lymphocytes (53). Ensuing work has reported that other cell types, including lung endothelial cells, are able to respond to IL2 stimulation through the intermediate affinity dimeric IL2 receptor complex (IL2Rβ and IL2Rγ) (46,57). We established that both human and murine BMECs express the intermediate affinity IL2 receptor (IL2Rβγ) (Fig. 11). These cells constitutively express IL2Rβ and IL2Rγ transcripts at a significantly higher level than comparative controls comprising human and murine cells (HEKs and MEFs). Correspondingly, I showed the expression of IL2Rβ and IL2Rγ proteins by immunoblotting cellular lysates of human and murine BMECs. Significantly, expression of IL2Rα, the high affinity subunit, was only observed after prolonged stimulation of endothelial cells with IL2 (Fig. 11). These results are in agreement with previous work documenting IL2-induced expression of the IL2Rα subunit following NFκB activation in murine lymphocytes (70). Consistent with these results, a κB regulatory element binding site within the promoter region of IL2Rα is conserved between humans and murine genes (70). Thus, I established the existence of a constitutively expressed dimeric IL2Rβγ and an inducibly expressed trimeric IL2αβγ receptor complex on human and murine BMECs.

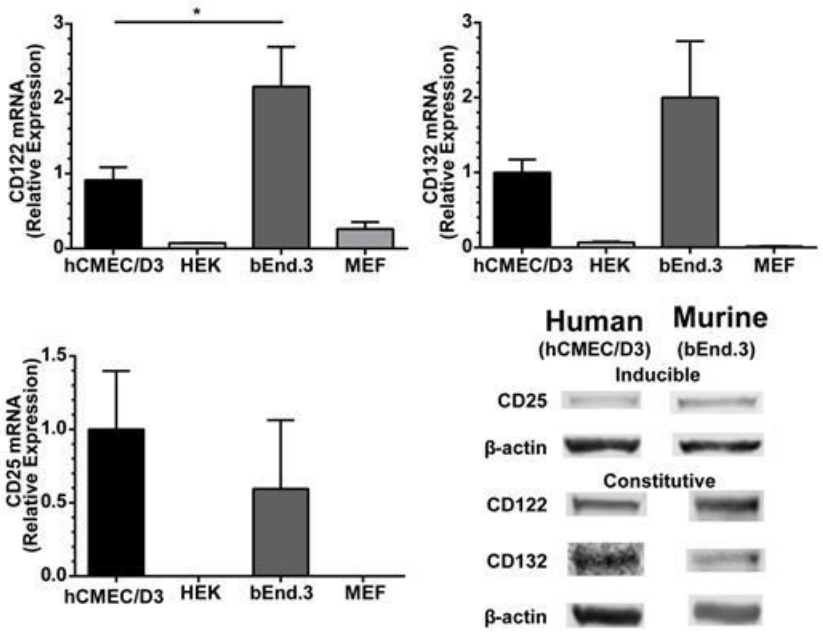

Figure 11. Expression of IL2 Receptor Complex in Human and Murine BMECs

Transcript levels of IL2R subunits were determined by qPCR, and protein expression was documented by immunoblotting. IL2Rβ (CD122) and IL2Rγ (CD132) were constitutively expressed in both human and murine BMECs. Transcript and protein levels for IL2Rα (CD25) were only detected following 24-h stimulation with 300 kilounits/ml of species-specific IL2. The level of mRNA transcript is presented as relative expression comparing human and murine BMECs. *Error bars* represent mean ±S.E. of three independent experiments performed in triplicates. Statistical significance was determined by Student's *t* test (*, $p < 0.05$).

IL2 Induces Degradation of IκBα, an Inhibitor that Sequesters NFκB in the Cytoplasm of BMECs

In an effort to demonstrate that the intermediate affinity dimeric IL2 receptor complex was competent and able to transduce NFκB activation in BMECs, we employed a three pronged approach. NFκB sequestration in the cytosol is controlled by interaction with IκBα. That restricts NFκB from interacting with the nuclear import machinery by concealing the nuclear localization signal (NLS), thereby preventing NFκB translocation to the nucleus. Dissociation of IκBα from NFκB occurs following phosphorylation of IκBα at Ser-32 and Ser-36 (71,72). Subsequent polyubiquitination of IκBα leads to degradation by the proteasome that allows NFκB nuclear translocation.

Our first approach documented the degradation of IκBα in IL2-stimulated human and murine BMECs and was comparable to the results evoked by a known endothelial agonist, lipopolysaccharide (LPS). Due to the very rapid turnover kinetics of IκBα (73), we included the protein synthesis inhibitor cycloheximide to prevent re-accumulation of newly synthesized IκBα. Constitutive turnover was measured following addition of cycloheximide and compared with degradation in BMECs stimulated with agonist. Stimulation with IL2 caused time-dependent degradation of IκBα with a loss of 30-70% of its basal level, mimicking IκBα degradation following activation with LPS (Fig. 12). Degradation and release of NFκB is the first step in translocation to the nucleus and activation. We show that IL2 stimulation can directly lead to IκBα degradation suggesting that NFκB can be translocated to the nucleus in BMECs.

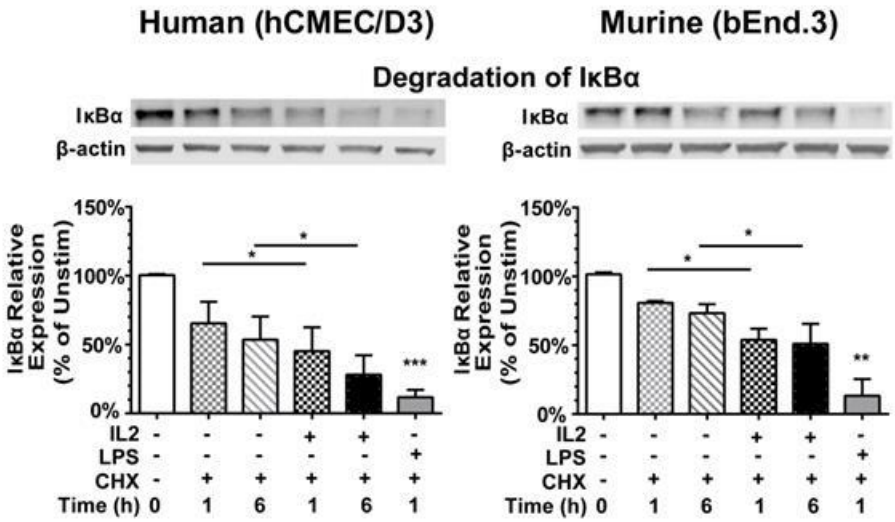

Figure 12. IL2 Activates the NFκB Pathway in Human and Murine BMECs

Degradation of IκBα in BMECs. Human (hCMEC/D3) and murine (bEnd.3) BMECs were left unstimulated (*Unstim*) (*0*) or stimulated with 300 kilounits/ml of species-specific IL2 or 1μg/ml LPS, a positive control, for the indicated times after pretreatment for 30 min with the protein synthesis inhibitor cycloheximide (*CHX*) (10 μg/ml) to block *de novo* protein synthesis. Cytosolic extracts were isolated, separated by SDS-PAGE, and immunoblotted for the degradation of IκBα. Protein levels were quantified by immunoblotting, and values at each time point were normalized to the β-actin loading control. *Error bars* represent mean ±S.D. of at least four independent experiments. Statistical significance was determined using an unpaired *t* test with Welch's correction (*, $p < 0.05$; **, $p < 0.005$; ***, $p < 0.0005$).

IL2-Induced Phosphorylation of NFκB p65 (RelA) and Nuclear Localization

Following degradation of IκBα, the NFκB p65/RelA subunit becomes phosphorylated conferring enhanced DNA binding capacity. It is shuttled to the nucleus through nuclear transport adaptors, importins/karyopherins alpha, that recognize the unmasked NLS. By isolating nuclear lysates from human and murine BMECs stimulated with or without IL2 we were able to demonstrate an increase in the proportion of phosphorylated RelA as compared to non-phosphorylated RelA implying activation of this transcription factor (Fig. 13). Both human and murine BMECs showed a time-dependent response to IL2, resulting in a 50% increase in Tyr-536 phosphorylation of NFκB RelA following agonist stimulation. Nuclear localization of NFκB was verified by immunofluorescence microscopy (Fig. 14). Indeed, as compared to unstimulated control, we noted elevated levels of nuclear NFκB in BMECs stimulated with IL2 or comparative control TNFα, which is a known inducer and activator of the NFκB pathway. Nuclear translocation of phosphorylated NFκB leads to the transcription of a number of target genes, including proinflammatory cytokines and chemokines.

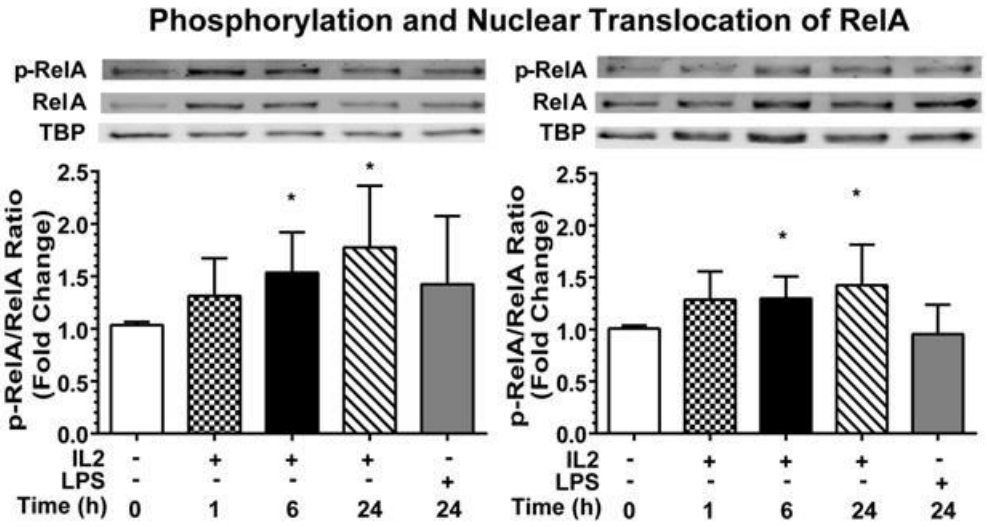

Figure 13. IL2-Induced Nuclear Translocation and Phosphorylation of NFκB

Translocation and phosphorylation of NFκb to the nucleus. Human and murine BMECs were stimulated with 300 kilounits/ml of species-specific IL2 or 1 μg/ml LPS for the indicated times, and nuclear extracts were isolated, separated by SDS-PAGE and immunoblotted for the presence of total NFκB and Tyr-536 phosphorylated NFκB (*p-RelA*). TATA-binding protein (*TBP*) serves as a loading control for nuclear lysates. Quantification of signal is shown as -fold change compared with the unstimulated control. *Error bars* represent mean ±S.D. of at least four independent experiments. Statistical significance was determined using an unpaired *t* test with Welch's correction (*, $p < 0.05$).

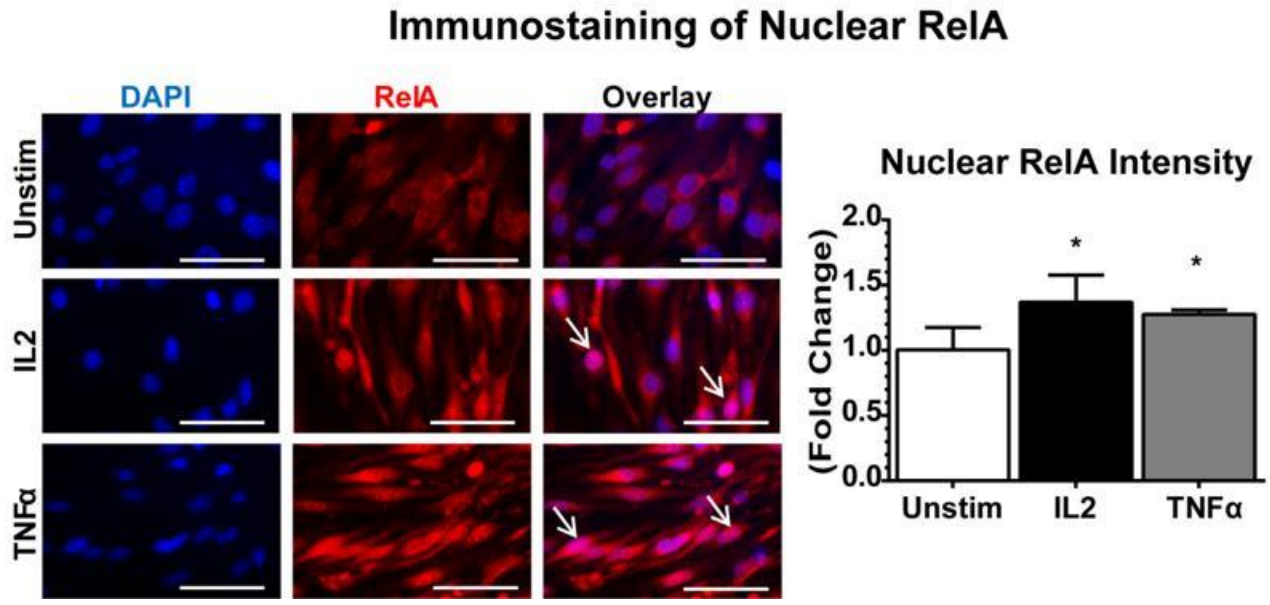

Figure 14. Detection of NFκB in the Nucleus by Immunofluorescence

Murine (bEnd.3) BMECs were analyzed following 24-h stimulation with 300 kilounits/ml of murine IL2 or 30 ng/ml murine TNFα. Cells were immunostained with anti-RelA antibodies (*red*), and nuclei were counterstained with DAPI (*blue*). *Arrows* indicate strong nuclear staining of RelA. Images are representative of three independent experiments. Quantification was determined using MetaMorph imaging software. Statistical significance was determined using an unpaired *t* test with Welch's correction (*, $p < 0.05$). *Magnification*, x63. *Scale bars*, 5 µm. *Error bars* represent mean ±S.D.

IL2-Induced Expression of Proinflammatory Cytokine and Chemokine

Productive transcription and translation of NFκB target genes were confirmed by measuring endothelial expression of cytokine interleukin 6 (IL6) and chemokine macrophage chemoattractant protein 1 (MCP1) upon IL2 stimulation. These two mediators of inflammation have been previously implicated in the activation and loss of barrier function in other endothelial barrier models (74-77). Both IL6 and MCP1 were elicited by IL2 in a concentration-dependent manner in human and murine BMECs (Fig. 15). Thus, IL2 signaling through the intermediate affinity receptor located on BMECs led to degradation of IκBα, nuclear translocation of NFκB p65 (RelA) and ultimately, to transcription of two NFκB-regulated genes, IL6 and MCP1.

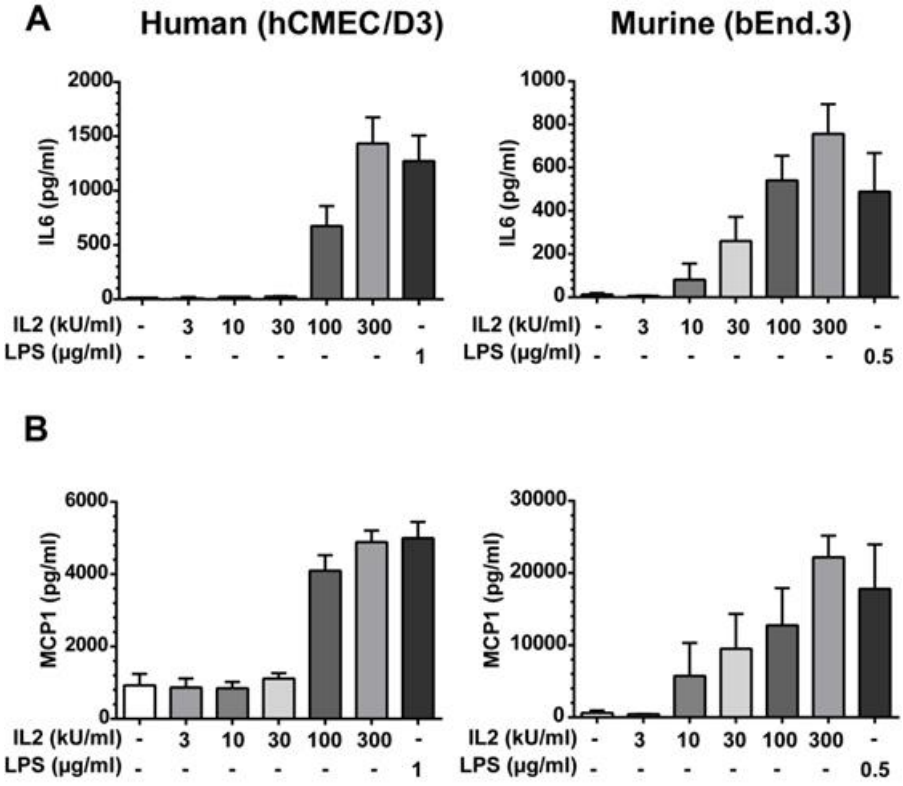

Figure 15. IL2-Induced Expression of Proinflammatory IL6 and MCP1 in Human and Murine BMECs

IL6 (*A*) and MCP1 (*B*) are expressed by activated BMECs in a dose-dependent manner. Protein levels of IL6 and MCP1 in culture media were measured 24 h after stimulation of hCMEC/D3 and bEnd.3 cells with increasing concentrations of species-specific IL2 as indicated (kilounits (*kU*)) or 1µg/ml LPS in hCMEC/D3 cells and 0.5µg/ml LPS in bEnd.3 cells. *Error bars* represent mean ±S.D. from three independent experiments performed in duplicate or triplicate.

Chapter III

INTERLEUKIN 2-INDUCED DISRUPTION OF ADHERENS JUNCTIONS

Synopsis

Harnessing the power of IL2 to stimulate the immune system to treat renal cell carcinoma and malignant melanoma has proven to be successful. However, these beneficial effects of IL2 are curtailed by the development of multi-organ edema including brain edema, a prominent manifestation of vascular leak syndrome. Some patients receiving IL2 immunotherapy begin experiencing these symptoms within a couple of days of initiation of treatment and a reversal of these side effects is seen upon cessation of therapy indicating its direct role in this serious complication. Moreover, IL2 has been documented to play a significant role in a number of chronic neurological autoimmune diseases, including Multiple Sclerosis, Neuromyelitis Optica and Neuropsychiatric Systemic Lupus Erythematosus (30,78,79). Disruption of the BBB is a critical step in the development of these neurological conditions but in many cases complete understanding of how this occurs is unknown. Gaining a better understanding of the effect of IL2 on BMECs may prove beneficial not only for patients receiving IL2 immunotherapy but also those suffering other autoimmune disease affecting the CNS. Here we report that IL2 increases BMEC monolayer permeability through the formation of intercellular gaps. IL2 induces disruption of adherens junctions responsible for maintaining the tight organization of BMECs. This occurs by increasing the phosphorylation state of VE-cadherin an important constituent of the adherens junction protein complex. The increase in phosphorylation of VE-cadherin is accompanied by concomitant loss of SHP2 phosphatase protein responsible for maintaining

adherens junction stability. Phosphorylation of VE-cadherin destabilizes the adherens junction complex and IL2 ultimately leads to dissociation of VE-cadherin, p120-catenin and β-catenin resulting in formation of intercellular gaps and increased permeability.

Introduction

The BBB is formed through the specialized properties of brain endothelial cells along with associated cell types which create a highly selective barrier protecting the CNS. While the term "barrier" implies a rigid structure, it is now known that many features of the BBB can be modulated. The maintenance of the BBB is largely vested in the cell-cell interactions which allow for exclusion of water, ions and plasma proteins from the CNS. A complex network of intercellular adhesion proteins are organized into adherens junctions (AJs) and tight junctions. They form the "physical barrier" limiting paracellular diffusion between adjoining endothelial cells. These junctions are intermingled in endothelial cells, whereas in epithelial cells, adherens and tight junctions are strictly separated from each other. (17). Adherens junctions are ubiquitously expressed in the vascular tree (80) and are of particular importance in microvascular circulation, which provides the largest surface area of exchange between blood and tissue (7). Furthermore, post-capillary venules comprise the main endothelial surface for blood-tissue exchange and have shown to be particularly vulnerable to opening by inflammatory mediators (17). Formation of AJs is dependent on the homotypic interaction of cell surface transmembrane proteins termed cadherins whose cytoplasmic tails associate with intracellular binding partners termed catenins. Destabilization of this interaction leads to dissociation of the complex and

internalization of VE-cadherin disrupting the barrier function of these proteins (81-83). IL2 administered during cancer immunotherapy causes vascular leak syndrome, manifested by a raise in brain water content that is attributed to increased permeability of the brain microvascular endothelium (84). Therefore, we hypothesize that IL2 is able to induce increased permeability of the BMEC monolayer through the disruption of the adherens junction protein complex leading to a loss of barrier function.

Results

IL2-Induced Increase in the Permeability of Human Microvascular Endothelial Cell Monolayers

Endothelial dysfunction following IL2 stimulation was measured by monitoring the passage of fluorescein labeled molecules as they pass across the endothelial monolayer. Fluoroscein isothiocyanate (FITC) conjugated dextran (FITC-dextran, 10kDa) was added to the upper chambers of Transwell chambers following stimulation with IL2 or with another known inducer of permeability, TNFα. Lower chamber supernatants were then sampled at multiple time points. IL2 induced a significant increase in the movement of FITC-dextran across the IL2-stimulated human BMEC monolayer compared with the non-stimulated control, indicating a gradual loss of endothelial barrier function and increased permeability (Fig. 16). As IL2-induced permeability can potentially be enhanced by other cytokines, namely IL6 and/or MCP1 both concurrently induced in BMECs, we utilized species-specific neutralizing antibodies against IL6 and MCP1. Neutralizing these two potential permeability agonists did not significantly alter an

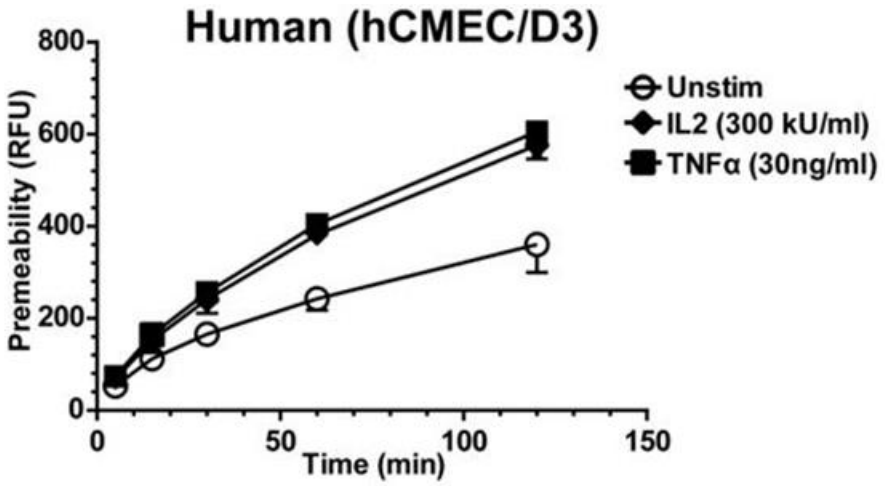

Figure 16. IL2-Induced Permeability of Human BMEC Monolayer

Human (hCMEC/D3) cells were grown to confluence on Transwell inserts and left unstimulated (*Unstim*) or stimulated with 300 kilounits (*kU*)/ml of human IL2 or 30 ng/ml human TNFα for 24 h as indicated. Shown are representative permeability tracings. To assess permeability, 10-kDa FITC-dextran was added to the top chamber of each insert, and fluorescence in the lower chamber was measured at the indicated times.

IL2-induced increase in permeability, although a trend toward lower permeability was observed. In contrast, IL2-induced permeability enhancement was countered in human BMECs by species-specific IL2Rβ-neutralizing antibody (Fig. 17). These significant results indicate that the IL2-induced increase in endothelial monolayer permeability is solely due to its signaling via the IL2 receptor. Consistent with these findings in human cells, we also documented increased BMEC monolayer permeability following IL2 stimulation in murine cells (Fig. 18). No significant decrease in permeability was noted following treatment with species-specific IL6 or MCP1 neutralizing antibodies in murine BMECs either (Fig. 19). An IL2Rβ antibody neutralizing experiment could not be performed in murine cells due to a lack of species-specific antibody against murine IL2Rβ. Murine bEnd.3 cells demonstrated greater change in endothelial permeability as compared to human hCMEC/D3 cells most likely due to constitutively higher expression of IL2Rβ as documented in Figure 11.

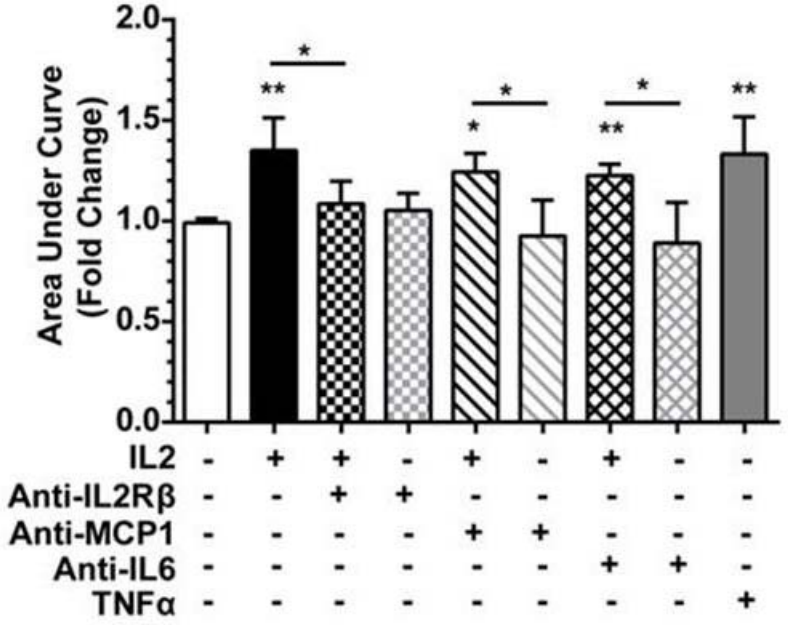

Figure 17. Human BMEC Monolayer Permeability following Cytokine and Chemokine Neutralizing Antibody Treatment

Human (hCMEC/D3) cells were grown to confluence on Transwell inserts and left unstimulated (*Unstim*) or stimulated with 300 kilounits (*kU*)/ml of human IL2 or 30 ng/ml human TNFα for 24 h as indicated. Concurrent with stimulation, a portion of the Transwell inserts were treated with species-specific neutralizing antibodies against IL6 and MCP1 as indicated. Shown are quantitative representation of all permeability tracings recorded at 120 min. To assess permeability, 10-kDa FITC-dextran was added to the top chamber of each insert, and fluorescence in the lower chamber was measured at the indicated times. *Error bars* represent mean ±S.D. of -fold change relative to the unstimulated control from five independent experiments performed in at least duplicate; *p* values shown were determined by an unpaired *t* test with Welch's correction of the area under the curves from each individual experiment (*, $p < 0.05$; **, $p < 0.005$).

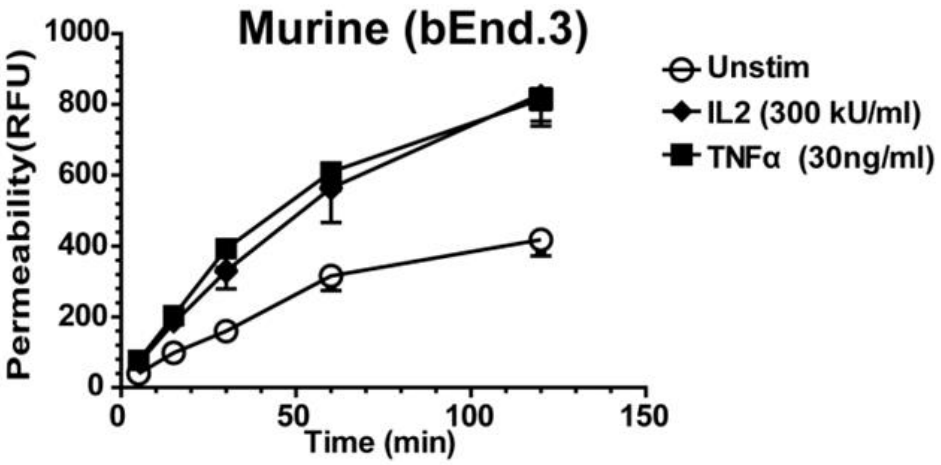

Figure 18. IL2-Induced Permeability of Murine BMCEC Monolayer

Murine (bEnd.3) cells were grown to confluence on Transwell inserts and left unstimulated (*Unstim*) or stimulated with 300 kilounits (*kU*)/ml of murine IL2 or 30 ng/ml murine TNFα for 24 h as indicated. Shown are representative permeability tracings. To assess permeability, 10-kDa FITC-dextran was added to the top chamber of each insert, and fluorescence in the lower chamber was measured at the indicated times.

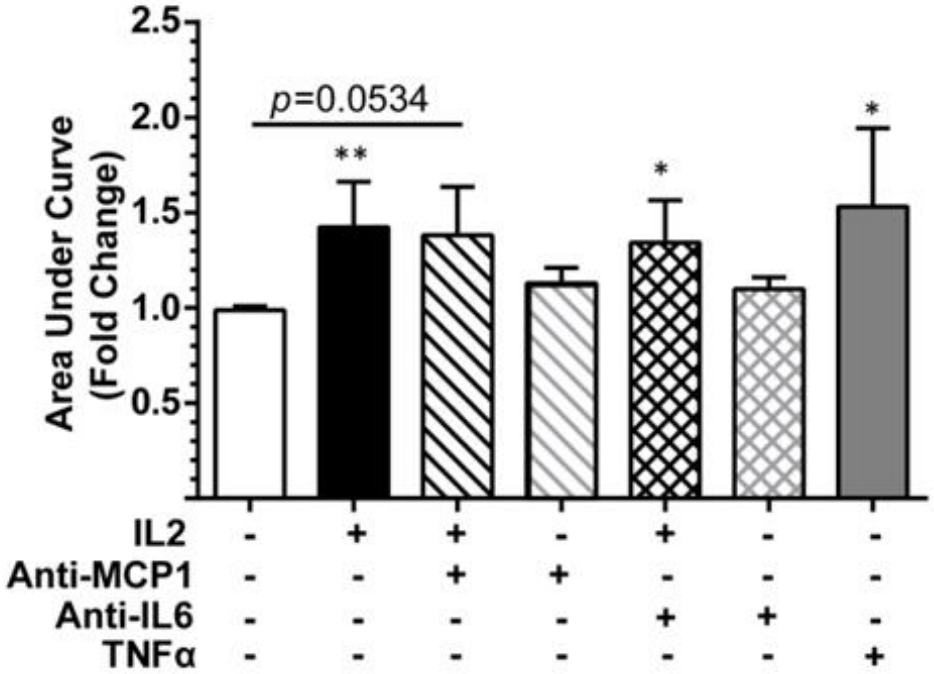

Figure 19. Murine BMEC Monolayer Permeability following Cytokine and Chemokine Neutralizing Antibody Treatment

Murine (bEnd.3) cells were grown to confluence on Transwell inserts and left unstimulated (*Unstim*) or stimulated for 24 h with 300 kilounits (*kU*)/ml of murine IL2 or 30 ng/ml murine TNFα as indicated. Concurrent with stimulation, a portion of the Transwell inserts were treated with species-specific neutralizing antibodies against IL6 and MCP1 as indicated. Shown are quantitative representation of all permeability tracings recorded at 120 min. To assess permeability, 10-kDa FITC-dextran was added to the top chamber of each insert, and fluorescence in the lower chamber was measured at the indicated times. *Error bars* represent mean ±S.D. of -fold change relative to the unstimulated control from at least three independent experiments performed in at least duplicate; *p* values shown were determined by unpaired *t* test with Welch's correction of the area under the curves from each individual experiment (*, $p < 0.05$; **, $p < 0.005$).

IL2-Induced Disruption of Adherens Junctions

To gain a better understanding of the mechanism of increased permeability we initiated experiments identifying changes associated with BMEC adherens junctions. Thus, we analyzed IL2's impact on the adherens junction protein complex by immunofluorescence after completion of the permeability analysis. VE-cadherin and p120-catenin, the main constituents of AJs, were labeled and the complex visualized by immunofluorescence microscopy. In quiescent human BMECs, immunostained VE-cadherin and p120 displayed a well-defined, contiguous border between adjoining endothelial cells. This border was strikingly lost after treatment with IL2 or TNFα, a comparative positive control (Fig. 20). Membrane-associated VE-cadherin•p120 complexes were disrupted with a concomitant reduction of these proteins along the periphery of the cells. These immunofluorescence images correlated with immunostaining of murine BMECs which showed a similar outcome with a significant loss of VE-cadherin•p120 complexes at the cellular border (Fig. 21). These results establish that the adherens junction is negatively impacted by IL2 stimulation and may be the key to increased BMEC microvascular permeability.

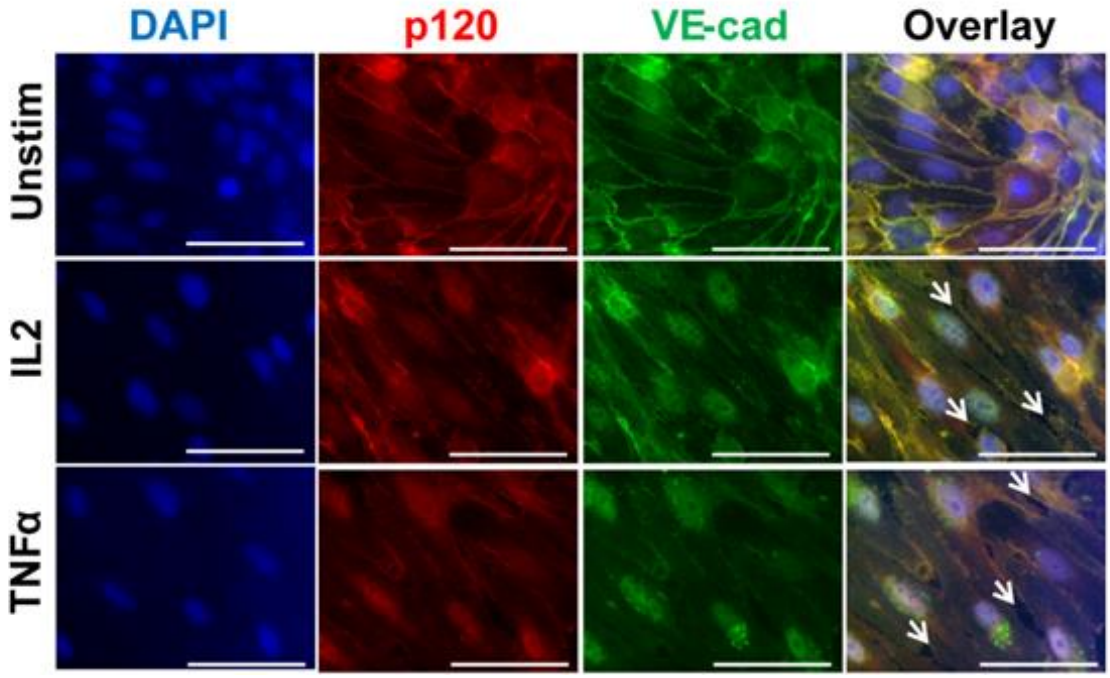

Figure 20. Loss of Cell Border Adherens Junctions in Human BMECs

Adherens junctions were observed by immunofluorescence of VE-cadherin (*VE-cad*) and p120 following agonist stimulation. hCMEC/D3 cells were grown to confluence and then left unstimulated or stimulated with 300 kilounits/ml of human IL2 or 30 ng/ml human TNFα for 24 h. Cells were immunostained with anti-p120 antibodies (*red*) and anti-VE-cadherin antibodies (*green*). Nuclei were counterstained with DAPI (*blue*). *Arrows* indicate openings between neighboring cells and disruption of both proteins at the cell membrane in agonist-stimulated human BMECs. *Magnification*, x63. *Scale bars*, 5 μm

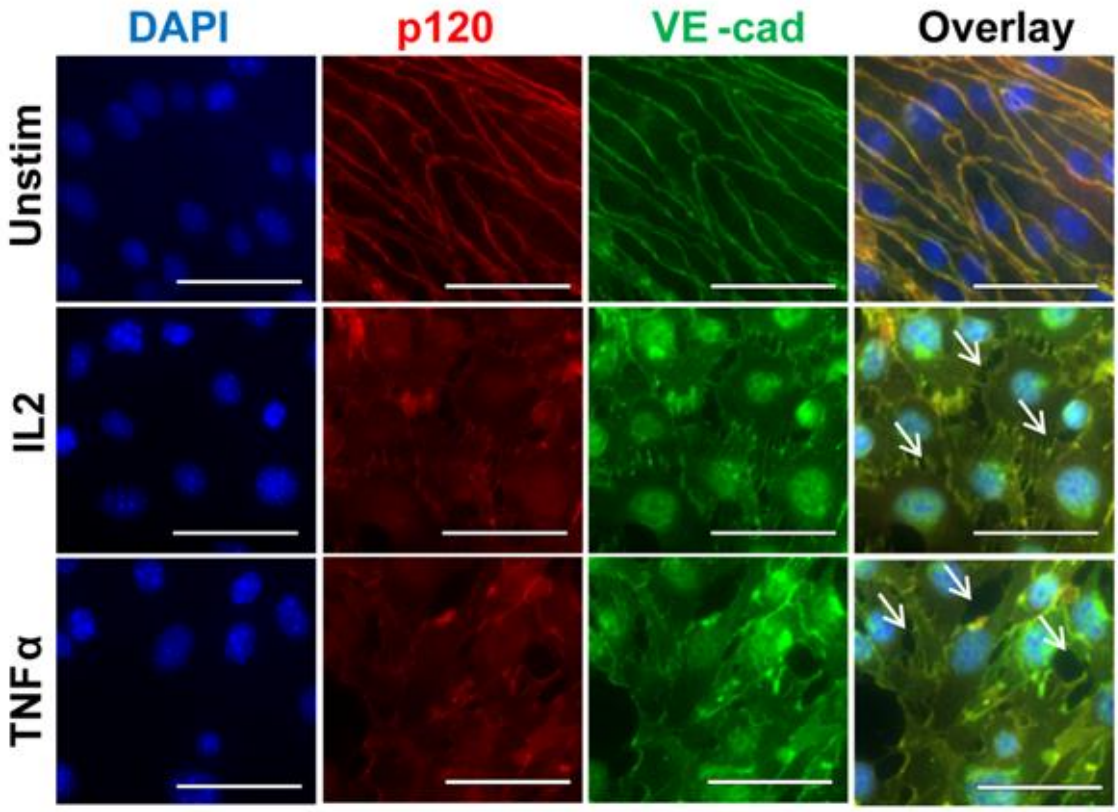

Figure 21. Loss of Cell Border Adherens Junctions of Murine BMECs

Adherens junctions were observed by immunofluorescence of VE-cadherin (*VE-cad*) and p120 following agonist stimulation. bEnd.3 cells were grown to confluence and then left unstimulated or stimulated with 300 kilounits/ml of murine IL2 or 30 ng/ml murine TNFα for 24 h. Cells were immunostained with anti-p120 antibodies (*red*) and anti-VE-cadherin antibodies (*green*). Nuclei were counterstained with DAPI (*blue*). *Arrows* indicate openings between neighboring cells and disruption of both proteins at the cell membrane in agonist-stimulated murine BMECs. *Magnification*, x63. *Scale bars*, 5 μm

Disruption of Adherens Junctions in Brain Microvascular Endothelial Cells Parallels their Activation

We verified that endothelial activation corresponded to the time course of increased permeability in human and murine BMECs by analyzing cytokine and chemokine expression in supernatant from the upper Transwell chamber prior to addition of FITC-dextran. In agreement with our prior analysis in a different culture system, we documented significantly higher levels of IL6 and MCP1 following IL2 stimulation compared with unstimulated controls (Fig. 22). However, within the time frame of our antibody-neutralizing permeability experiments, these two proinflammatory agonists evoked by IL2 did not significantly contribute to its effect on microvascular permeability. These results suggest that IL2 is concomitantly potentiating a proinflammatory environment through expression of IL6 and MCP1 while also disrupting AJs leading to increased microvascular permeability.

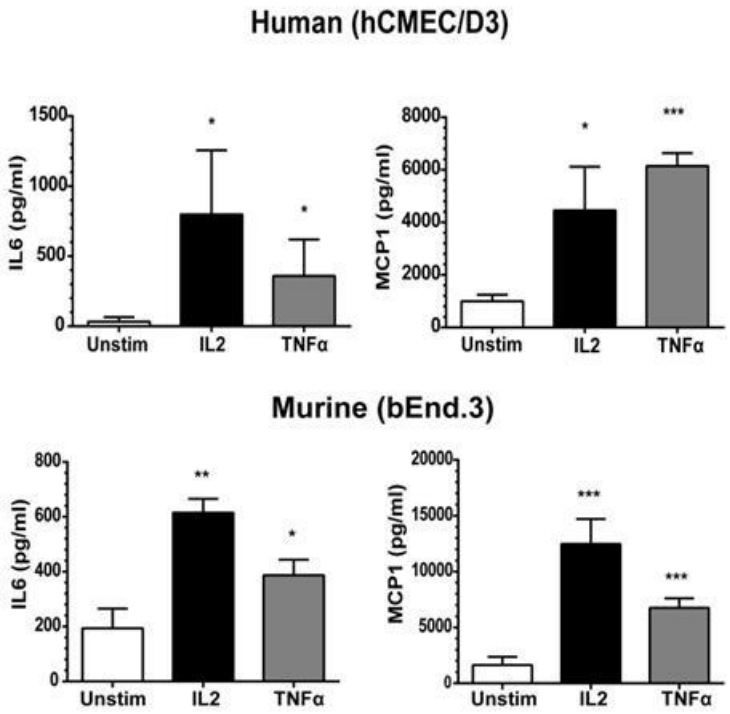

Figure 22. Agonist-Induced Expression of Cytokine IL6 and Chemokine MCP1 in Transwell Permeability Inserts

Human and murine cell activation state was assessed prior to initiation of the permeability assay utilizing identical cells for multiple analyses. Cells were grown to confluence on Transwell inserts and left unstimulated or stimulated with 300 kilounits/ml of species-specific IL2 or 30 ng/ml species-specific TNFα for 24 h as indicated. The supernatants were collected and analyzed for cytokine/chemokine production prior to addition of FITC-dextran for permeability analysis. *Error bars* represent mean ±S.D. of at least three independent experiments performed in duplicates or triplicates. Statistical significance was determined by unpaired *t* test with Welch's correction (*, p <0.05; **, p <0.005; ***, p <0.0005).

IL2-Induced Cytoskeletal Reorganization Manifested by an Increase in F-Actin Stress Fiber Formation

In addition to a loss of peripheral VE-cadherin•p120 complexes along the cell membrane, IL2 stimulation also resulted in striking changes in cellular morphology. Modification of bordering BMEC cellular membrane organization led to the formation of apparent gaps between neighboring endothelial cells. These changes are coupled to cytoskeletal reorganizations (62,85,86). We documented an increase in F-actin fiber bundles prominently displayed in IL2-activated murine bEnd.3 cells (Fig. 23). These cells exhibited thicker and more prominent F-actin fiber bundles compared with thin F-actin fibers sparsely crossing the cell body in unstimulated controls. Activation of endothelial cells, as well as loss of adherens junctions between adjoining cells, spur their detachment and initiate "anoikis" thereby contributing to microvascular injury (41). Endothelial injury manifested by an increased number of endothelial cells in the blood is being considered as a useful marker for vascular damage in a number of human diseases as well as in animal models (87-89). Indeed, we documented IL2-induced detachment and apoptosis in both human and murine BMECs (Fig. 24).

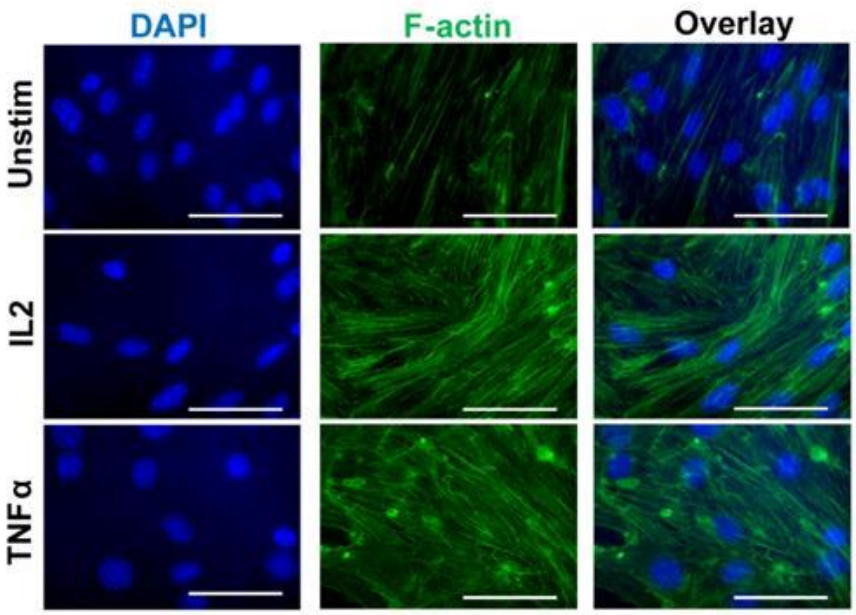

Figure 23. F-Actin Polymerization Changes in Agonist-Stimulated Murine BMECs

Murine bEnd.3 cells were grown to confluence and then left unstimulated (*Unstim*) or stimulated with 300 kilounits/ml of murine IL2 or 30 ng/ml murine TNFα for 24 h. Cells were stained with Alexa Fluor 488-labeled phalloidin (*green*) to visualize F-actin. Nuclei were counterstained with DAPI (*blue*). Images are representative of at least three independent experiments. *Magnification*, x63. *Scale bars*, 5 μm

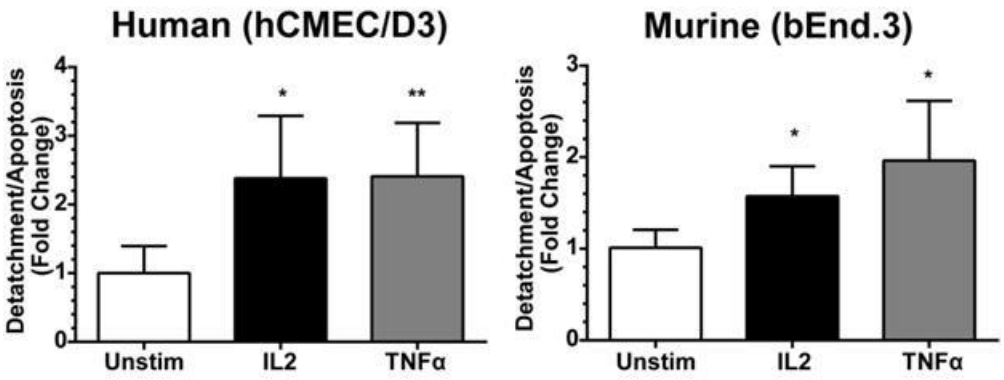

Figure 24. IL2-Induced Endothelial Cell Detachment and Apoptosis

Increased BMEC detachment and apoptosis following agonist stimulation from Transwell inserts. Both human and murine BMECs were grown to confluence on Transwell permeability inserts and then left unstimulated or stimulated with 300 kilounits/ml IL2 or 30 ng/ml of species-specific TNFα for 24 h. Supernatants were collected, and free floating endothelial cells detached from the Transwell membranes were counted. *Error bars* represent mean ±S.D. of at least three independent experiments performed in duplicates. Statistical significance was determined by unpaired *t* test with Welch's correction (*, $p < 0.05$; **, $p < 0.005$).

Analysis of Adherens Junction Protein Complex Composition

The striking disruption of the AJ protein complex following IL2 stimulation led us to analyze changes in AJ protein complex composition. In a series of co-immunoprecipitation experiments, we demonstrated that IL2-induced activation of BMECs results in a loss of interaction between VE-cadherin and p120 (Fig. 25). These results complement the findings that there was loss of co-localization of both junctional proteins following IL2 stimulation of BMECs analyzed by immunofluorescence (see Fig. 20 and 21). In addition to the two main components of the AJ complex, VE-cadherin and p120, we analyzed the interaction of β-catenin that also binds to VE-cadherin, stabilizing the complex and allowing its interaction with F-actin. Loss of both p120 and β-catenin leads to destabilization of adherens junctions and ultimately results in endocytosis of VE-cadherin (83,86,90). As documented with the VE-cadherin•p120 interaction, the VE-cadherin•β-catenin interaction was also disrupted following stimulation of both human and murine BMECs with IL2 (Fig. 26). Thus, IL2-induced dissociation of the AJ complex demonstrated by co-immunoprecipitation explains the loss of VE-cadherin•p120 immunostaining at cellular borders seen in agonist-stimulated BMECs contributing to an increase in monolayer permeability. The observed difference in the extent of measured adherens junction complex disruption by co-immunoprecipitation as compared to the more striking immunofluorescent images (compare Figures 20 and 25) can be attributed to the culturing conditions of these BMECs. The immunofluorescent images were obtained from BMECs grown on Transwell membranes while the co-immunoprecipitation results were derived from BMECs grown in tissue culture dishes. The latter comprise of a more abundant population of non-synchronized BMECs vs. monolayers grown in a smaller area on Transwell membranes. These differences may account for the variation in amplitude of junctional protein disruption observed between these two

experimental conditions. Nevertheless, these concordant results indicate IL2-induced dissociation of adherens junction protein complexes encompassing the main proteins responsible for AJs stability, VE-cadherin, p120-catenin and β-catenin.

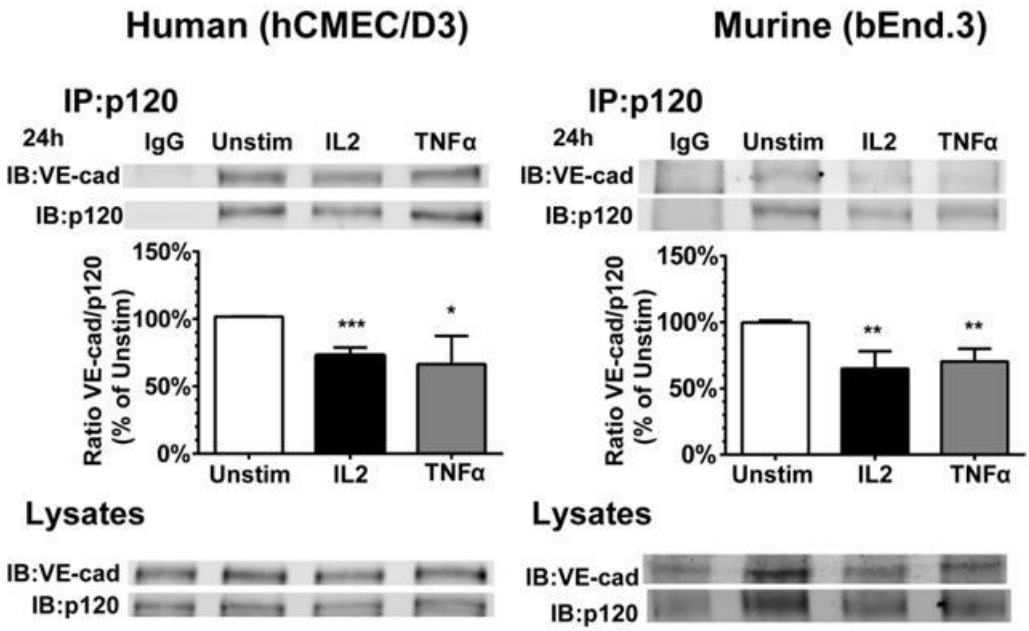

Figure 25. IL2-Induced Disruption of the p120-Catenin•VE-Cadherin Protein Complex

Analysis of the VE-cadherin•p120 complex. Human (hCMEC/D3) and murine (bEnd.3) endothelial cells were grown to confluence and left unstimulated (*Unstim*) or stimulated with 300 kilounits/ml of species-specific IL2 or 30 ng/ml species-specific TNFα for 24 h. Protein complexes in cytosolic lysates precipitated with anti-p120 (*IP*) or treated with control IgG were quantified by immunoblotting (*IB*) with protein-specific antibodies. Cell lysates serve as input controls prior to immunoprecipitation. *Error bars* represent mean ±S.D. of at least three independent experiments. Statistical significance was determined by Student's *t* test (*, $p < 0.05$; **, $p < 0.005$; ***, $p < 0.0005$).

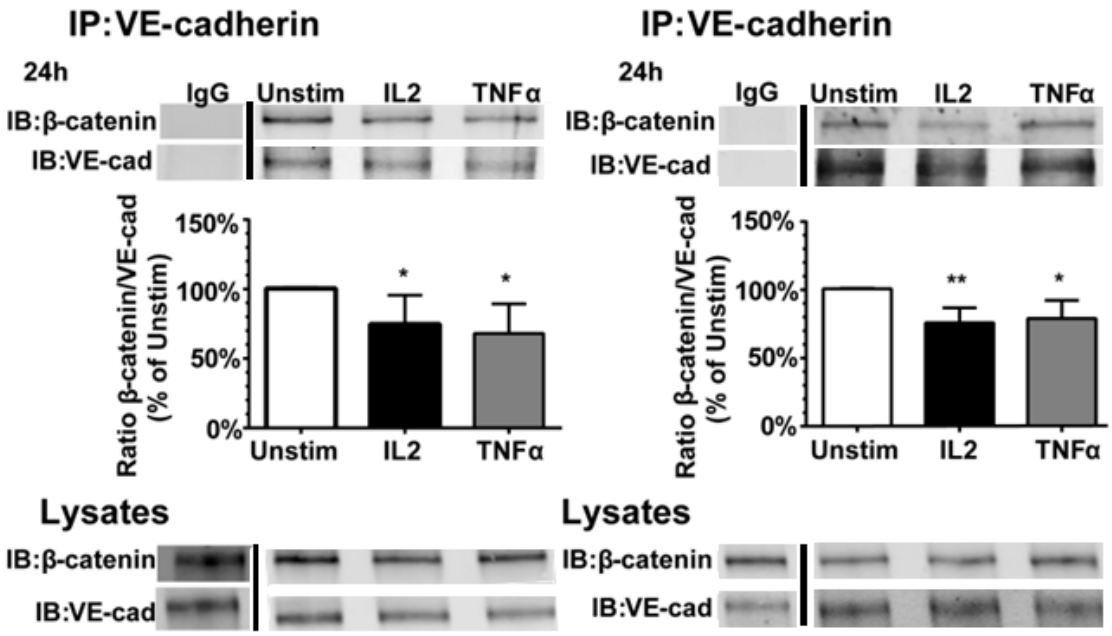

Figure 26. IL2-Induced Disruption of the β-Catenin•VE-Cadherin Protein Complex

Analysis of the VE-cadherin•β-catenin complex. Human (hCMEC/D3) and murine (bEnd.3) endothelial cells were grown to confluence and left unstimulated or stimulated with 300 kilounits/ml of species-specific IL2 or 30 ng/ml species-specific TNFα for 24 h. Protein complexes in cytosolic lysates precipitated with anti-VEcadherin (*IP*) or treated with control IgG were quantified by immunoblotting (*IB*) with protein-specific antibodies. Cell lysates serve as input controls prior to immunoprecipitation. *Error bars* represent mean ±S.D. of four independent experiments. Statistical significance was determined by Student's *t* test (*, p <0.05; **, p <0.005). *VE-cad*, VE-cadherin.

IL2-Induced Phosphorylation of VE-cadherin

To further our understanding of the dissociation of VE-cadherin and its associated adaptor proteins, in particular p120 and β-catenin, we analyzed the mechanism responsible for this process. Post-translational modifications, such as phosphorylation events, contribute to destabilization of the AJ complex and loss of endothelial barrier function in various endothelial subsets (83,91-93). We documented that IL2 evoked an increase in phosphorylation of Tyr-685 of VE-cadherin in both human and murine BMECs (Fig. 27). This process was time-dependent with maximal phosphorylation levels reached between 6 and 24 hours. Consistent with more robust activation and increased permeability recorded in murine bEnd.3 cells, we noted higher VE-cadherin phosphorylation in those cells than that of human hCMEC/D3 cells. Increased phosphorylation of VE-cadherin following stimulation of BMECs with IL2 leads to destabilization of the AJ complex. These results are consistent with findings obtained with other endothelial agonists. (26,92).

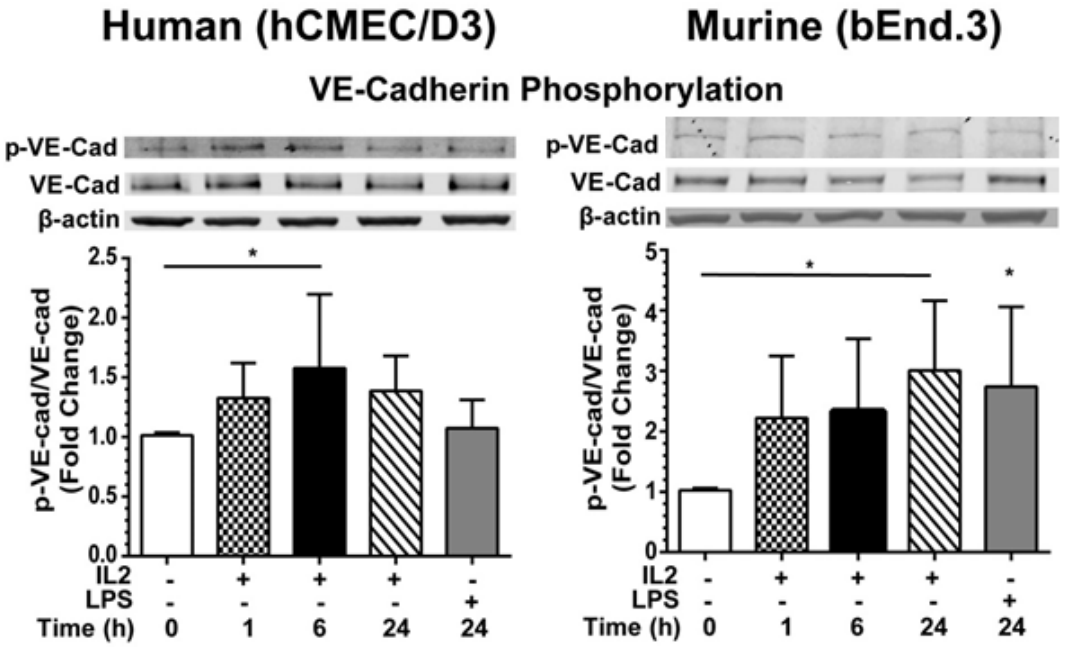

Figure 27. IL2-Induced Phosphorylation of VE-Cadherin

Analysis of VE-cadherin phosphorylation. Human (hCMEC/D3) and murine (bEnd.3) BMECs were left unstimulated or stimulated with 300 kilounits/ml of species-specific IL2 or 1 μg/ml LPS for 24 h prior to isolation of cytosolic extracts. Samples were separated by SDS-PAGE and immunoblotted for the presence of total VE-cadherin (*VE-cad*) and Tyr-685 phosphorylated VE-cadherin (*p-VE-cad*). β-Actin is a loading control for cytosolic lysates. Quantification of signal is shown as a ratio of p-VE-cadherin to total VE-cadherin as –fold change compared with unstimulated control. *Error bars* represent mean ±S.D. of seven independent experiments. Statistical significance was determined using one-way ANOVA with Bonferroni correction for multiple comparisons for IL2 and an unpaired *t* test with Welch's correction for LPS (*, $p < 0.05$).

IL2-Induced Degradation of SHP2

In an effort to identify proteins responsible for an increased VE-cadherin phosphorylation state we analyzed a number of kinases and phosphatases known to be associated with the IL2R or VE-cadherin. Src-homology domain containing phosphatase 2 (SHP2) was identified as one possible target for IL2 action. SHP2 phosphatase has been shown to counteract VE-cadherin phosphorylation, thereby contributing to the maintenance of lung microvascular endothelial barrier function (25,81,94). We found a significant decrease in expression of SHP2 phosphatase in IL2-stimulated BMECs that paralleled increased phosphorylation of VE-cadherin (Fig. 28). SHP2 protein levels were reduced by 40-50% in both human and murine BMECs following IL2 stimulation. In contrast, transcript levels of SHP2 phosphatase remained at the same level or were increased and SHP2 protein levels were not rescued following proteasomal inhibition. This result is in agreement with a published report suggesting that SHP2 is post-translationally degraded through the lysosome (25). Thus, degradative loss of SHP2 phosphatase accompanies an increase in the phosphorylation state of AJ-associated proteins and destabilization of the adherens junction complexes. This finding supports our proposed mechanism of adherens junction destabilization through increased phosphorylation of VE-cadherin and disruption of its association with adaptor proteins p120-catenin and β-catenin.

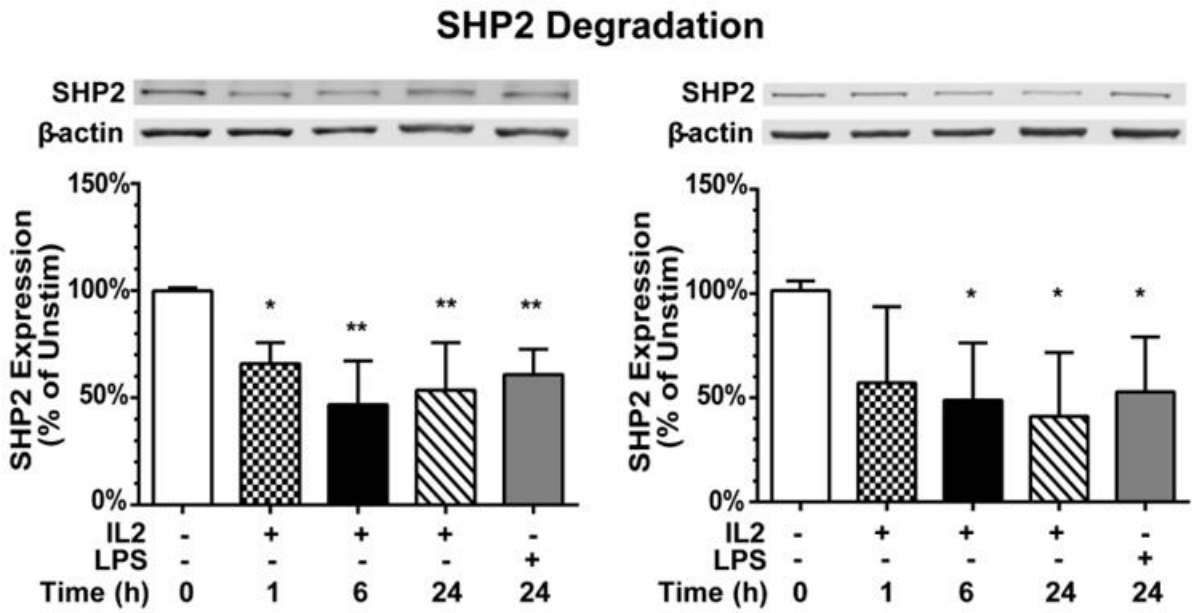

Figure 28. IL2-Induced Degradation of SHP2

Analysis of SHP2 expression. Human (hCMEC/D3) and murine (bEnd.3) BMECs were left unstimulated (*Unstim*) or stimulated with 300 kilounits/ml of species-specific IL2 or 1 μg/ml LPS for 24 h, and cytosolic extracts were isolated, separated by SDS-PAGE, and immunoblotted for the presence of SHP2. β-Actin is a loading control for cytosolic lysates. Normalized quantification of proteins is shown as a percent compared with the unstimulated control. *Error bars* represent mean ±S.D. of five independent experiments. Statistical significance was determined using one-way ANOVA with Bonferroni correction for multiple comparisons for IL2 and an unpaired *t* test with Welch's correction for LPS (*, $p < 0.05$; **, $p < 0.005$).

Chapter IV

DISCUSSION AND CONCLUSIONS

Interleukin 2 Activation of Brain Microvascular Endothelial Cells

Administration of IL2 as part of adoptive immunotherapy has been proven to be an effective cancer treatment but it is limited by serious, though infrequently lethal, systemic side effects. Importantly, many of these side effects are directly related to increased systemic capillary permeability. This endothelial dysfunction extends to the CNS where neuropsychiatric toxicity has been documented during IL2 therapy. The initial onset of neuropsychiatric symptoms appear toward the end of each treatment phase particularly on the last day and is dosage dependent (32). Furthermore, there is rapid recovery from neuropsychiatric toxicity upon cessation of treatment underscoring the specific effect of IL2. Interleukin 2 may directly affect CNS function by impacting neuronal activity. Alternatively, IL2 may indirectly affect brain function by enhancing the accumulation of behaviorally active substance or by increasing the permeability of the BBB, thereby exposing the CNS to behavior activating factors (32). While a number of suggested mechanisms of action have been proposed, the underlying mechanism of IL2-induced CNS toxicity has not been elucidated (65). Our work decodes the process through which IL2 activates BMECs and leads to loss of BMEC barrier function. As brain microvascular endothelial cells are the cardinal constituent of the "neurovascular unit" comprising the BBB, understanding the action of IL2 on these endothelial cells would be potentially beneficial for patients suffering from these side effects of IL2 immunotherapy as well as for patients suffering from autoimmune neurological disorders where IL2 plays an important role.

The ability of IL2 to sustain lymphocyte survival and function suggested that its administration could be harnessed to potentially stimulate functional lymphocytes *in vivo*. This rationale set the stage for IL2 cancer immunotherapy and spurred continued research into the properties of this molecule. Initial characterization of the IL2 receptor was undertaken in T cells and suggested the presence of an IL2 receptor complex (95). As presented above (see Figures 11-14), we established that brain microvascular endothelial cells express a competent IL2 receptor complex thereby adding them to a number of cells responding to IL2 signaling (see Table 3). The high affinity trimeric receptor complex is constitutively found on immune cells and was reported on lung endothelial cells (46). However, BMECs express IL2Rα only following 24hr stimulation with IL2. This result is consistent with previous discoveries that IL2 is able to modulate the expression of its own receptor α subunit in immune cells (96,97). Establishing that human and murine BMECs express a competent IL2 receptor complex suggests that IL2 immunotherapy can directly affect brain microvasculature.

Cell Type	IL2Rα (CD25)	IL2Rβ (CD122)	IL2Rγ (CD132;γ_c)	Refs
Thymocyte	-/+	-/+	+	(98,99)
Naïve T Cell†	-	-/+	+	(100-104)
Effector T Cell§	+++	++	+	(100-104)
Memory T Cell#	-	+/++	+	(46,100,102,104-106)
T_{FH} Cell	-	?	+	(103,104)
T_{Reg} Cell	+++	+	+	(107)
Immature B Cell¶	+	-	+	(98,108)
Mature B Cell	-	-	+	(98,108)
NK Cell	-	++	+	(46)
NKT Cell*	-/+	-/+	+	(109,110)
Dendritic Cell††	-/+	-	+	(111-117)
Langerhans Cell	+	?	+	(118)
Lung Endothelial Cell	+	+	+	(46,61)
Brain Microvascular Endothelial Cell	-	+	+	This project (119)
Fibroblast	+	+	-	(120,121)

Table 3. IL2 Receptor Expression by Immune and Non-Immune Cells

-, background expression level; +, low expression level; ++ high expression level; +++ very high expression level; γc, common cytokine receptor γ-chain; T_{FH}, follicular helper T cell; T_{Reg}, regulatory T cell; NK natural killer cell; NKT, natural killer T cell. † CD122 expression is undetectable on naïve CD4+ T cells, whereas CD8+ T cells have low but significant levels of CD122. § CD25 and CD122 are transiently upregulated on effector T cells. # CD122 expression levels are low on memory CD4+ cells but high on memory CD8+ T cells. ¶ Pre-B cells express significant levels of CD25 but no CD122. * NKT cells from the spleen express low to intermediate levels of CD25 †† There exists controversial data regarding CD 122 expression on human DCs; in mice, mature DCs do not express CD122, although CD122 may be present on DC precursors. Table adapted from Boyman, O., 2012. *Nat Rev Immunology* **12**, 180-190.

Interleukin 2 Signaling in Brain Microvascular Endothelial Cells

Signaling emanating from the IL2 receptor in lymphocytes involves the activation of the NFκB pathway (53). Likewise, NFκB was identified as a major mediator of Interleukin 15 action in BMECs (122). IL15 utilizes the IL2Rβ and IL2Rγ subunits as well as its specific IL15Rα subunit. Activation of the NFκB pathway following IL2Rβ and IL2Rγ engagement by IL15 suggests that IL2 signaling through this intermediate affinity IL2 receptor complex may also initiate NFκB signaling. Consequently, we endeavored to identify activation of the NFκB pathway by IL2 in BMECs. We were able to document IκBα degradation, NFκB RelA phosphorylation and nuclear localization following IL2 stimulation in BMECs (see Figures 13 and 14). NFκB activation and translocation to the nucleus is governed by its release from inhibitor, IκBα (123). Phosphorylation at Ser-536 of RelA has been documented to occur following NFκB activation and increases its transcriptional activity (124). These three lines of evidence support the activation of the NFκB pathway by IL2 in human and murine BMECs.

Proinflammatory cytokines and chemokines, in particular IL6 and MCP1, have been implicated in activating endothelial cells resulting in damage to the vasculature (47,55). We demonstrated that these two NFκB-regulated genes, IL6 and MCP1, are expressed following IL2 stimulation (see Figure 15). Induction of these two pleiotropic mediators of inflammation potentiates an inflammatory environment facilitating additional recruitment of immune cells capable of prolonged disruption of endothelial barrier function (74-77). IL2-evoked NFκB activation in lymphocytes is well known (53) but to our knowledge has not been previously reported in non-immune cells such as BMECs.

IL2 stimulation can potentially lead to the production of other proinflammatory mediators effecting endothelial activation and permeability. In particular, Interleukin 1 beta (IL1-β) is known to be expressed by endothelial cells (125) and IL2 is able to induce expression of IL1-β in immune cells (126). Furthermore, Vascular Endothelial Growth Factor (VEGF) that was initially discovered and named vascular permeability factor, is well known to destabilize adherens junctions through induction of VE-cadherin phosphorylation (127). In addition, TNFα is a potent inducer of vascular activation and is expressed following NFκB signaling in immune cells (128). TNFα production has also been documented in endothelial cells (129). With this in mind, it is important to realize that these mediators may play a role in the activation of BMECs and ultimate induction of permeability.

Structural and functional integrity of brain microvascular endothelial cells is of paramount importance in maintaining the physiologic function of the BBB (17,130). Patients receiving IL2 immunotherapy develop manifestations of capillary leak such as edema, weight gain and pulmonary congestion which are progressive with resolution of these side effects occurring quickly following termination of IL2 therapy (131). We hypothesized that IL2 activation of BMECs would also lead to loss of their ability to provide an effective barrier. In fact, we were able to document a direct IL2-induced increase in BMEC monolayer permeability (see Figures 16-19). Blocking proinflammatory mediators IL6 and MCP1 did not abate the significant increase in permeability induced by IL2 stimulation. These results confirm the direct role of IL2 in activating endothelial cells and causing an increase in monolayer permeability.

Destabilization of the Adherens Junction

To gain a better understanding of increased microvascular permeability we focused on IL2's effect on adherens junctions. Endothelial cell junctions are composed of tight junctions and adherens junctions with many reports suggesting that AJs and TJs are interconnected and influence their overall organization (132). These protein complexes work in tandem to restrict paracellular transport of molecules from the bloodstream into the surrounding tissues. We observed that IL2 stimulation led to disruption of the adherens junction protein complex with a distinct loss of VE-cadherin and p120 staining along the cellular border (see Figures 20 and 21). Disruption of the adherens junction protein complex leads to the internalization of VE-cadherin and dissociation of its adaptor proteins (26,86). Furthermore, changes in expression or organization of AJ proteins, in particular VE-cadherin, have been suggested to impact protein levels of claudin 5, a tight junction protein, leading to changes in barrier function and vascular permeability (27). Thus, disruption of adherens junctions may act, in turn, on TJs resulting in an endothelial dysregulation feed-forward loop. While we have not yet further investigated the effect of AJ disruption on the integrity of TJs in BMECs additional studies to corroborate this effect would be informative. Moreover, previous work has documented VE-cadherin redistribution in pulmonary endothelial cells treated with human sera from patients undergoing IL2 immunotherapy (62). These results lend support to our findings that IL2 signaling is operational in non-immune cells. Moreover, they offer the mechanism of adherens junction disruption in lung microvascular endothelial cells as the mechanism responsible for increased vascular permeability.

Adherens junction stability relies on the association of p120-catenin as well as β-catenin with VE-cadherin. Intriguingly, previous reports demonstrate that these adaptor proteins are critical regulators of VE-cadherin cell surface localization in endothelial cells (86) but may also be involved in further transcriptional activation, modifying endothelial activation and permeability (27,133). We were able to document the dissociation of the adherens junction protein complex (see Figures 25 and 26). There is growing evidence that p120 is associated with inflammation and in particular its ability to modulate NFκB activation in inflammatory responses (133). Furthermore, β-catenin has been reported to mediate the repression of tight junction proteins following release from the adherens junction complex (27). Thus, studying the nuclear translocation of these adaptor proteins following IL2 stimulation may allow for delineation of additional signaling pathways that are detrimental to endothelial barrier function.

Adherens junctions are stabilized in the plasma membrane through their anchoring to the F-actin cytoskeleton (26). Alteration of the F-actin cytoskeleton disrupts adherens junction complexes weakening cell-cell interactions. Stress fibers composed of bundles of polymerized actin and myosin filaments are the primary elements of the contractile machinery of endothelial cells (134). Edemagenic agonists rapidly induce actin reorganization from cortical actin into actin stress fibers, which induces AJ disruption and leads to interendothelial gap formation, resulting in increased endothelial permeability (85,86,135). The formation of these paracellular gaps is regulated by a balance of competing contractile forces intimately linked to the actin-based endothelial cytoskeleton where centripetal tension, adhesive cell-cell and cell-matrix tethering forces together regulate changes in cell shape (136). In concert with adherens junction alteration, cellular cytoskeleton architecture is changed following IL2 stimulation (see Figure

23). An increase in polymerized F-actin organized in thick bundles visually indicates an activated endothelial phenotype that promotes disruption of junctional protein complexes.

While the primary focus of this project was the barrier function of brain microvascular endothelial cells based on the stability of adherens junctions, it is important to note that other cellular constituents within the neurovascular unit depend on adherens junctions. Neural cadherin (N-cadherin) is abundantly expressed throughout the brain (137) and is responsible for intercellular contacts in a variety of cell types. They include pericyte-endothelial cell interactions during brain angiogenesis (138). Moreover, disruption of the N-cadherin•β-catenin complex leads to the activation of astrocytes within the brain (139). These findings suggest that adherens junctions other than VE-cadherin may contribute to dysregulation of the neurovascular unit. Therefore, it is plausible that IL2 can disrupt not only junctions between endothelial cells but also in the other constituents of the neurovascular contingent on identification of the IL2 receptor complex in these cells.

Mechanism of Adherens Junction Protein Complex Disruption

To investigate the underlying mechanism responsible for dissociation of the adherens junction complex we studied post-translational modification of VE-cadherin. Prior investigations of post-translational modifications of VE-cadherin have mostly focused on tyrosine phosphorylation sites and the effect these changes impart on vascular permeability and endothelial activation (27,83,91,92). Phosphorylation of catenins is associated with destabilization of adherens junction cell contacts (27,91). A complete consensus has yet to be

reached on the role of each specific phosphorylation site, although a number of proinflammatory mediators have been reported to preferentially lead to phosphorylation of Tyr-685 resulting in increased permeability (91,92). Thus, we focused on the potential of IL2 to increase phosphorylation of VE-cadherin at Tyr-685. Indeed, we documented increased phosphorylation of this residue (see Figure 27). Therefore, we conclude that IL2 can be added to the list of proinflammatory mediators able to induce Tyr-685 phosphorylation resulting in destabilization of the adherens junction complex.

A number of different kinases have been reported to be responsible for Tyr-685 phosphorylation VE-cadherin (91,92,140). In an effort to identify the kinase responsible for VE-cadherin phosphorylation in BMECs we analyzed a panel of IL2-associated and VE-cadherin associated kinases reported in the literature. They included focal adhesion kinase (FAK), src protein tyrosine kinase (src), spleen tyrosine kinase (syk) and zeta-chain-associated protein kinase 70 (ZAP70). To this end, we were unable to produce conclusive results. Changes in tyrosine phosphorylation are often transient by being regulated through the tandem action of kinases as well as phosphatases. Phosphorylation of VE-cadherin appears to be regulated in this way as multiple protein tyrosine phosphatases (PTP) including PTPμ, PTP1, VE-PTP and SHP2 have been implicated in the regulation of the adherens junction protein complex (81,141-143). We documented that SHP2 phosphatase expression was significantly reduced following IL2 stimulation (see Figure 28). These results suggest that an alteration in phosphatase expression may be the basis for VE-cadherin phosphorylation levels. Unlike kinases, which are recruited to the phosphorylation site, protein tyrosine phosphatase activity is largely determined by the expression level or proximity to the phosphorylation site and not by a specific recruiting event (25). Previous reports corroborate the role SHP2 phosphatase plays in regulation of the adherens

junction complex and in particular the phosphorylation state of VE-cadherin and its adaptor proteins (25,81,94,144). While identification of the kinase responsible remains elusive, our finding of decreased expression of SHP2 phosphatase in response to IL2 opens up an intriguing mechanistic link to dysregulation of adherens junctions in BMECs.

The Role of Adherens Junctions in other Diseases Affecting the BBB

The importance of adherens junction importance in maintaining a healthy CNS becomes apparent when one considers their potential involvement in other brain diseases mediated by inflammation caused by microbial, autoimmune and physical insults. Development of Multiple Sclerosis (MS), a well-known autoimmune disease, has been associated with disruption of adherens junctions. Decreased expression of VE-cadherin in endothelial cells following exposure to sera taken from MS patients experiencing an exacerbation in disease has been documented (145). Furthermore, MS leads to increased expression of VEGF, a well-known inducer of VE-cadherin phosphorylation, thereby disrupting adherens junctions (146). Dissociation of endothelial adherens junctions can also be initiated in the brain by hypoxia. Ischemic stroke results from a transient or persistent reduction in blood flow due to localized thrombosis or an embolism. In a murine model of transient middle cerebral artery occlusion, VE-cadherin protein levels were reduced by 33% suggesting disruption of the adherens junction complex subsequent to an ischemic episode (147). Moreover, developmental abnormalities of the brain microvasculature, in particular cerebral cavernous malformation, is linked to the destabilization

of adherens junctions (148). These diverse brain disorders underline the importance of adherens junctions in maintaining the integrity of the BBB and taming excessive brain inflammation.

Chapter V

FUTURE DIRECTIONS

Thesis Summary

Cumulatively, this work provides new evidence that a pleiotropic immune cytokine, IL2, activates brain microvascular endothelial cells and leads to deterioration of their barrier function (Fig. 29). A better understanding of IL2 action on brain microvascular endothelium, one of the cardinal components of the BBB, may aid in the development of new cytoprotective measures to protect the central nervous system from blood-borne mediators of endothelial injury. Developing new strategies to combat IL2-evoked vascular permeability would benefit patients suffering from VLS that complicates high dose IL2 immunotherapy as well as those afflicted with neurological autoimmune diseases in which IL2 plays a prominent role.

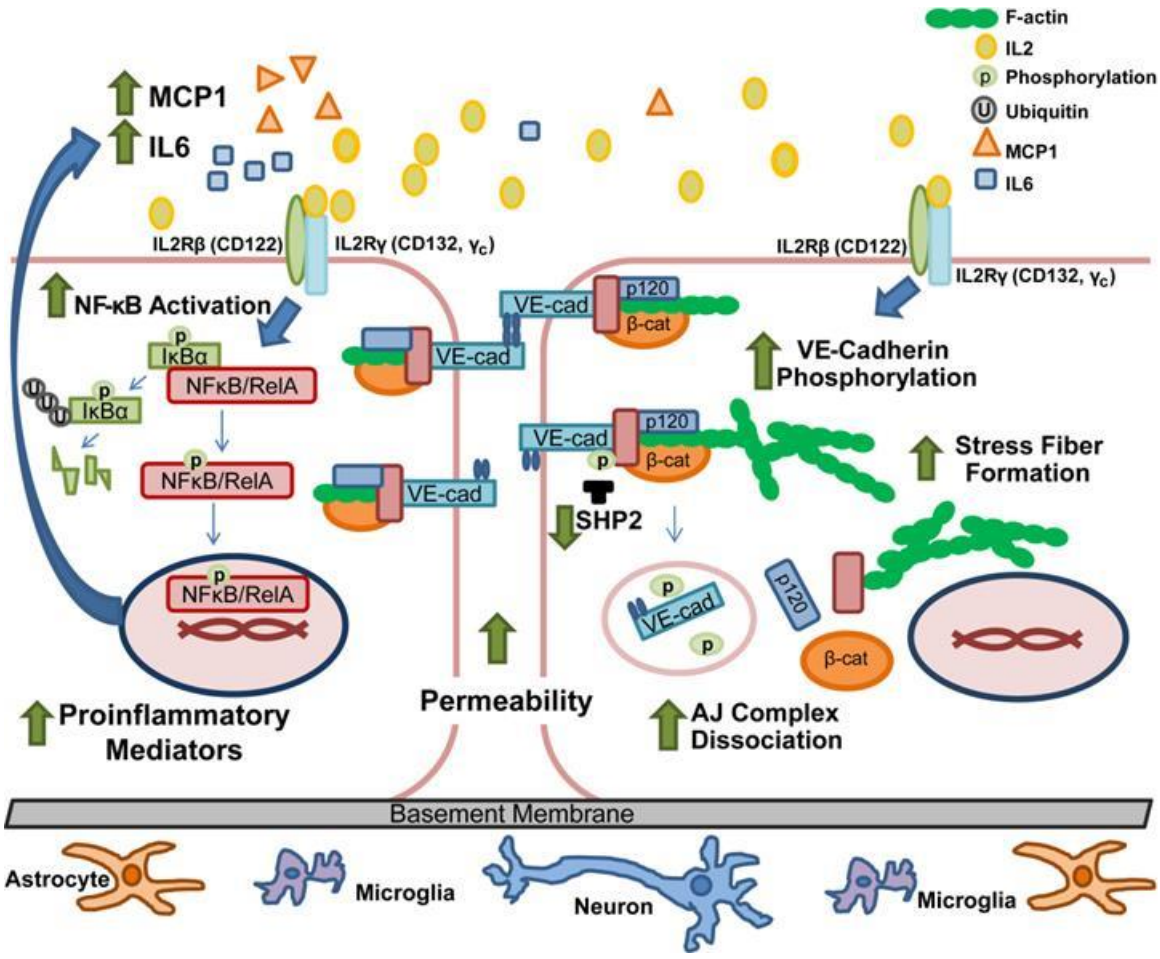

Figure 29. Diagrammatic Depiction of IL2-Induced Activation of BMECs

IL2 interacts with the constitutively expressed intermediate affinity IL2R complex (IL2Rβ and IL2Rγ), leading to degradation of IκBα and freeing NFκB to be translocated to the nucleus. Therein NFκB initiates transcription of its target genes, including two proinflammatory mediators, namely cytokine IL6 and chemokine MCP1, culminating in a feed-forward enhancement of the inflammatory process (*left*). In parallel, IL2 induces destabilization of adherens junctions through an increase in VE-cadherin (*VE-cad*) phosphorylation concomitant with a decrease in SHP2 phosphatase protein levels. An elevated VE-cadherin phosphorylation state results in diminished interaction between the constituents of the adherens junction complex, in particular p120 and β-catenin (β-*cat*). Furthermore, activation of the brain microvascular endothelial monolayer leads to increased F-actin stress fiber formation. Loss of adherens junction interaction between adjoining endothelial cells increases monolayer permeability (*right*). Thus, IL2 interaction with its cognate receptor on BMECs leads to a shift from a quiescent to an "activated" phenotype of BMECs and an increase in endothelial monolayer permeability.

Contribution of Alternative IL2 Receptor Signaling Pathways in Brain Microvascular Endothelial Cell Activation

This work has provided the foundation for understanding IL2's impact on brain microvascular endothelial cells. By identifying that BMECs express a competent IL2R complex which is able to activate the NFκB pathway we developed evidence to document induction of one of the signaling pathways emanating from the IL2R in BMECs. Prior work in immune cells documented the IL2R complex initiating three major signaling pathways: (i) the signal transducer and activator of transcription (STAT) pathway, (ii) the phosphoinositide 3-kinase (PI3k-Akt) pathway and (iii) the mitogen-activated protein kinase (MAPK) signaling pathway (59). Further investigation into which of these major signaling pathways leads to the activation of BMECs and disruption of adherens junctions would provide a more complete picture of IL2 signaling in BMECs. It is of significant note that activation of the NFκB pathway emanating from the IL2R complex in immune cells has been previously associated with the PI3K-Akt signaling pathway (149). Utilizing Akt-specific inhibitors would provide evidence that induction of this signaling pathway in BMECs also results in NFκB activation. Moreover, it was identified that signaling through the Akt pathway involved BCL10, a known mediator of canonical NFκB signaling in T and B lymphocytes (149). Importantly, we have previously reported activation of BCL10 in lung microvascular endothelial cells following proinflammatory stimuli (Appendix B) (85). We were able to show that knockdown of BCL10 resulted in reduction of NFκB signaling. This may be applicable to IL2 stimulation of BMECs. Further investigation into the role of BCL10 along with its physiologic suppressor CRADD/RAIDD would provide a distinct signaling pathway originating from the IL2 receptor complex culminating in activation of NFκB

in brain microvascular endothelial cells. Alternatively, potential IL2 signaling through the MAPK and STAT pathways could be probed in order to identify the extent of their specific activation and transcriptional targets. There have been reports of various agonists that increase vascular permeability following MAPK as well as STAT activation suggesting that these pathways may indeed be involved in IL2's action (150-153). These signaling intermediates can also be analyzed by single cell proteomics with cytometry by time of flight (CyTOF) (154).

Potentiation of Inflammation by p120-Catenin and β-Catenin

Documentation of IL2 induced adherens junction dissociation may allow alternative signaling by VE-cadherin associated adapter proteins. While principally responsible for stabilizing cell-cell interactions, p120 and β-catenin, in particular may have an alternative action. Emerging evidence has suggested that p120-catenin may function in an expanded role mediating both transcriptional regulation and inflammatory activation (133,155). p120 has been shown to interact with RhoA thereby modulating NFκB activation (133). As IL2 activates NFκB, p120 release from the protein complex may be directly impacting this transcription factor. p120 acts in the nucleus as a transcriptional repressor of proinflammatory genes (155). A disruption of p120 homeostasis following IL2 stimulation may disable its second function to attenuate a proinflammatory state. A more detailed investigation into the role of p120 following IL2 activation in BMECs may identify cooperative or secondary signaling capacity influencing the development of vascular permeability.

In addition to its role in stabilizing adherens junctions, β-catenin has been implicated in cross-talk with NFκB activation. β-catenin has been documented to positively influence the proinflammatory environment during NFκB signaling in pulmonary inflammation and colonic tumorigenesis (156,157). Increased nuclear localization of β-catenin enhances NFκB signaling potentiating a proinflammatory environment. As with p120, disruption of the VE-cadherin complex may increase the available pool of cytosolic β-catenin eligible for nuclear translocation. Further investigation of β-catenin in IL2 stimulated BMECs would determine a possible role in potentiating the proinflammatory NFκB signaling environment. Identifying other targets of β-catenin's transcriptional activity may unravel a new proinflammatory gene regulatory network.

Analysis of Adherens Junction and Tight Junction Crosstalk Following IL2 Stimulation

Further investigation on the crosstalk between adherens junctions and tight junctions would be necessary to gain a complete understanding of the effect of IL2 stimulation on the brain microvasculature. VE-cadherin associated with the adherens junction protein complex has been shown to upregulate the gene encoding claudin 5, a tight junction adhesive protein (27). IL2 action on the endothelium leading to dissociation of VE-cadherin from its adaptors p120 and β-catenin may magnify the deleterious process resulting in increased brain microvascular permeability. It has also been suggested that an increase in β-catenin localization to the nucleus leads to down regulation of claudin 5 expression (27). Experiments identifying β-catenin localization following dissociation from the adherens junction complex could potentially unlock a new avenue of investigation into crosstalk between AJs and TJs at the BBB. Due to the

functional and structural relationship between AJs and TJs an unraveling of any potential crosstalk between these crucial protein complexes would provide a more global picture of IL2 action on brain microvascular endothelial cell barrier function.

Analysis of Nuclear Transport Modifiers in NFκB Blockade

Conversely, further investigation into restricting NFκB activation may present potential therapeutic value. We have not yet been able to separate or directly link the activation of NFκB to the increase in monolayer permeability. Increased expression of proinflammatory cytokines and chemokines potentiate an environment conducive to increased endothelial monolayer permeability. Reducing endothelial NFκB activation would promote recovery of the endothelial monolayer. Our laboratory has developed a nuclear transport modifier which has been shown to reduce nuclear translocation of several stress responsive transcription factors (SRTFs), including NFκB (67,158,159). We have preliminary data suggesting that impairing nuclear transport of SRTFs reduces IL2-induced permeability in brain microvascular endothelial cells. Additionally, BAY 11-7082 a more selective inhibitor of the NFκB pathway (160) may be investigated to tease apart the specific role that NFκB activation plays in brain microvascular endothelial cell permeability. An alternative approach could involve the use of physiologic negative regulators of NFκB. We have previously been able to produce recombinant cell penetrating proteins able to control NFκB activation in response to proinflammatory signaling (38,40,85). These strategies would provide insight into the role of IL2-induced NFκB activation and its impact on the

development of BMEC permeability. Ultimately, these further studies may lead to the development of potential therapeutic approaches to counteract increased BBB permeability.

Further Analysis of IL2 Receptor Associated Kinases

In parallel with NFκB activation we observed disruption of the adherens junction leading to formation of intercellular gaps. Increased dissociation of VE-cadherin and its adapter proteins occurred due to the increased phosphorylation state of VE-cadherin. Further investigation into the link between the IL2 receptor and increased phosphorylation of VE-cadherin would provide a more robust story. While we investigated a number of kinases associated with the IL2 receptor (ZAP-70, syk and src) other VE-cadherin associated kinases should be examined for their potential activation in response to IL2 stimulation. One VE-cadherin associated kinase we have not yet analyzed is Rho kinase. VE-cadherin regulation has been associated with Rho kinase which has a duel role in modulating endothelial barrier function by both inducing barrier-protective and barrier-disruptive activity (161). Due to its association with endothelial barrier function it may prove to be involved in VE-cadherin phosphorylation. Again, these signaling events can be analyzed by single cell proteomics with cytometry by time of flight (CyTOF) (154).

A separate approach to get a better understanding of the association between activation of the IL2 receptor complex and the phosphorylation state of VE-cadherin would be to utilize newly developed IL2/anti-IL2 antibody complexes designed to target specific subunits of the IL2 receptor (46). Employing this tool in our model of brain microvascular permeability would allow

selective modulation of the IL2 receptor at the BBB. These complexes have been shown to activate the immune system yet spare the endothelium by avoiding interaction with IL2Rα (46). Identification of any differences in signaling, phosphorylation and adherens junction stability as compared to IL2 could provide a clue towards potential residues and/or proteins responsible for barrier dysfunction. Changes in endothelial permeability identified using these molecules may provide evidence to suggest other kinases and/or phosphatases as well as their target tyrosine residues implicated in barrier disruption.

Additionally, we have documented the importance of SHP2 in regulating VE-cadherin phosphorylation state. Investigating the recruitment and stabilization of SHP2 at the adherens junction would be important to analyze. Degradation of SHP2 could be a result of dissociation from adaptor/associated proteins which localize SHP2 at the adherens junction. Further investigation into other phosphatases associated with adherens junctions is potentially significant as regulation of VE-cadherin phosphorylation has been suggested to involve multiple protein tyrosine phosphatases including PTPμ, PTP1 and VE-PTP (81,141-143). Furthermore, identification of other proteins associated with the IL2 receptor complex may provide a clue to its signaling mechanism(s). These investigations would provide a better understanding of the link between the IL2 receptor and the phosphorylation state of VE-cadherin.

In Vivo Analysis of IL2-induced Brain Microvascular Endothelial Cell Permeability

Ultimately, the new knowledge gained from this study would be advanced with its application to *in vivo* models of VLS thus providing an integrated picture of IL2's role in

disrupting the BBB. Increased brain vascular permeability has been documented in human patients and murine models necessitating the development of a much needed new therapeutic approaches (32,45). Monitoring mice for increased BBB permeability following IL2 administration as well as their response to inhibitors of NFκB and other SRTFs would provide the basis for developing potential treatments to counter VLS. Employing physiologic negative regulators of inflammation or nuclear transport modifiers (NTMs) to reduce the level of NFκB and other SRTFs activation has been shown to be effective in other models of inflammation (37-39,67,85,158,162) and suggests that reducing NFκB signaling following IL2 activation of endothelial cells may prove beneficial. Utilizing new *in vivo* intravital microscopy techniques to track activation and disruption of the BBB would build on the results presented here. Protecting endothelial cell function following injury or insult is crucial to reducing collateral damage in adjoining brain tissue and preserving or restoring its function.

Chapter VI

MATERIALS AND METHODS

Cell Culture

The human BMEC line hCMEC/D3 was provided through the courtesy of Professor Babette Weksler (Weill Cornell Medical College, New York, NY) (163). hCMEC/D3 cells were cultured at 37 °C in 5% CO_2 in EBM-2 (Lonza) supplemented with 5% HI-FBS, 1% penicillin/streptomycin (Mediatech), 1.4 µM hydrocortisone (Sigma), 5 µg/ml of ascorbic acid (Fisher Scientific), chemically-defined lipid concentrate (Invitrogen) diluted 1:100, 10 mM HEPES (Mediatech) and 1 ng/ml of human b-FGF (Sigma). Cells used for experiments were between passages 20 and 30. The murine brain endothelioma cell line bEnd.3 (164) was purchased from American Type Culture Collection and cultured at 37 °C in 5% CO2 in Dulbecco's Modified Eagle's Medium (Mediatech) supplemented with 10% heat-inactivated fetal bovine serum (HI-FBS) and 1% penicillin/streptomycin. Murine embryonic fibroblasts (MEF) and the human embryonic kidney cell line (HEK) were cultured at 37 °C in 5% CO_2 in Dulbecco's Modified Eagle's Medium supplemented with 10% HI-FBS and 1% penicillin/streptomycin.

Quantitative Real Time PCR Analysis

Total RNA was isolated for quantitative real time PCR (qPCR) analysis using RNeasy Mini Kit (Qiagen) following manufacturer's instructions and reverse-transcribed utilizing the iScript cDNA synthesis kit (Bio-Rad). Targets were amplified by CFX96 Touch real-time PCR detection system (Bio-Rad) using the iQ SYBR Green Supermix kit (Bio-Rad) with specific primers listed in Table 1 and 2 for the indicated mRNAs. Results were analyzed by CFX Manager (Bio-Rad). Following normalization to GAPDH cDNA, relative levels were calculated using the $2^{-\Delta\Delta Ct}$ method (165).

Preparation of Cytosolic and Nuclear Extracts

Confluent BMEC monolayers were cultured and then stimulated for the indicated times in complete growth medium. Following stimulation, BMECs were washed with ice-cold PBS and then lysed using a cytosolic lysis buffer (10 mM HEPES [pH 7.9], 10 mM KCl, 0.1mM EDTA, 0.1 mM EGTA, 1% NP-40, 1mM DTT) containing phosphatase (Roche) and protease (Sigma) inhibitors as previously described (85). Nuclei were pelleted by centrifugation, supernatant was saved as the cytoplasmic extract, and the nuclear pellet was washed with cytosolic lysis buffer. Nuclear fractions were prepared by resuspension of the nuclear pellet in a high salt nuclear extraction buffer (20mM HEPES [pH 7.9], 400 mM NaCl, 1 mM EDTA, 1 mM EGTA, 1 mM DTT, with protease (Sigma) and phosphatase (Roche) inhibitor mixture) under

constant shaking for 30 min, centrifugation, and removal of genomic DNA as previously described (39).

Immunoblotting Analyses

The protein concentration of cytosolic and nuclear extracts was quantified using the Bradford Protein Assay (Bio-Rad) for equivalent protein loading. Samples were then separated by 10% SDS-PAGE, transferred onto nitrocellulose membranes (Bio-Rad), blocked with Odyessy Blocking Buffer (LI-COR) and incubated with the appropriate antibodies. Antibodies against NFκB p65 (Rel A; 1:1000; Santa Cruz), p120-catenin (p120; 1:1000; Santa Cruz), VE-cadherin (VE-cad; 1:1000; Santa Cruz), SHP2 (1:1000; Santa Cruz), β-catenin (1:1000; BD Biosciences), phospho-β-catenin (p-β-catenin; 1:500; Cell Signaling), IκBα, phospho-NFκB p65 (p-RelA; 1:500; Cell Signaling) and phospho-VE-cadherin (p-VE-cad; 1:500; ECM Biosciences) were used for immunoblot analyses. Obtained values were normalized in reference to β-actin (1:10,000; Abcam) or TATA-binding protein (TBP; 1:10,000; Abcam) detected with their cognate antibodies in cytosolic and nuclear extracts as indicated. Immunoblots were quantitatively analyzed by the LI-COR Odyssey Infrared Imaging System following incubation with appropriate secondary antibodies as previously described (39,85).

Immunoprecipitation Analyses

Adherens junction protein complexes were immunoprecipitated from cytosolic extracts with antibodies against p120 or VE-cadherin (Santa Cruz). The lysates we pre-cleared with protein A/G-agarose beads (Thermo) for 1hr at 4^{o}C prior to overnight incubation of antibodies or control IgG at 4^{o}C. Species specific IgG (Santa Cruz) was used as control. The immune complexes were then captured with protein A/G-agarose beads and analyzed by quantitative immunoblotting using antibodies against p120, VE-cadherin and β-catenin with the LI-COR Odyssey Infrared Imaging System as previously described (39,85) .

Cytokine and Chemokine Protein Expression Assay

Cytokines and chemokines in tissue culture medium supernatants were assayed by cytometric bead array (BD Biosciences) in the Vanderbilt Flow Cytometry Shared Resource according to manufacturer's instructions as previously described (85). During time- and concentration- dependent titration experiments, supernatant samples were taken following stimulation as indicated. Cytokine and chemokine expression was also analyzed in media from BMEC monolayers cultured in Transwell chambers for permeability experiments. Medium samples were taken from the upper chamber following stimulation as indicated but prior to addition of FITC-dextran tracer.

Immunofluorescence Staining

Human hCMEC/D3 or murine bEnd.3 cells grown to confluency on Transwell permeability supports were stimulated with species-specific IL2 (BD Biosciences, Prometheus) or TNFα (Invitrogen) as indicated. After stimulation, cells were fixed in 4% paraformaldehyde (Electron Microscopy Sciences), washed with PBS and permeabilized with 0.1% Triton X-100 (Invitrogen). For immunostaining, cells were blocked with 5% normal goat serum (Jackson ImmunoResearch) before overnight incubation at 4 °C with primary antibodies to NFκB p65 (Abcam) or VE-cadherin and p120 (Santa Cruz), followed by incubation with Alexa 488- (Invitrogen), Cy3- or Cy5-labeled (Jackson ImmunoResearch) secondary antibodies. F-actin polymerization was visualized in permeabilized cells with Alexa 488-labeled phalloidin (Cytoskeleton, Inc.). After staining, the semi-permeable membranes were removed from the Transwell permeability supports and mounted on slides with ProLong Gold Antifade reagent containing DAPI (Invitrogen) to counterstain nuclei.

Immunofluorescence Microscopy

Images were captured and analyzed with MetaMorph software on an Axioplan widefield microscope in the Vanderbilt Cell Imaging Core facility using a ×63 oil immersion objective.

Endothelial Cell Permeability Assay

Human hCMEC/D3 cells or murine bEnd.3 (1×10^5) were seeded onto 24-well Transwell semi-permeable supports (Costar) pre-coated with type 1 collagen (Cultrex) and incubated until confluent. Upon confluence, as verified by microscopy, growth media was exchanged for serum-depleted media that comprised growth media with a low concentration (0.5%) of HI-FBS. Following 24 h culture in low serum media, cells were left unstimulated or stimulated for 24 h with species-specific 300 kU/ml IL2 (kU=1000 U), or 30 ng/ml TNFα. In experiments utilizing neutralizing antibodies, species-specific murine anti-IL6, anti-MCP1 (R&D Systems) as well as human anti-IL6 (R&D Systems) and anti-MCP1 (Sigma) were added concomitantly with IL2. Human anti-IL2Rβ antibody (R&D Systems) was added 30 minutes prior to IL2 stimulation. Antibody concentrations necessary for neutralization were calculated from the levels of cytokine/chemokine expression during titration of IL2. Monolayer permeability was assessed by detection of FITC-dextran passage across an intact monolayer into the lower chamber. The lower chamber supernatant was sampled at the indicated time points after addition of 1mg/ml 10 kDa FITC-dextran (Sigma) to the upper chamber.

Cellular Detachment and Apoptosis Assay

Human and murine BMECs were cultured and stimulated as previously described during the permeability experiments. Following 24hr stimulation, the supernatant was removed from the

Transwell chambers and cellular detachment/apoptosis was measured using the trypan blue exclusion assay.

Statistical Analyses

Data analysis and statistical calculations were performed using Prism statistical software (GraphPad). Cytokine and chemokine levels in cultured cell supernatants were analyzed using an unpaired *t* test with Welch's correction. Quantified immunoblot results correlated to comparative controls were analyzed using Student's *t* test as indicated. Western blot quantifications of multiple time points were analyzed by one-way ANOVA with Bonferroni correction for multiple comparisons or by an unpaired *t* test with Welch's correction as indicated. Quantification of real time PCR results was calculated as a fold-change in transcripts compared to non-stimulated samples and statistical differences were determined by Student's *t* test. For permeability experiments, *p* values shown represent comparison of the area under the curve calculated for each experiment and/or condition analyzed by unpaired *t* test with Welch's correction. In all experiments, a p value of <0.05 was considered significant.

APPENDIX

A. “Interleukin 2 Activates Brain Microvascular Endothelial Cells Resulting in Destabilization of Adherens Junctions.” by **Lukasz Wylezinski** and Jacek Hawiger, *Journal of Biological Chemistry*, 2016. **291,** 22913-22923.

THE JOURNAL OF BIOLOGICAL CHEMISTRY VOL. 291, NO. 44, pp. 22913–22923, October 28, 2016
Published in the U.S.A.

Interleukin 2 Activates Brain Microvascular Endothelial Cells Resulting in Destabilization of Adherens Junctions *

Received for publication, March 23, 2016, and in revised form, August 12, 2016 Published, JBC Papers in Press, September 6, 2016, DOI 10.1074/jbc.M116.729038

Lukasz S. Wylezinski [‡1] and Jacek Hawiger [‡§¶2]

From the Departments of [‡]Molecular Physiology and Biophysics and [§]Medicine, Division of Allergy, Pulmonary and Critical Care Medicine, Vanderbilt University School of Medicine, Vanderbilt University Medical Center and [¶]Department of Veterans Affairs, Tennessee Valley Healthcare System, Nashville, Tennessee 37232-2363

The pleiotropic cytokine interleukin 2 (IL2) disrupts the blood-brain barrier and alters brain microcirculation, underlying vascular leak syndrome that complicates cancer immunotherapy with IL2. The microvascular effects of IL2 also play a role in the development of multiple sclerosis and other chronic neurological disorders. The mechanism of IL2-induced disruption of brain microcirculation has not been determined previously. We found that both human and murine brain microvascular endothelial cells express constituents of the IL2 receptor complex. Then we established that signaling through this receptor complex leads to activation of the transcription factor, nuclear factor κB, resulting in expression of proinflammatory interleukin 6 and monocyte chemoattractant protein 1. We also discovered that IL2 induces disruption of adherens junctions, concomitant with cytoskeletal reorganization, ultimately leading to increased endothelial cell permeability. IL2-induced phosphorylation of vascular endothelial cadherin (VE-cadherin), a constituent of adherens junctions, leads to dissociation of its stabilizing adaptor partners, p120-catenin and β-catenin. Increased phosphorylation of VE-cadherin was also accompanied by a reduction of Src homology 2 domain-containing protein-tyrosine phosphatase 2, known to maintain vascular barrier function. These results unravel the mechanism of deleterious effects induced by IL2 on brain microvascular endothelial cells and may inform the development of new measures to improve IL2 cancer immunotherapy, as well as treatments for autoimmune diseases affecting the central nervous system.

The blood-brain barrier (BBB) [3] is formed by endothelial cells that line the microcirculation and are part of the "neurovascular unit" composed of brain microvascular endothelial cells (BMECs), astrocytes, and neurons (1). BMECs play an essential role in these functional units, even prompting neurological changes following endothelial activation. For example, BMECs are stimulated by inflammatory mediator interleukin 1β, causing fever and lethargy (2). Likewise, IL2, the mainstay of the first effective cancer immunotherapy, induces neuropsychiatric changes in patients through a hitherto undefined mechanism (3). This therapy consists of IL2-induced activation and proliferation of tumor-infiltrating lymphocytes that lead to remission of renal cell carcinoma and malignant melanoma (4). However, these beneficial effects of IL2 are curtailed by the development of brain edema, a prominent manifestation of vascular leak syndrome (VLS). Brain edema subsides upon cessation of IL2 immunotherapy, indicating its direct role in this serious complication. Thus, IL2-induced vascular permeability in the central nervous system and other organs represents an undesirable off-target effect (5). Moreover, IL2 plays a significant role in several chronic neurological autoimmune diseases, including multiple sclerosis, neuromyelitis optica, and neuropsychiatric systemic lupus erythematosus (6–8). Disruption of the BBB is a critical step in development of these neurological conditions. However, the mechanism of adverse action of IL2 on the barrier function of brain microvascular endothelial cells remains unknown.

The maintenance of BBB function is largely vested in BMEC intercellular junctions, a complex network of adhesive proteins organized into adherens junctions (AJs) and tight junctions (9). AJs are ubiquitously expressed in the vascular tree (10) and are of particular importance in microvascular circulation, which provides the largest surface area of exchange between blood and tissue (11). Furthermore, postcapillary venules comprise the main endothelial surface for activation and emigration of immune cells that mediate inflammatory reactions (12). Formation of AJs is dependent on the homotypic interaction of cell surface transmembrane proteins termed cadherins whose cytoplasmic tails associate with intracellular binding partners termed catenins. Thus, the stability of AJs depends on complex formation between vascular endothelial cadherin (VE-cad-

* This work was supported by United States Public Health Service National Institutes of Health Grants HL069452 and HL085833 (to J. H.), National Institutes of Health Ruth Kirschstein Institutional National Service Award T32 HL069765 (to L. S. W.), the Vanderbilt Immunotherapy Program, the Vanderbilt University Medical School Department of Medicine, and Vanderbilt Clinical and Translational Science Award UL1TR000445. The authors declare that they have no conflicts of interest with the contents of this article. The content is solely the responsibility of the authors and does not necessarily represent the official views of the National Institutes of Health.

[1] Submitted as partial fulfillment of the requirements for the degree of Doctor of Philosophy, Vanderbilt University School of Medicine.

[2] To whom correspondence should be addressed: Dept. of Medicine, Division of Allergy, Pulmonary and Critical Care Medicine, Vanderbilt University School of Medicine, 1161 21st Ave. South, T1218 MCN, Nashville, TN 37232-2363. Tel.: 615-343-8280; Fax: 615-343-8278; E-mail: jacek.hawiger@vanderbilt.edu.

[3] The abbreviations used are: BBB, blood brain barrier; VE-cadherin, vascular endothelial cadherin; BMEC, brain microvascular endothelial cell; VLS, vascular leak syndrome; NFκB, nuclear factor κB; MCP1, macrophage chemoattractant protein 1; IL2R, IL2 receptor; AJ, adherens junction; p120, p120-catenin; SHP2, Src homology 2 domain-containing protein-tyrosine phosphatase 2; HI-FBS, heat-inactivated fetal bovine serum; MEF, mouse embryonic fibroblast; qPCR, quantitative real time PCR; vWF, von Willebrand factor; PECAM1, platelet endothelial cell adhesion molecule 1; ANOVA, analysis of variance.

herin), p120-catenin (p120), β-catenin, and plakoglobin (9). In contrast, destabilization of AJs is due to a loss of p120 and β-catenin binding, which causes the internalization of VE-cadherin (13–15). This process is induced by increased phosphorylation of VE-cadherin accompanied by a decrease in Src homology domain-containing protein-tyrosine phosphatase 2 (SHP2), which maintains vascular barrier function (15). Ultimately, disruption of AJs leads to leakiness of endothelial cell monolayers (9, 15–17).

In general, activation of endothelial cells results in expression of cell adhesion molecules along with proinflammatory cytokines and chemokines, enhancing an autoregulatory feed-forward loop that leads to further recruitment of immune cells and escalation of the inflammatory response (18). Genes encoding these mediators of inflammation are controlled by nuclear factor κB (NF κB), master regulator of immunity and inflammation. Increased expression of interleukin 6 (IL6), macrophage chemoattractant protein 1 (MCP1/CCL2), intercellular adhesion molecule 1, and vascular cell adhesion molecule 1 among others has been linked to the NF κB pathway (19, 20). In lymphocytes, IL2-evoked signaling mediated by its high affinity trimeric receptor (IL2R αβγ) has been previously coupled to activation of the NF κB pathway (21).

Here we analyze the mechanism of IL2-induced activation of human and murine brain microvascular endothelial cells and the resulting disruption of BMEC barrier function. We report that IL2 induces activation of the NF κB pathway, leading to increased expression of proinflammatory mediators. In parallel, IL2 causes disruption of AJs through an increase in VE-cadherin phosphorylation. As a consequence, microvascular endothelial monolayer permeability was increased. Whereas IL2-induced disruption of the BBB changes the central nervous system milieu and leads to subsequent brain edema, our study may contribute to the development of new strategies for protecting brain function from this deleterious process.

Experimental Procedures

Cell Culture—The human BMEC line hCMEC/D3 was provided through the courtesy of Professor Babette Weksler (Weill Cornell Medical College, New York, NY) (22). hCMEC/D3 cells were cultured at 37 °C in 5% CO_2 in EBM-2 (Lonza) supplemented with 5% heat-inactivated fetal bovine serum (HI-FBS), 1% penicillin/streptomycin (Mediatech), 1.4 μM hydrocortisone (Sigma), 5 μg/ml ascorbic acid (Fisher Scientific), chemically defined lipid concentrate (Invitrogen) diluted 1:100, 10 mM HEPES (Mediatech), and 1 ng/ml human basic FGF (Sigma). Cells used for experiments were between passages 20 and 30. The murine brain endothelioma cell line bEnd.3 (23) was purchased from American Type Culture Collection and cultured at 37 °C in 5% CO_2 in Dulbecco's modified Eagle's medium (Mediatech) supplemented with 10% HI-FBS and 1% penicillin/streptomycin. Murine embryonic fibroblasts (MEFs) and the human embryonic kidney (HEK) cell line were cultured at 37 °C in 5% CO_2 in Dulbecco's modified Eagle's medium supplemented with 10% HI-FBS and 1% penicillin/streptomycin.

Quantitative Real Time PCR Analysis—Total RNA was isolated for quantitative real time PCR (qPCR) analysis using the RNeasy Mini kit (Qiagen) following the manufacturer's instructions and reverse transcribed utilizing the iScript cDNA synthesis kit (Bio-Rad). Targets were amplified by the CFX96 Touch real time PCR detection system (Bio-Rad) using the iQ SYBR Green Supermix kit (Bio-Rad) with specific primers listed in Table 1 for the indicated mRNAs. Results were analyzed by CFX Manager (Bio-Rad). Following normalization to GAPDH cDNA, relative levels were calculated using the $2^{-\Delta\Delta Ct}$ method (24).

TABLE 1
Oligonucleotide PCR primer sequences used in current study
h, human; m, murine.

Gene	Primer sequences
h vWF	Forward, 5′-TGCTGACACCAGAAAAGTGC-3′
	Reverse, 5′-AGTCCCCAATGGACTCACAG-3′
m vWF	Forward, 5′-TTCATCCGGGACTTTGAGAC-3′
	Reverse, 5′-AGCCTTGGCAAAACTCTTCA-3′
h PECAM1	Forward, 5′-GATAATTGCCATTCCCATGC-3′
	Reverse, 5′-GGGTTTGCCCTCTTTTTCTC-3′
m PECAM1	Forward, 5′-ATGACCCAGCAACATTCACA-3′
	Reverse, 5′-CACAGAGCACCGAAGTACCA-3′
h IL2R α	Forward, 5′-ATCAGTGCGTCCAGGGATAC-3′
	Reverse, 5′-GTGACGAGGCAGGAAGTCTC-3′
m IL2R α	Forward, 5′-TACAAGAACGGCACCATCCTAA-3′
	Reverse, 5′-TTGCTGCTCCAGGAGTTTCC-3′
h IL2R β	Forward, 5′-GCTGATCAACTGCAGGAACA-3′
	Reverse, 5′-TGTCCCTCTCCAGCACTTCT-3′
m IL2R β	Forward, 5′-GGCTCTTCTTGGAGATGCTG-3′
	Reverse, 5′-GCCAGAAAAACAACCAAGGA-3′
h IL2R γ	Forward, 5′-CCACTCTGTGGAAGTGCTCA-3′
	Reverse, 5′-AGGTTCTTCAGGGTGGGAAT-3′
m IL2R γ	Forward, 5′-CTGGGGGAGTCATACTGTAGAGG-3′
	Reverse, 5′-AGGCTTCCGGCTTCAGAGAAT-3′

Immunoblotting and Immunoprecipitation Analysis—Antibodies against NF κB p65 (RelA), p120, VE-cadherin, SHP2 (Santa Cruz Biotechnology), β-catenin (BD Biosciences), phospho-β-catenin, IκBα, phospho-NF κB p65 (phospho-RelA) (Cell Signaling Technology), and phospho-VE-cadherin (ECM Biosciences) were used for immunoblotting analyses. Obtained values were normalized in reference to β-actin or TATA-binding protein detected with their cognate antibodies (Abcam) in cytosolic and nuclear extracts as indicated. Adherens junction protein complexes were immunoprecipitated from cell lysates with antibodies against p120 or VE-cadherin. Species-specific IgG (Santa Cruz Biotechnology) was used as a control. The lysates were precleared with protein A/G-agarose beads (Thermo) prior to addition of antibodies or control IgG. The immune complexes were then captured with protein A/G-agarose beads and analyzed by quantitative immunoblotting using antibodies against p120, VE-cadherin, and β-catenin with the LI-COR Odyssey infrared imaging system as described previously (25).

Cytokine/Chemokine Assays—Cytokines and chemokines in tissue culture medium supernatants were assayed by cytometric bead array (BD Biosciences) in the Vanderbilt Flow Cytometry Shared Resource according to the manufacturer's instructions as described previously (25). During time- and concentration-dependent titration experiments, supernatant samples were taken following stimulation as indicated. Cytokine and chemokine expression was also analyzed in medium from BMEC monolayers cultured in Transwell chambers for permeability experiments. Medium samples were taken from

the upper chamber following stimulation as indicated but prior to addition of FITC-dextran tracer.

Immunofluorescence Staining and Fluorescence Microscopy—Human hCMEC/D3 or murine bEnd.3 cells grown to confluence on Transwell permeability supports were stimulated with species-specific IL2 (BD Biosciences, Prometheus) or TNF α (Invitrogen) as indicated. After stimulation, cells were fixed in 4% paraformaldehyde (Electron Microscopy Sciences), washed with PBS, and permeabilized with 0.1% Triton X-100 (Invitrogen). For immunostaining, cells were blocked with 5% normal goat serum (Jackson ImmunoResearch Laboratories) before overnight incubation at 4 °C with primary antibodies to NF κB p65 (Abcam) or VE-cadherin and p120 (Santa Cruz Biotechnology) followed by incubation with Alexa Fluor 488 (Invitrogen)-, Cy3-, or Cy5-labeled (Jackson ImmunoResearch Laboratories) secondary antibodies. F-actin polymerization was visualized in permeabilized cells with Alexa Fluor 488-labeled phalloidin (Cytoskeleton, Inc.). After staining, the semipermeable membranes were removed from the Transwell permeability supports and mounted on slides with ProLong Gold antifade reagent containing DAPI (Invitrogen) to counterstain nuclei. Images were captured and analyzed with MetaMorph software on an Axioplan widefield microscope in the Vanderbilt Cell Imaging Core facility using a $\times$63 oil immersion objective.

Endothelial Cell Permeability—Human hCMEC/D3 or murine bEnd.3 cells (1×10^5) were seeded onto 24-well Transwell semipermeable supports (Costar) precoated with type 1 collagen (Cultrex) and incubated until confluent. Upon confluence, as verified by microscopy, growth medium was exchanged for serum-depleted medium that comprised growth medium with a low concentration (0.5%) of HI-FBS. Following 24-h culture in low serum medium, cells were left unstimulated or stimulated for 24 h with species-specific 300 kilounits/ml IL2 or 30 ng/ml TNF α. In experiments utilizing neutralizing antibodies, species-specific murine anti-IL6 and anti-MCP1 (R&D Systems) and human anti-IL6 (R&D Systems) and anti-MCP1 (Sigma) were added concomitantly with IL2. Human anti-IL2R β antibody (R&D Systems) was added 30 min prior to IL2 stimulation. Antibody concentrations necessary for neutralization were calculated from the levels of cytokine/chemokine expression during titration of IL2. Monolayer permeability was assessed by detection of FITC-dextran in the lower chamber at various times after addition of 1 mg/ml 10-kDa FITC-dextran (Sigma) to the upper chamber.

Cellular Detachment and Apoptosis—Human and murine BMECs were cultured and treated as described previously for permeability experiments. Following 24-h stimulation, the supernatant was removed from the Transwell chambers, and cellular detachment/apoptosis was measured using the trypan blue exclusion assay.

Statistical Analyses—Data analysis and statistical calculations were performed using Prism (GraphPad). Cytokine and chemokine levels in cultured cell supernatants and Western blotting quantification of comparative controls were analyzed using an unpaired t test with Welch's correction or Student's t test as indicated. Western blotting quantifications of multiple time points were analyzed by one-way ANOVA with Bonferroni correction for multiple comparisons. Quantification of real time PCR results was calculated as a -fold change in transcripts compared with non-stimulated samples, and statistical differences were determined by Student's t test. For permeability experiments, p values shown represent comparison of the area under the curve calculated for each experiment and/or condition analyzed by unpaired t test with Welch's correction. In all experiments, a p value of <0.05 was considered significant.

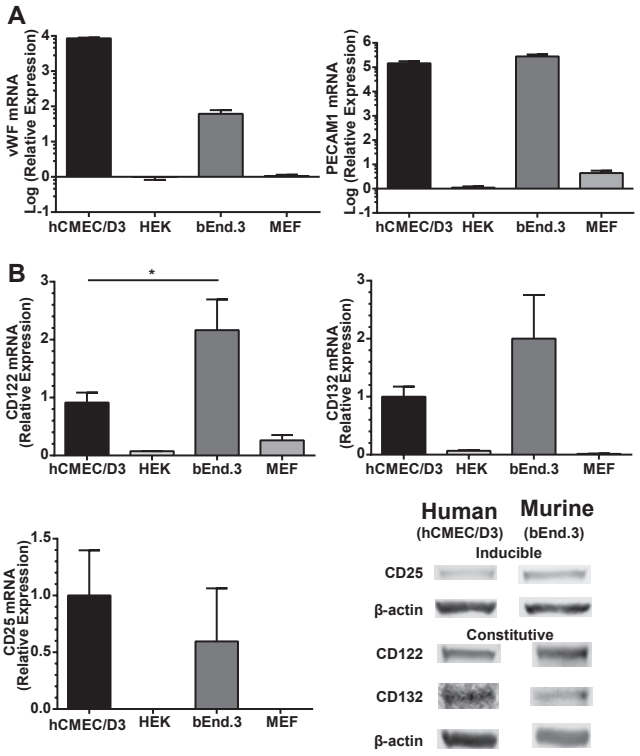

FIGURE 1. Expression of endothelial cell markers vWF, PECAM1, and IL2R subunits in human and murine BMECs. A, constitutive transcript levels of endothelial cell markers vWF and PECAM1 were assessed by qPCR. Following normalization to GAPDH, mRNA levels are presented as increased -fold change from species-specific non-endothelial cells: HEK 293 cells and MEFs. B, transcript levels of IL2R subunits were determined by qPCR, and protein expression was documented by immunoblotting. IL2Rβ (CD122) and IL2Rγ (CD132) were constitutively expressed in both human and murine BMECs. Transcript and protein levels for IL2Rα (CD25) were only detected following 24-h stimulation with species-specific 300 kilounits/ml IL2. The level of mRNA transcript is presented as relative expression comparing human and murine BMECs. Error bars represent mean $\pm$ S.E. of three independent experiments performed in triplicates. Statistical significance was determined by Student's t test (*, $p < 0.05$).

Results

Characterization of BMECs and Their Expression of the IL2 Receptor Subunits—In an effort to ensure that the endothelial cell phenotype was maintained in this study, we analyzed two well known markers specific for endothelial cells, von Willebrand factor (vWF) and platelet endothelial cell adhesion molecule 1 (PECAM1) (26). As expected, both human hCMEC/D3 and murine bEnd.3 cells constitutively expressed high levels of vWF and PECAM1 transcripts compared with human and murine non-endothelial cells (HEK cells and MEFs) when analyzed by qPCR (Fig. 1A). Our qPCR results in both human hCMEC/D3 and murine bEnd.3 cells complement previous

characterization in terms of protein expression of vWF and PECAM1 (22, 23, 27). Next, we assessed IL2 receptor subunit expression by qPCR and Western blotting to ascertain whether BMECs can respond to IL2. The IL2 receptor complex comprises the high affinity trimeric configuration (IL2R $\alpha\beta\gamma$) or the intermediate affinity dimer (IL2R $\beta\gamma$) (28). We documented that IL2R β (CD122) and IL2R γ (CD132) are expressed constitutively at both the transcript and protein levels. Conversely, these transcripts were barely detectable in control cell lines of human and murine origin (HEK cells and MEFs). IL2R α (CD25) transcripts were only detected in BMECs, but not control cells, after agonist stimulation for 24 h and corroborated with detection of the protein by Western blotting (Fig. 1B). Without constitutive expression of CD25 and formation of the trimeric receptor complex, affinity for IL2 is reduced 10–100 times (29). Therefore, we based our experimental protocol on using sufficiently high concentrations of IL2 to stimulate naïve BMECs and overcome their lower signaling capacity via the intermediate affinity receptor complex (IL2R $\beta\gamma$). As compared with human hCMEC/D3 cells, murine bEnd.3 cells displayed significantly higher transcript levels of IL2R β, the receptor subunit most attributed to mediating positive signal transduction (28, 30). No significant difference between human and murine cells was detected in transcript levels of inducible IL2R α subunit or constitutive IL2R γ subunit. However, a trend toward higher expression of IL2R γ was observed in murine bEnd.3 cells. Thus, these results establish the expression of the IL2 intermediate affinity receptor complex on both human and murine BMECs.

IL2-induced Activation of the NF κB Pathway—We hypothesized that IL2-induced activation of BMECs entails signaling through the NF κB pathway akin to IL15 (31). Therefore, we used three experimental approaches to analyze NF κB signaling in IL2-stimulated BMECs and compared the results with those evoked by a known endothelial agonist, lipopolysaccharide (LPS), a potent activator of the NF κB pathway (32). First, we determined that IκBα, the inhibitory protein responsible for sequestering NF κB p65 (RelA) in the cytoplasm, becomes degraded following IL2 stimulation in both human and murine BMECs (Fig. 2A). Due to the very rapid turnover kinetics of IκBα (33), we included the protein synthesis inhibitor cycloheximide to prevent reaccumulation of newly synthesized IκBα. Constitutive turnover was measured following addition of cycloheximide and compared with degradation in BMECs stimulated with agonist. Stimulation with IL2 caused time-dependent degradation of IκBα with a loss of 30–70% of its basal level, mimicking IκBα degradation following activation with LPS. Notably, the kinetics of IκBα degradation was faster in human hCMEC/D3 cells compared with murine bEnd.3 cells likely due to constitutively higher expression of physiologic suppressors of the NF κB signaling pathway such as A20 in murine cells (34). As a result of IκBα degradation, RelA is no longer sequestered in the cytoplasm, becomes phosphorylated, and is able to translocate into the nucleus. RelA phosphorylation enhances DNA binding and results in the activation of a number of proinflammatory genes (35). Accordingly, we detected an increase in phosphorylated RelA compared with total RelA in the nucleus (Fig. 2B). Both human and murine BMECs showed a time-dependent response to IL2, resulting in

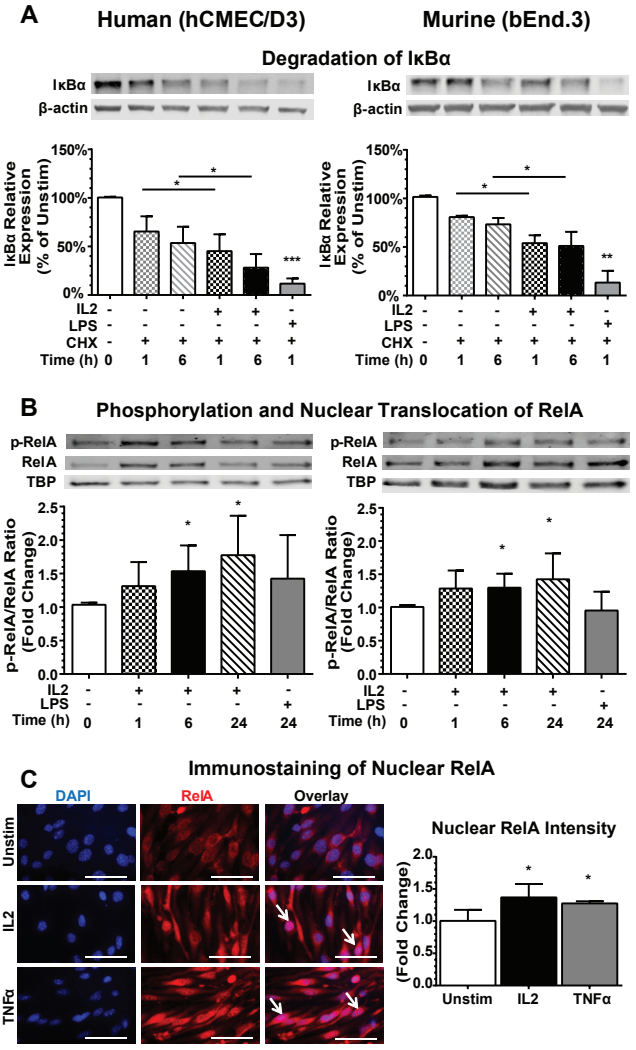

FIGURE 2. IL2 activates the NF κB pathway in human and murine BMECs. A, degradation of IκBα in BMECs. Human (hCMEC/D3) and murine (bEnd.3) BMECs were left unstimulated (Unstim) (0) or stimulated with species-specific 300 kilounits/ml IL2 or 1 μg/ml LPS, a positive control, for the indicated times after pretreatment for 30 min with the protein synthesis inhibitor cycloheximide (CHX) (10 μg/ml) to block de novo protein synthesis. Cytosolic extracts were isolated, separated by SDS-PAGE, and immunoblotted for the degradation of IκBα. Protein levels were quantified by immunoblotting, and values at each time point were normalized to the β-actin loading control. Error bars represent mean $\pm$ S.D. of at least four independent experiments. Statistical significance was determined using an unpaired t test with Welch's correction (*, $p < 0.05$; **, $p < 0.005$; ***, $p < 0.0005$). B, translocation of RelA to the nucleus. Human and murine BMECs were stimulated with 300 kilounits/ml species-specific IL2 or 1 μg/ml LPS for the indicated times, and nuclear extracts were isolated, separated by SDS-PAGE, and immunoblotted for the presence of total RelA and Tyr-536 phosphorylated RelA (p-RelA). TATA-binding protein (TBP) serves as a loading control for nuclear lysates. Quantification of signal is shown as -fold change compared with the unstimulated control. Error bars represent mean $\pm$ S.D. of at least four independent experiments. Statistical significance was determined using an unpaired t test with Welch's correction (*, $p < 0.05$). C, detection of RelA in the nucleus by immunofluorescence. Murine (bEnd.3) BMECs were analyzed following 24-h stimulation with 300 kilounits/ml murine IL2 or 30 ng/ml murine TNFα. Cells were immunostained with anti-RelA antibodies (red), and nuclei were counterstained with DAPI (blue). Arrows indicate strong nuclear staining of RelA. Images are representative of three independent experiments. Quantification was determined using MetaMorph imaging software. Statistical significance was determined using an unpaired t test with Welch's correction (*, $p < 0.05$). Magnification, $\times$63. Scale bars, 5 μm. Error bars represent mean $\pm$ S.D.

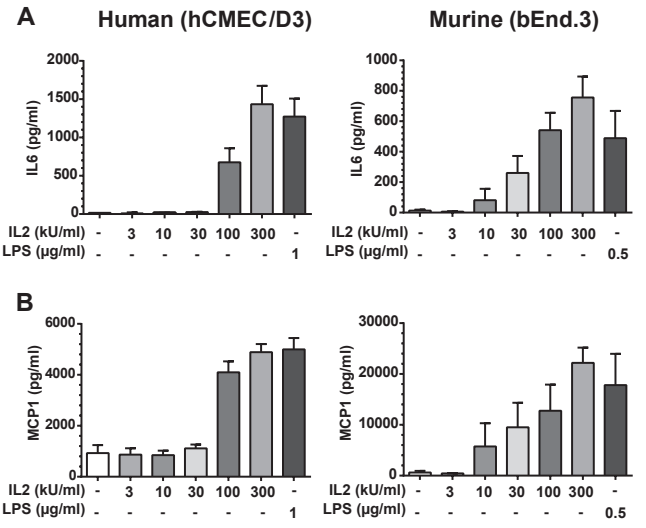

FIGURE 3. IL2-induced expression of proinflammatory IL6 and MCP1 in human and murine BMECs. IL6 (A) and MCP-1 (B) are expressed by activated BMECs in a dose-dependent manner. Protein levels of IL6 and MCP1 in culture medium were measured 24 h after stimulation of hCMEC/D3 and bEnd.3 cells with increasing concentrations of species-specific IL2 as indicated (kilounits (kU)) or 1 μg/ml LPS in hCMEC/D3 cells and 0.5 μg/ml LPS in bEnd.3 cells. Error bars represent mean ± S.D. from three independent experiments performed in duplicate or triplicate.

a 50% increase in Tyr-536 phosphorylation of RelA in nuclear extracts of agonist-treated cells. Finally, we verified nuclear translocation of RelA using immunofluorescence. Indeed, as compared with the unstimulated control, we noted elevated levels of nuclear RelA in BMECs stimulated with IL2 or TNF α, another known inducer and activator of the NF κB pathway (Fig. 2C). Taken together, our multipronged approach demonstrates that IL2 activates the NF κB signaling pathway in human and murine BMECs.

IL2 Induces Expression of Proinflammatory Cytokines and Chemokines—Several proinflammatory cytokines and chemokines have been previously implicated in endothelial activation and loss of barrier function, including IL6 and MCP1 (36–39). Both are regulated by the NF κB pathway (20, 40). Given that IL2 activated this pathway, we hypothesized that IL2 stimulation would also induce expression of these two proinflammatory mediators. Indeed, both pleiotropic cytokine IL6 and chemokine MCP1 were elicited by IL2 in a concentration-dependent manner in human and murine BMECs (Fig. 3). Thus, IL2 induces proinflammatory agonists that can also amplify signaling events involved in the potentiation of microvascular injury.

IL2-induced Permeability of the BMEC Monolayer—IL2 administered during cancer immunotherapy causes VLS, manifested by a rise in brain water content that is attributed to increased permeability of the brain microvascular endothelium (5). Therefore, we next analyzed the potential mechanism of IL2-induced disruption of endothelial barrier function in BMEC monolayers in Transwell chambers. We monitored the passage of FITC-labeled dextran across an intact monolayer. FITC-dextran was added to the upper Transwell chamber following 24-h stimulation of BMECs with species-specific IL2. The lower chamber supernatant was then sampled at the indicated time points. IL2 induced a significant increase in the movement of FITC-dextran across the IL2-stimulated BMEC monolayer compared with the non-stimulated control, indicating a gradual loss of endothelial barrier function and increased permeability (Figs. 4A and 5A). As IL2-induced permeability can potentially be enhanced by IL6 and/or MCP1, we utilized species-specific neutralizing antibodies against IL6 and MCP1. Neutralizing these two potential permeability agonists did not significantly alter an IL2-induced increase in permeability, although a trend toward lower permeability was observed. In contrast, IL2-induced permeability enhancement was counteracted in human hCMEC/D3 cells by species-specific IL2R β-blocking antibody (Fig. 4A). These results indicate that IL2 can directly increase endothelial monolayer permeability. A similar blocking experiment could not be performed in murine bEnd.3 cells due to a lack of species-specific antibody against IL2R β. Murine bEnd.3 cells demonstrated a greater change in endothelial permeability than human hCMEC/D3 cells most likely due to constitutively higher expression of IL2R β. Even though permeability increases in the hCMEC/D3 monolayer were not as robust, these results were significant and consistent. Endothelial monolayer confluence and integrity were checked by microscopy prior to initiating permeability assays. To this end, extending culture time from 24 to 72 h without agonist treatment in the Transwell system of both human hCMEC/D3 and murine bEnd.3 endothelial cells did not change their baseline permeability level for FITC-labeled dextran.

We verified changes in endothelial barrier function by immunostaining the adherens junction protein complex that includes VE-cadherin and one of its adaptors, p120-catenin. In quiescent human and murine BMECs, immunostained VE-cadherin and p120 displayed a well defined, contiguous border between adjoining cells. This border was strikingly lost after treatment with IL2 or TNF α, a comparative positive control. Membrane-associated VE-cadherin·p120 complexes were disrupted with a concomitant reduction of these proteins along the periphery of the cells (Figs. 4B and 5B). We verified that endothelial cell activation correlated with the time course of increased permeability in human hCMEC/D3 and murine bEnd.3 cells by analyzing cytokine and chemokine expression in supernatant collected from the upper Transwell chamber prior to addition of FITC-dextran. In agreement with prior analysis in a different culture system (see Fig. 3), we documented significantly higher levels of IL6 and MCP1 following IL2 stimulation compared with the unstimulated control (Figs. 4C and 5C). However, within the time frame of our antibody-neutralizing permeability experiments, these two proinflammatory agonists evoked by IL2 did not significantly contribute to its effect on microvascular permeability (see above; Figs. 4A and 5A).

IL2-induced Disruption of the Adherens Junction—Disruption of the AJ protein complex is accompanied by changes in cell morphology and resulted in the opening of gaps between neighboring cells. These changes in endothelial monolayer integrity are coupled to cytoskeletal reorganization (25, 41, 42). Indeed, an increase in F-actin fiber bundles was prominently displayed in IL2-activated murine bEnd.3 cells (Fig. 6A). These cells displayed thicker and more prominent F-actin fiber bun-

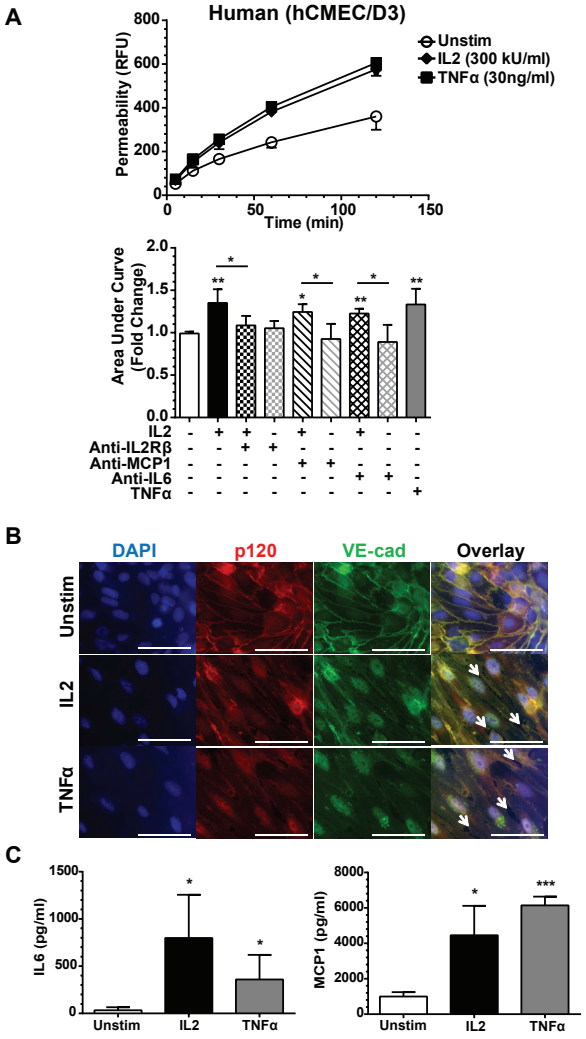

FIGURE 4. IL2-induced permeability and expression of proinflammatory mediators in human BMEC monolayer. A, human (hCMEC/D3) cells were grown to confluence on Transwell inserts and left unstimulated (Unstim) or stimulated with 300 kilounits (kU)/ml human IL2 or 30 ng/ml human TNFα for 24 h as indicated. Concurrent with stimulation, a portion of the Transwell inserts were treated with species-specific neutralizing antibodies against IL6 and MCP1 as indicated. Shown are representative permeability tracings (upper panel) and quantitative representation of all permeability tracings recorded at 120 min (bottompanel). To assess permeability, 10-kDa FITC-dextran was added to the top chamber of each insert, and fluorescence in the lower chamber was measured at the indicated times. Error bars represent mean ± S.D. of -fold change relative to the unstimulated control from five independent experiments performed in at least duplicate; p values shown were determined by an unpaired t test with Welch's correction of the area under the curves from each individual experiment (*, $p < 0.05$; **, $p < 0.005$). B, the loss of cell border adherens junctions documented by immunofluorescence of VE-cadherin (VE-cad) and p120 following agonist stimulation. hCMEC/D3 cells were grown to confluence and then left unstimulated or stimulated with 300 kilounits/ml human IL2 or 30 ng/ml human TNFα for 24 h. Cells were immunostained with anti-p120 antibodies (red) and anti-VE-cadherin antibodies (green). Nuclei were counterstained with DAPI (blue). Arrows indicate openings between neighboring cells and disruption of both proteins at the cell membrane in agonist-stimulated human BMECs. Magnification, X63; scale bars, 5 μm. C, agonist-induced expression of cytokine IL6 and chemokine MCP1 in hCMEC/D3 cell monolayer lining Transwell inserts. The hCMEC/D3 cell activation state was assessed prior to initiation of the permeability assay utilizing identical cells for multiple analyses. Cells were grown to confluence on Transwell inserts and left unstimulated or stimulated with 300 kilounits/ml human IL2 or 30 ng/ml human TNFα for 24 h as indicated. The supernatants were collected and analyzed for cytokine/chemokine production prior to addition of FITC-dextran for permeability analysis. Error bars represent mean ± S.D. of four independent experiments performed in technical duplicates or triplicates. Statistical significance was determined by unpaired t test with Welch's correction (*, $p < 0.05$; ***, $p < 0.0005$). RFU, relative fluorescence units.

dles compared with thin F-actin fibers sparsely crossing the cell body in unstimulated controls. Moreover, agonist-induced cell loss due to detachment and apoptosis was documented (Fig. 6B). Agonist stimulation resulted in significantly higher levels of cellular detachment and apoptosis in human and murine BMECs. Detached circulating endothelial cells have been described in a number of human diseases as well as in animal models of vascular injury (43, 44).

IL2 Changes the Composition of the AJ Complex—The striking disruption of the AJ protein complex following IL2 stimulation as demonstrated by immunostaining led us to analyze changes in AJ protein complex composition. In a series of co-immunoprecipitation experiments, we demonstrated that IL2-induced activation of BMECs results in a loss of interaction between VE-cadherin and p120 as reflected by their ratio (Fig. 7A). β-Catenin also binds to VE-cadherin, stabilizing the complex and allowing its interaction with F-actin. Loss of both p120 and β-catenin leads to destabilization of adherens junctions and endocytosis of VE-cadherin (12, 14, 42). Indeed, the VE-cadherin ·β-catenin complex is also altered due to IL2 activation in both human and murine BMECs (Fig. 7B). Thus, IL2-induced dissociation of the AJ complex documented by co-immunoprecipitation explains the loss of VE-cadherin immunostaining at cellular borders seen in agonist-stimulated BMECs (Figs. 4B and 5B).

IL2-induced Phosphorylation of VE-cadherin—We next analyzed the mechanism by which VE-cadherin and its associated adaptor proteins (p120 and β-catenin) are dissociated upon IL2 stimulation. Post-translational modifications, such as phosphorylation events, contribute to destabilization of the AJ complex and loss of endothelial barrier function in various endothelial cell subsets (14, 16, 17, 45). Indeed, IL2 evoked a significant increase in Tyr-685 phosphorylation of VE-cadherin in these cells (Fig. 8A). This process was time-dependent with maximal phosphorylation levels reached between 6 and 24 h. Consistent with more robust activation and increased permeability recorded in murine bEnd.3 cells, we noted higher VE-cadherin phosphorylation than in human hCMEC/D3 cells. Thus, IL2-induced phosphorylation of VE-cadherin leads to the destabilization of the AJ complex most likely through dissociation of VE-cadherin from its adaptor proteins as documented above (Fig. 7, A and B).

IL2-induced Loss of SHP2 Phosphatase—SHP2 phosphatase counteracts VE-cadherin phosphorylation, thereby contributing to the maintenance of lung microvascular endothelial barrier function (9, 15, 46). We found a significant decrease in expression of SHP2 phosphatase in IL2-stimulated BMECs that paralleled increased phosphorylation of VE-cadherin (Fig. 8B). SHP2 protein levels were reduced by 40–50% in both human and murine BMECs following IL2 stimulation. In contrast, observed transcript levels of SHP2 phosphatase remained at the

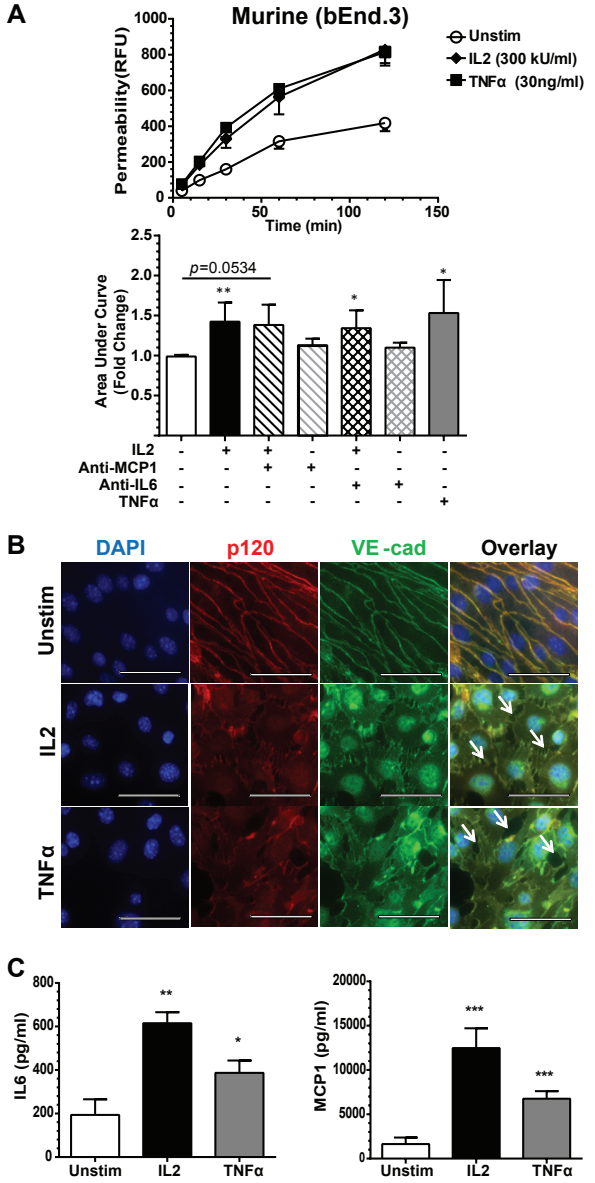

FIGURE 5. IL2-induced permeability and expression of proinflammatory mediators in murine BMEC monolayer. A, murine (bEnd.3) cells were grown to confluence on Transwell inserts and left unstimulated (Unstim) or stimulated for 24 h with 300 kilounits (kU)/ml murine IL2 or 30 ng/ml murine TNFα as indicated. Concurrent with stimulation, a portion of the Transwell inserts were treated with species-specific neutralizing antibodies against IL6 and MCP1 as indicated. Shown are representative permeability tracings (upper panel) and quantitative representation of all permeability tracings recorded at 120 min (bottom panel). To assess permeability, 10-kDa FITC-dextran was added to the top chamber of each insert, and fluorescence in the lower chamber was measured at the indicated times. Error bars represent mean $\pm$ S.D. of -fold change relative to the unstimulated control from at least three independent experiments performed in at least duplicate; p values shown were determined by unpaired t test with Welch's correction of the area under the curves from each individual experiment (*, $p < 0.05$; **, $p < 0.005$). B, the loss of cell border adherens junctions documented by immunofluorescence of VE-cadherin (VE-cad) and p120 following agonist stimulation. bEnd.3 cells were grown to confluence and then left unstimulated or stimulated with 300 kilounits/ml murine IL2 or 30 ng/ml murine TNFα for 24 h. Cells were immunostained with anti-p120 antibodies (red) and anti-VE-cadherin antibodies (green). Nuclei were counterstained with DAPI (blue). Arrows indicate openings between neighboring cells and disruption of both proteins at the cell membrane in agonist-stimulated murine BMECs. Magnification, X63; scale bars, 5 μm. C, agonist-induced expression of cytokine IL6 and chemokine MCP1 in bEnd.3 cell monolayer lining Transwell inserts. bEnd.3 cell activation state was assessed prior to initiation of the permeability assay utilizing identical cells for multiple analyses. Cells were grown to confluence on Transwell inserts and left unstimulated or stimulated with 300 kilounits/ml murine IL2 or 30 ng/ml murine TNFα for 24 h as indicated. The supernatants were collected and analyzed for cytokine/chemokine production prior to addition of FITC-dextran for permeability analysis. Error bars represent mean $\pm$ S.D. of at least three independent experiments performed in duplicates or triplicates. Statistical significance was determined by unpaired t test with Welch's correction (*, $p < 0.05$; **, $p < 0.005$; ***, $p < 0.0005$). RFU, relative fluorescence units.

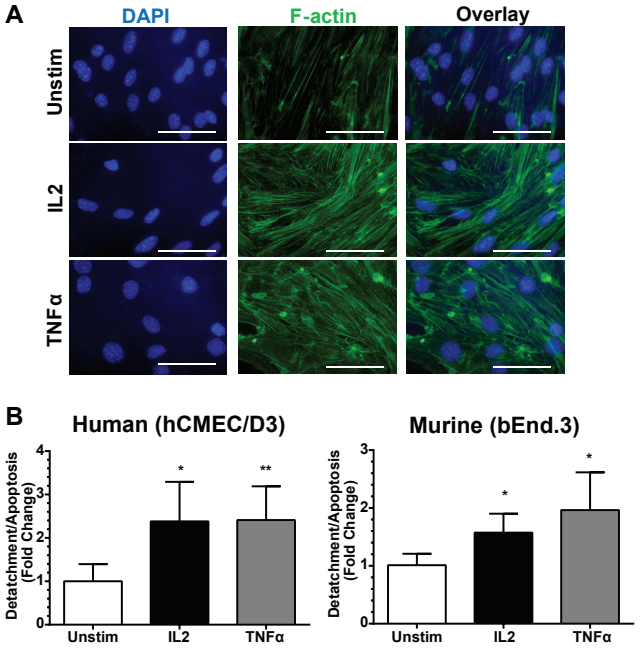

FIGURE 6. IL2-induced F-actin polymerization in BMECs and increased detachment following stimulation. A, F-actin polymerization changes in agonist-stimulated murine BMECs. bEnd.3 cells were grown to confluence and then left unstimulated (Unstim) or stimulated with 300 kilounits/ml murine IL2 or 30 ng/ml murine TNFα for 24 h. Cells were stained with Alexa Fluor 488-labeled phalloidin (green) to visualize F-actin. Nuclei were counterstained with DAPI (blue). Images are representative of at least three independent experiments. Magnification, $\times$63. Scale bars, 5 μm. B, increased BMEC detachment and apoptosis following agonist stimulation from Transwell inserts. Both human and murine BMECs were grown to confluence on Transwell permeability inserts and then left unstimulated or stimulated with species-specific IL2 (300 kilounits/ml) or TNFα (30 ng/ml) for 24 h. Supernatants were collected, and free floating endothelial cells detached from the Transwell membranes were counted. Error bars represent mean $\pm$ S.D. of at least three independent experiments performed in duplicates. Statistical significance was determined by unpaired t test with Welch's correction (*, $p < 0.05$; **, $p < 0.005$).

same level or were increased.[4] Thus, degradative loss of SHP2 phosphatase accompanies an increase in the phosphorylation state of AJ-associated proteins and destabilization of the complex.

Discussion

Taken together, our results decode the process through which IL2 activates BMECs and causes the loss of their barrier function. We found that human and murine BMECs constitutively express the intermediate affinity IL2 receptor comprising subunits β and γ (IL2R $\beta\gamma$), whereas subunit α (CD25) is induc-

[4] L. S. Wylezinski and J. Hawiger, unpublished data.

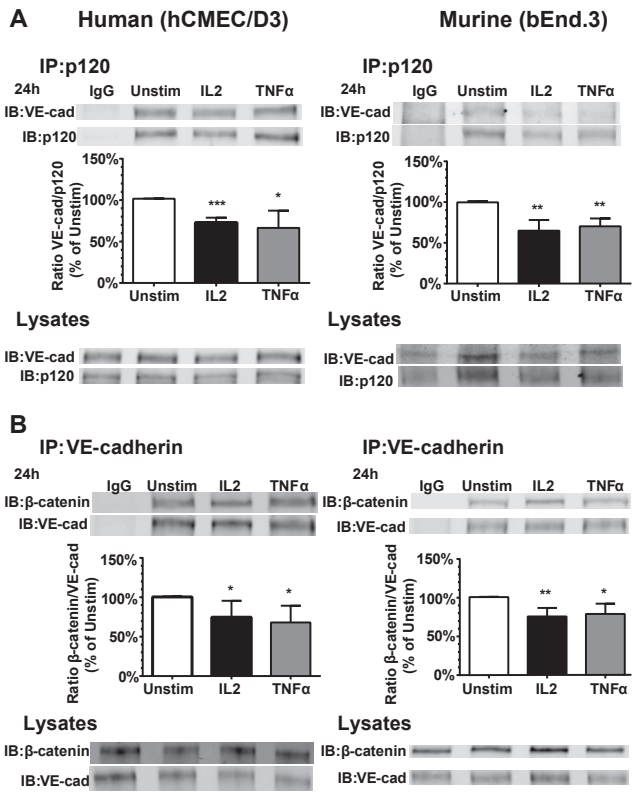

FIGURE 7. IL2-induced dissociation of the VE-cadherin·p120 and VE-cadherin·β-catenin complexes in human and murine BMECs. A, analysis of the VE-cadherin·p120 complex. Human (hCMEC/D3) and murine (bEnd.3) endothelial cells were grown to confluence and left unstimulated (Unstim) or stimulated with 300 kilounits/ml species-specific IL2 or 30 ng/ml species-specific TNFα for 24 h. Protein complexes in cell lysates precipitated with anti-p120 (IP) or treated with control IgG were quantified by immunoblotting (IB) with protein-specific antibodies. Cell lysates serve as input controls prior to immunoprecipitation. Error bars represent mean ± S.D. of at least three independent experiments. Statistical significance was determined by Student's t test (*, $p < 0.05$; **, $p < 0.005$; ***, $p < 0.0005$). B, analysis of the VE-cadherin·β-catenin complex. Human (hCMEC/D3) and murine (bEnd.3) endothelial cells were grown to confluence and left unstimulated or stimulated with 300 kilounits/ml species-specific IL2 or 30 ng/ml species-specific TNFα for 24 h. Protein complexes in cell lysates precipitated with anti-VE-cadherin (IP) or treated with control IgG were quantified by immunoblotting (IB) with protein-specific antibodies. Cell lysates serve as input controls prior to immunoprecipitation. Error bars represent mean ± S.D. of four independent experiments. Statistical significance was determined by Student's t test (*, $p < 0.05$; **, $p < 0.005$). VE-cad, VE-cadherin.

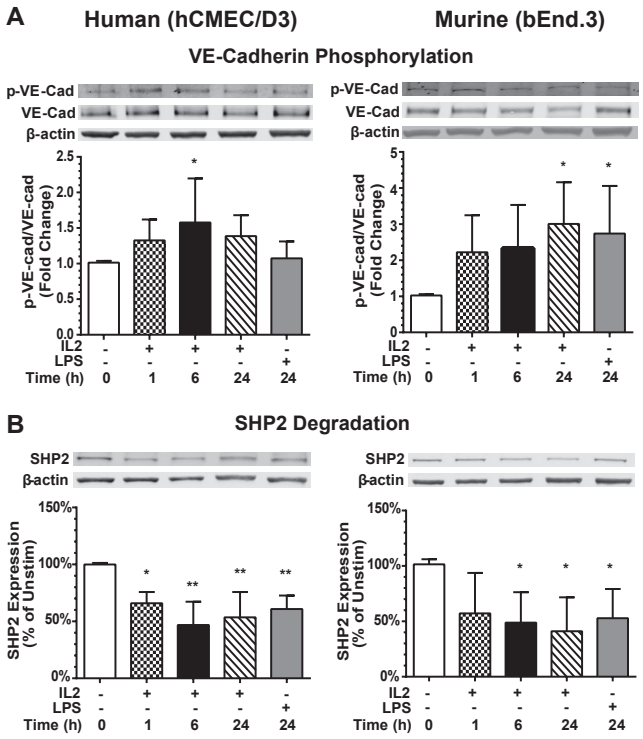

FIGURE 8. IL2-induced phosphorylation of VE-cadherin and degradation of SHP2 phosphatase in human and murine BMECs. A, analysis of VE-cadherin phosphorylation. Human (hCMEC/D3) and murine (bEnd.3) BMECs were left unstimulated or stimulated with 300 kilounits/ml species-specific IL2 or 1 μg/ml species-specific LPS for 24 h prior to isolation of cytosolic extracts. Samples were separated by SDS-PAGE and immunoblotted for the presence of total VE-cadherin (VE-cad) and Tyr-685 phosphorylated VE-cadherin (p-VE-cad). β-Actin is a loading control for cytosolic lysates. Quantification of signal is shown as a ratio of p-VE-cadherin to total VE-cadherin as -fold change compared with unstimulated control. Error bars represent mean ± S.D. of seven independent experiments. Statistical significance was determined using one-way ANOVA with Bonferroni correction for multiple comparisons for IL2 and an unpaired t test with Welch's correction for LPS (*, $p < 0.05$). B, analysis of SHP2 expression. Human (hCMEC/D3) and murine (bEnd.3) BMECs were left unstimulated (Unstim) or stimulated with 300 kilounits/ml species-specific IL2 or 1 μg/ml species-specific LPS for 24 h, and cytosolic extracts were isolated, separated by SDS-PAGE, and immunoblotted for the presence of SHP2. β-Actin is a loading control for cytosolic lysates. Normalized quantification of proteins is shown as a percent compared with the unstimulated control. Error bars represent mean ± S.D. of five independent experiments. Statistical significance was determined using one-way ANOVA with Bonferroni correction for multiple comparisons for IL2 and an unpaired t test with Welch's correction for LPS (*, $p < 0.05$; **, $p < 0.005$).

ibly expressed following IL2 stimulation. We documented that IL2-induced signaling in BMECs involves transcription factor NF κB through (i) degradation of NF κB inhibitor IκBα, (ii) phosphorylation of NF κB p65 (RelA), and (iii) its nuclear translocation. Subsequently, we demonstrated that among NF κB-regulated genes in BMECs two pleiotropic mediators of inflammation, cytokine IL6 and chemokine MCP1 (CCL2), are expressed following IL2 stimulation. Both IL6 and MCP1 are known inducers of endothelial instability (19, 20). IL2-evoked NF κB activation in lymphocytes is well known (21) but to our knowledge has not been reported previously in non-immune cells.

Furthermore, we demonstrated that IL2 causes the loss of barrier function of BMECs. Their stimulation disrupts the interaction of AJ complex proteins by inducing phosphorylation of VE-cadherin along with a concomitant decline in SHP2 phosphatase. Thus, IL2 changes the phenotype of BMECs from basal physiologic quiescence to an activated state, contributing to an inflammatory milieu affecting brain neurovascular units that comprise the BBB (1). As schematically depicted in Fig. 9, IL2 interaction with its intermediate affinity receptor expressed on brain microvascular endothelial cells activates signaling mediated by the transcription factor NF κB, master regulator of inflammation. This feed-forward loop results in expression of proinflammatory mediators exemplified by IL6 and MCP1. In parallel, IL2 destabilizes adherens junctions through phosphorylation of VE-cadherin and dissociation of its complex with p120 and β-catenin. This process is enhanced by an IL2-induced decrease in SHP2 phosphatase expression and stress fiber formation. Increased microvascular permeability ensues,

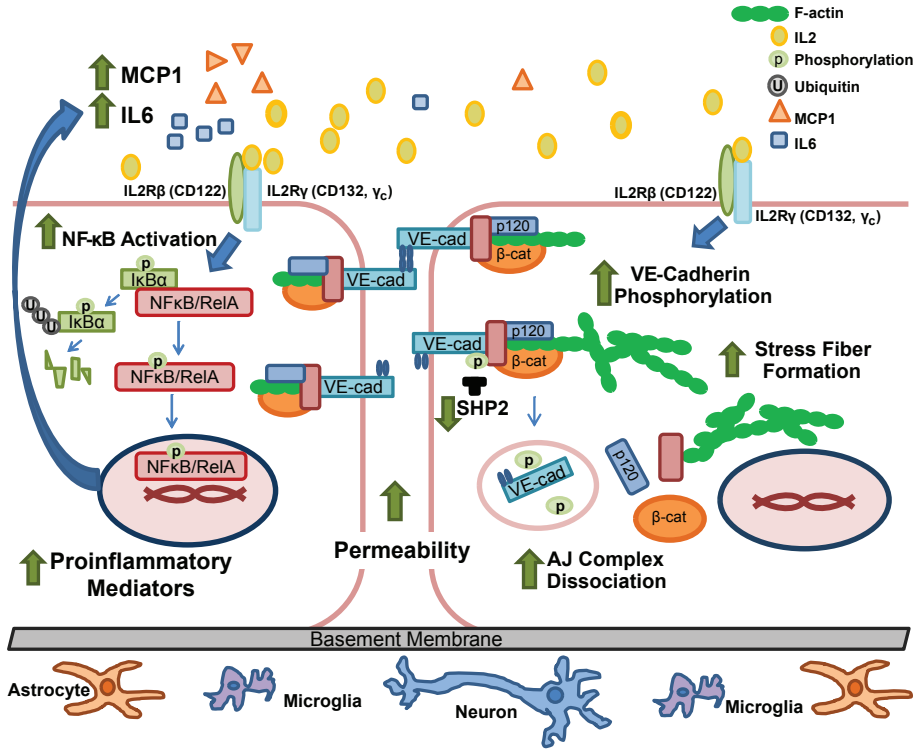

FIGURE 9. Diagrammatic depiction of IL2-induced activation of brain microvascular endothelial cells. IL2 interacts with the constitutively expressed intermediate affinity IL2R complex (IL2Rβ and IL2Rγ), leading to degradation of IκBα and freeing NFκB to be translocated to the nucleus. Therein NFκB initiates transcription of its target genes, including two proinflammatory mediators, namely cytokine IL6 and chemokine MCP1, culminating in a feed-forward enhancement of the inflammatory process (left). In parallel, IL2 induces destabilization of adherens junctions through an increase in VE-cadherin (VE-cad) phosphorylation concomitant with a decrease in SHP2 phosphatase protein levels. An elevated VE-cadherin phosphorylation state results in diminished interaction between the constituents of the adherens junction complex, in particular p120 and β-catenin (β-cat). Furthermore, activation of the brain microvascular endothelial monolayer leads to increased F-actin stress fiber formation. Loss of adherens junction interaction between adjoining endothelial cells increases monolayer permeability (right). Thus, IL2 interaction with its cognate receptor on BMECs leads to a shift from a quiescent to an "activated" phenotype of BMECs and an increase in endothelial monolayer permeability.

thereby explaining vascular leak syndrome and brain edema observed during IL2 cancer immunotherapy.

As was initially reported (3), neuropsychiatric effects of IL2 are both dose- and time -dependent during IL2 cancer immunotherapy. The latency period in development of IL2 neurotoxicity points to a cumulative effect and/or increased availability of the inducible IL2R α subunit (CD25). Therefore, in an effort to overcome this receptor limitation on naïve BMECs, we utilized a much higher agonist concentration range of IL2 in BMEC-based experiments.

Consistent with our study, expression of the IL2 receptor complex has been previously documented in pulmonary endothelial cells studied in a lung edema model (29, 41). Signaling through the IL2 receptor complex expressed on BMECs induces activation of the NF κB pathway similarly to the previously reported action of IL15, another member of the IL2 family. IL15 utilizes two subunits of IL2 receptor, IL2R β and IL2R γ, in addition to the IL15-binding α subunit (31).

The structural and functional integrity of brain microvascular endothelium is of paramount importance for maintaining the physiologic function of the BBB (1, 47). IL2 stimulation of BMECs caused significant and consistent increases in endothelial monolayer permeability. VE-cadherin, the transmembrane protein responsible for homotypic interactions between adjacent endothelial cells, is stabilized by a group of cytoplasmic adaptor proteins, including p120 and β-catenin. We established that IL2 stimulation of BMECs disrupts this interaction of AJ proteins (see Fig. 7). Consistent with our study, VE-cadherin distribution in pulmonary microvascular endothelial cells was altered by blood serum obtained from patients treated with IL2 (41). Although our investigation was focused on AJs, it is important to note that tight junctions are also involved in restricting paracellular permeability in endothelial cells. It is likely that activation of BMECs also influences the barrier function of tight junctions (48).

Our study offers a deeper understanding of the mechanism of IL2-induced brain edema, which along with lung edema limits the effectiveness of IL2 cancer immunotherapy. This IL2-evoked mechanism includes Tyr-685 phosphorylation of VE-cadherin in BMECs (Fig. 8A) that is rapid and persists up to 24 h poststimulation, coinciding with the loss of AJs at endothelial cell borders. It is noteworthy that other VE-cadherin phosphorylation sites have been described in regulating AJ stability, and they contribute to destabilization of the AJ complex in response to agonists other than IL2 (9, 16, 17, 49). Thus, more than one phosphorylation site within VE-cadherin, along with other IL2-induced signaling events, may contribute to increased endothelial permeability.

We also discovered that IL2 stimulation resulted in the loss of SHP2 protein in BMECs (Fig. 8B). SHP2 is one of several

phosphatases responsible for VE-cadherin dephosphorylation linked to maintenance of endothelial monolayer barrier function (9, 15, 46). The loss of SHP2 protein following IL2 stimulation enhances the phosphorylation status of VE-cadherin and/or its adaptor proteins and exacerbates the destabilization of AJs. Modification of protein-tyrosine phosphatases, including SHP2, as opposed to kinases has been proposed as the principal driver in modulating VE-cadherin phosphorylation levels (9).

In summary, our study provides new evidence that IL2 activates BMECs and leads to deterioration of their barrier function (see Fig. 9). A better understanding of IL2 action on brain microvascular endothelium, the cardinal component of the brain's neurovascular unit, may aid in the development of new measures to protect the central nervous system against IL2-induced VLS complicating high dose IL2 cancer immunotherapy and shed light on the role of IL2 in autoimmune inflammation associated with several brain diseases.

Author Contributions—L. S. W. designed and performed the experiments, analyzed the data, and prepared the manuscript. J. H. conceived the study and revised the manuscript. Both authors reviewed the results and approved the final version of the manuscript.

Acknowledgments—We thank Professor Babette Weksler (Weil-Cornell Medical College, New York, NY) and Professor Pierre-Olivier Couraud and Dr. Nacho Romero (Institute Cochin, INSERM, Paris, France) for generously providing human BMEC line hCMEC/D3 and for helpful comments concerning the manuscript. We also thank Alyssa Hasty, Roger Colbran, David G. Harrison, Luc Van Kaer, and Ruth Ann Veach for valuable and constructive comments during the course of this study. Additionally, we thank Jozef Zienkiewicz for insightful discussions and suggestions throughout the course of experimentation and preparation of this manuscript. Fluorescence microscopy and analysis were performed in part through the use of the Vanderbilt University Medical Center Cell Imaging Shared Resource (supported by National Institutes of Health Grants CA68485, DK20593, DK58404, DK59637, and EY08126). Flow cytometry experiments were performed in the Vanderbilt Medical Center (VMC) Flow Cytometry Shared Resource. The VMC Flow Cytometry Shared Resource is supported by the Vanderbilt Ingram Cancer Center (National Institutes of Health Grant P30 CA68485) and the Vanderbilt Digestive Disease Research Center (National Institutes of Health Grant DK058404).

References

1. Abbott, N. J., Rönnbäck, L., and Hansson, E. (2006) Astrocyte-endothelial interactions at the blood-brain barrier. Nat. Rev. Neurosci. 7, 41–53
2. Ridder, D. A., Lang, M. F., Salinin, S., Röderer, J. P., Struss, M., Maser-Gluth, C., and Schwaninger, M. (2011) TAK1 in brain endothelial cells mediates fever and lethargy. J. Exp. Med. 208, 2615–2623
3. Denicoff, K. D., Rubinow, D. R., Papa, M. Z., Simpson, C., Seipp, C. A., Lotze, M. T., Chang, A. E., Rosenstein, D., and Rosenberg, S. A. (1987) The neuropsychiatric effects of treatment with interleukin-2 and lymphokine-activated killer cells. Ann. Intern. Med. 107, 293–300
4. Rosenberg, S. A. (2014) IL-2: the first effective immunotherapy for human cancer. J. Immunol. 192, 5451–5458
5. Saris, S. C., Patronas, N. J., Rosenberg, S. A., Alexander, J. T., Frank, J., Schwartzentruber, D. J., Rubin, J. T., Barba, D., and Oldfield, E. H. (1989) The effect of intravenous interleukin-2 on brain water content. J. Neurosurg. 71, 169–174
6. Ichinose, K., Arima, K., Ushigusa, T., Nishino, A., Nakashima, Y., Suzuki, T., Horai, Y., Nakajima, H., Kawashiri, S. Y., Iwamoto, N., Tamai, M., Nakamura, H., Origuchi, T., Motomura, M., and Kawakami, A. (2015) Distinguishing the cerebrospinal fluid cytokine profile in neuropsychiatric systemic lupus erythematosus from other autoimmune neurological diseases. Clin. Immunol. 157, 114–120
7. Martins, T. B., Rose, J. W., Jaskowski, T. D., Wilson, A. R., Husebye, D., Seraj, H. S., and Hill, H. R. (2011) Analysis of proinflammatory and anti-inflammatory cytokine serum concentrations in patients with multiple sclerosis by using a multiplexed immunoassay. Am. J. Clin. Pathol. 136, 696–704
8. Gallo, P., Pagni, S., Piccinno, M. G., Giometto, B., Argentiero, V., Chiusole, M., Bozza, F., and Tavolato, B. (1992) On the role of interleukin-2 (IL-2) in multiple sclerosis (MS). IL-2-mediated endothelial cell activation. Ital. J. Neurol. Sci. 13, 65– 68
9. Hatanaka, K., Lanahan, A. A., Murakami, M., and Simons, M. (2012) Fibroblast growth factor signaling potentiates VE-cadherin stability at adherens junctions by regulating SHP2. PLoS One 7, e37600
10. Lampugnani, M. G., and Dejana, E. (2007) Adherens junctions in endothelial cells regulate vessel maintenance and angiogenesis. Thromb. Res. 120, Suppl. 2, S1–S6
11. Hawiger, J., Veach, R. A., and Zienkiewicz, J. (2015) New paradigms in sepsis: from prevention to protection of failing microcirculation. J. Thromb. Haemost. 13, 1743–1756
12. Abu Taha, A., and Schnittler, H. J. (2014) Dynamics between actin and the VE-cadherin/catenin complex: novel aspects of the ARP2/3 complex in regulation of endothelial junctions. Cell Adh. Migr. 8, 125–135
13. Xiao, K., Garner, J., Buckley, K. M., Vincent, P. A., Chiasson, C. M., Dejana, E., Faundez, V., and Kowalczyk, A. P. (2005) p120-catenin regulates clathrin-dependent endocytosis of VE-cadherin. Mol. Biol. Cell 16, 5141–5151
14. Potter, M. D., Barbero, S., and Cheresh, D. A. (2005) Tyrosine phosphorylation of VE-cadherin prevents binding of p120- and β-catenin and maintains the cellular mesenchymal state. J. Biol. Chem. 280, 31906–31912
15. Ukropec, J. A., Hollinger, M. K., Salva, S. M., and Woolkalis, M. J. (2000) SHP2 association with VE-cadherin complexes in human endothelial cells is regulated by thrombin. J. Biol. Chem. 275, 5983–5986
16. Orsenigo, F., Giampietro, C., Ferrari, A., Corada, M., Galaup, A., Sigismund, S., Ristagno, G., Maddaluno, L., Koh, G. Y., Franco, D., Kurtcuoglu, V., Poulikakos, D., Baluk, P., McDonald, D., Grazia Lampugnani, M., et al. (2012) Phosphorylation of VE-cadherin is modulated by haemodynamic forces and contributes to the regulation of vascular permeability in vivo. Nat. Commun. 3, 1208
17. Wessel, F., Winderlich, M., Holm, M., Frye, M., Rivera-Galdos, R., Vockel, M., Linnepe, R., Ipe, U., Stadtmann, A., Zarbock, A., Nottebaum, A. F., and Vestweber, D. (2014) Leukocyte extravasation and vascular permeability are each controlled in vivo by different tyrosine residues of VE-cadherin. Nat. Immunol. 15, 223–230
18. Greenwood, J., Heasman, S. J., Alvarez, J. I., Prat, A., Lyck, R., and Engelhardt, B. (2011) Review: leucocyte-endothelial cell crosstalk at the blood-brain barrier: a prerequisite for successful immune cell entry to the brain. Neuropathol. Appl. Neurobiol. 37, 24–39
19. Kempe, S., Kestler, H., Lasar, A., and Wirth, T. (2005) NF-κB controls the global pro-inflammatory response in endothelial cells: evidence for the regulation of a pro-atherogenic program. Nucleic Acids Res. 33, 5308–5319
20. Libermann, T. A., and Baltimore, D. (1990) Activation of interleukin-6 gene expression through the NF-κB transcription factor. Mol. Cell. Biol. 10, 2327–2334
21. Arima, N., Kuziel, W. A., Grdina, T. A., and Greene, W. C. (1992) IL-2-induced signal transduction involves the activation of nuclear NF-κB expression. J. Immunol. 149, 83–91
22. Weksler, B. B., Subileau, E. A., Perrière, N., Charneau, P., Holloway, K., Leveque, M., Tricoire-Leignel, H., Nicotra, A., Bourdoulous, S., Turowski, P., Male, D. K., Roux, F., Greenwood, J., Romero, I. A., and Couraud, P. O. (2005) Blood-brain barrier-specific properties of a human adult brain endothelial cell line. FASEB J. 19, 1872–1874

23. Montesano, R., Pepper, M. S., Möhle-Steinlein, U., Risau, W., Wagner, E. F., and Orci, L. (1990) Increased proteolytic activity is responsible for the aberrant morphogenetic behavior of endothelial cells expressing the middle T oncogene. Cell 62, 435–445
24. Livak, K. J., and Schmittgen, T. D. (2001) Analysis of relative gene expression data using real-time quantitative PCR and the $2(-\Delta\Delta C_T)$ method. Methods 25, 402–408
25. Qiao, H., Liu, Y., Veach, R. A., Wylezinski, L., and Hawiger, J. (2014) The adaptor CRADD/RAIDD controls activation of endothelial cells by proinflammatory stimuli. J. Biol. Chem. 289, 21973–21983
26. Middleton, J., Americh, L., Gayon, R., Julien, D., Mansat, M., Mansat, P., Anract, P., Cantagrel, A., Cattan, P., Reimund, J. M., Aguilar, L., Amalric, F., and Girard, J. P. (2005) A comparative study of endothelial cell markers expressed in chronically inflamed human tissues: MECA-79, Duffy antigen receptor for chemokines, von Willebrand factor, CD31, CD34, CD105 and CD146. J. Pathol. 206, 260–268
27. Sheibani, N., and Frazier, W. A. (1998) Down-regulation of platelet endothelial cell adhesion molecule-1 results in thrombospondin-1 expression and concerted regulation of endothelial cell phenotype. Mol. Biol. Cell 9, 701–713
28. Minami, Y., Kono, T., Miyazaki, T., and Taniguchi, T. (1993) The IL-2 receptor complex: its structure, function, and target genes. Annu. Rev. Immunol. 11, 245–268
29. Krieg, C., Létourneau, S., Pantaleo, G., and Boyman, O. (2010) Improved IL-2 immunotherapy by selective stimulation of IL-2 receptors on lymphocytes and endothelial cells. Proc. Natl. Acad. Sci. U.S.A. 107, 11906–11911
30. Ruiz-Medina, B. E., Ross, J. A., and Kirken, R. A. (2015) Interleukin-2 receptor β Thr-450 phosphorylation is a positive regulator for receptor complex stability and activation of signaling molecules. J. Biol. Chem. 290, 20972–20983
31. Stone, K. P., Kastin, A. J., and Pan, W. (2011) NF κB is an unexpected major mediator of interleukin-15 signaling in cerebral endothelia. Cell. Physiol. Biochem. 28, 115–124
32. Cordle, S. R., Donald, R., Read, M. A., and Hawiger, J. (1993) Lipopolysaccharide induces phosphorylation of MAD3 and activation of c-Rel and related NF-κB proteins in human monocytic THP-1 cells. J. Biol. Chem. 268, 11803–11810
33. Donald, R., Ballard, D. W., and Hawiger, J. (1995) Proteolytic processing of NF-κB/IκB in human monocytes. ATP-dependent induction by pro-inflammatory mediators. J. Biol. Chem. 270, 9–12
34. Cooper, J. T., Stroka, D. M., Brostjan, C., Palmetshofer, A., Bach, F. H., and Ferran, C. (1996) A20 blocks endothelial cell activation through a NF-κB-dependent mechanism. J. Biol. Chem. 271, 18068–18073
35. Wang, D., Westerheide, S. D., Hanson, J. L., and Baldwin, A. S., Jr. (2000) Tumor necrosis factor α-induced phosphorylation of RelA/p65 on Ser^{529} is controlled by casein kinase II. J. Biol. Chem. 275, 32592–32597
36. Tieu, B. C., Lee, C., Sun, H., Lejeune, W., Recinos, A., 3rd, Ju, X., Spratt, H., Guo, D. C., Milewicz, D., Tilton, R. G., and Brasier, A. R. (2009) An adventitial IL-6/MCP1 amplification loop accelerates macrophage-mediated vascular inflammation leading to aortic dissection in mice. J. Clin. Investig. 119, 3637–3651
37. Desai, T. R., Leeper, N. J., Hynes, K. L., and Gewertz, B. L. (2002) Interleukin-6 causes endothelial barrier dysfunction via the protein kinase C pathway. J. Surg. Res. 104, 118–123
38. Jee, Y., Yoon, W. K., Okura, Y., Tanuma, N., and Matsumoto, Y. (2002) Upregulation of monocyte chemotactic protein-1 and CC chemokine receptor 2 in the central nervous system is closely associated with relapse of autoimmune encephalomyelitis in Lewis rats. J. Neuroimmunol. 128, 49–57
39. Stamatovic, S. M., Keep, R. F., Kunkel, S. L., and Andjelkovic, A. V. (2003) Potential role of MCP-1 in endothelial cell tight junction 'opening': signaling via Rho and Rho kinase. J. Cell Sci. 116, 4615–4628
40. Brasier, A. R. (2010) The nuclear factor-κB-interleukin-6 signalling pathway mediating vascular inflammation. Cardiovasc. Res. 86, 211–218
41. Kim, D. W., Zloza, A., Broucek, J., Schenkel, J. M., Ruby, C., Samaha, G., and Kaufman, H. L. (2014) Interleukin-2 alters distribution of CD144 (VE-cadherin) in endothelial cells. J. Transl. Med. 12, 113
42. Rajput, C., Kini, V., Smith, M., Yazbeck, P., Chavez, A., Schmidt, T., Zhang, W., Knezevic, N., Komarova, Y., and Mehta, D. (2013) Neural Wiskott-Aldrich syndrome protein (N-WASP)-mediated p120-catenin interaction with Arp2-actin complex stabilizes endothelial adherens junctions. J. Biol. Chem. 288, 4241–4250
43. Dignat-George, F., and Sampol, J. (2000) Circulating endothelial cells in vascular disorders: new insights into an old concept. Eur. J. Haematol. 65, 215–220
44. Westlin, W. F., and Gimbrone, M. A., Jr. (1993) Neutrophil-mediated damage to human vascular endothelium. Role of cytokine activation. Am. J. Pathol. 142, 117–128
45. Chang, S. F., Chen, L. J., Lee, P. L., Lee, D. Y., Chien, S., and Chiu, J. J. (2014) Different modes of endothelial-smooth muscle cell interaction elicit differential β-catenin phosphorylations and endothelial functions. Proc. Natl. Acad. Sci. U.S.A. 111, 1855–1860
46. Grinnell, K. L., Casserly, B., and Harrington, E. O. (2010) Role of protein tyrosine phosphatase SHP2 in barrier function of pulmonary endothelium. Am. J. Physiol. Lung Cell Mol. Physiol. 298, L361–L370
47. Lippmann, E. S., Azarin, S. M., Kay, J. E., Nessler, R. A., Wilson, H. K., Al-Ahmad, A., Palecek, S. P., and Shusta, E. V. (2012) Derivation of blood-brain barrier endothelial cells from human pluripotent stem cells. Nat. Biotechnol. 30, 783–791
48. Taddei, A., Giampietro, C., Conti, A., Orsenigo, F., Breviario, F., Pirazzoli, V., Potente, M., Daly, C., Dimmeler, S., and Dejana, E. (2008) Endothelial adherens junctions control tight junctions by VE-cadherin-mediated upregulation of claudin-5. Nat. Cell Biol. 10, 923–934
49. Adam, A. P., Sharenko, A. L., Pumiglia, K., and Vincent, P. A. (2010) Src-induced tyrosine phosphorylation of VE-cadherin is not sufficient to decrease barrier function of endothelial monolayers. J. Biol. Chem. 285, 7045–7055

APPENDIX

B. “The Adaptor CRADD/RAIDD Controls Activation of Endothelial Cells by Proinflammaroy Stimuli.” By Huan Qiao, Yan Liu, Ruth Ann Veach, **Lukasz Wylezinski** and Jacek Hawiger, *Journal of Biological Chemistry*, 2014. **289,** 21973-21983.

THE JOURNAL OF BIOLOGICAL CHEMISTRY VOL. 289, NO. 32, pp. 21973–21983, August 8, 2014

The Adaptor CRADD/RAIDD Controls Activation of Endothelial Cells by Proinflammatory Stimuli *

Received for publication, June 11, 2014 Published, JBC Papers in Press, June 23, 2014, DOI 10.1074/jbc.M114.588723

Huan Qiao ‡, Yan Liu ‡, Ruth A. Veach ‡, Lukasz Wylezinski §, and Jacek Hawiger ‡§1

From the Departments of ‡Medicine, Division of Allergy, Pulmonary and Critical Care Medicine and §Molecular Physiology and Biophysics, Vanderbilt University School of Medicine, Vanderbilt University Medical Center, Nashville, Tennessee 37232

Background: The role of CRADD in endothelial cells is unknown.
Results: CRADD attenuates responses to proinflammatory agonists in endothelial cells and stabilizes their barrier function.
Conclusion: CRADD plays a pivotal role in maintaining the integrity of the endothelial barrier.
Significance: Understanding the role of CRADD as a physiologic rheostat of perturbed endothelial cells informs development of CRADD-based measures to stabilize endothelial integrity.

A hallmark of inflammation, increased vascular permeability, is induced in endothelial cells by multiple agonists through stimulus-coupled assembly of the CARMA3 signalosome, which contains the adaptor protein BCL10. Previously, we reported that BCL10 in immune cells is targeted by the "death" adaptor CRADD/RAIDD (CRADD), which negatively regulates nuclear factor κB (NF κB)-dependent cytokine and chemokine expression in T cells (Lin, Q., Liu, Y., Moore, D. J., Elizer, S. K., Veach, R. A., Hawiger, J., and Ruley, H. E. (2012) J. Immunol. 188, 2493–2497). This novel anti-inflammatory CRADD-BCL10 axis prompted us to analyze CRADD expression and its potential anti-inflammatory action in non-immune cells. We focused our study on microvascular endothelial cells because they play a key role in inflammation. We found that CRADD-deficient murine endothelial cells display heightened BCL10-mediated expression of the pleotropic proinflammatory cytokine IL-6 and chemokine monocyte chemoattractant protein-1 (MCP-1/CCL2) in response to LPS and thrombin. Moreover, these agonists also induce significantly increased permeability in cradd $^{-/-}$, as compared with cradd $^{+/+}$, primary murine endothelial cells. CRADD-deficient cells displayed more F-actin polymerization with concomitant disruption of adherens junctions. In turn, increasing intracellular CRADD by delivery of a novel recombinant cell-penetrating CRADD protein (CP-CRADD) restored endothelial barrier function and suppressed the induction of IL-6 and MCP-1 evoked by LPS and thrombin. Likewise, CP-CRADD enhanced barrier function in CRADD-sufficient endothelial cells. These results indicate that depletion of endogenous CRADD compromises endothelial barrier function in response to inflammatory signals. Thus, we define a novel function for CRADD in endothelial cells as an inducible suppressor of BCL10, a key mediator of responses to proinflammatory agonists.

Inflammation represents a fundamental mechanism of diseases caused by microbial, autoimmune, metabolic, and physical insults. For example, the action of microbial insults on endothelial cells in severe microbial infections evolving into sepsis leads to endothelial dysfunction that contributes to major organ failure, disseminated intravascular coagulation, and acute respiratory distress syndrome (1). To counteract the deleterious action of proinflammatory cytokines and chemokines, an intracellular negative feedback system has evolved to limit the duration and strength of proinflammatory signaling. This system is comprised of intracellular physiologic proteins that control excessive inflammatory responses. They include interleukin-1 receptor-associated kinase (IRAK) [2]-M, an inhibitory member of the IRAK family, the inhibitor of nuclear factor κB (NF κB) transcription factors IκB, the suppressors of cytokine signaling (SOCS) proteins that inhibit activated STAT transcription factors, and the ubiquitin-modifying enzyme A20 (2–5). Recently, we added the "death" adaptor caspase and receptor interacting protein adaptor with death domain/receptor interacting protein-associated ICH-1/CED-3 homologous protein with a death domain (CRADD/RAIDD), hereafter designated as CRADD, to this list. CRADD negatively regulates NF κB-dependent cytokine and chemokine expression in T cells by targeting the NH_2-terminal caspase recruitment domain (CARD) of B-cell CLL/Lymphoma 10 (BCL10) (6). In immune cells, the CARD of BCL10 functions as an oligomerization region and interacts with the CARD of the CARD membrane-associated guanylate kinase (CARMA) 1 (6, 7), which is required for activation of the NF κB pathway (8–12). In non-immune cells, such as endothelial cells, a CARMA3 signalo-

* This work was supported, in whole or in part, by National Institutes of Health Grants HL069452, HL085833, and AA015752 (to J. H.) from the United States Public Health Service, Ruth Kirschstein Institutional National Service Award T32 HL069765 (to H. Q.), the Vanderbilt Immunotherapy Program and Department of Medicine, and Vanderbilt Clinical and Translational Science Award UL1TR000445.

[1] To whom correspondence should be addressed: Dept. of Medicine, Division of Allergy, Pulmonary and Critical Care Medicine, Vanderbilt University Medical Center, 1161 21st Ave. S., Nashville, TN 37232-2650. Tel.: 615-343-8280; Fax: 615-343-8278; E-mail: jacek.hawiger@vanderbilt.edu.

[2] The abbreviations used are: IRAK, interleukin-1 receptor-associated kinase; BCL10, B-cell CLL/lymphoma 10; CARD caspase-recruitment domain; CARMA, CARD membrane-associated guanylate kinase; CP, cell-penetrating; CRADD, caspase and receptor interacting protein adaptor with Death domain; K/D, knockdown; LMEC, lung microvascular endothelial cells; MALT1, mucosa-associated lymphoid tissue lymphoma translocation protein 1; MCP-1, monocyte chemoattractant protein-1; NFκB, nuclear factor κB; PAR-1, protease-activated receptor 1; RAIDD, receptor interacting protein-associated ICH-1/CED-3 homologous protein with a Death domain; SOCS, suppressor of cytokine signaling; TBP, TATA-binding protein; TLR4, Toll-like receptor 4; TRAF6, TNF receptor-associated factor 6; VE-cadherin, vascular endothelial cadherin.

some containing BCL10 and mucosa-associated lymphoid tissue lymphoma translocation protein 1 (MALT1), operates to regulate the NF κB signaling pathway (13, 14). Disruption of the CARMA3 signalosome by genetic deletion of Bcl10 leads to dramatic reduction of vascular inflammation, illustrating that BCL10 is an essential component of the signaling complex (15).

The CARMA3 signalosome also modulates endothelial barrier function in response to proinflammatory agonists that induce increased vascular permeability (16). Induction of vascular permeability causes swelling, one of the four classic signs of inflammation, due to the action of proinflammatory agonists sensed by their cognate receptors expressed on microvascular endothelial cells (17). The CARMA3 signalosome amplifies signaling in response to proinflammatory agonists and mediates stimulus-dependent nuclear reprogramming (13–15, 18), which depends on transcription factors NF κB and AP-1 (13, 16, 18, 19). Thus, the CARMA3 signalosome plays a pivotal role in shifting microvascular endothelial cells from a resting to activated state, integrating signaling pathways evoked by recognition of diverse agonists. This signaling promulgates an inflammatory response, based in part on disruption of endothelial barrier function by altering cell-cell junctions that include adherens junctions and tight junctions (20, 21). These mainstays of endothelial monolayer integrity dynamically guard barrier function in major organs that contain an extensive network of microcirculation, such as lungs, kidneys, liver, and brain. Vascular endothelial cadherin (VE-cadherin) is a strictly endothelial specific cell adhesion molecule and the major determinant of endothelial cell contact integrity. Its adhesive function requires association with the cytoplasmic catenin protein p120 (22). LPS and thrombin induce F-actin reorganization and subsequent reductions in VE-cadherin at endothelial cell junctions, resulting in increased vascular permeability (22–24). The target of CRADD, BCL10, and its effector, NF κB, have been implicated in mediating these changes (25–27).

Here we analyzed the potential role of CRADD in endothelial cell homeostasis by employing three approaches: (i) reduction of CRADD expression in murine endothelial cells with shRNA, (ii) analysis of microvascular endothelial cells isolated from CRADD-deficient mice (6), and (iii) intracellular delivery of a novel recombinant cell-penetrating CRADD protein homolog (CP-CRADD) to CRADD-deficient and sufficient endothelial cells. We documented a protective role for CRADD in maintaining the permeability barrier of primary lung microvascular endothelial cells (LMEC) by demonstrating increased agonist-induced permeability of cradd$^{-/-}$ LMEC monolayers compared with cradd$^{+/+}$ LMEC monolayers. Moreover, treatment with CP-CRADD restored barrier function in endothelial monolayers of human and murine cells challenged with proinflammatory agonists.

EXPERIMENTAL PROCEDURES

Mice—Wild-type cradd$^{+/+}$ and knock-out cradd$^{-/-}$ mice were generated and maintained as previously described (6). All work with animals was carried out in strict accordance with the recommendations in the Guide for the Care and Use of Laboratory Animals of the National Institutes of Health, and approved by the Vanderbilt University Institutional Animal Care and Use Committee.

Endothelial Cell Culture—Primary human umbilical vein endothelial cells were purchased from ScienCell and cultured in ECM (ScienCell). Primary murine LMEC were isolated from cradd$^{+/+}$ and cradd$^{-/-}$ mice using a lung dissociation kit and purified by immunomagnetic separation, with anti-CD45-conjugated and anti-CD31-conjugated MicroBeads according to protocols provided by the manufacturer (Miltenyi Biotec), then cultured in collagen-coated tissue culture dishes with EBM-2 (Lonza) supplemented with 5% heat-inactivated FBS, 25 μg/ml of endothelial mitogen (Biomedical Technologies), and 1% penicillin/streptomycin solution (Mediatech). The human lung microvascular endothelial cell line HPMEC-ST1.6R was generously provided by C. J. Kirkpatrick (28) and cultured in M199 (Mediatech) supplemented with 10% heat-inactivated FBS, 25 μg/ml of endothelial mitogen, 50 μg/ml of heparin (Sigma), and 1% penicillin/streptomycin. The endothelial cell line LEII (mouse lung capillary) was a kind gift from T. Maciag (29). EA.hy926, EOMA, and SVEC4 –10 cell lines were purchased from ATCC. LEII and cell lines from ATCC were cultured in DMEM (Mediatech) supplemented with 10% heat-inactivated FBS and 1% penicillin/streptomycin.

Immunoprecipitation and Immunoblot Analysis—Antibodies to CRADD (Proteintech Group), BCL10 and NF κB p65/RelA (Santa Cruz) were used for immunoblot analyses. GAPDH, β-actin, or TATA-binding protein (TBP) antibodies (Abcam) were used for normalization of cytosolic and nuclear extracts as indicated in the figure legends. Complexes were immunoprecipitated from cell lysates with antibody to IRAK-1 (Santa Cruz) and protein A/G-agarose beads (Thermo) then analyzed by quantitative immunoblotting using antibodies to IRAK-1 and BCL10. All immunoblots were analyzed with the LI-COR Odyssey Infrared Imaging System as previously described (6, 30).

Lentiviral shRNA Knockdown of CRADD and BCL10 in Endothelial Cells—Lentiviral packaging and shRNA transduction were performed as previously described (31). CRADD and BCL10 knockdown (K/D) efficiency was assessed at the transcript and protein level after 96 h, when shRNA-mediated knockdown experiments were performed.

RT-PCR Analysis—Total RNA was isolated for RT-PCR analysis using TRIzol reagent (Invitrogen) and reverse-transcribed using the iScript cDNA synthesis kit (Bio-Rad). Targets were amplified by PCR using PCR Master Mix (Promega) with specific primers listed in Table 1 for the indicated protein mRNAs. PCR products were separated on 1% agarose gels. Ethidium bromide-stained gels were imaged on a Gel Doc EZ Imager (Bio-Rad) and analyzed with Image Lab 5.0 software to quantify bands.

Cytokine/Chemokine Assays—Cytokines and chemokines in tissue culture media were assayed by cytometric bead array (BD Biosciences) in the Vanderbilt Flow Cytometry Core according to the manufacturer's instructions and as described previously (6). In some experiments, cells were treated with CP-CRADD or non-CP-CRADD before stimulation.

Immunofluorescence Staining and Fluorescence Microscopy—LMEC or LEII cells were plated into Lab-Tek II chamber slides

TABLE 1
Oligonucleotide PCR primer sequences used in the current study

Gene		Primer sequences (5′ to 3′)
hCRADD	Forward	5-AGTACTCCGCTCACTTCGC-3
	Reverse	5-CTGCAGGCAGGTCGGTCAT-3
mCRADD	Forward	5-GAAGAAATGGAAGCCAGAG-3
	Reverse	5-CTGTAGGCAGCTCGGCTG-3
hBCL10	Forward	5-CCCGCTCCGCCTCCTCTCCTT-3
	Reverse	5-GGCGCTTCTTCCGGGTCCG-3
mBCL10	Forward	5-GAGAGCATCCACTGTCATG-3
	Reverse	5-GGAGAAACATCTCACTTGAG-3
mTNF- α	Forward	5-GCGACGTGGAACTGGCAGAAG-3
	Reverse	5-GGTACAACCCATCGGCTGGCA-3
mIL-6	Forward	5-TTCCATCCAGTTGCCTTCTTGG-3
	Reverse	5-CTTCATGTACTCCAGGTAG-3
mIL-1 α	Forward	5-CTCTAGAGCACCATGCTACAGAC-3
	Reverse	5-TGGAATCCAGGGGAAACACTG-3
mβ-actin	Forward	5-TTCTTTGCAGCTCCTTCGTTGCCG-3
	Reverse	5-TGGATGGCTACGTACATGGCTGGG-3

(Thermo Scientific) and stimulated with LPS or thrombin (Sigma) as indicated. After stimulation, cells were fixed in 4% paraformaldehyde (Electron Microscopy Sciences), then washed in PBS and permeabilized with 0.1% Triton X-100 (Invitrogen). For immunofluorescence staining, cells were blocked with 5% normal goat serum (Jackson ImmunoResearch) before overnight incubation at 4 °C with antibodies to NF κB p65/RelA (Abcam) or VE-Cadherin and p120 (Santa Cruz) followed by incubation with Alexa 488- (Invitrogen) or Cy-3-labeled (Jackson ImmunoResearch) secondary antibodies. Alexa 488-labeled phalloidin (Cytoskeleton, Inc.) was used to visualize F-actin polymerization in permeabilized cells. Slides were mounted with ProLong Gold Antifade reagent containing DAPI (Invitrogen) to stain nuclei. Images were captured with MetaMorph software on an Axioplan widefield microscope in the Vanderbilt Cell Imaging Core facility using $\times$40 or $\times$63 oil immersion objectives, as indicated.

Design, Preparation, and Intracellular Delivery of Recombinant CRADD Proteins—Design, production, and analysis of recombinant murine CRADD proteins followed our previously published protocols (30, 32). Plasmid constructs for wild type (non-CP-CRADD) and cell penetrating (CP-CRADD) were produced using standard molecular biology techniques. CP-CRADD contains a membrane-translocating motif that enables it to cross the plasma membrane. Proteins were isolated from bacterial inclusion bodies using previously described protocols (30, 32) and dialyzed into DMEM supplemented with 1% penicillin/streptomycin and 66 μM PEG3350. LPS content in all recombinant protein preparations was below the level of detection (0.06 EU/ml) by Limulus assay (Endosafe, Charles River), performed according to the manufacturer's instructions. To confirm intracellular delivery of CP-CRADD, human ST1.6R endothelial cells were treated for 1 h with equimolar concentrations (10 μM) of non-CP-CRADD and CP-CRADD or medium alone. The cells were washed with warm DMEM without serum and treated with 7 μg/ml of proteinase K (Sigma) for 10 min to remove proteins attached to the cell surface, followed by a wash in warm DMEM supplemented with 5% FBS. Pelleted cells were lysed in RIPA buffer supplemented with protease inhibitors (Sigma). Lysates were cleared by centrifugation then analyzed by immunoblotting using antibodies to CRADD and β-actin. Although some membrane-associated non-CP-CRADD is detected by immunoblotting, CP-CRADD is 2–3-fold more abundant when recombinant proteins are normalized to endogenous CRADD or β-actin.

Endothelial Cell Permeability—LMEC (1×10^4, passage 3 or 4) isolated from cradd$^{+/+}$ and cradd$^{-/-}$ mice, or human ST1.6R cells were seeded onto 24-well Transwell insets (Costar) pre-coated with type I collagen and incubated until confluent. Confluent monolayers were serum-starved in 0.5% heat-inactivated FBS for 24 h, then left unstimulated or stimulated with vascular permeability inducers as indicated. In some experiments, cells were treated with CP-CRADD or non-CP-CRADD before stimulation. Monolayer permeability was assessed by detection of FITC-dextran in the lower chamber at various times after addition of 1 mg/ml of 10-kDa FITC-dextran or the molar equivalent of 70-kDa FITC-dextran (Invitrogen) to the top chamber. We determined that the relative fluorescence of 70-kDa FITC-dextran is ~6-fold greater than that of 10-kDa FITC-dextran at equal molarities.

Statistical Analyses—Data analysis and statistical calculations were performed using Prism (GraphPad). Cytokine and chemokine levels in cultured cell supernatants, and nuclear levels of p65/RelA were compared using an unpaired t test with Welch's correction for unequal standard deviations. Quantification of RT-PCR bands was used to calculate the fold-change in transcripts compared with non-transduced cells stimulated with LPS or thrombin and statistical differences were determined by Student's t test. For permeability experiments, the p values shown compare the area under the curve calculated for each condition, analyzed by an unpaired t test with Welch's correction for unequal standard deviations. Additional evaluation of permeability curves by repeated measures two-way analysis of variance resulted in a p value of <0.0001 for all indicated comparisons. In all experiments, a p value of <0.05 was considered significant.

RESULTS

The outcome of inflammation depends on the balance between proinflammatory mediators and anti-inflammatory suppressors. Our prior studies in immune cells (T lymphocytes) established that CRADD inhibits pro-inflammatory signaling at the level of BCL10-dependent NF κB activation (6, 7). We investigated the possibility of a similar function for CRADD in non-immune cells (endothelial cells) in which BCL10 plays a pivotal role in the CARMA3 signalosome-dependent activation of the NF κB pathway.

Expression of CRADD in Endothelial Cells—We hypothesized that CRADD could negatively regulate BCL10, an essential component of the CARMA3 signalosome assembled in endothelial cells following their response to proinflammatory stimuli. To test this hypothesis, we first examined expression of CRADD mRNA and protein in primary human endothelial cells, primary murine LMEC, and human and murine endothelial cell lines. We show by RT-PCR (Fig. 1A) and immunoblot analysis (Fig. 1B) that the human umbilical vein endothelial cell, LMEC, and endothelial cell lines constitutively express CRADD.

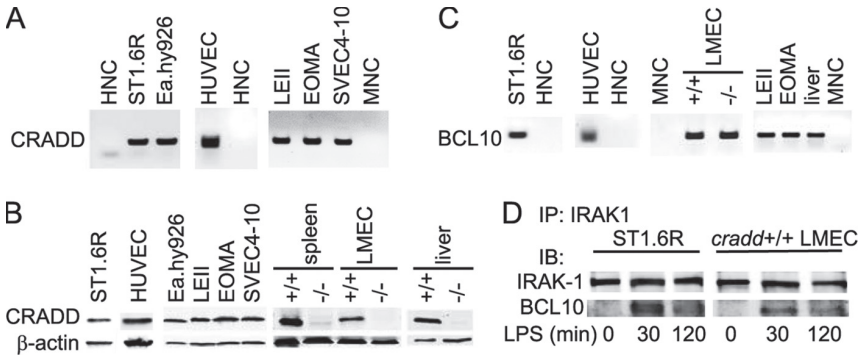

FIGURE 1. Expression of CRADD and BCL10 in human and mouse endothelial cells and association of BCL10 with IRAK-1 in the proinflammatory TLR4 signaling pathway induced by LPS. CRADD mRNA and protein expression in endothelial cells was assessed by RT-PCR (A) and immunoblot analysis (B). C, BCL10 mRNA was assessed by RT-PCR in endothelial cells. In RT-PCR analyses, human negative control (HNC) and mouse negative control (MNC) reactions were performed using human or mouse primers, respectively, without cDNA. In immunoblot analyses, mouse spleen and liver extracts derived from cradd$^{+/+}$ and cradd$^{-/-}$ mice served as positive (+/+) and negative (−/−) controls for CRADD protein, respectively, and -actin served as a cellular protein loading control. D, co-immunoprecipitation of BCL10 with IRAK-1 is stimulus- and time-dependent. Primary cradd$^{+/+}$ LMEC cells or human ST1.6 R endothelial cells were stimulated with 1 g/ml of LPS for the indicated times. Protein complexes precipitated with anti-IRAK-1 (IP) from cell lysates were immunoblotted (IB) with antibodies to the indicated proteins. All gels and blots shown are representative of three independent experiments.

The Anti-inflammatory Action of CRADD Is Dependent on BCL10 —We previously identified BCL10 as a direct target of CRADD responsible for suppression of T cell receptor agonist-evoked signaling in T lymphocytes (6). This new function of CRADD is dependent on its CARD domain, which binds to BCL10 and impedes its interaction with CARMA1 (6). Thus, the CRADD-BCL10 axis prevents formation of a complete CARMA1 signalosome required for activation of the NF κB signaling pathway in immune cells (6). BCL10 is expressed in endothelial cells (Fig. 1C), consistent with other reports that also documented expression of CARMA3 and MALT1 (15, 16, 18). BCL10 has been identified as an important mediator of NF κB activation, and is recruited to Toll-like receptor 4 (TLR4) signaling complexes in response to LPS stimulation by interacting with IRAK-1 (33, 34). We confirmed this interaction in LPS-stimulated LMEC from cradd$^{+/+}$ mice and human lung microvascular endothelial HPMEC-ST1.6R cells by showing stimulus- and time-dependent association of BCL10 with IRAK-1 (Fig. 1D). We chose HPMEC-ST1.6R cells because they display the major constitutive and inducible endothelial cell characteristics and show an angiogenic response on Matrigel similar to that of primary human endothelial cells isolated from umbilical vein (HUVEC), lung (HPMEC), and skin (HDMEC) (28).

Subsequently, we demonstrated that the regulatory action of CRADD depends on BCL10 in stimulated endothelial cells by employing shRNA knockdown of CRADD and/or BCL10 (Fig. 2, A and B). Upon stimulation with the TLR4 agonist LPS, or the proteinase-activated receptor 1 (PAR-1) agonist thrombin, CRADD K/D LEII cells display significantly increased transcripts for cytokines TNF- α, IL-6, and IL-1 α (Fig. 3). Consistent with increased expression of IL-6 mRNA transcripts, IL-6 protein expression was also increased in response to LPS and thrombin (Fig. 2, C and D, right). Thus, endothelial production of this pleotropic cytokine and permeability inducer (35) is negatively controlled by CRADD, regulating signaling pathways evoked by two distinct agonists, LPS and thrombin, in endothelial cells. Although CRADD K/D cells produced more IL-6 in response to LPS or thrombin, BCL10 K/D endothelial cells displayed the opposite effect (Fig. 2, C and D, left). Simultaneous reduction in CRADD and BCL10 expression (CRADD/BCL10 K/D) abrogated the increased IL-6 expression observed in CRADD-deficient cells stimulated with LPS and thrombin (Fig. 2, C and D, right). Thus, increased IL-6 expression in CRADD-depleted cells depends on BCL10. This enhancement of LPS-induced signaling to the nucleus in CRADD K/D LEII cells resulted in predicted downstream activation events as demonstrated by elevated levels of nuclear NF κB RelA/p65 (p65) in LPS-stimulated CRADD K/D cells compared with LPS-stimulated control cells (Fig. 2E).

Proinflammatory Agonist-induced Cytokine Expression Is Suppressed by Replenishing Endogenous CRADD with a Novel Recombinant Cell Penetrating (CP) Protein, CP-CRADD— We reasoned that by increasing the intracellular content of CRADD in endothelial cells we can attenuate their responses to proinflammatory agonists. Consistent with our prior evidence with recombinant cell penetrating SOCS1 and -3 that inhibited inflammation and apoptosis (30, 32, 36), we developed a novel recombinant CP-CRADD protein (Fig. 4A) to restore CRADD protein in CRADD-deficient endothelial cells and analyze its regulatory function. Purity and yields of the recombinant CRADD protein homologs were comparable (Fig. 4B). Intracellular delivery of CP-CRADD was verified in human and murine endothelial cells by immunoblot analysis (Fig. 4C) before use in functional assays, which ultimately provided proof of CP-CRADD intracellular activity.

As final evidence of the negative regulatory function of CRADD in endothelial cells, CP-CRADD protein delivery to CRADD-depleted LEII cells (CRADD K/D) significantly suppressed both LPS- and thrombin-induced IL-6 expression (Fig. 5A). Consistent with the changes in protein expression, increased mRNA transcripts for TNF- α, IL-6, and IL-1 α in CRADD K/D cells were reduced by treatment with CP-CRADD to the levels displayed by CRADD-sufficient LEII cells after stimulation with LPS or thrombin (see Fig. 3, B and C). Moreover, treatment with CP-CRADD significantly reduced the IL-6 protein in CRADD-sufficient LEII control cells stimulated with LPS, although a similar reduction in IL-6 induced by thrombin in the control LEII cells was not apparent (Fig. 5A).

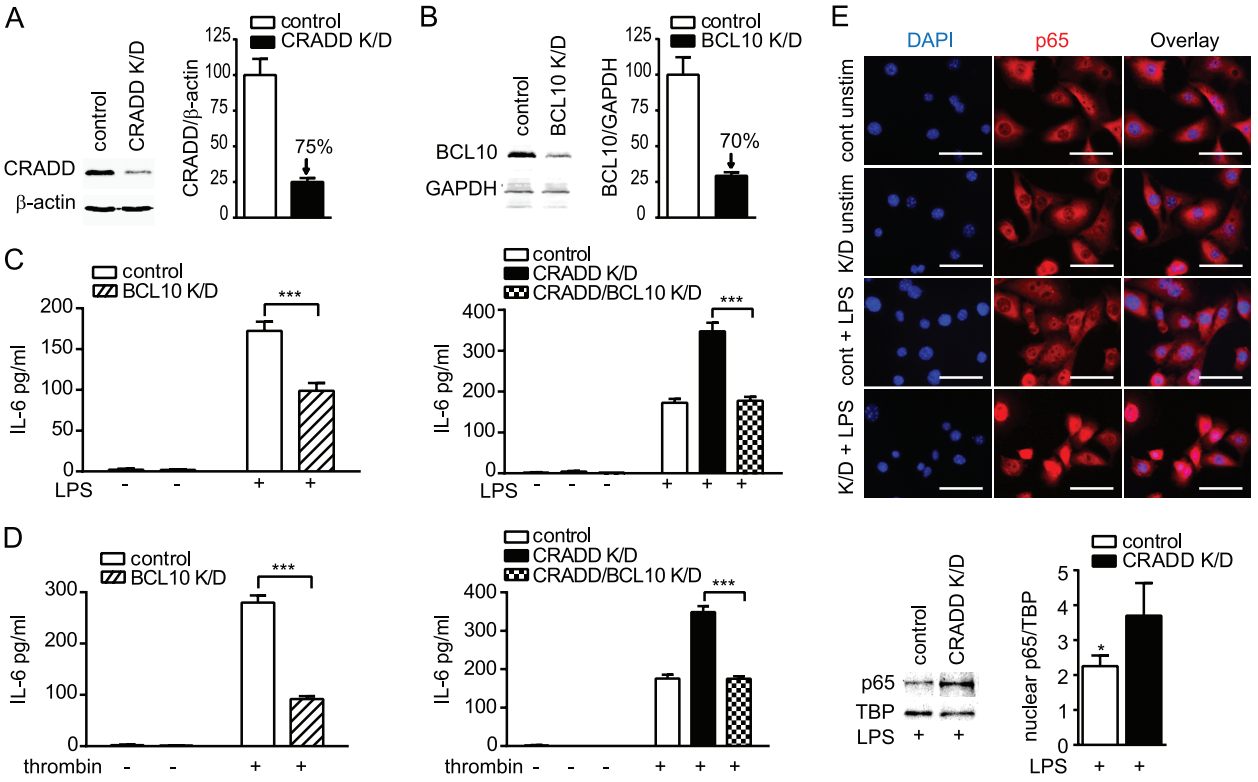

FIGURE 2. Expression of IL-6 induced by proinflammatory agonists in CRADD-depleted endothelial cells is dependent on BCL10. CRADD (A) and BCL10 (B) protein knockdown (K/D) induced by shRNA transduction in LEII cells was assessed by immunoblot analysis after 96 h. Shown are immunoblots and mean ± S.D. of proteins from at least 3 independent immunoblots normalized to β-actin and GAPDH cellular protein loading controls for CRADD and BCL10, respectively, with calculation of percent suppression of CRADD and BCL10. C and D, LEII cells were transduced with control, CRADD, and/or BCL10 shRNA as indicated for 96 h then treated with 100 ng/ml of LPS (C) or 1.5 units/ml of thrombin (D). IL-6 in culture media was measured 24 h after stimulation. Results are presented as mean ± S.D. from three independent experiments performed in duplicate (***, $p < 0.0001$ by t test). E, LEII cells were transduced with control, or CRADD shRNA as indicated for 96 h then treated with 10 ng/ml of LPS for 1 h. Nuclear translocation of NFκB p65/RelA (p65) was assessed by immunofluorescence staining and immunoblot analysis of nuclear extracts. Shown are immunofluorescence and immunoblot images representative of at least 3 independent experiments. Quantification of immunoblots is based on analysis of 6 lanes and shown as mean ± S.D. of proteins normalized to TBP nuclear protein loading control in that lane. Magnification ×40, scale bars = 5 μm. (*, $p < 0.05$ by t test.)

We next compared the inflammatory response to LPS in LMEC derived from previously characterized cradd$^{-/-}$ and wild-type cradd$^{+/+}$ control mice (6). As shown in Fig. 1B, LMEC isolated from cradd$^{-/-}$ mice are deficient in CRADD protein, whereas LMEC from wild-type cradd$^{+/+}$ mice contain endogenous CRADD. Concordant with results obtained in LEII cells, primary LMEC isolated from cradd$^{-/-}$ mice also displayed an enhanced response to LPS stimulation compared with LMEC from wild-type cradd$^{+/+}$ mice (Fig. 5B). Treatment with CP-CRADD suppressed IL-6 production of LMEC from cradd$^{-/-}$ mice by 43%, and, significantly, in LMEC from cradd$^{+/+}$ mice, CP-CRADD supplemented endogenous CRADD to reduce their IL-6 production in response to LPS by 35% (Fig. 5C). This beneficial effect of CRADD augmentation was further explored in the human lung microvascular endothelial cell line HPMEC-ST1.6R. The enhanced production of IL-6 and monocyte chemoattractant protein-1 (MCP-1/CCL2) in response to LPS was counteracted by treatment with CP-CRADD, reducing their expression by 40 and 47%, respectively (Fig. 5D). Additionally, thrombin-induced IL-6 and MCP-1 were reduced by 63 and 64%, respectively. The chemokine MCP-1 is known to induce reorganization of tight junctions proteins and increase endothelial permeability (37). Thus, intracellular delivery of recombinant CP-CRADD complemented the negative regulation of cytokine/chemokine expression by endogenous CRADD. The contrast between the results from ST1.6R cells and control LEII cells (Fig. 5A) may be attributed to low expression of IL-6 by LEII cells in response to thrombin.

Agonist-induced Endothelial Monolayer Permeability Is Enhanced in CRADD-deficient Endothelial Cells—We analyzed the role of CRADD in maintaining endothelial barrier function by first comparing permeability of LMEC monolayers from cradd$^{+/+}$ and cradd$^{-/-}$ mice. This assay was based on monitoring the passage of FITC-labeled dextran through the monolayer. In the absence of stimulation, there was no difference in permeability between monolayers from cradd$^{-/-}$ and cradd$^{+/+}$ LMEC (Fig. 6A). We then tested the barrier function of primary LMEC in agonist-induced permeability assays. Proinflammatory agonists LPS and thrombin induced significantly increased permeability in cradd$^{-/-}$ LMEC monolayers as compared with cradd$^{+/+}$ LMEC monolayers (Fig. 6, B and C). Notably, agonist-induced permeability of endothelial monolayers to both small and large tracers (10-kDa FITC-dextran and 70-kDa FITC-dextran, respectively) was similar (Fig. 6, D–F). CP-CRADD treatment restored barrier function to cradd$^{-/-}$ LMEC (Fig. 6, G and H) stimulated with either LPS or thrombin, providing

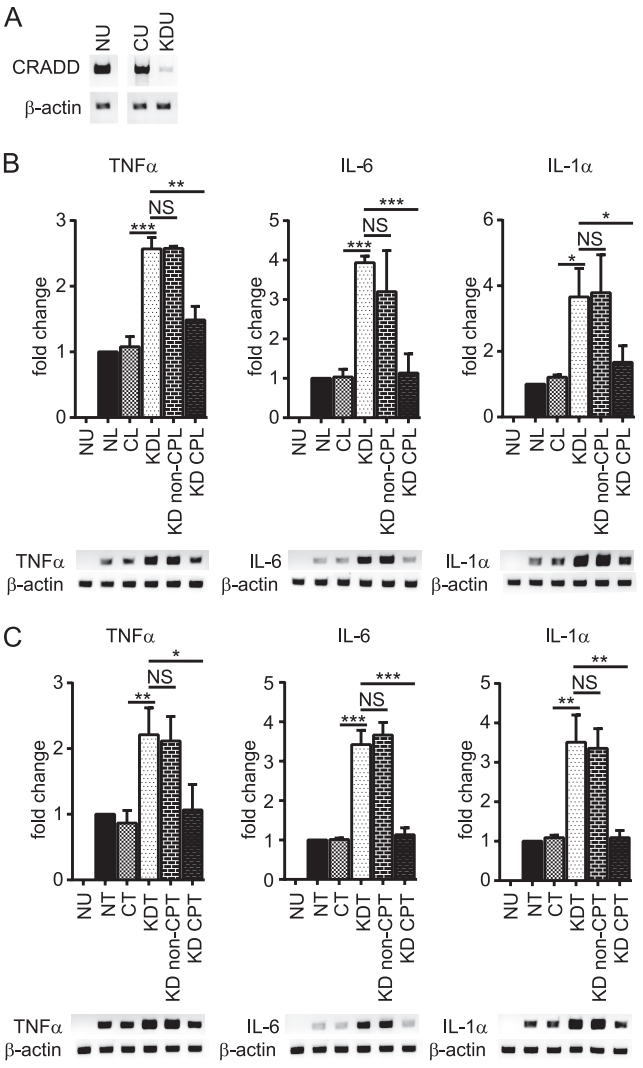

FIGURE 3. Endothelial CRADD suppresses mRNA expression of cytokines TNF α, IL-6, and IL-1 α in response to proinflammatory agonists. Murine lung capillary endothelial LEII cells were left non-transduced (N), or were transduced with shRNA for CRADD knockdown (KD), or with scrambled control shRNA (C). After 96 h, control and CRADD K/D LEII cells were left unstimulated (U) or stimulated with 1 μg/ml of LPS (L) or with 10 units/ml of thrombin (T) for 24 h. Some CRADD K/D cells were treated with CP-CRADD (CP) or non-CP-CRADD (non-CP) for 2 h before stimulation. β-Actin was used as a control for RT-PCR. A, in unstimulated cells, CRADD expression is reduced by shRNA targeting CRADD but not by non-target scrambled shRNA. LPS (B) and thrombin (C) stimulation increased transcripts for TNFα, IL-6, and IL-1α in cells not transduced with shRNA. Knockdown of CRADD with shRNA targeting CRADD further increases mRNA expression. Treatment with CP-CRADD reduces expression to that of cells without CRADD knockdown. Gels shown are representative of 3 independent experiments. Graphs represent quantification of bands from three gels. Values from unstimulated samples were set as background and NL or NT bands were set to 1. Fold-change from stimulated non-transduced samples (NL or NT) are shown as $\pm$S.D. from three independent experiments (NS, not significant; *, $p < 0.05$; **, $p < 0.01$; ***, $p < 0.001$ by t test).

definitive proof of the negative regulatory function of CRADD in endothelial cells. Moreover, in CRADD-sufficient human ST1.6R cell monolayers, thrombin-induced permeability was reduced by supplementation with CP-CRADD (Fig. 6I), suggesting that supplementation of endogenous CRADD with CP-CRADD may stabilize endothelial barrier function during protracted inflammatory signaling.

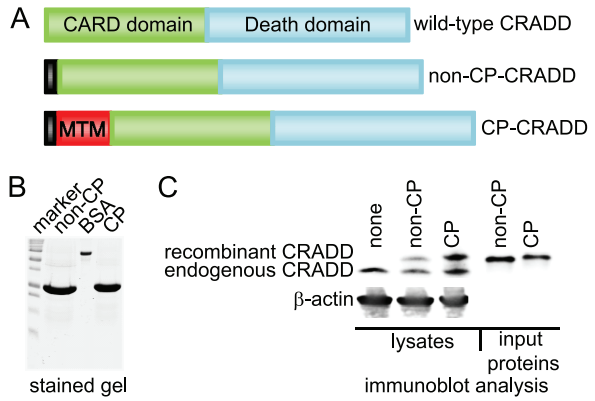

FIGURE 4. Design, purity, and intracellular delivery of recombinant CP-CRADD. A, schematic representation of full-length wild-type CRADD, showing different functional domains of the protein including the CARD domain (green) and Death domain (blue). Non-CP-CRADD lacks the membrane translocating motif but contains an N-terminal His_6 tag (black), whereas CP-CRADD contains the N-terminal His_6 tag (black), followed by a 12-amino acid membrane-translocating motif (red). B, protein staining with Coomassie Blue displays recombinant non-CP-CRADD (25 kDa) and CP-CRADD (26 kDa) proteins. BSA is shown between them for size reference. C, tracking intracellular delivery of CP-CRADD by protease resistance and quantitative immunoblotting. Left, lysates from ST1.6R cells incubated for 1 h with equimolar doses (10 μM) of non-CP-CRADD or CP-CRADD, then treated with proteinase K to remove extracellular proteins. Right, recombinant protein preparations added to cells. All samples were run on the same gel and immunoblotted with an anti-CRADD antibody that recognizes both endogenous and recombinant CRADD in cell lysates as indicated. Immunoblot is representative of two independent experiments performed in triplicate.

F-Actin Polymerization and Adherens Junctions Are Altered in CRADD-deficient Cells—Stimulation of endothelial cell monolayers with agonists triggers morphological changes through reorganization of the actin cytoskeleton, leading to increased permeability (25, 38–40). We explored the mechanism of increased agonist-induced permeability in CRADD-deficient endothelial monolayers by investigating changes in F-actin organization (Fig. 7) and the adherens junction protein VE-cadherin and its adaptor p120 (Fig. 8) in cradd$^{+/+}$ and cradd$^{-/-}$ LMEC stimulated with the permeability inducers LPS or thrombin.

Unstimulated LMEC from both cradd$^{+/+}$ and cradd$^{-/-}$ mice stained with fluorescent phalloidin exhibited an actin cytoskeleton with thin F-actin fibers sparsely crossing the body of cells (Fig. 7, A and B). LPS and thrombin stimulation induced changes in F-actin organization (Fig. 7, C–F), displaying a strong pattern of polymerized actin with prominently thick F-actin fiber bundles. However, loss of peripheral F-actin and more prominent retraction of the cell mass toward the center were evident in cradd$^{-/-}$ LMEC, leading to increased gaps in the monolayer (indicated by arrows) (Fig. 7, D and F).

Immunostaining for the adherens junction protein VE-cadherin and its adaptor p120 produced a strong signal, which appeared as a contiguous line of varied thickness along cell borders in quiescent endothelial cells (Fig. 8, A and B). Please note that unstimulated cradd$^{-/-}$ endothelial cells displayed a spindle-like shape rather than the typical cobblestone pattern of cradd$^{+/+}$ endothelial cells. LPS and thrombin stimulation triggered a striking distortion of the VE-cadherin/p120 contiguous border pattern with a visible reduction of VE-cadherin/p120 peripheral staining (Fig. 8, C–F). Stimulated cradd$^{-/-}$ LMEC

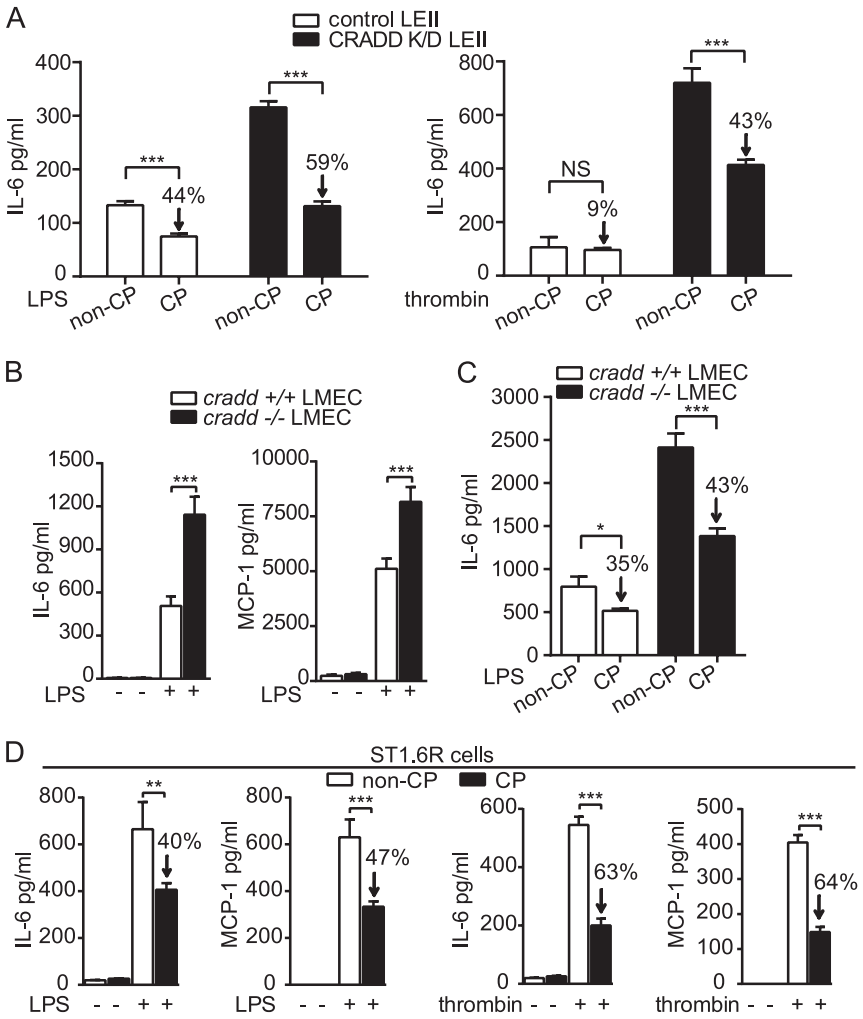

FIGURE 5. Intracellular delivery of CP-CRADD suppresses agonist-induced IL-6 and MCP-1 expression in wild-type and CRADD-deficient endothelial cells. A, after a 2-h treatment of control or CRADD K/D LEII cells with equimolar doses (6 μM) of non-CP-CRADD or CP-CRADD, cells were stimulated with 100 ng/ml of LPS (left) or 1.5 units/ml of thrombin (right). B, LMEC were isolated from cradd$^{+/+}$ and cradd$^{-/-}$ mice. Cells were stimulated with 100 ng/ml of LPS. C, LMEC isolated from cradd$^{+/+}$ and cradd$^{-/-}$ mice were treated for 3 h with equimolar doses (11 μM) of non-CP-CRADD or CP-CRADD, then stimulated with 100 ng/ml of LPS. D, human ST1.6R endothelial cells were treated for 3 h with equimolar doses (11 μM) of non-CP-CRADD or CP-CRADD, then stimulated as in A. IL-6 and MCP-1 in culture media were measured 24 h after stimulation. Results are presented as mean ± S.D. from three independent experiments performed in duplicate (*, $p < 0.05$; **, $p < 0.01$; ***, $p < 0.0001$ by t test).

displayed a more dramatic disturbance in the border pattern compared with cradd$^{+/+}$ LMEC, evidenced by areas of deficient staining surrounding the gaps formed in the initially integral monolayer (indicated by arrows) (Fig. 8, D and F). These results indicate that BCL10-mediated F-actin disorganization (27) and adherens junction disruption are controlled by CRADD.

DISCUSSION

Here we show that the intracellular adaptor CRADD is expressed in non-immune cells. In primary human and murine endothelial cells, CRADD is involved in maintaining their integrity by acting as a negative regulator of the inflammatory response. We document that this physiologic action of CRADD is dependent on its interaction with BCL10, a key component of the CARMA3 signalosome in microvascular endothelial cells. This anti-inflammatory function of CRADD in endothelial cells is consistent with its role as a negative regulator of the BCL10-containing CARMA1 signalosome in immune cells, as documented in our initial study of CRADD (6). BCL10 interacts not only with CARMA1, which is restricted to cells of the immune system, but also with its close homolog, CARMA3, which has a much broader expression pattern including endothelial and epithelial cells (13–16, 18, 41, 42). Therefore, expression of CRADD in endothelial and other cell types, e.g. epithelial cells,[3] follows that of BCL10 and may also provide an anti-inflammatory CRADD-BCL10 axis in those cells. CRADD interaction with BCL10 transcends its engagement in the CARMA3 signalosome as BCL10 is known to interact with IRAK-1 (34). CRADD negatively regulates LPS-triggered signaling to the nucleus mediated by NF κB (see Fig. 2E), a process that depends

[3] H. Qiao and J. Hawiger, unpublished data.

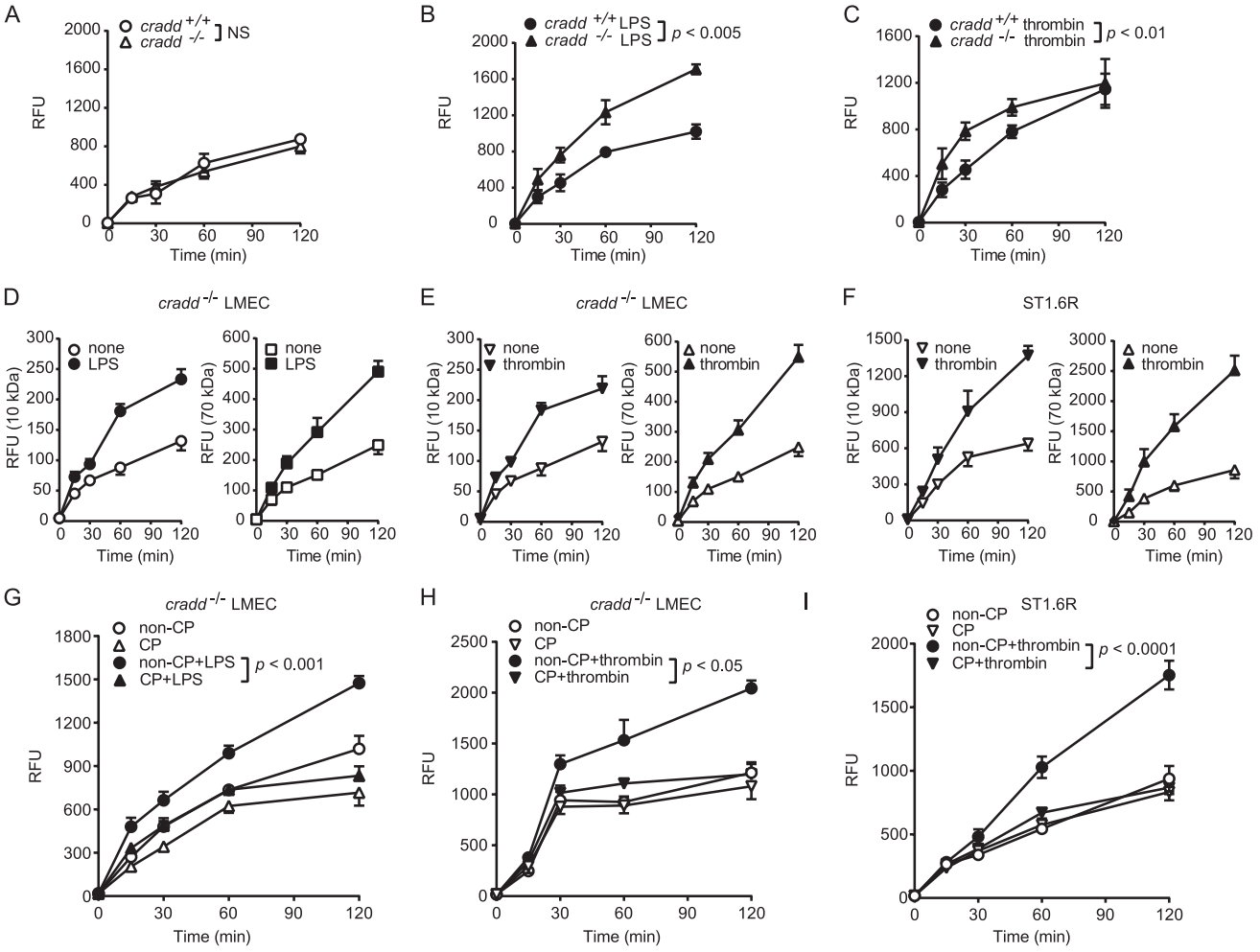

FIGURE 6. Endothelial permeability of CRADD-deficient primary murine LMEC and CRADD-sufficient human ST1. 6R endothelial monolayers is regulated by CP-CRADD. A–C, LMEC isolated from cradd$^{+/+}$ and cradd$^{-/-}$ mice were grown to confluence on Transwell inserts and left unstimulated (A) or stimulated with 1 μg/ml of LPS for 24 h (B) or 10 units/ml of thrombin for 6 h (C). D–F, permeability of 10-kDa compared with 70-kDa FITC-dextran. LMEC isolated from cradd$^{-/-}$ mice (D and E) were stimulated with LPS (D) or thrombin (E) as in B and C. F, human ST1.6R cells were stimulated with 30 units/ml of thrombin for 20 min. G and H, LMEC isolated from cradd$^{-/-}$ mice were treated for 3 h with equimolar doses (12 μM) of non-CP-CRADD or CP-CRADD, then stimulated with LPS (G) or thrombin (H) as in B and C. I, human ST1.6R cells were stimulated with thrombin as in F. To assess permeability, FITC-dextran (10 kDa in A–C and G–I) was added to each insert and fluorescence in the lower chamber was measured at the indicated times. Results are presented as mean ± S.D. in relative fluorescence units (RFU) from three independent experiments performed in duplicate (p values shown were determined by t test of the area under the curves from 3 independent experiments).

on TLR4-evoked activation of IRAK-1 that binds BCL10 (34). Hence CRADD targeting of BCL10 may reduce the outcome of LPS action on endothelial cells.

Although direct involvement of the CARMA3 signalosome in the LPS/TLR4 pathway is unclear, previous studies have reported that BCL10 and MALT1 play major roles by mediating NF κB activation via the IRAK-1-BCL10-MALT1-TRAF6-TAK1 cascade in the LPS/TLR4 pathway (43, 44). An investigation of Bcl10/Malt1-mediated NF κB signaling in non-immune cells showed that IL-6 production was blocked in the absence of BCL10 (45). Our results, based on co-immunoprecipitation analysis (Fig. 1D) and BCL10 silencing (Fig. 2), also demonstrate BCL10 involvement in the LPS/TLR4 signaling pathway. This pathway is negatively regulated by CRADD and its novel recombinant cell-penetrating homolog CP-CRADD.

Thrombin/PAR-1 signaling to mobilize NF κB for nuclear translocation depends on initial protein kinase C activation, with subsequent steps mediated by BCL10 to engage the canonical NF κB machinery and shift endothelial function toward an "activated" phenotype (46–50). As documented in our current study, thrombin dramatically increased cytokine and chemokine production and significantly induced permeability of the endothelial monolayer. The CARMA3 signalosome links PAR-1-evoked signaling to activation of the I κB kinase signaling complex assembled around TRAF6 through ubiquitination of the NF κB essential modulator (NEMO/IKK γ), the regulatory subunit of the I κB kinase complex (51). In immune cells, BCL10 activates the NF κB pathway through the NF κB essential modulator (52). Although there are significant differences in how the CARMA1 and CARMA3 signalosomes communicate with PAR-1 and other receptors, such as the choice of 3-phosphoinositide-dependent protein kinase 1 and β-arrestin 2, the CARMA3 signalosome shares its positive regulator BCL10 with the CARMA1 signalosome found in lymphocytes (18). Hence

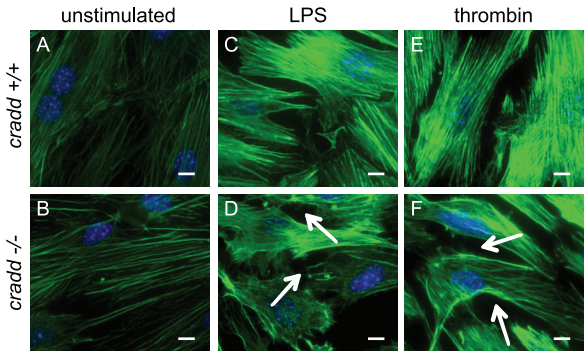

FIGURE 7. F-actin polymerization and cellular contraction are enhanced in cradd$^{-/-}$ as compared with cradd$^{+/+}$ LMEC monolayers after stimulation with LPS or thrombin. LMEC isolated from cradd$^{+/+}$ and cradd$^{-/-}$ mice were grown to confluence, then left unstimulated (A and B) or stimulated with 1 μg/ml of LPS for 24 h (C and D) or 10 units/ml of thrombin for 6 h (E and F). Cells were stained with Alexa 488-labeled phalloidin (green) to visualize F-actin. Nuclei are counterstained with DAPI (blue). Arrows indicate gaps in the monolayer caused by cellular retraction in stimulated cells. Images are representative of at least 3 independent experiments. Magnification ×63, scale bars = 1 μm.

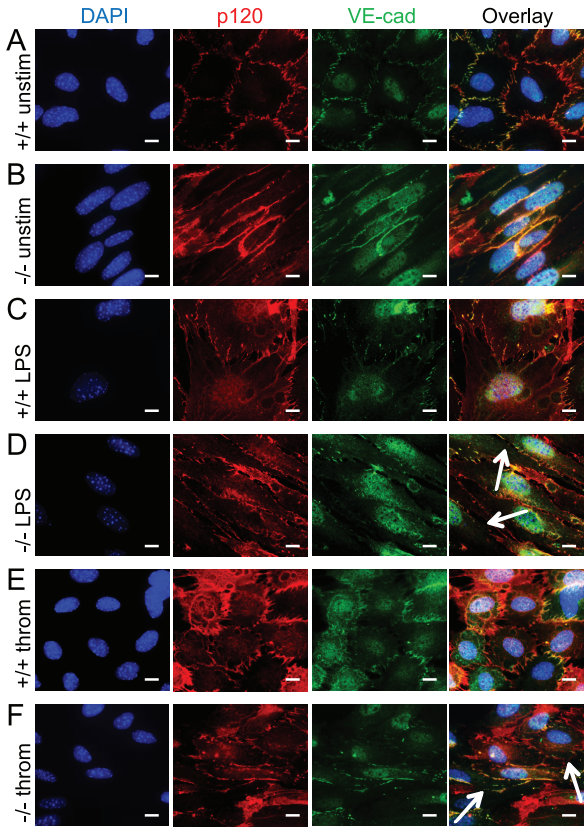

FIGURE 8. CRADD deficiency exacerbates the loss of monolayer integrity in LPS- or thrombin-stimulated LMEC monolayers analyzed by immunofluorescence of VE-cadherin and p120. LMEC isolated from cradd$^{+/+}$ and cradd$^{-/-}$ mice were grown to confluence, then left unstimulated (A and B) or stimulated with 1 μg/ml of LPS for 24 h (C and D) or 10 units/ml of thrombin for 6 h (E and F). Cells were immunostained with p120 (red) and VE-cadherin (green). Nuclei are counterstained with DAPI (blue). Arrows indicate disruption of both proteins in cell membranes of stimulated cradd$^{-/-}$ LMEC. Images are representative of at least 3 independent experiments. Magnification ×63, scale bars = 1 μm.

BCL10 presents itself as an easy target for CRADD negative regulation of both CARMA1 and CARMA3 signalosomes in agonist-stimulated immune and non-immune cells, respectively.

BCL10 has emerged as a key positive mediator of inflammatory signals, as it has been reported to interact with other CARD domain-containing proteins, including CARD 9, 10, 11, and 14, which are thought to function as upstream regulators in NF κB signaling (43–45, 53). Independent of NF κB signaling, BCL10 is also linked to remodeling of F-actin (27), which is connected to transmembrane junctional proteins that control the barrier function of endothelial cells (26, 40). As the non-immune mainstays of the blood-tissue barrier, endothelial cells are connected by highly regulated tight and adherens junctions, which control paracellular leakage of plasma fluid and proteins that contribute to increased endothelial permeability (54, 55). LPS induces F-actin remodeling through activation of a Src family kinase and TNF receptor-associated factor 6 (TRAF6) (56–58). As shown in Fig. 7, CRADD-deficient cells demonstrate an altered pattern of F-actin polymerization in response to LPS and thrombin stimulation compared with CRADD-sufficient cells. Therefore, CRADD, by targeting BCL10, plays an important role in the negative regulation of BCL10-mediated F-actin polymerization. CRADD deficiency thereby increases inducible but not constitutive permeability of endothelial monolayers compared with CRADD-sufficient endothelium.

Proinflammatory agonist-induced stress fiber formation overlaps with redistributed VE-cadherin (59), an endothelium-specific member of the cadherin family of adhesion proteins found in adherens junctions. Inside the cell, VE-cadherin interacts with its adaptor p120. As shown in Fig. 8, the VE-cadherin/p120 system was highly perturbed in CRADD-deficient cells upon their stimulation with proinflammatory agonists. Thus, the evidence presented here points to another important role for endothelial CRADD as an inducible physiologic regulator of vascular permeability, a cardinal sign of inflammation.

Previous studies have demonstrated that the proinflammatory cytokine IL-6 (35) and chemokine MCP-1 (37) contribute to increased endothelial permeability. This study shows significantly increased IL-6 and MCP-1 expression by CRADD-deficient endothelial cells in response to LPS and thrombin, suggesting that depletion of endogenous CRADD by inflammatory signaling may contribute to the enhanced action of IL-6 and MCP-1 as endothelial permeability inducers. We show that the changes induced by inflammatory signaling are sufficient to allow permeability to large molecules (Fig. 6, D–F), such as plasma proteins. In turn, reduction of BCL10-mediated inflammatory signaling by a novel recombinant protein, CP-CRADD, offers a new strategy to control vascular inflammatory responses not only in non-immune cells (endothelial cells) as demonstrated in this study but also in immune cells. CRADD is also expressed in human brain microvascular endothelial cells (60), suggesting its potential anti-inflammatory function there as well.

In summary, this study provides new evidence that CRADD plays a pivotal role in maintaining the integrity of endothelial monolayers. A better appreciation of the role of CRADD in endothelium may contribute to a deeper understanding of endothelial dysfunction and inform the development of a novel treatment for inflammatory vascular disorders.

Acknowledgments—Fluorescence microscopy and analysis was performed in part through the use of the VUMC Cell Imaging Shared Resource. Cell Imaging and other Core Services were funded in part through Vanderbilt University Medical Center's Digestive Disease Research Center supported by National Institutes of Health Grant P30DK058404 and the Vanderbilt Ingram Cancer Center supported by National Institutes of Health Grant P30CA068485.

REFERENCES

1. Hawiger, J., and Musser, J. M. (2011) How to approach genome wars in sepsis? Crit. Care 15, 1007
2. Alexander, W. S., and Hilton, D. J. (2004) The role of suppressors of cytokine signaling (SOCS) proteins in regulation of the immune response. Annu. Rev. Immunol. 22, 503–529
3. Liew, F. Y., Xu, D., Brint, E. K., and O'Neill, L. A. (2005) Negative regulation of toll-like receptor-mediated immune responses. Nat. Rev. Immunol. 5, 446–458
4. Rakesh, K., and Agrawal, D. K. (2005) Controlling cytokine signaling by constitutive inhibitors. Biochem. Pharmacol. 70, 649–657
5. Coornaert, B., Carpentier, I., and Beyaert, R. (2009) A20: central gatekeeper in inflammation and immunity. J. Biol. Chem. 284, 8217–8221
6. Lin, Q., Liu, Y., Moore, D. J., Elizer, S. K., Veach, R. A., Hawiger, J., and Ruley, H. E. (2012) Cutting edge: the "death" adaptor CRADD/RAIDD targets BCL10 and suppresses agonist-induced cytokine expression in T lymphocytes. J. Immunol. 188, 2493–2497
7. Paul, S., and Schaefer, B. C. (2013) A new look at T cell receptor signaling to nuclear factor-κB. Trends Immunol. 34, 269–281
8. Egawa, T., Albrecht, B., Favier, B., Sunshine, M. J., Mirchandani, K., O'Brien, W., Thome, M., and Littman, D. R. (2003) Requirement for CARMA1 in antigen receptor-induced NF-κB activation and lymphocyte proliferation. Curr. Biol. 13, 1252–1258
9. Gaide, O., Favier, B., Legler, D. F., Bonnet, D., Brissoni, B., Valitutti, S., Bron, C., Tschopp, J., and Thome, M. (2002) CARMA1 is a critical lipid raft-associated regulator of TCR-induced NF-κB activation. Nat. Immunol. 3, 836–843
10. Hara, H., Wada, T., Bakal, C., Kozieradzki, I., Suzuki, S., Suzuki, N., Nghiem, M., Griffiths, E. K., Krawczyk, C., Bauer, B., D'Acquisto, F., Ghosh, S., Yeh, W. C., Baier, G., Rottapel, R., and Penninger, J. M. (2003) The MAGUK family protein CARD11 is essential for lymphocyte activation. Immunity 18, 763–775
11. Jun, J. E., Wilson, L. E., Vinuesa, C. G., Lesage, S., Blery, M., Miosge, L. A., Cook, M. C., Kucharska, E. M., Hara, H., Penninger, J. M., Domashenz, H., Hong, N. A., Glynne, R. J., Nelms, K. A., and Goodnow, C. C. (2003) Identifying the MAGUK protein Carma-1 as a central regulator of humoral immune responses and atopy by genome-wide mouse mutagenesis. Immunity 18, 751–762
12. Newton, K., and Dixit, V. M. (2003) Mice lacking the CARD of CARMA1 exhibit defective B lymphocyte development and impaired proliferation of their B and T lymphocytes. Curr. Biol. 13, 1247–1251
13. Sun, J. (2010) CARMA3 : A novel scaffold protein in regulation of NF-kappaB activation and diseases. World J. Biol. Chem. 1, 353–361
14. Jiang, C., and Lin, X. (2012) Regulation of NF-κB by the CARD proteins. Immunol. Rev. 246, 141–153
15. McAllister-Lucas, L. M., Jin, X., Gu, S., Siu, K., McDonnell, S., Ruland, J., Delekta, P. C., Van Beek, M., and Lucas, P. C. (2010) The CARMA3-Bcl10-MALT1 signalosome promotes angiotensin II-dependent vascular inflammation and atherogenesis. J. Biol. Chem. 285, 25880–25884
16. Martin, D., Galisteo, R., and Gutkind, J. S. (2009) CXCL8/IL8 stimulates vascular endothelial growth factor (VEGF) expression and the autocrine activation of VEGFR2 in endothelial cells by activating NF κB through the CBM (Carma3/Bcl10/Malt1) complex. J. Biol. Chem. 284, 6038–6042
17. Kenne, E., and Lindbom, L. (2011) Imaging inflammatory plasma leakage in vivo. Thromb. Haemost. 105, 783–789
18. Delekta, P. C., Apel, I. J., Gu, S., Siu, K., Hattori, Y., McAllister-Lucas, L. M., and Lucas, P. C. (2010) Thrombin-dependent NF-κB activation and monocyte/endothelial adhesion are mediated by the CARMA3 ·Bcl10· MALT1 signalosome. J. Biol. Chem. 285, 41432–41442
19. Blonska, M., and Lin, X. (2009) CARMA1-mediated NF-κB and JNK activation in lymphocytes. Immunol. Rev. 228, 199–211
20. Colgan, O. C., Ferguson, G., Collins, N. T., Murphy, R. P., Meade, G., Cahill, P. A., and Cummins, P. M. (2007) Regulation of bovine brain microvascular endothelial tight junction assembly and barrier function by laminar shear stress. Am. J. Physiol. Heart Circ. Physiol. 292, H3190–H3197
21. Goldenberg, N. M., Steinberg, B. E., Slutsky, A. S., and Lee, W. L. (2011) Broken barriers: a new take on sepsis pathogenesis. Sci. Transl. Med. 3, 88ps25
22. Vestweber, D. (2008) VE-cadherin: the major endothelial adhesion molecule controlling cellular junctions and blood vessel formation. Arterioscler. Thromb. Vasc. Biol. 28, 223–232
23. Herwig, M. C., Tsokos, M., Hermanns, M. I., Kirkpatrick, C. J., and Müller, A. M. (2013) Vascular endothelial cadherin expression in lung specimens of patients with sepsis-induced acute respiratory distress syndrome and endothelial cell cultures. Pathobiology 80, 245–251
24. Garcia, J. G., Verin, A. D., and Schaphorst, K. L. (1996) Regulation of thrombin-mediated endothelial cell contraction and permeability. Semin. Thromb. Hemost. 22, 309–315
25. Wang, Y., Chen, H., Li, H., Zhang, J., and Gao, Y. (2013) Effect of angiopoietin-like protein 4 on rat pulmonary microvascular endothelial cells exposed to LPS. Int. J. Mol. Med. 32, 568–576
26. Marion, S., Mazzolini, J., Herit, F., Bourdoncle, P., Kambou-Pene, N., Hailfinger, S., Sachse, M., Ruland, J., Benmerah, A., Echard, A., Thome, M., and Niedergang, F. (2012) The NF-κB signaling protein Bcl10 regulates actin dynamics by controlling AP1 and OCRL-bearing vesicles. Dev. Cell 23, 954–967
27. Rueda, D., Gaide, O., Ho, L., Lewkowicz, E., Niedergang, F., Hailfinger, S., Rebeaud, F., Guzzardi, M., Conne, B., Thelen, M., Delon, J., Ferch, U., Mak, T. W., Ruland, J., Schwaller, J., and Thome, M. (2007) Bcl10 controls TCR- and FcγR-induced actin polymerization. J. Immunol. 178, 4373–4384
28. Unger, R. E., Krump-Konvalinkova, V., Peters, K., and Kirkpatrick, C. J. (2002) In vitro expression of the endothelial phenotype: comparative study of primary isolated cells and cell lines, including the novel cell line HPMEC-ST1.6R. Microvasc. Res. 64, 384–397
29. Schreiber, A. B., Kenney, J., Kowalski, W. J., Friesel, R., Mehlman, T., and Maciag, T. (1985) Interaction of endothelial cell growth factor with heparin: characterization by receptor and antibody recognition. Proc. Natl. Acad. Sci. U.S.A. 82, 6138–6142
30. Fletcher, T. C., DiGiandomenico, A., and Hawiger, J. (2010) Extended anti-inflammatory action of a degradation-resistant mutant of cell-penetrating suppressor of cytokine signaling 3. J. Biol. Chem. 285, 18727–18736
31. Qiao, H., and May, J. M. (2012) Interaction of the transcription start site core region and transcription factor YY1 determine ascorbate transporter SVCT2 exon 1a promoter activity. PloS One 7, e35746
32. Jo, D., Liu, D., Yao, S., Collins, R. D., and Hawiger, J. (2005) Intracellular protein therapy with SOCS3 inhibits inflammation and apoptosis. Nat. Med. 11, 892–898
33. Bhattacharyya, S., Borthakur, A., Dudeja, P. K., and Tobacman, J. K. (2010) Lipopolysaccharide-induced activation of NF-κB non-canonical pathway requires BCL10 serine 138 and NIK phosphorylations. Exp. Cell Res. 316, 3317–3327
34. Dong, W., Liu, Y., Peng, J., Chen, L., Zou, T., Xiao, H., Liu, Z., Li, W., Bu, Y., and Qi, Y. (2006) The IRAK-1-BCL10-MALT1-TRAF6-TAK1 cascade mediates signaling to NF-κB from Toll-like receptor 4. J. Biol. Chem. 281, 26029–26040
35. Desai, T. R., Leeper, N. J., Hynes, K. L., and Gewertz, B. L. (2002) Interleukin-6 causes endothelial barrier dysfunction via the protein kinase C pathway. J. Surg. Res. 104, 118–123
36. DiGiandomenico, A., Wylezinski, L. S., and Hawiger, J. (2009) Intracellular delivery of a cell-penetrating SOCS1 that targets IFN-γ signaling. Sci. Signal. 2, ra37
37. Stamatovic, S. M., Keep, R. F., Kunkel, S. L., and Andjelkovic, A. V. (2003)

Potential role of MCP-1 in endothelial cell tight junction "opening": signaling via Rho and Rho kinase. J. Cell Sci. 116, 4615–4628
38. He, F., Peng, J., Deng, X. L., Yang, L. F., Wu, L. W., Zhang, C. L., and Yin, F. (2011) RhoA and NF-κB are involved in lipopolysaccharide-induced brain microvascular cell line hyperpermeability. Neuroscience 188, 35–47
39. Bogatcheva, N. V., Zemskova, M. A., Kovalenkov, Y., Poirier, C., and Verin, A. D. (2009) Molecular mechanisms mediating protective effect of cAMP on lipopolysaccharide (LPS)-induced human lung microvascular endothelial cells (HLMVEC) hyperpermeability. J. Cell Physiol. 221, 750–759
40. van der Heijden, M., van Nieuw Amerongen, G. P., van Bezu, J., Paul, M. A., Groeneveld, A. B., and van Hinsbergh, V. W. (2011) Opposing effects of the angiopoietinson the thrombin-induced permeability of human pulmonary microvascular endothelial cells. PloS One 6, e23448
41. Wegener, E., and Krappmann, D. (2007) CARD-Bcl10-Malt1 Signalosomes: missing link to NF-κB. Sci. STKE 2007, pe21
42. Fraser, C. C. (2008) G protein-coupled receptor connectivity to NF-κB in inflammation and cancer. Int. Rev. Immunol. 27, 320–350
43. Bhattacharyya, S., Borthakur, A., Pant, N., Dudeja, P. K., and Tobacman, J. K. (2007) Bcl10 mediates LPS-induced activation of NF-κB and IL-8 in human intestinal epithelial cells. Am. J. Physiol. Gastrointest. Liver Physiol. 293, G429–G437
44. Wang, D., You, Y., Lin, P. C., Xue, L., Morris, S. W., Zeng, H., Wen, R., and Lin, X. (2007) Bcl10 plays a critical role in NF-κB activation induced by G protein-coupled receptors. Proc. Natl. Acad. Sci. U.S.A. 104, 145–150
45. Klemm, S., Zimmermann, S., Peschel, C., Mak, T. W., and Ruland, J. (2007) Bcl10 and Malt1 control lysophosphatidicacid-induced NF-κB activation and cytokine production. Proc. Natl. Acad. Sci. U.S.A. 104, 134–138
46. Coughlin, S. R. (2000) Thrombin signalling and protease-activated receptors. Nature 407, 258–264
47. Minami, T., Sugiyama, A., Wu, S. Q., Abid, R., Kodama, T., and Aird, W. C. (2004) Thrombin and phenotypic modulation of the endothelium. Arterioscler. Thromb. Vasc. Biol. 24, 41–53
48. Major, C. D., Santulli, R. J., Derian, C. K., and Andrade-Gordon, P. (2003) Extracellular mediators in atherosclerosis and thrombosis: lessons from thrombin receptor knockout mice. Arterioscler. Thromb. Vasc. Biol. 23, 931–939
49. Hirano, K. (2007) The roles of proteinase-activated receptors in the vascular physiology and pathophysiology. Arterioscler. Thromb. Vasc. Biol. 27, 27–36
50. Martorell, L., Martínez-González, J., Rodríguez, C., Gentile, M., Calvayrac, O., and Badimon, L. (2008) Thrombin and protease-activated receptors (PARs) in atherothrombosis. Thromb. Haemost. 99, 305–315
51. Chen, Z. J. (2012) Ubiquitination in signaling to and activation of IKK. Immunol. Rev. 246, 95–106
52. Zhou, H., Wertz, I., O'Rourke, K., Ultsch, M., Seshagiri, S., Eby, M., Xiao, W., and Dixit, V. M. (2004) Bcl10 activates the NF-κB pathway through ubiquitination of NEMO. Nature 427, 167–171
53. McAllister-Lucas, L. M., Ruland, J., Siu, K., Jin, X., Gu, S., Kim, D. S., Kuffa, P., Kohrt, D., Mak, T. W., Nuñez, G., and Lucas, P. C. (2007) CARMA3/Bcl10/MALT1-dependent NF-κB activation mediates angiotensin II-responsive inflammatory signaling in nonimmune cells. Proc. Natl. Acad. Sci. U.S.A. 104, 139–144
54. Aghajanian, A., Wittchen, E. S., Allingham, M. J., Garrett, T. A., and Burridge, K. (2008) Endothelial cell junctions and the regulation of vascular permeability and leukocyte transmigration. J. Thromb. Haemost. 6, 1453–1460
55. Vandenbroucke, E., Mehta, D., Minshall, R., and Malik, A. B. (2008) Regulation of endothelial junctional permeability. Ann. N.Y. Acad. Sci. 1123, 134–145
56. Bannerman, D. D., and Goldblum, S. E. (1999) Direct effects of endotoxin on the endothelium: barrier function and injury. Lab. Investig. 79, 1181–1199
57. Gong, P., Angelini, D. J., Yang, S., Xia, G., Cross, A. S., Mann, D., Bannerman, D. D., Vogel, S. N., and Goldblum, S. E. (2008) TLR4 signaling is coupled to SRC family kinase activation, tyrosine phosphorylation of zonula adherens proteins, and opening of the paracellular pathway in human lung microvascular endothelia. J. Biol. Chem. 283, 13437–13449
58. Liu, A., Gong, P., Hyun, S. W., Wang, K. Z., Cates, E. A., Perkins, D., Bannerman, D. D., Puché, A. C., Toshchakov, V. Y., Fang, S., Auron, P. E., Vogel, S. N., and Goldblum, S. E. (2012) TRAF6 protein couples Toll-like receptor 4 signaling to Src family kinase activation and opening of paracellular pathway in human lung microvascular endothelia. J. Biol. Chem. 287, 16132–16145
59. Yuan, D., and He, P. (2012) Vascular remodeling alters adhesion protein and cytoskeleton reactions to inflammatory stimuli resulting in enhanced permeability increases in rat venules. J. Appl. Physiol. 113, 1110–1120
60. Londoño, D., Carvajal, J., Strle, K., Kim, K. S., and Cadavid, D. (2011) IL-10 Prevents apoptosis of brain endothelium during bacteremia. J. Immunol. 186, 7176–7186

APPENDIX

C. "The "Genomic Storm" Induced by Bacterial Endotoxin is Calmed by a Nuclear Transport Modifier that Attenuates Localized and Systemic Inflammation." By Antonio DiGiandomenico, Ruth Ann Veach, Jozef Zienkiewicz, Daniel Moore, **Lukasz Wylezinski**, Martha Hutchens and Jacek Hawiger, *PLoS One*. 2014. **9,** e110183.

OPEN ACCESS Freely available online

PLOS ONE

The "Genomic Storm" Induced by Bacterial Endotoxin Is Calmed by a Nuclear Transport Modifier That Attenuates Localized and Systemic Inflammation

Antonio DiGiandomenico [1.¤a], Ruth Ann Veach [2,3.], Jozef Zienkiewicz [2,3.], Daniel J. Moore [2,4,5], Lukasz S. Wylezin ski [2,6], Marth a A. Hutchen s [1,2¤b], Jacek Hawiger [2,3,6*]

1 Department of Microbiology and Immunology Vanderbilt University School of Medicine, Nashville, Tennessee, United States of America, 2 Immunotherapy Program at Vanderbilt University School of Medicine, Nashville, Tennessee, United States of America, 3 Department of Medicine, Division of Allergy, Pulmonary and Critical Care Medicine, Vanderbilt University School of Medicine, Nashville, Tennessee, United States of America, 4 Department of Pediatrics, Ian Burr Division of Endocrinology and Diabetes, Vanderbilt University School of Medicine, Nashville, Tennessee, United States of America, 5 Department of Pathology, Microbiology and Immunology, Vanderbilt University School of Medicine, Nashville, Tennessee, United States of America, 6 Department of Molecular Physiology and Biophysics, Vanderbilt University School of Medicine, Nashville, Tennessee, United States of America

Abstract

Lipopolysaccharide (LPS) is a potent microbial virulence factor that can trigger production of proinflammatory mediators involved in the pathogenesis of localized and systemic inflammation. Importantly, the role of nuclear transport of stress responsive transcription factors in this LPS-generated "genomic storm" remains largely undefined. We developed a new nuclear transport modifier (NTM) peptide, cell-penetrating cSN50.1, which targets nuclear transport shuttles importin a5 and importin b1, to analyze its effect in LPS-induced localized (acute lung injury) and systemic (lethal endotoxic shock) murine inflammation models. We analyzed a human genome database to match 46 genes that encode cytokines, chemokines and their receptors with transcription factors whose nuclear transport is known to be modulated by NTM. We then tested the effect of cSN50.1 peptide on proinflammatory gene expression in murine bone marrow-derived macrophages stimulated with LPS. This NTM suppressed a proinflammatory transcriptome of 37 out of 84 genes analyzed, without altering expression of housekeeping genes or being cytotoxic. Consistent with gene expression analysis in primary macrophages, plasma levels of 23 out of 26 LPS-induced proinflammatory cytokines, chemokines, and growth factors were significantly attenuated in a murine model of LPS-induced systemic inflammation (lethal endotoxic shock) while the anti-inflammatory cytokine, interleukin 10, was enhanced. This anti-inflammatory reprogramming of the endotoxin-induced genomic response was accompanied by complete protection against lethal endotoxic shock with prophylactic NTM treatment, and 75% protection when NTM was first administered after LPS exposure. In a murine model of localized lung inflammation caused by direct airway exposure to LPS, expression of cytokines and chemokines in the bronchoalveolar space was suppressed with a concomitant reduction of neutrophil trafficking. Thus, calming the LPS-triggered "genomic storm" by modulating nuclear transport with cSN50.1 peptide attenuates the systemic inflammatory response associated with lethal shock as well as localized lung inflammation.

Citation: DiGiandomenico A, Veach RA, Zienkiewicz J, Moore DJ, Wylezinski LS, et al. (2014) The "Genomic Storm" Induced by Bacterial Endotoxin Is Calmed by a Nuclear Transport Modifier That Attenuates Localized and Systemic Inflammation. PLoS ONE 9(10): e110183. doi:10.1371/journal.pone.0110183

Editor: Liwu Li, Virginia Polytechnic Institute and State University, United States of America

Received June 16, 2014; Accepted September 9, 2014; Published October 20, 2014

Data Av ailability: The authors confirm that all data underlying the findings are fully available without restriction. All relevant data are within the paper.

Funding: This work was supported by the National Institutes of Health grants R01HL087531, R01HL069452, T32HL069765 (JH), 5K08DK090146 (DJM) and F32HL087531 (AD). Scholarships for core services were provided by Vanderbilt University Medical Center's Digestive Disease Research Center supported by NIH grant P30DK058404 and the Vanderbilt Ingram Cancer Center supported by NIH grant 2P30CA68485. Additional support was provided through the Vanderbilt University Medical Center Immunotherapy Program and the Vanderbilt Clinical and Translational Science Award (CTSA). The funders had no role in study design, data collection and analysis, decision to publish, or preparation of the manuscript.

Competing Interests: JH, RAV, and JZ are co-inventors of patents relating to cell-penetrating NTM peptides and their use for anti-inflammatory therapy. All rights are assigned to Vanderbilt University. JH is co-founder and shareholder of AGH Therapeutics, Inc. This does not alter the authors' adherence to PLOS ONE policies on sharing data and materials. The authors have no other financial conflicts of interest relating to the subject matter or materials discussed in this article. All work performed by AD was completed during his post-doctoral training at Vanderbilt University prior to and not related to his current employment at MedImmune.

* Email: jacek.hawiger@vanderbilt.edu

. These authors contributed equally to this work.

¤a Current address: MedImmune, LLC, Gaithersburg, Maryland, United States of America
¤b Current address: School of Biological Sciences, Lake Superior State University, Sault Sainte Marie, Minnesota, United States of America

Introduction

Bacterial endotoxin, known as lipopolysaccharide(LPS), is one of the most potent microbial virulence factors in the pathogenesis of localized and systemic inflammation caused by Gram-negative bacteria [1]. LPS is the primary component of the Gram-negative bacterial outer membrane and the most proinflammatory of all bacterial pathogen-associated molecular patterns recognized by

Toll-like receptors (TLRs). TLRs are expressed on multiple cell types, including myeloid and lymphoid cells, vascular endothelial cells, and respiratory epithelial cells [2,3]. Binding of LPS to its cognate receptor, TLR4, induces robust signaling to the nucleus mediated by a cascade of signal transducers engaged in a stream of protein-protein interactions and post translational modifications [4], culminating in nuclear translocation of NF-kB along with other stress-responsive transcription factors (SRTFs), including activator protein-1 (AP-1), nuclear factor of activated T cells (NFAT), and signal transducer and activator of transcription 1 (STAT-1) [5]. These SRTFs, either alone or in various combinations, regulate the genomic response to Gram-negative bacteria and other microbial agents [5]. Similarly, SRTFs respond to signaling pathways emanating from cytokine/chemokine receptors [6,7].

SRTFs and other nuclear proteins larger than 45 kDa are transported to the nucleus by a set of adaptor proteins known as importins (Imp)/karyopherins a which in tandem with importin b1, ferry the SRTF cargo to the nucleus [5,6,8,9]. Therein, they activate a plethora of genes that encode inflammatory cytokines and chemokines, signal transducers (cyclooxygenase, nitric oxide synthase), and cell adhesion molecules, a response denoted as a ''genomic storm''. The concept of a ''genomic storm'' induced by trauma and burns in critically injured patients was extended to subjects challenged with bacterial endotoxin, and therefore represents a fundamental human response to severe inflammatory stress [10]. A tidal wave of gene expression raises blood levels of cytokines and chemokines and mobilizes expression of other mediators. Cumulatively, these products of genomic reprogramming induce fever, endothelial instability and detachment, disseminated intravascular coagulation, acute lung inflammation (ALI), acute respiratory distress syndrome (ARDS), and multiple organ dysfunction, culminating in vascular collapse refractory to fluid resuscitation (septic shock), and death [11,12].

Though prompt initiation of anti-microbial therapy is crucial in limiting the extent of Gram-negative bacterial infections [13], residual circulating LPS can sustain production of inflammatory mediators by blood leukocytes and microvascular endothelial cells [14]. Given the plethora of proinflammatory mediators that are produced [15], focusing therapy on single inflammatory molecules will likely not alleviate the morbidity associated with this disease [16]. Rather, a more comprehensive countermeasure to reduce the flow of SRTFs to the nucleus would be preferable. Therefore, we hypothesized that targeting the nuclear transport machinery, which integrates multiple signaling pathways emanating from endotoxin-stimulated TLR4 and from subsequently produced cytokines and chemokines [5], would calm the ''genomic storm''. Thus, it would be plausible to reduce lethal endotoxic shock (systemic inflammation) while also attenuating expression of inflammatory mediators in the lungs (localized inflammation). Using computer-based analysis of a public database, we identified the regulatory elements in 46 human genes that encode mediators of inflammation. These regulatory elements are recognized by SRTFs dependent on nuclear translocation mediated by importins a and b [5,7]. To test our hypothesis, we used the next generation NTM, cSN50.1, a highly soluble 28 amino acid cell-penetrating peptide [6] that targets Imp a5 and Imp b1 [9]. We assessed its impact on the inflammatory transcriptome of primary bone marrow-derived macrophages stimulated with LPS. Then, we compared the action of NTM in primary macrophages with in vivo analysis in murine models of systemic and localized inflammation induced by LPS.

Here we report that the modulating nuclear transport with the cell-penetrating NTM, cSN50.1 peptide, leads to selective attenuation of the LPS-induced transcriptome of murine bone marrow-derived macrophages and striking suppression of LPS-induced systemic endotoxic shock and localized lung inflammation. These results support the concept of targeting nuclear import of transcription factors as a means to control the LPS-induced ''genomic storm'' and its resultant inflammatory responses.

Materials and Methods

Peptide synthesis and purification

Highly soluble cell-penetrating NTM peptide cSN50.1 (Table 1), was synthesized, purified, and filter-sterilized as described elsewhere [6,9].

Transcription Factor/Targeted Gene pair selection

Human genes encoding the cytokines, chemokines, receptors and growth factors studied in this manuscript, were analyzed for specific binding sites of transcription factors whose nuclear translocation was previously shown to be modulated by NTM (Table 2). The prediction process was conducted based on the presence of a binding site in the promoter region of the targeted gene. To accomplish this task we employed the UCSC Genome Browser publicly available on the website of the Center for Biomolecular Science and Engineering at the University of California Santa Cruz (UCSC Genome Bioinformatics, http://genome.ucsc.edu).

Isolation and cultivation of bone marrow-derived macrophages (BMDMs)

Bone marrow cells were isolated from femurs and tibias of C57BL/6 mice and suspended in Dulbecco's Modified Eagle Medium supplemented with 10% FBS, 10 mM HEPES, 100 U/ml penicillin, 100 mg/ml streptomycin, and 20% L929-conditioned medium. Non-adherent cells were removed and culture media replaced every three days. Cells were used in experiments after 10 days of culture for up to 2 weeks after maturation. Prior to use in experiments, culture purity of adherent cells was verified by fluorescence-activated cell sorting where $ 95% were MAC3^{+}, CD11b^{+}, CD3^{-}, CD11c^{-} and B220^{-}. Viability was $ 80% as determined by trypan blue exclusion.

LPS treatment of BMDMs and quantitative real-time PCR (qRT-PCR)

BMDMs were left unstimulated for preparation of control RNA, or stimulated with 2 ng/ml LPS from E. coli O127:B8 (Sigma) and concurrently treated with cSN50.1 (30 mM) or saline (diluent). After incubation at 37uC for 6 h, RNA was prepared from cells using the Qiagen RNeasy Kit (Qiagen) and converted to cDNA using the RT^{2} First Strand Kit, then analyzed using the RT^{2} Profiler PCR array system (Qiagen) according the manufacturer's instructions.

Ethics statement

All animal handling and experimental procedures were performed in strict accordance with the recommendations in the Guide for the Care and Use of Laboratory Animals of the National Institutes of Health. The protocol was approved by the Vanderbilt University Animal Care and Use Program (Permit Number: A3227-01), which has been accredited by the American Association of Accreditation of Laboratory Animal Care International (file # 000020). Animals were housed in groups of five in the animal care facility of Vanderbilt University in a 12 hour light/dark cycle. Regular rodent chow and water were provided ad

Table 1. Amino acid sequence of cSN50.1 peptide and its congeners SN50 and cSN50.

Peptide	Sequence	MW [Da]	Solubility in Water	
			[mg/mL]	[mM]
SN50	AAVALLPAVL LALLAP VQRKRQKLMP	2781	13	4.7
cSN50	AAVALLPAVL LALLAP CYVQRKRQKLMPC	3149	38	12.1
cSN50.1	AAVALLPAVL LALLAP CVQRKRQKLMPC	2986	100	33.5

Fragment-linked peptides comprising the Signal Sequence Hydrophobic Region of Fibroblast Growth Factor 4 (bolded) and the NLS region of NFkB1/p50 (italicized) were analyzed for their solubility in water. In cSN50 and cSN50.1, an intra-molecular disulfide bond is formed between the two cysteines, which cyclizes the NLS motif.
doi:10.1371/journal.pone.0110183.t001

libitum. After administration of inflammatory agonists, mice are carefully monitored and any that exhibit end-stage symptoms consistent with acute toxic shock are euthanized as soon as it is apparent they will not recover.

Murine models of LPS-induced systemic (lethal shock) and localized (lung) inflammation

Randomized groups of five female C57BL/6 mice (The Jackson Laboratory) 8–12 weeks of age (~ 20 g weight) and LPS from E. coli O127:B8 (Sigma) were used in all animal experiments. To evaluate the protective efficacy of NTM (cSN50.1 peptide) against systemic inflammation, two models of lethal endotoxic shock were used: high-dose LPS; or low-dose LPS under conditions of metabolic stress imposed by 2-amino-2-deoxy-D-galactosamine (D-Gal), which sensitizes mice to the pro-inflammatory action of LPS [17]. In the high-dose LPS model, 800 mg LPS in 0.2 ml saline was administered by intraperitoneal (i.p.) injection. In the LPS +D-Gal model, mice were injected i.p. with 1 mg of LPS and 20 mg of D-Gal, each in 0.2 ml saline. Two NTM treatment protocols, prophylactic and therapeutic, were tested in the high-dose LPS model. In the prophylactic protocol, mice were given NTM (cSN50.1 peptide, 0.66 mg/injection), or diluent (saline) by i.p. injections of 0.2 ml at 30 min before and 30, 90, 150, 210, 360 and 720 min after LPS challenge, while in the therapeutic protocol, NTM was administered at 15, 90, 150, 210, 360, and 720 min post-LPS challenge. Blood samples (~ 40 mL) were collected from the saphenous vein in heparinized tubes (Sarstedt) before and at 2, 4, 6 and 24 h post-LPS challenge. All injected reagents were sterile and prepared in pyrogen-free saline. These experiments are based on the death of animals as an experimental endpoint, so mice were allowed to progress to a moribund state before being euthanized by isoflurane asphyxiation. Since multiple organ systems are affected in the mechanism of systemic inflammation, any pain medication may inadvertently interfere with the progression of endotoxic shock. Therefore, we could not use agents that alleviate pain. However, we attempted to minimize the amount of pain experienced by the animals by closely monitoring mice, at least hourly for the first 24 hours and three times a day thereafter, and euthanizing any mice that exhibit end-stage symptoms consistent with acute toxic shock (lack of reaction to cage motion, or any of the following signs: ataxia, paralysis, cyanosis, or severe respiratory distress) as soon as it is apparent they will not recover. Any surviving mice were euthanized after 72 h.

For induction of localized acute lung inflammation, intranasal instillations of 50 ng of LPS in 50 mL saline (25 mL/nostril) were performed under ketamine/xylazine anesthesia (0.2 ml of 6.7 mg/ml ketamine and 1.3 mg/ml xylazine administered by i.p. injection). Mice were treated with NTM (cSN50.1 peptide, 0.66 mg/injection) or diluent (saline) administered by i.p. injections of 0.2 ml at 30 min before and at 30, 90, and 120 min after LPS challenge. Six hours post-LPS challenge, mice were euthanized by isoflurane asphyxiation. Bronchoalveolar lavage (BAL) collection and differential cell counts were performed as previously described [18]. For comparison, BAL was also collected from naïve mice not exposed to any intranasal instillation before euthanasia.

Analysis of chemokines, cytokines, and growth factors in BAL fluid and plasma

The effect of cSN50.1 on expression of chemokines, cytokines and growth factors was analyzed in cell-free BAL fluid or blood plasma from mice by cytometric bead array (BD BioSciences) or a 32-analyte Milliplex mouse panel (Millipore) according to the manufacturers' instructions. Analytes included eotaxin, granulocyte colony-stimulating factor (G-CSF), granulocyte macrophage colony-stimulating factor (GM-CSF), interferon gamma (IFN-c), interleukin (IL) 2 1a, IL-1 b, IL-2, IL-3, IL-4, IL-5, IL-6, IL-7, IL-9, IL-10, IL-12 (p40), IL-12 (p70), IL-13, IL-15, IL-17, IFN-c-induced protein 10 (IP-10), keratinocyte chemoattractant (KC), leukemia inhibitory factor (LIF), LPS-induced CXC chemokine (LIX), macrophage colony-stimulating factor (M-CSF), monocyte chemoattractant protein-1 (MCP-1), monokine induced by gamma interferon (MIG), macrophage inflammatory protein (MIP) 2 1a, MIP-1 b, MIP-2, regulated upon activation normal T-cell expressed, and presumably secreted (RANTES), tumor necrosis factor alpha (TNF-a), and vascular endothelial growth factor (VEGF).

Statistical analyses

Threshold cycle values from qRT-PCR were exported to Excel and analyzed using the Qiagen web-based PCR Array Data Analysis Software. Genes showing a ~ 0.5 log fold change versus control were considered significant. Other data analysis and statistical calculations were performed using Prism (GraphPad). Cell counts and chemokine, cytokine, and growth factor levels in BAL were compared using the non-parametric Mann–Whitney U test. Survival data were analyzed by the log-rank test. Cytokine, chemokine and growth factor levels in plasma collected from the same animals at different time points were evaluated by repeated measures two-way analysis of variance with Sidak's post-test. A p value of ~ 0.05 was considered significant.

Results

Design and characterization of the next generation NTM, cSN50.1 peptide, and its previous congeners

A fragment-linked peptide strategy to analyze signal-dependent nuclear transport is based on fusing a motif from the nuclear localization sequence (NLS) region of the NF-kB1/p50 subunit

Table 2. Genes encoding mediators of inflammation are regulated by transcription factors that require nuclear transport shuttles targeted by NTM.

	Transcription Factor (MW/kDa)	Nuclear Targeting Motif	# of targeted genes	Cytokines and Growth Factors																						Chemokines																Receptors/Transporters									
				Il1a	Il1b	Il6	Il9	Il10	Il12p40	Il12p70	Il13	Il15	Il17	Il18/IGIF	Ifng	Lif	Lta	Tnf	Spp1	G-csf/Csf3	M-csf/Cs f1	Gm-csf/C sf2	Vegf	Ccl2/MCP -1	Ccl3/MIP- 1a	Ccl4/MIP- 1b	Ccl5/RANT ES	Ccl7/MCP -3	Ccl8/MCP -2	Ccl17/TAR C	Ccl19/MI P-3 b	Ccl20/MI P-3 a	Ccl22/MDC	Ccl24/MPI F-2	Cx3cl1/ABC D-3	Cxcl2/MIP-2 a	Cxcl5/LIX	Cxcl9/MIG	Cxcl10/IP -10	Cxcl11/IP -9	Cxcr5/CD1 85	Ccr2/CD19 2	Ccr3/CD19 3	Ccr7/CD19 7	Ccr10/GP R2	Il6ra	Il6st	Tnfrsf1b	Abcf1
1	NF-kB1/p50 (48)	mNLS	46	+	+	+	+	+	+	+	+	+	+	+	+	+	+	+	+	+	+	+	+	+	+	+	+	+	+	+	+	+	+	+	+	+	+	+	+	+	+	+	+	+	+	+	+	+	+
2	STAT-1 (87)	uNLS	34	+			+	+	+	+	+		+	+	+	+	+	+	+	+	+	+	+	+	+	+		+	+							+		+	+	+	+	+	+	+	+	+	+	+	+
3	AP-1 c-Jun (36)	bNLS	32	+	+	+	+				+		+	+		+	+	+	+	+	+	+	+	+	+	+	+	+	+					+		+			+	+	+	+	+	+	+		+	+	+
4	Rel A (60)	mNLS	32	+	+	+	+	+	+		+				+	+	+	+	+		+	+	+		+			+	+	+	+	+		+	+	+	+	+	+	+	+	+	+	+	+	+	+	+
5	NF-kB2/p52 (49)	mNLS	31	+	+	+		+	+	+					+	+	+	+	+			+	+	+		+	+	+	+		+	+	+	+	+	+	+	+	+	+	+	+	+	+	+	+	+	+
6	c-Rel (68)	mNLS	26		+	+	+	+			+	+				+	+	+		+	+			+			+	+		+			+		+	+	+	+	+	+				+	+	+		
7	nSREBP1 (51)	bHLH	19										+	+	+	+	+	+		+	+	+	+							+				+				+	+			+							+
8	NFATc4 (96)	mNLS	15		+	+	+	+			+		+			+	+	+		+	+								+				+									+						+
9	NFATc1 (77)	mNLS	14		+	+	+	+			+					+	+	+		+	+								+				+									+						+
10	NFATc2 (100)	mNLS	14		+	+	+	+			+					+	+	+		+	+								+				+									+						+
11	NFATc3 (116)	mNLS	14		+	+	+	+			+					+	+	+		+	+								+				+									+						+
12	NRF-2 (68)	mNLS	6					+								+	+	+																					+									+

Analysis was performed in silico using The UCSC Genome Browser (The UCSC Genome Bioinformatics). mNLS - classical monopartite Nuclear Localization Sequence; bNLS - nonclassical bipartite Nuclear Localization Sequence; uNLS - unconventional, structural or dimer-specific Nuclear Localization Sequence; bHLH - basic helix-loop-helix motif; ''+'' - the transcription factor specific binding site is present in the gene promoter.

doi:10.1371/journal.pone.0110183.t002

with the signal sequence hydrophobic region (SSHR) of human fibroblast growth factor 4 [7,19]. NLS- and SSHR-containing NTMs (SN50, cSN50 and cSN50.1; see Table 1 for their composition and solubility) were designed to function at the nuclear transport level by binding to importins a during stimulus-initiated signaling and thereby modulate nuclear import of NLS-bearing SRTFs. The SSHR motif allows peptides to cross the plasma membrane of cells in culture or in experimental animals through an ATP- and endosome-independent mechanism [20]. In this study, we used cSN50.1, an improved version of our previously described cell-penetrating NTM peptides [6,9,21,22] that shows increased solubility (100 mg/ml) in water, compared to cSN50 (38 mg/ml) and SN50 (13 mg/ml) (see Table 1), thereby increasing its potency [6,21]. The functional utility of NTMs has been reported in numerous preclinical models of inflammation caused by microbial and autoimmune insults [18,21–26]. Most recently, and unexpectedly, we found that cSN50.1 not only modulates nuclear transport of SRTFs such as NF-kB, but also sterol regulatory element-binding protein (SREBP) transcription factors that regulate lipid homeostasis [6].

NTM has a calming effect on the "genomic storm" induced by LPS in primary macrophages

Recently, it was shown that injection of bacterial endotoxin into healthy adult volunteers was associated with a robust genomic response in combined blood leukocyte populations [10]. Among the genes reported in that study, several encoded cytokines, chemokines, and their receptors as reflected by transcriptome analysis. We used a publicly available database to match genes encoding mediators of inflammation with transcription factors containing nuclear targeting motifs known to require nuclear transport shuttles recognized by cSN50.1 [6] (Table 2). We found that all 46 proinflammatory genes are potentially regulated by NF-kB1, 34 genes by STAT-1, 32 genes by c-Jun, and 19 genes by SREBP1. Most of these genes are combinatorially regulated by two or more transcription factors that are transported to the nucleus as monomers or homodimers/heterodimers by importins a and b. Their transport function is modulated by NTMs that encompass cell penetrating SN50, cSN50, and cSN50.1 peptides [6,9] (Table 1). It is thus plausible that cSN50.1 peptide can suppress expression of multiple proinflammatory genes by modulating nuclear transport of transcription factors analyzed in Table 2.

We tested this hypothesis through analysis of the proinflammatory transcriptome in bone marrow-derived macrophages. These primary cells are one of the main myeloid lineage targets of LPS [27]. A mouse inflammatory cytokine/chemokine and receptor PCR array allowed us to assess the effects of NTM on 84 genes compared to untreated controls. Remarkably, NTM modified expression of 37 of the 84 genes tested. While NTM suppressed gene expression in LPS-activated inflammatory pathways (Figure 1), it did not alter gene expression of five housekeeping genes (Gusb, Hprt1, Hsp90ab1, Gapdh, Actb, , 0.5 fold change versus control, not shown). Genes encoding most cytokines and CC chemokines were down-regulated by NTM whereas those for most CC chemokine receptors, cytokine receptors, and CX chemokines and their receptors were not affected. There were a few notable exceptions: LIX/CXCL5, MIG/CXCL9, and IP-10/CXCL10. Importantly, this suppression of genomic changes by NTM in primary macrophages challenged with LPS was not associated with changes in cell viability (data not shown), indicating that NTM has no adverse effect on cell growth. Thus, targeting nuclear transport pathways for LPS-activated SRTFs with cSN50.1 peptide prevented a "genomic storm" by reducing

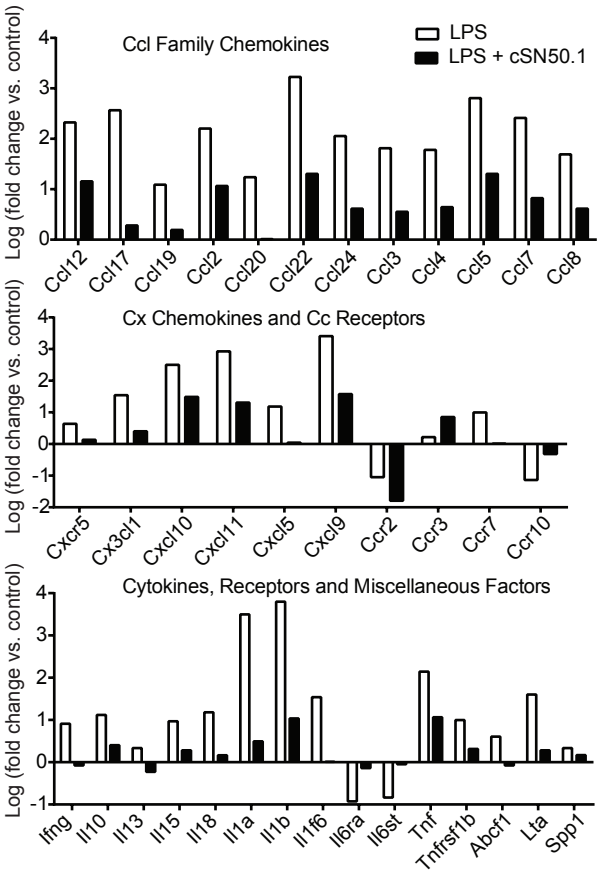

Figure 1. qRT-PCR -based gene expression analysis of LPS-challenged BMDMs in the absence or presence of NTM. Ccl family chemokines, Cx chemokines and Cc receptors, and cytokines, receptors and miscellaneous factors from an 84 gene array exhibiting a . 0.5 log fold change in LPS-stimulated primary macrophages compared to unstimulated control cells.
doi:10.1371/journal.pone.0110183.g001

transcription of a wide array of genes that encode mediators of inflammation in primary macrophages.

NTM attenuates LPS-induced systemic inflammation in the form of lethal endotoxic shock accompanied by a burst of proinflammatory cytokines and chemokines in blood

After analysis of the primary macrophage response to LPS modulated by NTM, we studied its effect on two models of LPS-induced systemic inflammation exemplified by lethal shock. In a high-dose LPS model, both prophylactic and therapeutic NTM treatment protocols were employed. In the prophylactic protocol, the first dose of NTM was administered before LPS challenge while in the therapeutic protocol, NTM treatment was begun after LPS administration. As shown in Figure 2A, animals treated with NTM by the prophylactic protocol in the high-dose LPS model were completely protected, compared to only 10% survival in saline-treated control animals (p, 0.0001). Strikingly, when a therapeutic NTM treatment protocol was employed in the high-dose LPS model, 75% of mice survived, compared to 100% mortality in the saline-treated control group (Figure 2B, p,

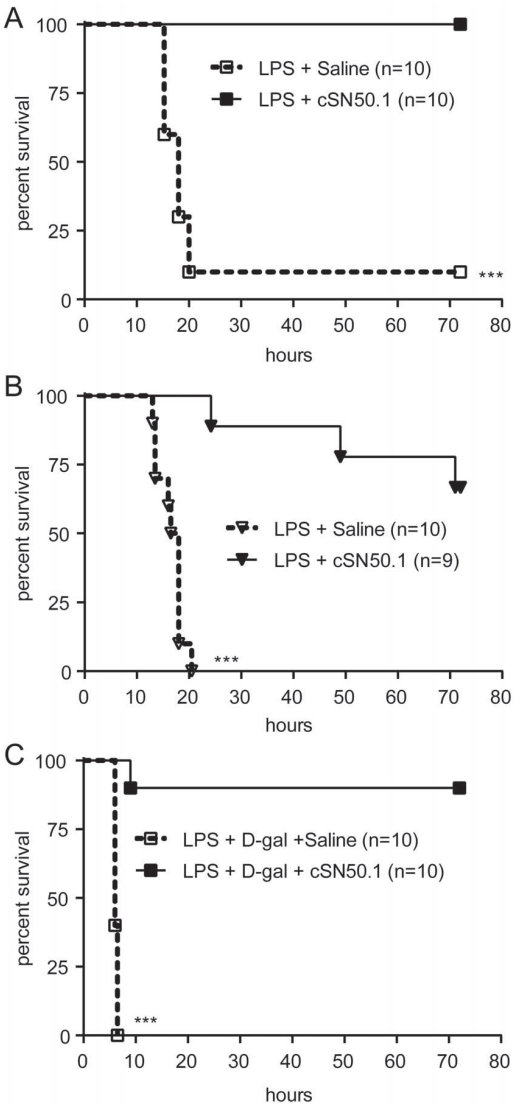

Figure 2. NTM treatment enhances survival from lethal endotoxic shock. Survival curves for mice challenged i.p. with high-dose LPS (A and B) or low-dose LPS+D-Gal (C). In (A) and (C) mice were administered the first NTM (cSN50.1 peptide) treatment 30 min before LPS challenge (prophylactic protocol), while in (B), the first treatment was administered 15 min after LPS challenge (therapeutic protocol). Saline injections were administered to control mice challenged with LPS following the same treatment schedule in each protocol, as described in "Materials and Methods". ***p, 0.0005 by log rank test.
doi:10.1371/journal.pone.0110183.g002

0.0001). Thus, NTM was highly effective against high-dose LPS with both prophylactic and therapeutic protocols.

To further evaluate the effectiveness of the NTM, we tested its anti-inflammatory effect under conditions of metabolic stress imposed by D-Gal, which sensitizes mice to LPS [17]. In contrast to the high-dose LPS model, which requires at least 800 mg of LPS per 20 g mouse for induction of lethal shock, only 1 mg of LPS per 20 g mouse is required for lethality when mice are metabolically stressed with D-Gal, and death occurs much more rapidly (5–7 h after low-dose LPS +D-gal compared to 16–20 h post-LPS in the high-dose model). Consistent with results from the high-dose LPS shock model, prophylactic NTM treatment afforded robust protection (90%) in mice challenged with LPS +D-Gal. In contrast, no mice survived in the control group treated with saline (Figure 2C, p, 0.0005).

We analyzed the striking gain in survival of NTM-treated mice that were challenged with LPS in the context of systemic proinflammatory cytokine and chemokine production. As expected, in the prophylactic protocol, NTM treatment engendered significant inhibition of 11 out of 13 proinflammatory cytokines whose plasma levels were increased by LPS challenge (Figure 3A, upper). An exception was the anti-inflammatory cytokine, IL-10, which was elevated. 2 fold in NTM-treated animals. In parallel, a wide array of LPS-elevated chemokines and growth factors was suppressed in NTM-treated mice (Figure 3A, lower). Overall, of 26 cytokines, chemokines and growth factors elevated in plasma after LPS challenge, 23 were reduced by NTM treatment, two were unchanged (eotaxin/CCL11 and IL-5, not shown) and one was increased (IL-10). Plasma levels of the remaining six of the 32 analytes tested were not increased by administration of LPS (not shown). These results are consistent with the genomic response of primary macrophages in the qRT-PCR analysis (see Figure 1), indicating that NTM, under the conditions of these in vivo experiments, suppresses expression of multiple mediators of inflammation. A comparable trend in suppression of proinflammatory cytokines and chemokines TNF- a, IL-6, IFN- c and MCP-1 was observed in mice treated with NTM when employing the therapeutic protocol, albeit to a lesser degree. Interestingly in the therapeutic protocol, IL-10 is suppressed instead of enhanced by NTM (Figure 3B), consistent with suppression of the Il10 gene in primary macrophages (see Figure 1).

Cumulatively, our results indicate that NTM affords robust protection of mice from LPS-induced systemic inflammation in two distinct models of lethal shock. Concurrently, we noted a striking reprogramming of the inflammatory response that entails suppression of many proinflammatory cytokines and chemokines in plasma.

NTM attenuates proinflammatory cytokine and chemokine expression after direct airway exposure to LPS

We next sought to correlate our transcriptome analysis of primary macrophages with the production of inflammatory mediators in the bronchoalveolar space in a murine model of LPS-induced ALI. After challenging mice intranasally with LPS, we analyzed inflammatory mediators and cell populations in BAL fluid. We determined that i.p. administration of NTM suppressed the LPS-induced increase of 14 out of 32 proinflammatory chemokines, cytokines and growth factors analyzed in BAL fluid (Figure 4). Consistent with genomic reprogramming in primary macrophages (see Figure 1), NTM treatment effectively reduced chemokines linked to lung inflammation by their roles in mediating inflammatory cell migration to the lung: MCP-1/CCL2, MIP-1 a/CCL3, and LIX/CXCL5. Suppressed production of cytokines IL-1 a, IL-1 b, IFN- c, and IL-13 also correlated with results from BMDMs. Conversely, some inflammatory mediators, such as MIG, were not induced by direct airway exposure to LPS, while TNF- a, MIP-1 b/CCL4, RANTES/CCL5 and IP-10/CXCL10 were induced by LPS but not suppressed by NTM treatment. However, these discrepancies between the qRT-PCR assay and BAL analysis can be attributed to the different cell populations present in each assay. NTM did reduce BAL levels of a number of other inflammatory mediators that were not analyzed by qRT-PCR: cytokines LIF, IL-9, and IL-12p70; chemokine MIP-2/CXCL2; and growth factors G-CSF, M-CSF, and VEGF,

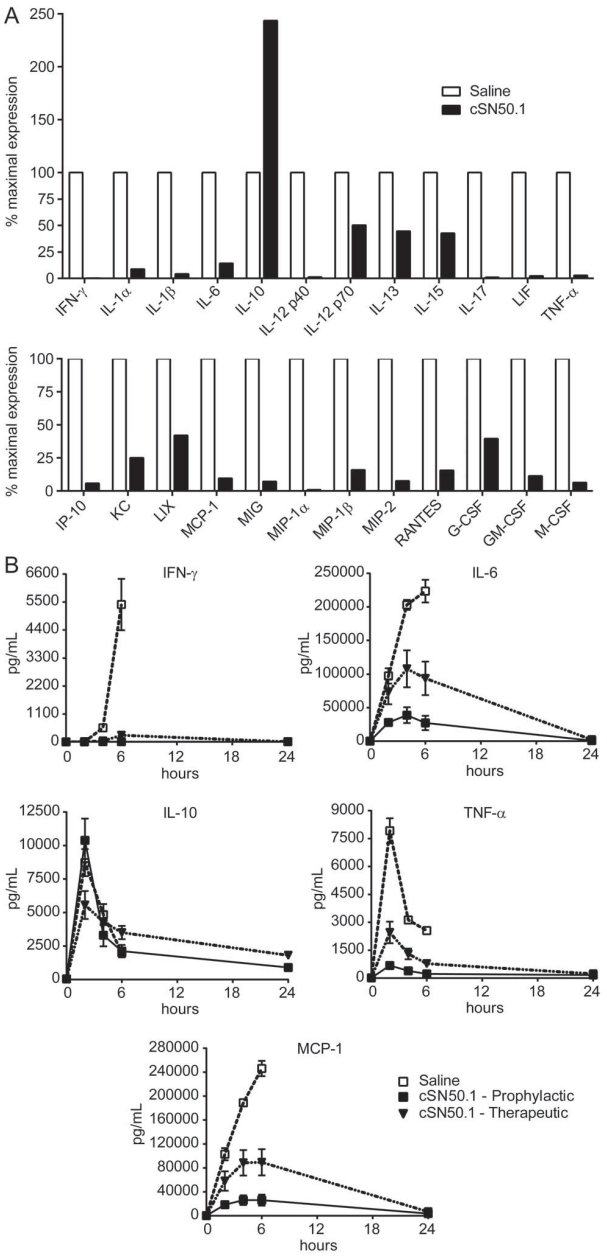

Figure 3. NTM treatmen t reduces plasma levels of multiple cytokines, chemokin es and growth factors induced by LPS. (A) Wild type C57BL/6 mice were challenged i.p. with a lethal dose of LPS (800 mg) and treated with i.p. injections of NTM (cSN50.1 peptide) or diluent (saline) following a prophylactic protocol as in Figure 4A. Blood was collected at baseline and 2 or 6 h after LPS challenge and a multiplex assay was used to measure 32 analytes in plasma. Twenty-four analytes were significantly altered by NTM treatment, as determined by repeated measures two-way analysis of variance with Sidak's post-test. Twenty-three were reduced, while anti-inflammatory IL-10 was increased by NTM treatment. Results are shown as the % inhibition or increase by NTM compared to saline control set to 100% at the time point demonstrating maximal expression for that analyte. n = 10 animals/group. (B) Comparison of prophylactic and therapeutic NTM treatment protocols on selected plasma cytokine and chemokine levels in the high-dose LPS model of endotoxic shock. Data are presented as mean 6 standard error, n = 5 2 10 animals/group.
doi:10.1371/journal.pone.0110183.g003

which is implicated in vascular permeability[28]. Overall, analysis of BAL documents the effectiveness of NTM in suppressing mediators of ALI after direct airway exposure to LPS.

Suppression of chemokines MCP-1/CCL2, MIP-1 a/CCL3, MIP-1 b/CCL4, and LIX/CXCL5 in the inflammatory transcriptome analysis of NTM-treated primary macrophages and in BAL following direct airway exposure to LPS, led us to postulate that NTM would reduce leukocyte trafficking to the lung. As shown in Figure 5, we observed a 5-fold reduction in total cell count in BAL fluid from mice treated with NTM in comparison to the saline-treated control group (p, 0.005), reducing the total cell count in BAL from NTM-treated mice to that of naive mice. A reduction in neutrophils (, 80%, p, 0.05) accounted for most of the difference in BAL cellularity. Trafficking of monocytes/macrophages, the primary cell type detected in BAL fluid from naïve mice was moderately reduced (30%), but not significantly. Lymphocytes represented less than 1% of cells detected in BAL and their numbers were unchanged by NTM treatment (Figure 5). Thus, migration of neutrophils to the bronchoalveolar space in response to direct airway exposure to LPS, which evokes a robust expression of chemokine genes, is profoundly reduced by systemic administration of NTM. As neutrophils are the main source of oxidative stress to the delicate structure of the blood-air barrier [29], NTM's suppression of chemokines responsible for massive neutrophil trafficking to the bronchoalveolar space may engender a new approach to lung cytoprotection. Thus, LPS-induced respiratory and systemic blood inflammatory responses and their lethal outcomes are averted.

Discus sion

Cumulatively, our results document the essential role of nuclear transport in development of a "genomic storm" and its sequelae induced by bacterial endotoxin. This evidence rests on the design and application of a highly soluble NTM, cSN50.1 peptide, which targets nuclear transport shuttles required for translocation of proinflammatory SRTFs and metabolism-regulating SREBPs. The emerging concept of a "genomic storm" in critically injured patients has been extended to human subjects challenged with bacterial endotoxin[10]. Our analysis of 46 genes encoding a wide array of mediators of inflammation (see Table 2) indicated that these genes are regulated by a group of transcription factors responsible for proinflammatory and metabolic signaling to the nucleus. As nuclear translocation of these transcription factors depends on nuclear transport machinery, we showed how modulation of this machinery with a cell-penetrating peptide targeting Imp a5 and Imp b1 calms the "genomic storm" triggered by bacterial endotoxin in primary BMDMs, and attenuates systemic and localized inflammation. These results obtained in murine macrophages are congruent with the gene expression profile of human peripheral blood leukocytes following endotoxin challenge [30]. Though it was recently asserted that humans and mice display discordant genomic responses to severe injury [31], subsequent reanalysis of the datasets employed in that study indicates that the gene expression profiles in the mouse models were highly similar to human responses[30].

We show that cSN50.1 had a profound suppressing effect on the inflammatory transcriptome of LPS-stimulated primary macrophages. This effect was paralleled by suppression of multiple cytokines, chemokines and, growth factors in plasma in response to LPS. Furthermore, NTM protected mice from lethality in two endotoxic shock models NTM also attenuated proinflammatory cytokines and chemokines in inflamed lungs accompanied by reduced trafficking of neutrophils to the LPS-challenged bronchoalveolar space. These

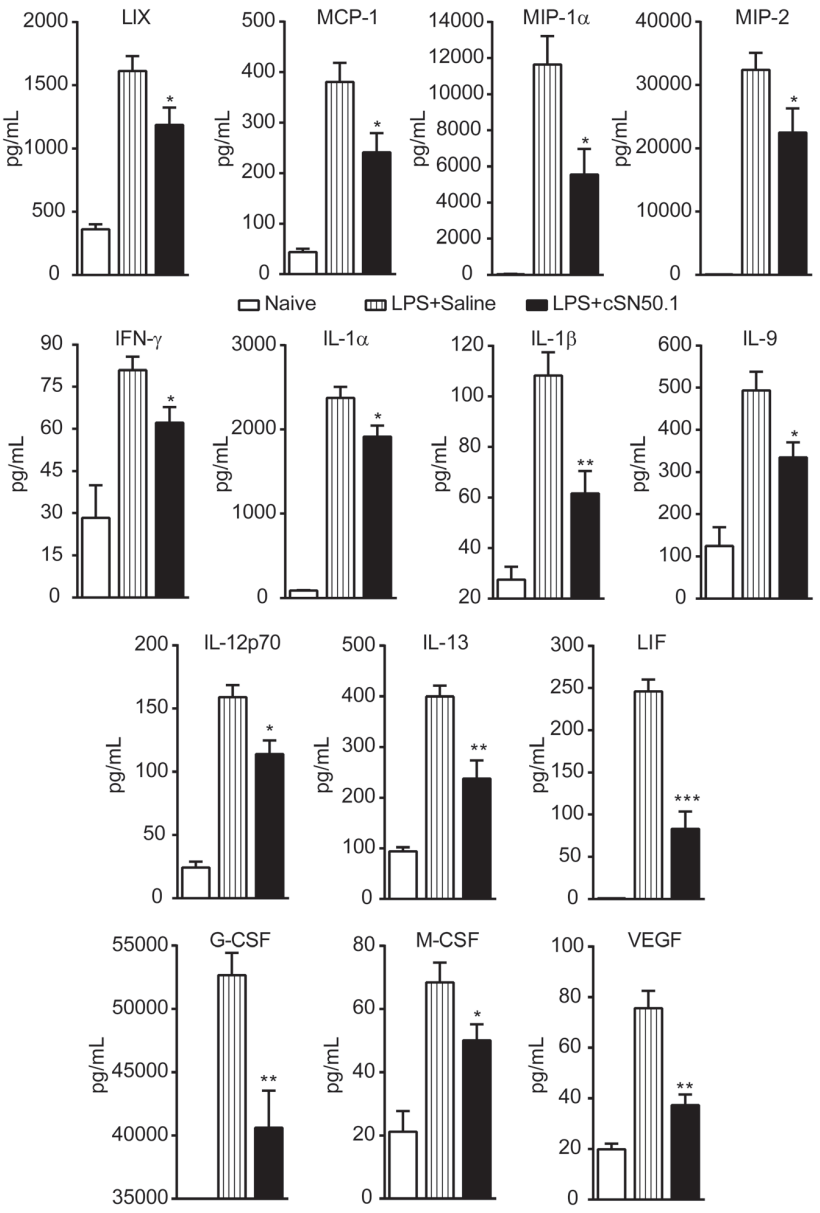

Figure 4. LPS-induced expression of chemokines, cytokines, and growth factors in the lung is suppressed by NTM. Fourteen cytokines, chemokines and growth factors elevated in BAL after direct airway exposure to LPS are significantly suppressed by NTM (cSN50.1 peptide) treatment. Data are presented as mean 6 standard error, n = 4 naïve and 8–9 NTM- or saline-treated animals/group from 3 independent experiments. *p, 0.05, **p, 0.005, and ***p, 0.0005 by Mann-Whitney U test comparing LPS-challenged groups.
doi:10.1371/journal.pone.0110183.g004

results indicate that the more soluble, next generation NTM modulates nuclear signaling induced by LPS, thereby effectively reducing its deleterious effects in systemic (endotoxic shock) and localized (lung) inflammation.

NTM is rapidly delivered (within 30–60 min after i.p. injection) through a receptor-and endocytosis-independent mechanism [20] to mouse blood cells and organs where it reaches sufficient intracellular concentration to engender localized (lung) and systemic (endotoxic shock) anti-inflammatory effects. Thus, the microvascular compartment of multiple organs that are vulnerable to LPS toxicity (e.g. lungs, liver, and kidneys) can be protected [18,22]. Unlike anti-inflammatory glucocorticosteroids which produced discordant results in sepsis clinical trials [32,33] and have potentially adverse side effects on metabolic balance (e.g. hyperglycemia and hyperlipidemia) [34–36], NTM not only suppresses pulmonary and systemic inflammation induced by LPS but also corrected metabolic derangements in an experimental model of hyperlipidemia by targeting nuclear transport of SREBPs [6]. This new function of cSN50.1 resulted in significant amelioration of hyperlipidemia and hyperglycemia. Metabolic dysregulation is a consequence of the systemic action of LPS, which in turn accelerates the vascular complications of hyperlipidemia [37–39]. SREBPs lack an NLS for binding to importins a and are shuttled to the nucleus by binding to Imp b1 [40]. We

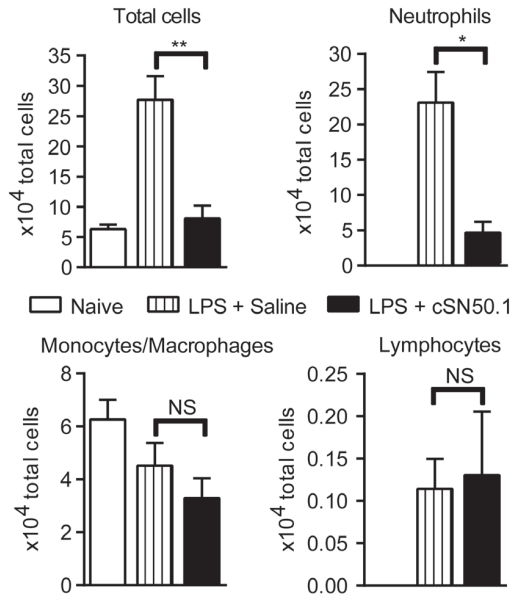

Figure 5. LPS-in duced cellular trafficking to lungs is reduced in NTM-treated mice. Cell counts in BAL fluid collected from unchallenged mice (naïve) and 6 h after direct airway exposure to LPS, with i.p. NTM peptide (cSN50.1) or diluent control (saline) treatment. The LPS-induced increase in total cells is comprised primarily of neutrophils. Neutrophil trafficking to BAL is significantly reduced by NTM treatment while monocytes/macrophages and lymphocytes are not affected. Data are presented as mean 6 standard error, n = 4 naïve and 5–7 NTM- or saline-treated animals/group from two independent experiments. *p, 0.05, **p, 0.005 by Mann-Whitney U test comparing LPS-challenged groups.
doi:10.1371/journal.pone.0110183.g005

discovered that the SSHR motif of cSN50.1 binds Imp b1, thereby reducing nuclear translocation of SREBP-1 and 2 2. To the best of our knowledge, the immunoregulatory function of SREBP1 toward genes that encode proinflammatory cytokines and chemokinesis not well understood.

Three interwoven mechanisms of LPS-induced systemic inflammation: endothelial injury, apoptosis, and microvascular dysfunction, depend on modulation of a nuclear transport-regulated genomic response [5,22,41,42]. Significantly, we documented that systemic production of proinflammatory cytokines, chemokines and growth factors, which contribute to the subsequent development of endotoxic shock, was attenuated, while only IL-10 was increased by NTM, and only in plasma. Whereas elevation of IL-10 is notable in the profile of cytokine and chemokine responses in human sepsis studies [43–45], other critical proinflammatory mediators are consistently suppressed by NTM, and NTM treatment is highly protective against lethal shock. Since many small transcription factors (, 45 kDa) essential to cell viability can traverse the nuclear pore without assistance from importins a and b [46], which are the targets of NTM [6], it is unlikely that NTM is involved in their nucleocytoplasmic trafficking. Thus, targeted modulation of nuclear transport of proinflammatory SRTFs, the master regulators of innate immunity and inflammation, and SREBPs, the master regulators of metabolic inflammation, offers a new approach to suppression of inflammatory, metabolic, and apoptotic mediators in the lung, liver, and other organs to interrupt rapidly progressing microvascular injury induced by bacterial endotoxin. Importantly, in polymicrobial sepsis and a pulmonary anthrax model, addition of NTM to antimicrobial therapy improved the outcome in terms of clearance of bacteria and survival [24,26]. These studies militate against the notion that using NTM to modulate nuclear transport of SRTFs would compromise the outcome of microbial inflammatory diseases.

Important to these considerations of novel countermeasures toward LPS toxicity is the rise of multidrug-resistant Gram-negative bacterial infections in intensive care units throughout the United States, Europe, and Asia. These infections cause localized and systemic inflammation leading to septic shock and are a growing concern in immunocompromised hosts [47,48]. Alarmingly, Gram-negative bacteria are isolated from 62% of patients with severe sepsis; approximately half of these cases result in individuals dependent upon mechanical ventilation [49]. The rate of acquiring bacterial pneumonia increases up to 21% in intubated patients and rises even higher as the length of intubation persists [50–52]. In total, Gram-negative bacteria account for more than 30% of hospital-acquired infections causing pneumonia [53].

A cardinal feature of localized inflammation of the lungs (pneumonia and ARDS) caused by Gram-negative bacteria is endothelial and epithelial injury [29]. The response to microbial virulence factors leads to uncontrolled production of proinflammatory chemokines and cytokines that contribute to collateral damage of the air-blood barrier. We postulate that simultaneous reduction of multiple proinflammatory cytokines and chemokines induced by direct airway exposure to LPS has a salutary effect on other lung-associated inflammatory cells. For example, intracellular delivery of NTM significantly reduced trafficking of neutrophils to the bronchoalveolar space. At least three NTM-suppressed cytokines, IL-6, IL-17, and IFN- c, through their localized action, contribute to the disruption of lung endothelial and epithelial barriers [54,55], manifested by migration of leukocytes to the bronchoalveolar space, leakiness of plasma proteins therein, and impairment of respiratory function. Consistent with localized suppression of LIX, MCP-1, MIP-1 a, and MIP-2 by NTM, a significant migration of neutrophils to the bronchoalveolar space was attenuated, thereby reducing potential oxidant injury to the respiratory epithelium and vascular endothelium. Systemic suppression by NTM of chemokines IP-10, MCP-1, MIG, MIP-1 b and RANTES in plasma is also of significance due to their role in induction of inflammatory cell migration to the bronchoalveolar space [56,57].

The need for new therapeutic approaches to protect lungs and other major organs from LPS-induced injury is apparent as there is currently no available FDA-approved drug to counteract collateral organ injury during sepsis, ALI, and ARDS [11]. The prospect for an effective countermeasure based on a single cytokine/chemokine target for monoclonal antibodies or soluble cytokine receptor antagonists [58–60] is dimmed by the potential for significant redundancy in cytokine signaling. We have now demonstrated the beneficial effects of NTM in two diverse models of localized lung inflammation: one induced by LPS, a potent agonist of TLR4-expressing myeloid, endothelial, and epithelial cells as documented in this study, and the second, induced by staphylococcal enterotoxin B, a superantigenic immunotoxin, which is a robust agonist of T cell receptor-expressing cells [18]. Our findings document the potential utility of targeting the nuclear transport shuttles with cell-penetrating peptides to simultaneously suppress production of multiple cytokines and chemokines and potentially correct metabolic derangements [6]. Survivors of sepsis have strikingly lower levels of NF- kB in the nuclear compartment of peripheral blood mononuclear leukocytes than non-survivors [61]. Using an established formula for extrapolating a human equivalent dose from the animal dose

through normalization to body surface area [62], the effective cSN50.1 peptide dose of 0.66 mg/20 g mouse translates to a manageable human dose of 200 mg/70 kg. This is similar to a standard oral dose of ibuprofen, a non-steroidal anti-inflammatory drug, which at a daily intravenous dose of 800 mg, was proven ineffective in reducing shock, ARDS, and mortality in a human sepsis trial [63]. However, further studies will be required to determine the pharmacokinetics, toxicity, and therapeutic efficacy of NTMs.

Given its efficient delivery to the lungs and rapid action, a cell-penetrating NTM peptide targeting nuclear import of SRTFs and SREBPs may represent a much-needed adjunctive therapy to complement antimicrobials that target Gram-negative bacteria in systemic (endotoxic shock) and localized (lung) infections. In such a combined treatment, antimicrobials would limit the proliferation of Gram-negative bacteria that shed LPS and express exotoxins while the collateral damage to lungs and other organs through uncontrolled inflammation would be contained by NTM. Thus, the serious and costly consequences of Gram-negative infections can be potentially reduced.

Acknowledgments

We dedicate this paper to the memory of Dr. Robert D. Collins, our mentor, collaborator, advisor and friend.

Author Contributions

Conceived and designed the experiments: AD RAV JZ JH. Performed the experiments: AD RAV JZ DJM LSW MAH. Analyzed the data: AD RAV JZ JH. Contributed to the writing of the manuscript: AD RAV JZ JH.

References

1. Rosenberg HF, Gallin JI (2003) Inflammation. In: Paul WE, editor. Fundamental Immunology. 5th ed. Philadelphia, PA: Lippincott Williams & Wilkins. pp. 1151–1169.
2. Beutler B (2004) Innate immunity: an overview. Mol Immunol 40: 845–859.
3. Opal SM (2010) New perspectives on immunomodulatory therapy for bacteraemia and sepsis. Int J Antimicrob Agents 36 Suppl 2: S70–73.
4. Beutler BA (2009) TLRs and innate immunity. Blood 113: 1399–1407.
5. Hawiger J (2001) Innate immunity and inflammation: a transcriptional paradigm. Immunol Res 23: 99–109.
6. Liu Y, Major AS, Zienkiewicz J, Gabriel CL, Veach RA, et al. (2013) Nuclear transport modulation reduces hypercholesterolemia, atherosclerosis, and fatty liver. J Am Heart Assoc 2: e000093.
7. Torgerson TR, Colosia AD, Donahue JP, Lin YZ, Hawiger J (1998) Regulation of NF-kappa B, AP-1, NFAT, and STAT1 nuclear import in T lymphocytes by noninvasive delivery of peptide carrying the nuclear localization sequence of NF-kappa B p50. J Immunol 161: 6084–6092.
8. Weis K (2003) Regulating access to the genome: nucleocytoplasmic transport throughout the cell cycle. Cell 112: 441–451.
9. Zienkiewicz J, Armitage A, Hawiger J (2013) Targeting nuclear import shuttles, importins/karyopherins alpha by a peptide mimicking the NFkappaB1/p50 nuclear localization sequence. J Am Heart Assoc 2: e000386.
10. Xiao W, Mindrinos MN, Seok J, Cuschieri J, Cuenca AG, et al. (2011) A genomic storm in critically injured humans. J Exp Med 208: 2581–2590.
11. Angus DC, van der Poll T (2013) Severe sepsis and septic shock. N Engl J Med 369: 840–851.
12. Hawiger J, Musser JM (2011) How to approach genome wars in sepsis? Crit Care 15: 1007.
13. Kumar A, Roberts D, Wood KE, Light B, Parrillo JE, et al. (2006) Duration of hypotension before initiation of effective antimicrobial therapy is the critical determinant of survival in human septic shock. Crit Care Med 34: 1589–1596.
14. Levin J, Poore TE, Young NS, Margolis S, Zauber NP, et al. (1972) Gram-negative sepsis: detection of endotoxemia with the limulus test. With studies of associated changes in blood coagulation, serum lipids, and complement. Ann Intern Med 76: 1–7.
15. Sjovall F, Morota S, Asander Frostner E, Hansson MJ, Elmer E (2014) Cytokine and nitric oxide levels in patients with sepsis- temporal evolvement and relation to platelet mitochondrial respiratory function. PLoS One 9: e97673.
16. Lorente JA, Marshall JC (2005) Neutralization of tumor necrosis factor in preclinical models of sepsis. Shock 24 Suppl 1: 107–119.
17. Galanos C, Freudenberg MA, Reutter W (1979) Galactosamine-induced sensitization to the lethal effects of endotoxin. Proc Natl Acad Sci U S A 76: 5939–5943.
18. Liu D, Zienkiewicz J, DiGiandomenico A, Hawiger J (2009) Suppression of acute lung inflammation by intracellular peptide delivery of a nuclear import inhibitor. Mol Ther 17: 796–802.
19. Lin YZ, Yao SY, Veach RA, Torgerson TR, Hawiger J (1995) Inhibition of nuclear translocation of transcription factor NF-kappa B by a synthetic peptide containing a cell membrane-permeable motif and nuclear localization sequence. J Biol Chem 270: 14255–14258.
20. Veach RA, Liu D, Yao S, Chen Y, Liu XY, et al. (2004) Receptor/transporter-independent targeting of functional peptides across the plasma membrane. J Biol Chem 279: 11425–11431.
21. Liu XY, Robinson D, Veach RA, Liu D, Timmons S, et al. (2000) Peptide-directed suppression of a pro-inflammatory cytokine response. J Biol Chem 275: 16774–16778.
22. Liu D, Li C, Chen Y, Burnett C, Liu XY, et al. (2004) Nuclear import of proinflammatory transcription factors is required for massive liver apoptosis induced by bacterial lipopolysaccharide. J Biol Chem 279: 48434–48442.
23. Duffy JY, McLean KM, Lyons JM, Czaikowski AJ, Wagner CJ, et al. (2009) Modulation of nuclear factor-kappaB improves cardiac dysfunction associated with cardiopulmonary bypass and deep hypothermic circulatory arrest. Crit Care Med 37: 577–583.
24. O'Sullivan AW, Wang JH, Redmond HP (2009) NF-kappaB and p38 MAPK inhibition improve survival in endotoxin shock and in a cecal ligation and puncture model of sepsis in combination with antibiotic therapy. J Surg Res 152: 46–53.
25. Moore DJ, Zienkiewicz J, Kendall PL, Liu D, Liu X, et al. (2010) In vivo islet protection by a nuclear import inhibitor in a mouse model of type 1 diabetes. PLoS One 5: e13235.
26. Veach RA, Zienkiewicz J, Collins RD, Hawiger J (2012) Lethality in a Murine Model of Pulmonary Anthrax is Reduced by Combining Nuclear Transport Modifier with Antimicrobial Therapy. PLoS ONE 7: e30527.
27. Miller SI, Ernst RK, Bader MW (2005) LPS, TLR4 and infectious disease diversity. Nat Rev Microbiol 3: 36–46.
28. Aird WC (2007) Phenotypic heterogeneity of the endothelium: I. Structure, function, and mechanisms. Circ Res 100: 158–173.
29. Matthay MA, Ware LB, Zimmerman GA (2012) The acute respiratory distress syndrome. J Clin Invest 122: 2731–2740.
30. Takao K, Miyakawa T (2014) Genomic responses in mouse models greatly mimic human inflammatory diseases. Proc Natl Acad Sci U S A; published ahead of print August 4, 2014, doi:10.1073/pnas.1401965111.
31. Seok J, Warren HS, Cuenca AG, Mindrinos MN, Baker HV, et al. (2013) Genomic responses in mouse models poorly mimic human inflammatory diseases. Proc Natl Acad Sci U S A 110: 3507–3512.
32. Annane D, Sebille V, Charpentier C, Bollaert PE, Francois B, et al. (2002) Effect of treatment with low doses of hydrocortisone and fludrocortisone on mortality in patients with septic shock JAMA 288: 862–871.
33. Sprung CL, Annane D, Keh D, Moreno R, Singer M, et al. (2008) Hydrocortisone therapy for patients with septic shock. N Engl J Med 358: 111–124.
34. Stanbury RM, Graham EM (1998) Systemic corticosteroid therapy–side effects and their management. Br J Ophthalmol 82: 704–708.
35. Lemke U, Kron es-Herzig A, Berriel Diaz M, Narvekar P, Ziegler A, et al. (2008) The glucocorticoid receptor controls hepatic dyslipidemia through Hes1. Cell Metab 8: 212–223.
36. Wang JC, Gray NE, Kuo T, Harris CA (2012) Regulation of triglyceride metabolism by glucocorticoid receptor. Cell Biosci 2: 19.
37. Barcia AM, Harris HW (2005) Triglyceride-rich lipoproteins as agents of innate immunity. Clin Infect Dis 41 Suppl 7: S498–503.
38. Tweedell A, Mulligan KX, Martel JE, Chueh FY, Santomango T, et al. (2011) Metabolic response to endotoxin in vivo in the conscious mouse: role of interleukin-6. Metabolism 60: 92–98.
39. Lehr HA, Sagban TA, Ihling C, Zahringer U, Hungerer KD, et al. (2001) Immunopathogenesis of atherosclerosis: endotoxin accelerates atherosderosis in rabbits on hypercholesterolemic diet. Circulation 104: 914–920.
40. Lee SJ, Sekimoto T, Yamashita E, Nagoshi E, Nakagawa A, et al. (2003) The structure of importin-beta bound to SREBP-2: nuclear import of a transcription factor. Science 302: 1571–1575.
41. Dauphinee SM, Karsan A (2006) Lipopolysaccharide signaling in endothelial cells. Lab Invest 86: 9–22.
42. Bannerman DD, Goldblum SE (2003) Mechanisms of bacterial lipopolysaccharide-induced endothelial apoptosis. Am J Physiol Lung Cell Mol Physiol 284: L899–914.
43. Rose WE, Eickhoff JC, Shukla SK, Pantrangi M, Rooijakkers S, et al. (2012) Elevated serum interleukin-10 at time of hospital admission is predictive of mortality in patients with Staphylococcus aureus bacteremia J Infect Dis 206: 1604–1611.
44. Bozza FA, Salluh JI, Japiassu AM, Soares M, Assis EF, et al. (2007) Cytokine profiles as markers of disease severity in sepsis: a multiplex analysis. Crit Care 11: R49.

45. Andaluz-Ojeda D, Bobillo F, Iglesias V, Almansa R, Rico L, et al. (2012) A combined score of pro- and anti-inflammatory interleukins improves mortality prediction in severe sepsis. Cytokine 57: 332–336.
46. Jans DA, Hubner S (1996) Regulation of protein transport to the nucleus: central role of phosphorylation. Physiol Rev 76: 651–685.
47. Chopra I, Schofield C, Everett M, O'Neill A, Miller K, et al. (2008) Treatment of health-care-associated infections caused by Gram-negative bacteria: a consensus statement. Lancet Infect Dis 8: 133–139.
48. Peleg AY, Hooper DC (2010) Hospital-acquired infections due to gram-negative bacteria. N Engl J Med 362: 1804–1813.
49. Vincent JL, Rello J, Marshall J, Silva E, Anzueto A, et al. (2009) International study of the prevalence and outcomes of infection in intensive care units. JAMA 302: 2323–2329.
50. Fagon JY, Chastre J, Hance AJ, Montravers P, Novara A, et al. (1993) Nosocomial pneumonia in ventilated patients: a cohort study evaluating attributable mortality and hospital stay. Am J Med 94: 281–288.
51. Hoffken G, Niederman MS (2002) Nosocomial pneumonia: the importance of a de-escalating strategy for antibiotic treatment of pneumonia in the ICU. Chest 122: 2183–2196.
52. Boyer A, Doussau A, Thiebault R, Venier AG, Tran V, et al. (2011) Pseudomonas aeruginosa acquisition on an intensive care unit: relationship between antibiotic selective pressure and patients' environment. Crit Care 15: R55.
53. Jarvis WR (2007) The Lowbury Lecture. The United States approach to strategies in the battle against healthcare-associated infections, 2006: transitioning from benchmarking to zero tolerance and clinician accountability. J Hosp Infect 65 Suppl 2: 3–9.
54. Frank KM, Zhou T, Moreno-Vinasco L, Hollett B, Garcia JG, et al. (2012) Host response signature to Staphylococcus aureus alpha-hemolysin implicates pulmonary Th17 response. Infect Immun 80: 3161–3169.
55. Vial T, Descotes J (1995) Clinical toxicity of cytokines used as haemopoietic growth factors. Drug Saf 13: 371–406.
56. Raghavendran K, Davidson BA, Mullan BA, Hutson AD, Russo TA, et al. (2005) Acid and particulate-induced aspiration lung injury in mice: importance of MCP-1. Am J Physiol Lung Cell Mol Physiol 289: L134–143.
57. Reutershan J, Morris MA, Burcin TL, Smith DF, Chang D, et al. (2006) Critical role of endothelial CXCR2 in LPS-induced neutrophil migration into the lung. J Clin Invest 116: 695–702.
58. Nakahara H, Song J, Sugimoto M, Hagihara K, Kishimoto T, et al. (2003) Anti-interleukin-6 receptor antibody therapy reduces vascular endothelial growth factor production in rheumatoid arthritis. Arthritis Rheum 48: 1521–1529.
59. Lorenz HM, Antoni C, Valerius T, Repp R, Grunke M, et al. (1996) In vivo blockade of TNF-alpha by intravenous infusion of a chimeric monoclonal TNF-alpha antibody in patients with rheumatoid arthritis. Short term cellular and molecular effects. J Immunol 156: 1646–1653.
60. Wendling D, Racadot E, Wijdenes J (1993) Treatment of severe rheumatoid arthritis by anti-interleukin 6 monoclonal antibody. J Rheumatol 20: 259–262.
61. Bohrer H, Qiu F, Zimmermann T, Zhang Y, Jllmer T, et al. (1997) Role of NFkappaB in the mortality of sepsis. J Clin Invest 100: 972–985.
62. Reagan-Shaw S, Nihal M, Ahmad N (2008) Dose translation from animal to human studies revisited. Faseb Journal 22: 659–661.
63. Bernard GR, Wheeler AP, Russell JA, Schein R, Summer WR, et al. (1997) The effects of ibuprofen on the physiology and survival of patients with sepsis. The Ibuprofen in Sepsis Study Group. N Engl J Med 336: 912–918.

REFERENCES

1. Carmeliet, P. (2003) Angiogenesis in health and disease. *Nat. Med.* **9**, 653-660
2. Zweifach, B. W. (1959) The microcirculation of the blood. *Sci. Am.* **200**, 54-60
3. Harb, R., Whiteus, C., Freitas, C., and Grutzendler, J. (2013) In vivo imaging of cerebral microvascular plasticity from birth to death. *J. Cereb. Blood Flow Metab.* **33**, 146-156
4. Adler, A. C., Nathanson, B. H., Raghunathan, K., and McGee, W. T. (2012) Misleading indexed hemodynamic parameters: the clinical importance of discordant BMI and BSA at extremes of weight. *Crit Care* **16**, 471
5. Wolinsky, H. (1980) A proposal linking clearance of circulating lipoproteins to tissue metabolic activity as a basis for understanding atherogenesis. *Circul. Res.* **47**, 301-311
6. Jacob, M., Chappell, D., and Becker, B. F. (2016) Regulation of blood flow and volume exchange across the microcirculation. *Crit Care* **20**, 319
7. Hawiger, J., Veach, R. A., and Zienkiewicz, J. (2015) New paradigms in sepsis: from prevention to protection of failing microcirculation. *J Thromb Haemost* **13**, 1743-1756
8. Roumenina, L. T., Rayes, J., Frimat, M., and Fremeaux-Bacchi, V. (2016) Endothelial cells: source, barrier, and target of defensive mediators. *Immunol. Rev.* **274**, 307-329
9. Bergman, R. A., Afifi, A.K., Heidger, P.M. (2016) Atlas of Microscopic Anatomy; Section 4: Blood.
10. Steiniger, B., Bette, M., and Schwarzbach, H. (2011) The open microcirculation in human spleens: a three-dimensional approach. *J. Histochem. Cytochem.* **59**, 639-648
11. Vollmar, B., and Menger, M. D. (2009) The hepatic microcirculation: mechanistic contributions and therapeutic targets in liver injury and repair. *Physiol. Rev.* **89**, 1269-1339
12. Gil, J. (1988) The normal lung circulation. State of the art. *Chest* **93**, 80S-82S
13. Hudlicka, O. (2011) Microcirculation in skeletal muscle. *Muscles Ligaments Tendons J* **1**, 3-11
14. Yuan, L., Chan, G. C., Beeler, D., Janes, L., Spokes, K. C., Dharaneeswaran, H., Mojiri, A., Adams, W. J., Sciuto, T., Garcia-Cardena, G., Molema, G., Kang, P. M., Jahroudi, N., Marsden, P. A., Dvorak, A., Regan, E. R., and Aird, W. C. (2016) A role of stochastic phenotype switching in generating mosaic endothelial cell heterogeneity. *Nat Commun* **7**, 10160
15. Kolinko, Y., Krakorova, K., Cendelin, J., Tonar, Z., and Kralickova, M. (2015) Microcirculation of the brain: morphological assessment in degenerative diseases and restoration processes. *Rev. Neurosci.* **26**, 75-93
16. Banks, W. A. (2016) From blood-brain barrier to blood-brain interface: new opportunities for CNS drug delivery. *Nat Rev Drug Discov* **15**, 275-292
17. Abbott, N. J., Ronnback, L., and Hansson, E. (2006) Astrocyte-endothelial interactions at the blood-brain barrier. *Nat Rev Neurosci* **7**, 41-53
18. Armulik, A., Abramsson, A., and Betsholtz, C. (2005) Endothelial/pericyte interactions. *Circul. Res.* **97**, 512-523
19. Amiry-Moghaddam, M., and Ottersen, O. P. (2003) The molecular basis of water transport in the brain. *Nat Rev Neurosci* **4**, 991-1001
20. Papadopoulos, M. C., and Verkman, A. S. (2013) Aquaporin water channels in the nervous system. *Nat Rev Neurosci* **14**, 265-277
21. Obermeier, B., Daneman, R., and Ransohoff, R. M. (2013) Development, maintenance and disruption of the blood-brain barrier. *Nat. Med.* **19**, 1584-1596
22. Carson, M. J., Doose, J. M., Melchior, B., Schmid, C. D., and Ploix, C. C. (2006) CNS immune privilege: hiding in plain sight. *Immunol. Rev.* **213**, 48-65
23. Holman, D. W., Klein, R. S., and Ransohoff, R. M. (2011) The blood-brain barrier, chemokines and multiple sclerosis. *Biochim. Biophys. Acta* **1812**, 220-230

24. Greenwood, J., Heasman, S. J., Alvarez, J. I., Prat, A., Lyck, R., and Engelhardt, B. (2011) Review: leucocyte-endothelial cell crosstalk at the blood-brain barrier: a prerequisite for successful immune cell entry to the brain. *Neuropathol. Appl. Neurobiol.* **37**, 24-39
25. Hatanaka, K., Lanahan, A. A., Murakami, M., and Simons, M. (2012) Fibroblast growth factor signaling potentiates VE-cadherin stability at adherens junctions by regulating SHP2. *PLoS One* **7**, e37600
26. Gavard, J. (2014) Endothelial permeability and VE-cadherin: a wacky comradeship. *Cell Adh Migr* **8**, 158-164
27. Taddei, A., Giampietro, C., Conti, A., Orsenigo, F., Breviario, F., Pirazzoli, V., Potente, M., Daly, C., Dimmeler, S., and Dejana, E. (2008) Endothelial adherens junctions control tight junctions by VE-cadherin-mediated upregulation of claudin-5. *Nat Cell Biol* **10**, 923-934
28. Abbott, N. J. (2005) Dynamics of CNS barriers: evolution, differentiation, and modulation. *Cell. Mol. Neurobiol.* **25**, 5-23
29. Simard, M., and Nedergaard, M. (2004) The neurobiology of glia in the context of water and ion homeostasis. *Neuroscience* **129**, 877-896
30. Ichinose, K., Arima, K., Ushigusa, T., Nishino, A., Nakashima, Y., Suzuki, T., Horai, Y., Nakajima, H., Kawashiri, S. Y., Iwamoto, N., Tamai, M., Nakamura, H., Origuchi, T., Motomura, M., and Kawakami, A. (2015) Distinguishing the cerebrospinal fluid cytokine profile in neuropsychiatric systemic lupus erythematosus from other autoimmune neurological diseases. *Clin. Immunol.* **157**, 114-120
31. Dendrou, C. A., Fugger, L., and Friese, M. A. (2015) Immunopathology of multiple sclerosis. *Nat Rev Immunol* **15**, 545-558
32. Denicoff, K. D., Rubinow, D. R., Papa, M. Z., Simpson, C., Seipp, C. A., Lotze, M. T., Chang, A. E., Rosenstein, D., and Rosenberg, S. A. (1987) The neuropsychiatric effects of treatment with interleukin-2 and lymphokine-activated killer cells. *Ann. Intern. Med.* **107**, 293-300
33. Lawrence, T., Willoughby, D. A., and Gilroy, D. W. (2002) Anti-inflammatory lipid mediators and insights into the resolution of inflammation. *Nat Rev Immunol* **2**, 787-795
34. Mozaffarian, D., Benjamin, E. J., Go, A. S., Arnett, D. K., Blaha, M. J., Cushman, M., Das, S. R., de Ferranti, S., Despres, J. P., Fullerton, H. J., Howard, V. J., Huffman, M. D., Isasi, C. R., Jimenez, M. C., Judd, S. E., Kissela, B. M., Lichtman, J. H., Lisabeth, L. D., Liu, S., Mackey, R. H., Magid, D. J., McGuire, D. K., Mohler, E. R., 3rd, Moy, C. S., Muntner, P., Mussolino, M. E., Nasir, K., Neumar, R. W., Nichol, G., Palaniappan, L., Pandey, D. K., Reeves, M. J., Rodriguez, C. J., Rosamond, W., Sorlie, P. D., Stein, J., Towfighi, A., Turan, T. N., Virani, S. S., Woo, D., Yeh, R. W., and Turner, M. B. (2016) Heart Disease and Stroke Statistics-2016 Update: A Report From the American Heart Association. *Circulation* **133**, e38-360
35. Nwankwo, T., Yoon, S. S., Burt, V., and Gu, Q. (2013) Hypertension among adults in the United States: National Health and Nutrition Examination Survey, 2011-2012. *NCHS Data Brief*, 1-8
36. Sena, C. M., Pereira, A. M., and Seica, R. (2013) Endothelial dysfunction - a major mediator of diabetic vascular disease. *Biochim. Biophys. Acta* **1832**, 2216-2231
37. Jo, D., Liu, D., Yao, S., Collins, R. D., and Hawiger, J. (2005) Intracellular protein therapy with SOCS3 inhibits inflammation and apoptosis. *Nat. Med.* **11**, 892-898
38. DiGiandomenico, A., Wylezinski, L. S., and Hawiger, J. (2009) Intracellular delivery of a cell-penetrating SOCS1 that targets IFN-gamma signaling. *Sci Signal* **2**, ra37
39. Lin, Q., Liu, Y., Moore, D. J., Elizer, S. K., Veach, R. A., Hawiger, J., and Ruley, H. E. (2012) Cutting edge: the "death" adaptor CRADD/RAIDD targets BCL10 and suppresses agonist-induced cytokine expression in T lymphocytes. *J. Immunol.* **188**, 2493-2497

40. Fletcher, T. C., DiGiandomenico, A., and Hawiger, J. (2010) Extended anti-inflammatory action of a degradation-resistant mutant of cell-penetrating suppressor of cytokine signaling 3. *J. Biol. Chem.* **285**, 18727-18736
41. Gilmore, A. P. (2005) Anoikis. *Cell Death Differ.* **12 Suppl 2**, 1473-1477
42. Kerrigan, S. W., and McDonnell, C. (2015) Dysregulation of the endothelium following Staphylococcus aureus infection. *Biochem. Soc. Trans.* **43**, 715-719
43. Baluna, R., and Vitetta, E. S. (1997) Vascular leak syndrome: a side effect of immunotherapy. *Immunopharmacology* **37**, 117-132
44. Xie, Z., Ghosh, C. C., Patel, R., Iwaki, S., Gaskins, D., Nelson, C., Jones, N., Greipp, P. R., Parikh, S. M., and Druey, K. M. (2012) Vascular endothelial hyperpermeability induces the clinical symptoms of Clarkson disease (the systemic capillary leak syndrome). *Blood* **119**, 4321-4332
45. Irwan, Y. Y., Feng, Y., Gach, H. M., Symanowski, J. T., McGregor, J. R., Veni, G., Schabel, M., and Samlowski, W. E. (2009) Quantitative analysis of cytokine-induced vascular toxicity and vascular leak in the mouse brain. *J. Immunol. Methods* **349**, 45-55
46. Krieg, C., Letourneau, S., Pantaleo, G., and Boyman, O. (2010) Improved IL-2 immunotherapy by selective stimulation of IL-2 receptors on lymphocytes and endothelial cells. *Proc. Natl. Acad. Sci. U. S. A.* **107**, 11906-11911
47. Kempe, S., Kestler, H., Lasar, A., and Wirth, T. (2005) NF-kappaB controls the global pro-inflammatory response in endothelial cells: evidence for the regulation of a pro-atherogenic program. *Nucleic Acids Res* **33**, 5308-5319
48. Hawiger, J. (2001) Innate immunity and inflammation: a transcriptional paradigm. *Immunol. Res.* **23**, 99-109
49. Baltimore, D. (2011) NF-kappaB is 25. *Nat Immunol* **12**, 683-685
50. Karin, M., and Ben-Neriah, Y. (2000) Phosphorylation meets ubiquitination: the control of NF-[kappa]B activity. *Annu. Rev. Immunol.* **18**, 621-663
51. Zienkiewicz, J., Armitage, A., and Hawiger, J. (2013) Targeting nuclear import shuttles, importins/karyopherins alpha by a peptide mimicking the NFkappaB1/p50 nuclear localization sequence. *J Am Heart Assoc* **2**, e000386
52. Li, C. C., Dai, R. M., Chen, E., and Longo, D. L. (1994) Phosphorylation of NF-KB1-p50 is involved in NF-kappa B activation and stable DNA binding. *J. Biol. Chem.* **269**, 30089-30092
53. Arima, N., Kuziel, W. A., Grdina, T. A., and Greene, W. C. (1992) IL-2-induced signal transduction involves the activation of nuclear NF-kappa B expression. *J. Immunol.* **149**, 83-91
54. Denk, A., Goebeler, M., Schmid, S., Berberich, I., Ritz, O., Lindemann, D., Ludwig, S., and Wirth, T. (2001) Activation of NF-kappa B via the Ikappa B kinase complex is both essential and sufficient for proinflammatory gene expression in primary endothelial cells. *J. Biol. Chem.* **276**, 28451-28458
55. Libermann, T. A., and Baltimore, D. (1990) Activation of interleukin-6 gene expression through the NF-kappa B transcription factor. *Mol. Cell. Biol.* **10**, 2327-2334
56. Lotze, M. T., Frana, L. W., Sharrow, S. O., Robb, R. J., and Rosenberg, S. A. (1985) In vivo administration of purified human interleukin 2. I. Half-life and immunologic effects of the Jurkat cell line-derived interleukin 2. *J. Immunol.* **134**, 157-166
57. Minami, Y., Kono, T., Miyazaki, T., and Taniguchi, T. (1993) The IL-2 receptor complex: its structure, function, and target genes. *Annu. Rev. Immunol.* **11**, 245-268
58. Stauber, D. J., Debler, E. W., Horton, P. A., Smith, K. A., and Wilson, I. A. (2006) Crystal structure of the IL-2 signaling complex: paradigm for a heterotrimeric cytokine receptor. *Proc. Natl. Acad. Sci. U. S. A.* **103**, 2788-2793
59. Sim, G. C., and Radvanyi, L. (2014) The IL-2 cytokine family in cancer immunotherapy. *Cytokine Growth Factor Rev.* **25**, 377-390

60. Cotran, R. S., Pober, J. S., Gimbrone, M. A., Jr., Springer, T. A., Wiebke, E. A., Gaspari, A. A., Rosenberg, S. A., and Lotze, M. T. (1988) Endothelial activation during interleukin 2 immunotherapy. A possible mechanism for the vascular leak syndrome. *J. Immunol.* **140**, 1883-1888
61. Downie, G. H., Ryan, U. S., Hayes, B. A., and Friedman, M. (1992) Interleukin-2 directly increases albumin permeability of bovine and human vascular endothelium in vitro. *Am. J. Respir. Cell Mol. Biol.* **7**, 58-65
62. Kim, D. W., Zloza, A., Broucek, J., Schenkel, J. M., Ruby, C., Samaha, G., and Kaufman, H. L. (2014) Interleukin-2 alters distribution of CD144 (VE-cadherin) in endothelial cells. *J Transl Med* **12**, 113
63. Rosenberg, S. A., Lotze, M. T., Muul, L. M., Leitman, S., Chang, A. E., Ettinghausen, S. E., Matory, Y. L., Skibber, J. M., Shiloni, E., Vetto, J. T., and et al. (1985) Observations on the systemic administration of autologous lymphokine-activated killer cells and recombinant interleukin-2 to patients with metastatic cancer. *New Engl. J. Med.* **313**, 1485-1492
64. Rosenberg, S. A. (2014) IL-2: the first effective immunotherapy for human cancer. *J. Immunol.* **192**, 5451-5458
65. Lerner, D. M., Stoudemire, A., and Rosenstein, D. L. (1999) Neuropsychiatric toxicity associated with cytokine therapies. *Psychosomatics* **40**, 428-435
66. Klapper, J. A., Downey, S. G., Smith, F. O., Yang, J. C., Hughes, M. S., Kammula, U. S., Sherry, R. M., Royal, R. E., Steinberg, S. M., and Rosenberg, S. (2008) High-dose interleukin-2 for the treatment of metastatic renal cell carcinoma : a retrospective analysis of response and survival in patients treated in the surgery branch at the National Cancer Institute between 1986 and 2006. *Cancer* **113**, 293-301
67. DiGiandomenico, A., Veach, R. A., Zienkiewicz, J., Moore, D. J., Wylezinski, L. S., Hutchens, M. A., and Hawiger, J. (2014) The "genomic storm" induced by bacterial endotoxin is calmed by a nuclear transport modifier that attenuates localized and systemic inflammation. *PLoS One* **9**, e110183
68. Stewart, R. J., Kashour, T. S., and Marsden, P. A. (1996) Vascular endothelial platelet endothelial adhesion molecule-1 (PECAM-1) expression is decreased by TNF-alpha and IFN-gamma. Evidence for cytokine-induced destabilization of messenger ribonucleic acid transcripts in bovine endothelial cells. *J. Immunol.* **156**, 1221-1228
69. Zanetta, L., Marcus, S. G., Vasile, J., Dobryansky, M., Cohen, H., Eng, K., Shamamian, P., and Mignatti, P. (2000) Expression of Von Willebrand factor, an endothelial cell marker, is up-regulated by angiogenesis factors: a potential method for objective assessment of tumor angiogenesis. *Int. J. Cancer* **85**, 281-288
70. Sperisen, P., Wang, S. M., Soldaini, E., Pla, M., Rusterholz, C., Bucher, P., Corthesy, P., Reichenbach, P., and Nabholz, M. (1995) Mouse interleukin-2 receptor alpha gene expression. Interleukin-1 and interleukin-2 control transcription via distinct cis-acting elements. *J. Biol. Chem.* **270**, 10743-10753
71. Brockman, J. A., Scherer, D. C., McKinsey, T. A., Hall, S. M., Qi, X., Lee, W. Y., and Ballard, D. W. (1995) Coupling of a signal response domain in I kappa B alpha to multiple pathways for NF-kappa B activation. *Mol. Cell. Biol.* **15**, 2809-2818
72. Brown, K., Gerstberger, S., Carlson, L., Franzoso, G., and Siebenlist, U. (1995) Control of I kappa B-alpha proteolysis by site-specific, signal-induced phosphorylation. *Science* **267**, 1485-1488
73. Donald, R., Ballard, D. W., and Hawiger, J. (1995) Proteolytic processing of NF-kappa B/I kappa B in human monocytes. ATP-dependent induction by pro-inflammatory mediators. *J. Biol. Chem.* **270**, 9-12
74. Tieu, B. C., Lee, C., Sun, H., Lejeune, W., Recinos, A., 3rd, Ju, X., Spratt, H., Guo, D. C., Milewicz, D., Tilton, R. G., and Brasier, A. R. (2009) An adventitial IL-6/MCP1 amplification loop accelerates

macrophage-mediated vascular inflammation leading to aortic dissection in mice. *J. Clin. Invest.* **119**, 3637-3651
75. Desai, T. R., Leeper, N. J., Hynes, K. L., and Gewertz, B. L. (2002) Interleukin-6 causes endothelial barrier dysfunction via the protein kinase C pathway. *J. Surg. Res.* **104**, 118-123
76. Jee, Y., Yoon, W. K., Okura, Y., Tanuma, N., and Matsumoto, Y. (2002) Upregulation of monocyte chemotactic protein-1 and CC chemokine receptor 2 in the central nervous system is closely associated with relapse of autoimmune encephalomyelitis in Lewis rats. *J. Neuroimmunol.* **128**, 49-57
77. Stamatovic, S. M., Keep, R. F., Kunkel, S. L., and Andjelkovic, A. V. (2003) Potential role of MCP-1 in endothelial cell tight junction 'opening': signaling via Rho and Rho kinase. *J. Cell Sci.* **116**, 4615-4628
78. Martins, T. B., Rose, J. W., Jaskowski, T. D., Wilson, A. R., Husebye, D., Seraj, H. S., and Hill, H. R. (2011) Analysis of proinflammatory and anti-inflammatory cytokine serum concentrations in patients with multiple sclerosis by using a multiplexed immunoassay. *Am. J. Clin. Pathol.* **136**, 696-704
79. Gallo, P., Pagni, S., Piccinno, M. G., Giometto, B., Argentiero, V., Chiusole, M., Bozza, F., and Tavolato, B. (1992) On the role of interleukin-2 (IL-2) in multiple sclerosis (MS). IL-2-mediated endothelial cell activation. *Ital. J. Neurol. Sci.* **13**, 65-68
80. Lampugnani, M. G., and Dejana, E. (2007) Adherens junctions in endothelial cells regulate vessel maintenance and angiogenesis. *Thromb. Res.* **120, Supplement 2**, S1-S6
81. Ukropec, J. A., Hollinger, M. K., Salva, S. M., and Woolkalis, M. J. (2000) SHP2 association with VE-cadherin complexes in human endothelial cells is regulated by thrombin. *J. Biol. Chem.* **275**, 5983-5986
82. Xiao, K., Garner, J., Buckley, K. M., Vincent, P. A., Chiasson, C. M., Dejana, E., Faundez, V., and Kowalczyk, A. P. (2005) p120-Catenin regulates clathrin-dependent endocytosis of VE-cadherin. *Mol. Biol. Cell* **16**, 5141-5151
83. Potter, M. D., Barbero, S., and Cheresh, D. A. (2005) Tyrosine phosphorylation of VE-cadherin prevents binding of p120- and beta-catenin and maintains the cellular mesenchymal state. *J. Biol. Chem.* **280**, 31906-31912
84. Saris, S. C., Patronas, N. J., Rosenberg, S. A., Alexander, J. T., Frank, J., Schwartzentruber, D. J., Rubin, J. T., Barba, D., and Oldfield, E. H. (1989) The effect of intravenous interleukin-2 on brain water content. *J. Neurosurg.* **71**, 169-174
85. Qiao, H., Liu, Y., Veach, R. A., Wylezinski, L., and Hawiger, J. (2014) The adaptor CRADD/RAIDD controls activation of endothelial cells by proinflammatory stimuli. *J. Biol. Chem.* **289**, 21973-21983
86. Rajput, C., Kini, V., Smith, M., Yazbeck, P., Chavez, A., Schmidt, T., Zhang, W., Knezevic, N., Komarova, Y., and Mehta, D. (2013) Neural Wiskott-Aldrich syndrome protein (N-WASP)-mediated p120-catenin interaction with Arp2-Actin complex stabilizes endothelial adherens junctions. *J. Biol. Chem.* **288**, 4241-4250
87. Tenreiro, M. M., Ferreira, R., Bernardino, L., and Brito, M. A. (2016) Cellular response of the blood-brain barrier to injury: Potential biomarkers and therapeutic targets for brain regeneration. *Neurobiol. Dis.* **91**, 262-273
88. Dignat-George, F., Blann, A., and Sampol, J. (2000) Circulating endothelial cells in acute coronary syndromes. *Blood* **95**, 728
89. Westlin, W. F., and Gimbrone, M. A., Jr. (1993) Neutrophil-mediated damage to human vascular endothelium. Role of cytokine activation. *Am. J. Pathol.* **142**, 117-128

90. Abu Taha, A., and Schnittler, H. J. (2014) Dynamics between actin and the VE-cadherin/catenin complex: novel aspects of the ARP2/3 complex in regulation of endothelial junctions. *Cell Adh Migr* **8**, 125-135
91. Orsenigo, F., Giampietro, C., Ferrari, A., Corada, M., Galaup, A., Sigismund, S., Ristagno, G., Maddaluno, L., Koh, G. Y., Franco, D., Kurtcuoglu, V., Poulikakos, D., Baluk, P., McDonald, D., Grazia Lampugnani, M., and Dejana, E. (2012) Phosphorylation of VE-cadherin is modulated by haemodynamic forces and contributes to the regulation of vascular permeability in vivo. *Nat Commun* **3**, 1208
92. Wessel, F., Winderlich, M., Holm, M., Frye, M., Rivera-Galdos, R., Vockel, M., Linnepe, R., Ipe, U., Stadtmann, A., Zarbock, A., Nottebaum, A. F., and Vestweber, D. (2014) Leukocyte extravasation and vascular permeability are each controlled in vivo by different tyrosine residues of VE-cadherin. *Nat Immunol* **15**, 223-230
93. Chang, S. F., Chen, L. J., Lee, P. L., Lee, D. Y., Chien, S., and Chiu, J. J. (2014) Different modes of endothelial-smooth muscle cell interaction elicit differential beta-catenin phosphorylations and endothelial functions. *Proc. Natl. Acad. Sci. U. S. A.* **111**, 1855-1860
94. Grinnell, K. L., Casserly, B., and Harrington, E. O. (2010) Role of protein tyrosine phosphatase SHP2 in barrier function of pulmonary endothelium. *Am J Physiol Lung Cell Mol Physiol* **298**, L361-370
95. Taniguchi, T., Matsui, H., Fujita, T., Hatakeyama, M., Kashima, N., Fuse, A., Hamuro, J., Nishi-Takaoka, C., and Yamada, G. (1986) Molecular analysis of the interleukin-2 system. *Immunol. Rev.* **92**, 121-133
96. Depper, J. M., Leonard, W. J., Drogula, C., Kronke, M., Waldmann, T. A., and Greene, W. C. (1985) Interleukin 2 (IL-2) augments transcription of the IL-2 receptor gene. *Proc. Natl. Acad. Sci. U. S. A.* **82**, 4230-4234
97. Lowenthal, J. W., Ballard, D. W., Bogerd, H., Bohnlein, E., and Greene, W. C. (1989) Tumor necrosis factor-alpha activation of the IL-2 receptor-alpha gene involves the induction of kappa B-specific DNA binding proteins. *J. Immunol.* **142**, 3121-3128
98. Malek, T. R. (2008) The biology of interleukin-2. *Annu. Rev. Immunol.* **26**, 453-479
99. Hanke, T., Mitnacht, R., Boyd, R., and Hunig, T. (1994) Induction of interleukin 2 receptor beta chain expression by self-recognition in the thymus. *J. Exp. Med.* **180**, 1629-1636
100. Boyman, O., Kovar, M., Rubinstein, M. P., Surh, C. D., and Sprent, J. (2006) Selective stimulation of T cell subsets with antibody-cytokine immune complexes. *Science* **311**, 1924-1927
101. Obar, J. J., Molloy, M. J., Jellison, E. R., Stoklasek, T. A., Zhang, W., Usherwood, E. J., and Lefrancois, L. (2010) CD4+ T cell regulation of CD25 expression controls development of short-lived effector CD8+ T cells in primary and secondary responses. *Proc. Natl. Acad. Sci. U. S. A.* **107**, 193-198
102. Kalia, V., Sarkar, S., Subramaniam, S., Haining, W. N., Smith, K. A., and Ahmed, R. (2010) Prolonged interleukin-2Ralpha expression on virus-specific CD8+ T cells favors terminal-effector differentiation in vivo. *Immunity* **32**, 91-103
103. Choi, Y. S., Kageyama, R., Eto, D., Escobar, T. C., Johnston, R. J., Monticelli, L., Lao, C., and Crotty, S. (2011) ICOS receptor instructs T follicular helper cell versus effector cell differentiation via induction of the transcriptional repressor Bcl6. *Immunity* **34**, 932-946
104. Pepper, M., Pagan, A. J., Igyarto, B. Z., Taylor, J. J., and Jenkins, M. K. (2011) Opposing signals from the Bcl6 transcription factor and the interleukin-2 receptor generate T helper 1 central and effector memory cells. *Immunity* **35**, 583-595
105. Boyman, O., Letourneau, S., Krieg, C., and Sprent, J. (2009) Homeostatic proliferation and survival of naive and memory T cells. *Eur. J. Immunol.* **39**, 2088-2094

106. Ku, C. C., Murakami, M., Sakamoto, A., Kappler, J., and Marrack, P. (2000) Control of homeostasis of CD8+ memory T cells by opposing cytokines. *Science* **288**, 675-678
107. Setoguchi, R., Hori, S., Takahashi, T., and Sakaguchi, S. (2005) Homeostatic maintenance of natural Foxp3(+) CD25(+) CD4(+) regulatory T cells by interleukin (IL)-2 and induction of autoimmune disease by IL-2 neutralization. *J. Exp. Med.* **201**, 723-735
108. Letourneau, S., Krieg, C., Pantaleo, G., and Boyman, O. (2009) IL-2- and CD25-dependent immunoregulatory mechanisms in the homeostasis of T-cell subsets. *J. Allergy Clin. Immunol.* **123**, 758-762
109. Ohteki, T., Ho, S., Suzuki, H., Mak, T. W., and Ohashi, P. S. (1997) Role for IL-15/IL-15 receptor beta-chain in natural killer 1.1+ T cell receptor-alpha beta+ cell development. *J. Immunol.* **159**, 5931-5935
110. Lau-Kilby, A. W., Kretz, C. C., Pechhold, S., Price, J. D., Dorta, S., Ramos, H., Trinchieri, G., and Tarbell, K. V. (2011) Interleukin-2 inhibits FMS-like tyrosine kinase 3 receptor ligand (flt3L)-dependent development and function of conventional and plasmacytoid dendritic cells. *Proc. Natl. Acad. Sci. U. S. A.* **108**, 2408-2413
111. Crowley, M., Inaba, K., Witmer-Pack, M., and Steinman, R. M. (1989) The cell surface of mouse dendritic cells: FACS analyses of dendritic cells from different tissues including thymus. *Cell. Immunol.* **118**, 108-125
112. Freudenthal, P. S., and Steinman, R. M. (1990) The distinct surface of human blood dendritic cells, as observed after an improved isolation method. *Proc. Natl. Acad. Sci. U. S. A.* **87**, 7698-7702
113. Kronin, V., Vremec, D., and Shortman, K. (1998) Does the IL-2 receptor alpha chain induced on dendritic cells have a biological function? *Int. Immunol.* **10**, 237-240
114. von Bergwelt-Baildon, M. S., Popov, A., Saric, T., Chemnitz, J., Classen, S., Stoffel, M. S., Fiore, F., Roth, U., Beyer, M., Debey, S., Wickenhauser, C., Hanisch, F. G., and Schultze, J. L. (2006) CD25 and indoleamine 2,3-dioxygenase are up-regulated by prostaglandin E2 and expressed by tumor-associated dendritic cells in vivo: additional mechanisms of T-cell inhibition. *Blood* **108**, 228-237
115. Wuest, S. C., Edwan, J. H., Martin, J. F., Han, S., Perry, J. S., Cartagena, C. M., Matsuura, E., Maric, D., Waldmann, T. A., and Bielekova, B. (2011) A role for interleukin-2 trans-presentation in dendritic cell-mediated T cell activation in humans, as revealed by daclizumab therapy. *Nat. Med.* **17**, 604-609
116. Velten, F. W., Rambow, F., Metharom, P., and Goerdt, S. (2007) Enhanced T-cell activation and T-cell-dependent IL-2 production by CD83+, CD25high, CD43high human monocyte-derived dendritic cells. *Mol. Immunol.* **44**, 1544-1550
117. Mnasria, K., Lagaraine, C., Velge-Roussel, F., Oueslati, R., Lebranchu, Y., and Baron, C. (2008) Anti-CD25 antibodies affect cytokine synthesis pattern of human dendritic cells and decrease their ability to prime allogeneic CD4+ T cells. *J. Leukocyte Biol.* **84**, 460-467
118. Steiner, G., Tschachler, E., Tani, M., Malek, T. R., Shevach, E. M., Holter, W., Knapp, W., Wolff, K., and Stingl, G. (1986) Interleukin 2 receptors on cultured murine epidermal Langerhans cells. *J. Immunol.* **137**, 155-159
119. Wylezinski, L. S., and Hawiger, J. (2016) Interleukin 2 Activates Brain Microvascular Endothelial Cells Resulting in Destabilization of Adherens Junctions. *J. Biol. Chem.* **291**, 22913-22923
120. Plaisance, S., Rubinstein, E., Alileche, A., Benoit, P., Jasmin, C., and Azzarone, B. (1993) The IL-2 receptor present on human embryonic fibroblasts is functional in the absence of P64/IL-2R gamma chain. *Int. Immunol.* **5**, 843-848
121. Gruss, H. J., Scott, C., Rollins, B. J., Brach, M. A., and Herrmann, F. (1996) Human fibroblasts express functional IL-2 receptors formed by the IL-2R alpha- and beta-chain subunits:

association of IL-2 binding with secretion of the monocyte chemoattractant protein-1. *J. Immunol.* **157**, 851-857
122. Stone, K. P., Kastin, A. J., and Pan, W. (2011) NFkB is an unexpected major mediator of interleukin-15 signaling in cerebral endothelia. *Cell. Physiol. Biochem.* **28**, 115-124
123. Sen, R., and Baltimore, D. (1986) Inducibility of kappa immunoglobulin enhancer-binding protein Nf-kappa B by a posttranslational mechanism. *Cell* **47**, 921-928
124. Yang, F., Tang, E., Guan, K., and Wang, C. Y. (2003) IKK beta plays an essential role in the phosphorylation of RelA/p65 on serine 536 induced by lipopolysaccharide. *J. Immunol.* **170**, 5630-5635
125. Warner, S. J., Auger, K. R., and Libby, P. (1987) Interleukin 1 induces interleukin 1. II. Recombinant human interleukin 1 induces interleukin 1 production by adult human vascular endothelial cells. *J. Immunol.* **139**, 1911-1917
126. Kovacs, E. J., Brock, B., Varesio, L., and Young, H. A. (1989) IL-2 induction of IL-1 beta mRNA expression in monocytes. Regulation by agents that block second messenger pathways. *J. Immunol.* **143**, 3532-3537
127. Giannotta, M., Trani, M., and Dejana, E. (2013) VE-cadherin and endothelial adherens junctions: active guardians of vascular integrity. *Dev Cell* **26**, 441-454
128. Liu, H., Sidiropoulos, P., Song, G., Pagliari, L. J., Birrer, M. J., Stein, B., Anrather, J., and Pope, R. M. (2000) TNF-alpha gene expression in macrophages: regulation by NF-kappa B is independent of c-Jun or C/EBP beta. *J. Immunol.* **164**, 4277-4285
129. Imaizumi, T., Itaya, H., Fujita, K., Kudoh, D., Kudoh, S., Mori, K., Fujimoto, K., Matsumiya, T., Yoshida, H., and Satoh, K. (2000) Expression of tumor necrosis factor-alpha in cultured human endothelial cells stimulated with lipopolysaccharide or interleukin-1alpha. *Atertio. Thromb. Vasc. Biol.* **20**, 410-415
130. Lippmann, E. S., Azarin, S. M., Kay, J. E., Nessler, R. A., Wilson, H. K., Al-Ahmad, A., Palecek, S. P., and Shusta, E. V. (2012) Derivation of blood-brain barrier endothelial cells from human pluripotent stem cells. *Nat. Biotechnol.* **30**, 783-791
131. Schwartzentruber, D. J. (2001) Guidelines for the safe administration of high-dose interleukin-2. *J. Immunother.* **24**, 287-293
132. Hartsock, A., and Nelson, W. J. (2008) Adherens and tight junctions: structure, function and connections to the actin cytoskeleton. *Biochim. Biophys. Acta* **1778**, 660-669
133. Qin, L., Qin, S., Zhang, Y., Zhang, C., Ma, H., Li, N., Liu, L., Wang, X., and Wu, R. (2014) p120 modulates LPS-induced NF-kappaB activation partially through RhoA in bronchial epithelial cells. *Biomed Res Int* **2014**, 932340
134. Mehta, D., and Malik, A. B. (2006) Signaling mechanisms regulating endothelial permeability. *Physiol. Rev.* **86**, 279-367
135. Gong, P., Angelini, D. J., Yang, S., Xia, G., Cross, A. S., Mann, D., Bannerman, D. D., Vogel, S. N., and Goldblum, S. E. (2008) TLR4 signaling is coupled to SRC family kinase activation, tyrosine phosphorylation of zonula adherens proteins, and opening of the paracellular pathway in human lung microvascular endothelia. *J. Biol. Chem.* **283**, 13437-13449
136. Dudek, S. M., and Garcia, J. G. (2001) Cytoskeletal regulation of pulmonary vascular permeability. *J Appl Physiol (1985)* **91**, 1487-1500
137. Redies, C., and Takeichi, M. (1993) Expression of N-cadherin mRNA during development of the mouse brain. *Dev. Dyn.* **197**, 26-39
138. Gerhardt, H., Wolburg, H., and Redies, C. (2000) N-cadherin mediates pericytic-endothelial interaction during brain angiogenesis in the chicken. *Dev. Dyn.* **218**, 472-479
139. Yang, C., Iyer, R. R., Yu, A. C., Yong, R. L., Park, D. M., Weil, R. J., Ikejiri, B., Brady, R. O., Lonser, R. R., and Zhuang, Z. (2012) beta-Catenin signaling initiates the activation of astrocytes and its

dysregulation contributes to the pathogenesis of astrocytomas. *Proc. Natl. Acad. Sci. U. S. A.* **109**, 6963-6968
140. Adam, A. P., Sharenko, A. L., Pumiglia, K., and Vincent, P. A. (2010) Src-induced tyrosine phosphorylation of VE-cadherin is not sufficient to decrease barrier function of endothelial monolayers. *J. Biol. Chem.* **285**, 7045-7055
141. Nawroth, R., Poell, G., Ranft, A., Kloep, S., Samulowitz, U., Fachinger, G., Golding, M., Shima, D. T., Deutsch, U., and Vestweber, D. (2002) VE-PTP and VE-cadherin ectodomains interact to facilitate regulation of phosphorylation and cell contacts. *EMBO J.* **21**, 4885-4895
142. Sui, X. F., Kiser, T. D., Hyun, S. W., Angelini, D. J., Del Vecchio, R. L., Young, B. A., Hasday, J. D., Romer, L. H., Passaniti, A., Tonks, N. K., and Goldblum, S. E. (2005) Receptor protein tyrosine phosphatase micro regulates the paracellular pathway in human lung microvascular endothelia. *Am. J. Pathol.* **166**, 1247-1258
143. Nakamura, Y., Patrushev, N., Inomata, H., Mehta, D., Urao, N., Kim, H. W., Razvi, M., Kini, V., Mahadev, K., Goldstein, B. J., McKinney, R., Fukai, T., and Ushio-Fukai, M. (2008) Role of protein tyrosine phosphatase 1B in vascular endothelial growth factor signaling and cell-cell adhesions in endothelial cells. *Circul. Res.* **102**, 1182-1191
144. Timmerman, I., Hoogenboezem, M., Bennett, A. M., Geerts, D., Hordijk, P. L., and van Buul, J. D. (2012) The tyrosine phosphatase SHP2 regulates recovery of endothelial adherens junctions through control of beta-catenin phosphorylation. *Mol. Biol. Cell* **23**, 4212-4225
145. Minagar, A., Ostanin, D., Long, A. C., Jennings, M., Kelley, R. E., Sasaki, M., and Alexander, J. S. (2003) Serum from patients with multiple sclerosis downregulates occludin and VE-cadherin expression in cultured endothelial cells. *Multiple Sclerosis* **9**, 235-238
146. Argaw, A. T., Asp, L., Zhang, J., Navrazhina, K., Pham, T., Mariani, J. N., Mahase, S., Dutta, D. J., Seto, J., Kramer, E. G., Ferrara, N., Sofroniew, M. V., and John, G. R. (2012) Astrocyte-derived VEGF-A drives blood-brain barrier disruption in CNS inflammatory disease. *J. Clin. Invest.* **122**, 2454-2468
147. Wacker, B. K., Freie, A. B., Perfater, J. L., and Gidday, J. M. (2012) Junctional protein regulation by sphingosine kinase 2 contributes to blood-brain barrier protection in hypoxic preconditioning-induced cerebral ischemic tolerance. *J. Cereb. Blood Flow Metab.* **32**, 1014-1023
148. Dejana, E., and Orsenigo, F. (2013) Endothelial adherens junctions at a glance. *J. Cell Sci.* **126**, 2545-2549
149. Chan, K. K., Shen, L., Au, W. Y., Yuen, H. F., Wong, K. Y., Guo, T., Wong, M. L., Shimizu, N., Tsuchiyama, J., Kwong, Y. L., Liang, R. H., and Srivastava, G. (2010) Interleukin-2 induces NF-kappaB activation through BCL10 and affects its subcellular localization in natural killer lymphoma cells. *J. Pathol.* **221**, 164-174
150. Nwariaku, F. E., Chang, J., Zhu, X., Liu, Z., Duffy, S. L., Halaihel, N. H., Terada, L., and Turnage, R. H. (2002) The role of p38 map kinase in tumor necrosis factor-induced redistribution of vascular endothelial cadherin and increased endothelial permeability. *Shock* **18**, 82-85
151. Lal, B. K., Varma, S., Pappas, P. J., Hobson, R. W., 2nd, and Duran, W. N. (2001) VEGF increases permeability of the endothelial cell monolayer by activation of PKB/akt, endothelial nitric-oxide synthase, and MAP kinase pathways. *Microvasc. Res.* **62**, 252-262
152. Korpelainen, E. I., Karkkainen, M., Gunji, Y., Vikkula, M., and Alitalo, K. (1999) Endothelial receptor tyrosine kinases activate the STAT signaling pathway: mutant Tie-2 causing venous malformations signals a distinct STAT activation response. *Oncogene* **18**, 1-8
153. Sprague, A. H., and Khalil, R. A. (2009) Inflammatory cytokines in vascular dysfunction and vascular disease. *Biochem. Pharmacol.* **78**, 539-552
154. Proserpio, V., and Lonnberg, T. (2016) Single-cell technologies are revolutionizing the approach to rare cells. *Immunol. Cell Biol.* **94**, 225-229

155. O'Donnell, J. J., 3rd, Zhuge, Y., Holian, O., Cheng, F., Thomas, L. L., Forsyth, C. B., and Lum, H. (2011) Loss of p120 catenin upregulates transcription of pro-inflammatory adhesion molecules in human endothelial cells. *Microvasc. Res.* **82**, 105-112
156. Chandrakesan, P., Jakkula, L. U., Ahmed, I., Roy, B., Anant, S., and Umar, S. (2013) Differential effects of beta-catenin and NF-kappaB interplay in the regulation of cell proliferation, inflammation and tumorigenesis in response to bacterial infection. *PLoS One* **8**, e79432
157. Jang, J., Ha, J. H., Chung, S. I., and Yoon, Y. (2014) Beta-catenin regulates NF-kappaB activity and inflammatory cytokine expression in bronchial epithelial cells treated with lipopolysaccharide. *Int. J. Mol. Med.* **34**, 632-638
158. Liu, X. Y., Robinson, D., Veach, R. A., Liu, D., Timmons, S., Collins, R. D., and Hawiger, J. (2000) Peptide-directed suppression of a pro-inflammatory cytokine response. *J. Biol. Chem.* **275**, 16774-16778
159. Torgerson, T. R., Colosia, A. D., Donahue, J. P., Lin, Y. Z., and Hawiger, J. (1998) Regulation of NF-kappa B, AP-1, NFAT, and STAT1 nuclear import in T lymphocytes by noninvasive delivery of peptide carrying the nuclear localization sequence of NF-kappa B p50. *J. Immunol.* **161**, 6084-6092
160. Pierce, J. W., Schoenleber, R., Jesmok, G., Best, J., Moore, S. A., Collins, T., and Gerritsen, M. E. (1997) Novel inhibitors of cytokine-induced IkappaBalpha phosphorylation and endothelial cell adhesion molecule expression show anti-inflammatory effects in vivo. *J. Biol. Chem.* **272**, 21096-21103
161. van Nieuw Amerongen, G. P., Beckers, C. M., Achekar, I. D., Zeeman, S., Musters, R. J., and van Hinsbergh, V. W. (2007) Involvement of Rho kinase in endothelial barrier maintenance. *Atertio. Thromb. Vasc. Biol.* **27**, 2332-2339
162. Liu, Y., Major, A. S., Zienkiewicz, J., Gabriel, C. L., Veach, R. A., Moore, D. J., Collins, R. D., and Hawiger, J. (2013) Nuclear transport modulation reduces hypercholesterolemia, atherosclerosis, and fatty liver. *J Am Heart Assoc* **2**, e000093
163. Weksler, B. B., Subileau, E. A., Perriere, N., Charneau, P., Holloway, K., Leveque, M., Tricoire-Leignel, H., Nicotra, A., Bourdoulous, S., Turowski, P., Male, D. K., Roux, F., Greenwood, J., Romero, I. A., and Couraud, P. O. (2005) Blood-brain barrier-specific properties of a human adult brain endothelial cell line. *FASEB J.* **19**, 1872-1874
164. Montesano, R., Pepper, M. S., Mohle-Steinlein, U., Risau, W., Wagner, E. F., and Orci, L. (1990) Increased proteolytic activity is responsible for the aberrant morphogenetic behavior of endothelial cells expressing the middle T oncogene. *Cell* **62**, 435-445
165. Livak, K. J., and Schmittgen, T. D. (2001) Analysis of relative gene expression data using real-time quantitative PCR and the 2(-Delta Delta C(T)) Method. *Methods* **25**, 402-408